frontiers | Research Topics

Beneficial and pathological roles of myeloid cells during COVID-19

Edited by
Lokesh Sharma, Thierry Roger and Shaon Sengupta

Published in
Frontiers in Immunology

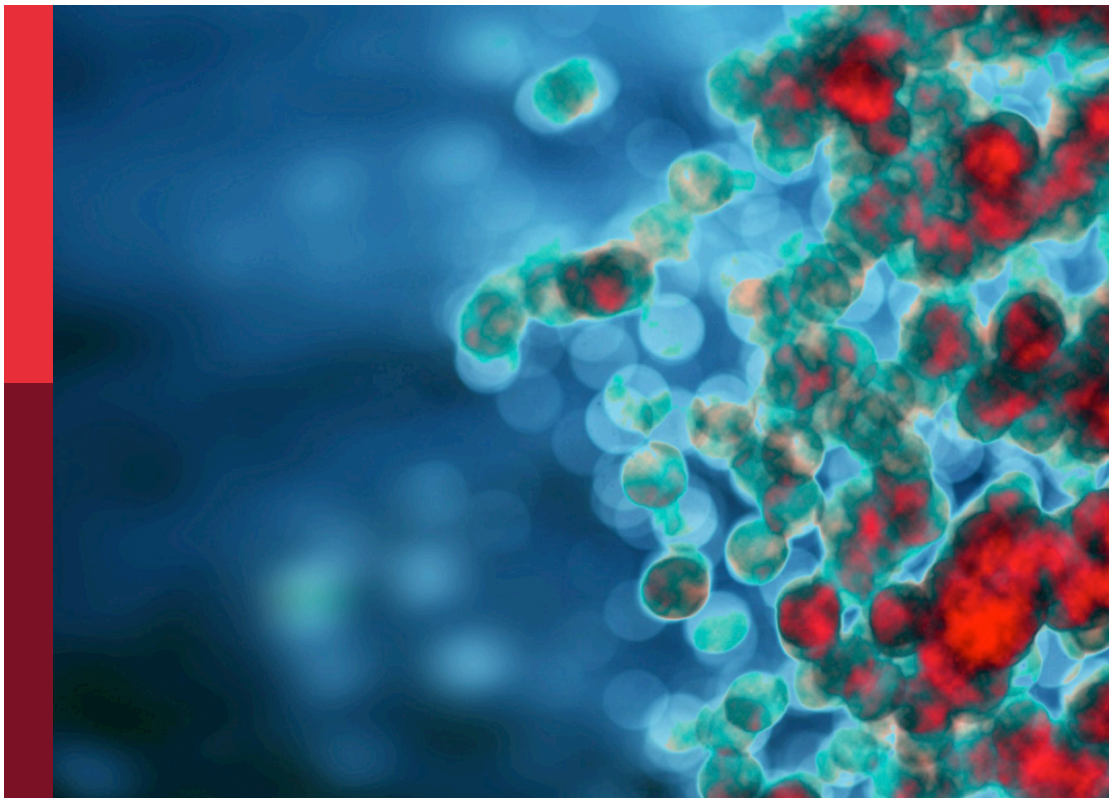

ISSN 1664-8714
ISBN 978-2-8325-2207-3
DOI 10.3389/978-2-8325-2207-3

About Frontiers

Frontiers is more than just an open access publisher of scholarly articles: it is a pioneering approach to the world of academia, radically improving the way scholarly research is managed. The grand vision of Frontiers is a world where all people have an equal opportunity to seek, share and generate knowledge. Frontiers provides immediate and permanent online open access to all its publications, but this alone is not enough to realize our grand goals.

Frontiers journal series

The Frontiers journal series is a multi-tier and interdisciplinary set of open-access, online journals, promising a paradigm shift from the current review, selection and dissemination processes in academic publishing. All Frontiers journals are driven by researchers for researchers; therefore, they constitute a service to the scholarly community. At the same time, the *Frontiers journal series* operates on a revolutionary invention, the tiered publishing system, initially addressing specific communities of scholars, and gradually climbing up to broader public understanding, thus serving the interests of the lay society, too.

Dedication to quality

Each Frontiers article is a landmark of the highest quality, thanks to genuinely collaborative interactions between authors and review editors, who include some of the world's best academicians. Research must be certified by peers before entering a stream of knowledge that may eventually reach the public - and shape society; therefore, Frontiers only applies the most rigorous and unbiased reviews. Frontiers revolutionizes research publishing by freely delivering the most outstanding research, evaluated with no bias from both the academic and social point of view. By applying the most advanced information technologies, Frontiers is catapulting scholarly publishing into a new generation.

What are Frontiers Research Topics?

Frontiers Research Topics are very popular trademarks of the *Frontiers journals series*: they are collections of at least ten articles, all centered on a particular subject. With their unique mix of varied contributions from Original Research to Review Articles, Frontiers Research Topics unify the most influential researchers, the latest key findings and historical advances in a hot research area.

Find out more on how to host your own Frontiers Research Topic or contribute to one as an author by contacting the Frontiers editorial office: frontiersin.org/about/contact

Beneficial and pathological roles of myeloid cells during COVID-19

Topic editors

Lokesh Sharma — Yale University, United States

Thierry Roger — Centre Hospitalier Universitaire Vaudois (CHUV), Switzerland

Shaon Sengupta — University of Pennsylvania, United States

Citation

Sharma, L., Roger, T., Sengupta, S., eds. (2023). *Beneficial and pathological roles of myeloid cells during COVID-19*. Lausanne: Frontiers Media SA.

doi: 10.3389/978-2-8325-2207-3

Table of contents

frontiers | Frontiers in Immunology

TYPE Editorial
PUBLISHED 04 April 2023
DOI 10.3389/fimmu.2023.1194826

OPEN ACCESS

EDITED AND REVIEWED BY
Francesca Granucci,
University of Milano-Bicocca, Italy

*CORRESPONDENCE
Lokesh Sharma
lokeshkumar.sharma@yale.edu

†These authors have contributed equally to this work

SPECIALTY SECTION
This article was submitted to Molecular Innate Immunity, a section of the journal Frontiers in Immunology

RECEIVED 27 March 2023
ACCEPTED 30 March 2023
PUBLISHED 04 April 2023

CITATION
Sharma L, Sengupta S and Roger T (2023) Editorial: Beneficial and pathological roles of myeloid cells during COVID-19. *Front. Immunol.* 14:1194826. doi: 10.3389/fimmu.2023.1194826

Editorial: Beneficial and pathological roles of myeloid cells during COVID-19

Lokesh Sharma [1*†], Shaon Sengupta [2†] and Thierry Roger [3†]

[1]Section of Pulmonary, Critical Care and Sleep Medicine, School of Medicine, Yale University, New Haven, CT, United States, [2]The Children's Hospital of Philadelphia, University of Pennsylvania Perelman School of Medicine, Philadelphia, PA, United States, [3]Infectious Diseases Service, Department of Medicine, Lausanne University Hospital and University of Lausanne, Epalinges, Switzerland

KEYWORDS

COVID - 19, neutrophils (PMNs), macrophage, SARS-CoV-2, infection - immunology

Editorial on the Research Topic
Beneficial and pathological roles of myeloid cells during COVID-19

Since its emergence, coronavirus disease-2019 (COVID-19) disease has become one of the greatest challenges to human health. Extensive research efforts have been devoted to the development of novel antiviral agents and effective vaccinations against severe acute respiratory syndrome coronavirus 2 (SARS-CoV-2), the etiologic agent of COVID-19. In comparison, there are relatively few studies investigating the role of an innate immune response during COVID-19, especially that mediated by myeloid cells. Myeloid cells including monocytes, macrophages, neutrophils, and dendritic cells play a key role in host antiviral response as well as in the pathological processes that occur in infected individuals. Antiviral mechanisms mediated by myeloid cells include virus sensing and phagocytosis, production of cytokines, and activation of the adaptive immune response through antigen presentation. However, myeloid cells can also trigger hypercytokinemia and release tissue-damaging factors that contribute to the host pathology. In this Research Topic, we aimed to include studies that investigated beneficial and pathological mechanisms of myeloid cells in the pathogenesis of COVID-19.

Neutrophils, the most prominent leukocyte subpopulation in the blood, are known to have profound tissue-damaging effects that result from the release of soluble proteases and reactive oxygen species. DNA released as neutrophil extracellular traps (NETs) may have significant adverse effects participating to lung pathology and inflammation. Moreover, elevated levels of neutrophil-derived calprotectin have been associated with severe COVID-19 disease, however, its role in the pathogenesis of COVID-19 is not well understood. Loh et al. investigated the molecular mechanisms by which neutrophils sense and respond to SARS-CoV-2 to produce calprotectin, a neutrophil protein. Loh et al. described a critical role of Dok-3 in limiting calprotectin secretion by deactivating MyD88 and subsequent downstream JAK2-STAT3 signaling, revealing potential therapeutic targets in COVID-19. Another facet of the role of neutrophils is highlighted by Calvert et al. who used co-culture models to reveal that the presence of neutrophils with epithelial cells increases cytokine/chemokine response and weakens epithelial barrier function. Furthermore, neutrophils enhance viral replication and increase SARS-CoV-2 infection of the epithelium including

basal stem cells. The authors confirm the deleterious role played by neutrophils using autopsy studies on the lungs of patients who died from COVID-19. Overall, these studies underline the pathological role of neutrophils during severe COVID-19.

A proportion of children with COVID-19 show signs of hyperinflammation with multi-organ involvement, defining a new syndrome called multisystem inflammatory syndrome in children (MIS-C). MIS-C has symptoms consistent with Kawasaki disease. Further exploring neutrophil biology in COVID-19, Chen et al. use whole blood single-cell RNA sequencing to compare neutrophil response in Kawasaki disease and COVID-19 disease. They demonstrate that neutrophils from these two diseases have similar transcriptomic profiles, characterized by neutrophil activation and low MHC class II expression. Confirming the role of neutrophil activation in lung pathology, Prével et al. report that high blood levels of biomarkers of neutrophil extracellular traps (NETs) are associated with disease severity. NET biomarkers are most prominently associated with acute respiratory distress syndrome (ARDS) and survival, but not pulmonary embolism. These apparently conflicting observations may be due to the limited number of patients analyzed. The authors propose that NET biomarkers be used as prognostic biomarkers in COVID-19, and that NETosis be targeted early during disease development to prevent the development of ARDS.

Beyond original research on neutrophil biology, two insightful reviews summarize specific aspects of the role of neutrophils in COVID-19. McKenna et al. provide a comprehensive review of potential mechanisms by which neutrophils contribute to lung injury and host response in SARS-CoV-2 infection. They highlight the changes in neutrophils, both in abundance and transcriptome profile, during COVID-19 disease. Further, they discuss how neutrophils may contribute to injury through the production of NETs and activation of inflammasomes. Potential approaches to target excessive neutrophil infiltration and activation in COVID-19 are proposed as possible therapeutic strategies. Along similar lines, Ventura-Santana et al. review the role of NETs in mediating viral sepsis in COVID-19. Consistent with the observations reported by Calvert et al. and Prével et al., the authors propose that direct viral infection of neutrophils exacerbates tissue damage *via* the release of NETs without aiding viral clearance.

Macrophages are one of the first responders to viral infection including by SARS-CoV-2. Atmeh et al. investigate the host-virus interaction using monocyte-derived macrophages. They report that α, β, γ, δ and o strains of SARS-CoV-2 successfully infect, but do not replicate in monocyte-derived macrophages. Further they demonstrate that infected macrophages are able to activate a γδ T cell line to secrete IFNγ and TNF. Schroeder and Beineman show that myeloid cells isolated from human blood such as basophils, dendritic cells and monocytes respond to S1, S2, and S1/S2 subunits of the spike protein (S) of SARS-CoV-2. The magnitude of the response, measured by the secretion of cytokines and chemokines, differs according to the cell type and S subunit. Monocytes respond robustly to S1 stimulation by releasing IL-1β, IL-6 and TNF, which are abundantly expressed in severe COVID-19 patients.

Finally, Trombetta et al. used multiparameter flow cytometry to investigate the frequency and phenotype of myeloid cells in patients with severe COVID-19 analyzed at admission and discharge from intensive care units (ICU). The authors describe major alterations, especially in the monocyte population. The levels of M-2 like classical monocytes are high in patients with SARS-CoV-2 viremia at ICU admission, increased at time of ICU discharge, and correlate with SARS-CoV-2 specific antibody response. In contrast, $Slan^+$ non-classical monocytes are expressed at low levels in patients regardless of disease severity. These data support the idea that the resolution of acute infection and recovery from COVID-19 are related to the acquisition of an immunoregulatory phenotype by monocytic cells.

In summary, this Research Topic includes a collection of original research articles and insightful reviews supporting the role of myeloid cells in the pathogenesis of COVID-19. The key mechanisms discussed in the articles offer insights into the study of host antiviral responses. We believe that this Research Topic will stimulate interest in the role of myeloid cells in COVID-19 and for research to contribute to the development of strategies improving the management of infected patients.

Author contributions

LS, SS, and TR have contributed to the writing of this editorial article. All authors contributed to the article and approved the submitted version.

Funding

LS acknowledges support from Parker B Francis Fellowship Program and American Lung Association. SS was supported by NHLBI R01HL155934-01A1 and NHLBI-R01HL147472. TR was supported by the Swiss National Science Foundation (310030_207418), the Carigest Foundation (Switzerland), and the European Union Horizon 2020 grants ImmunoSep (847422) and HDM-FUN (847507).

Acknowledgments

We thank all the authors for their contributions to this Research Topic. We also thank the reviewers for their evaluation of the manuscripts.

Conflict of interest

The authors declare that the research was conducted in the absence of any commercial or financial relationships that could be construed as a potential conflict of interest.

Publisher's note

frontiers in Immunology

ORIGINAL RESEARCH
published: 23 June 2021
doi: 10.3389/fimmu.2021.691725

Severe COVID-19 Recovery Is Associated with Timely Acquisition of a Myeloid Cell Immune-Regulatory Phenotype

Amelia C. Trombetta[1], Guilherme B. Farias[1], André M. C. Gomes[1,2], Ana Godinho-Santos[1], Pedro Rosmaninho[1], Carolina M. Conceição[1], Joel Laia[1], Diana F. Santos[1], Afonso R. M. Almeida[1], Catarina Mota[1,3], Andreia Gomes[1], Marta Serrano[1], Marc Veldhoen[1], Ana E. Sousa[1] and Susana M. Fernandes[1,2,4]*

[1] Instituto de Medicina Molecular João Lobo Antunes, Faculdade de Medicina, Universidade de Lisboa, Lisbon, Portugal, [2] Clinica Universitária de Medicina Intensiva, Faculdade de Medicina, Universidade de Lisboa, Lisbon, Portugal, [3] Serviço de Medicina II, Hospital de Santa Maria, Centro Hospitalar Universitário Lisboa Norte, Lisbon, Portugal, [4] Serviço de Medicina Intensiva, Hospital de Santa Maria, Centro Hospitalar Universitário Lisboa Norte, Lisbon, Portugal

OPEN ACCESS

Edited by:
Nabila Seddiki,
Commissariat à l'Energie Atomique et aux Energies Alternatives (CEA), France

Reviewed by:
Nicolas Ruffin,
Karolinska Institutet, Sweden
Sylvain Cardinaud,
Institut National de la Santé et de la Recherche Médicale (INSERM), France

***Correspondence:**
Amelia C. Trombetta
amelia.trombetta@medicina.ulisboa.pt

Specialty section:
This article was submitted to Viral Immunology, a section of the journal Frontiers in Immunology

Received: 06 April 2021
Accepted: 31 May 2021
Published: 23 June 2021

Citation:
Trombetta AC, Farias GB, Gomes AMC, Godinho-Santos A, Rosmaninho P, Conceição CM, Laia J, Santos DF, Almeida ARM, Mota C, Gomes A, Serrano M, Veldhoen M, Sousa AE and Fernandes SM (2021) Severe COVID-19 Recovery Is Associated With Timely Acquisition of a Myeloid Cell Immune-Regulatory Phenotype. Front. Immunol. 12:691725. doi: 10.3389/fimmu.2021.691725

After more than one year since the COVID-19 outbreak, patients with severe disease still constitute the bottleneck of the pandemic management. Aberrant inflammatory responses, ranging from cytokine storm to immune-suppression, were described in COVID-19 and no treatment was demonstrated to change the prognosis significantly. Therefore, there is an urgent need for understanding the underlying pathogenic mechanisms to guide therapeutic interventions. This study was designed to assess myeloid cell activation and phenotype leading to recovery in patients surviving severe COVID-19. We evaluated longitudinally patients with COVID-19 related respiratory insufficiency, stratified according to the need of intensive care unit admission (ICU, n = 11, and No-ICU, n = 9), and age and sex matched healthy controls (HCs, n = 11), by flow cytometry and a wide array of serum inflammatory/immune-regulatory mediators. All patients featured systemic immune-regulatory myeloid cell phenotype as assessed by both unsupervised and supervised analysis of circulating monocyte and dendritic cell subsets. Specifically, we observed a reduction of CD14lowCD16+ monocytes, and reduced expression of CD80, CD86, and Slan. Moreover, mDCs, pDCs, and basophils were significantly reduced, in comparison to healthy subjects. Contemporaneously, both monocytes and DCs showed increased expression of CD163, CD204, CD206, and PD-L1 immune-regulatory markers. The expansion of M2-like monocytes was significantly higher at admission in patients featuring detectable SARS-CoV-2 plasma viral load and it was positively correlated with the levels of specific antibodies. In No-ICU patients, we observed a peak of the alterations at admission and a progressive regression to a phenotype similar to HCs at discharge. Interestingly, in ICU patients, the expression of immuno-suppressive markers progressively increased until discharge. Notably, an increase of M2-like HLA-DRhighPD-L1+ cells in CD14++CD16– monocytes and in dendritic cell subsets was observed at ICU discharge. Furthermore, IFN-γ and IL-12p40

showed a decline over time in ICU patients, while high values of IL1RA and IL-10 were maintained. In conclusion, these results support that timely acquisition of a myeloid cell immune-regulatory phenotype might contribute to recovery in severe systemic SARS-CoV-2 infection and suggest that therapeutic agents favoring an innate immune system regulatory shift may represent the best strategy to be implemented at this stage.

Keywords: innate immunity, SARS-CoV-2, COVID-19, M2-like differentiation, immune-regulation

INTRODUCTION

After more than 1 year from the coronavirus disease (COVID-19) outbreak in Wuhan, China, more than 100 million cases and 2,5 million deaths have been confirmed worldwide (1). The etiological agent, the severe acute respiratory syndrome Coronavirus (SARS-CoV)-2, determines a mild illness in the majority of the patients. In 5% of the cases, rapid viral replication, immune cell infiltration, and uncontrolled inflammatory response occur, causing acute lung injury (ALI) or acute respiratory distress syndrome (ARDS), with or without multi-organ failure, resulting in a high case-fatality ratio (2).

Critically ill COVID-19 patients represent the bottleneck of the pandemic management, leading to an overwhelming impact on available health care resources. Most of the available therapies used for severe cases are still today of supportive nature, while several immune-modulating agents are under trial (3, 4). Cytokine storm and macrophage activation syndrome were reported in fatal COVID-19 cases. Interferon-γ (IFN-γ), interleukin-1 (IL-1), IL-6, tumor necrosis factor-α (TNF-α), and IL-18 have central immunopathogenic roles in the hyper-inflammation (5, 6). Decoy receptors for pro-inflammatory cytokines such as IL-1RA, as well as anti-inflammatory cytokines such as IL-10, constitute negative feedback mechanisms preventing immune hyper-activation and immunopathology (5).

Interestingly, Coronaviruses (CoVs) encode multiple proteins that antagonize the activation of type I, II, and III IFN responses (7–12). The inhibition of IFN pathways has been associated to the insidious clinical course of COVID-19, until late deterioration (7). Several reports have assessed aspects of systemic innate immune response to SARS-CoV-2, initially with contrasting results: increased or decreased levels of classical, intermediate, and non-classical monocytes and presence of both pro- and anti-inflammatory markers in circulating myeloid cells have been described (8, 9). More recently, systemic loss and functional impairment of pro-inflammatory monocytes, conventional and plasmacytoid dendritic cells (pDCs) populations, sustaining for a loss of M1-like/pro-inflammatory cells, were reported as distinctive features of the severe compared to moderate disease (10–12).

Nevertheless, to our knowledge, few data are available on longitudinal comprehensive characterization of myeloid cell phenotype, allowing elucidation of their role in COVID-19 recovery.

Here we performed a detailed longitudinal evaluation of circulating monocytes/macrophages and dendritic cells (DCs), along with a wide range of circulating cytokines and chemokines. We aimed to clarify if these elements of the innate immune response might direct towards inflammation or immune-suppression in COVID-19 associated with severe symptoms. Moreover, we assessed in hospitalized patients whether intensive care unit (ICU) requirement or symptoms resolution and discharge might be linked to a particular systemic myeloid cell and circulating cytokine/chemokine signature, with the ultimate goal to identify pathways to be targeted to induce the recovery.

MATERIALS AND METHODS

Patients and Healthy Controls

Twenty-one adult patients affected by COVID-19 related pneumonia, admitted at the Centro Hospitalar Universitário Lisboa Norte (CHULN, Lisboa, Portugal), between April and October 2020, and 11 healthy controls (HCs), were enrolled in the study (**Table 1**). Age and sex distribution were homogeneous in patient and healthy control groups. Informed consent was obtained from all participants and the study was approved by the Ethics committee at the CHULN/Faculdade de Medicina da Universidade de Lisboa. SARS-CoV-2 infection was confirmed by real-time PCR (RT-PCR) for nucleic acid testing of nasopharyngeal swabs.

The first time point for clinical and laboratory evaluation was performed at admission to the intensive care unit (ICU group) and at hospital admission (HA) for the patients not requiring high flux nasal oxygen (HFNO patients) or mechanical ventilation (MV) respiratory support (No-ICU group). Afterwards, all patients were evaluated at recovery, when discharged from hospital or from ICU. Collection of all clinical information (**Table 1**) was monitored by the same clinician, that integrates the research team (SMF). At each time point, clinical data, whole blood, plasma, and serum were collected for all individuals. To obtain a more homogenous set of patient samples, the study participants were screened for co-infections, and one case of HIV-1/SARS-CoV-2 co-infection was excluded and considered to be analyzed separately. Furthermore, three No-ICU patients were lost at the follow up and two ICU patients died after the ICU admission time point. Whole blood was processed immediately after sampling and no difference in sample handling or material used existed among patient and control groups.

Flow Cytometry

Multi-parameter flow cytometry for immune-phenotyping of circulating monocyte/macrophage and DCs was performed on whole blood, immediately after sampling.

TABLE 1 | Clinical and routine laboratory data from patients and healthy controls.

Clinical variables		No-ICU	ICU	HCs	p (Global)[a]	p (ICU *vs* HCs)[b]	p (No ICU *vs* HCs)[b]	p (ICU *vs* No-ICU)[b]
n		9	11	11				
Age in years		50 (39–65)	57 (45.5–64)	58 (39–65)	0.485	0.965	0.965	0.965
Male sex, n (%)[c]		7 (77.7)	10 (91)	9 (73)	0.671	0.315	0.882	0.413
Arterial hypertension, n (%)[c]		4 (44)	5 (46)	1 (9)	0.264	0.056	0.069	0.964
Diabetes type 2, n (%)[c]		3 (33)	3 (27)	0	0.251	0.062	**0.038**	0.2942
Obesity, n (%)[c]		1 (11)	5 (45)	0	**0.032**	**0.011**	0.257	0.095
Lung emphysema, n (%)[c]		0	2 (18)	0	0.313	0.138	>0.999	0.178
Time from symptoms start to admission (days)		8 (4–10)	9 (7–12)	NA	0.302	NA	NA	0.302
Time from symptoms start to recovery (days)		12 (11–17)	20 (17–21.5)	NA	**0.009**	NA	NA	**0.009**
Time from admission to discharge (days)		9 (8–10)	12 (9.5–15)	NA	**0.034**	NA	NA	**0.034**
P/F	A	287.4 (270–323)	122.1 (104.5–272.2)	NA	NA	NA	NA	**<0.001**
	D	447.6 (340–461)	283.3 (273–392.9)	NA	NA	NA	NA	**0.03**
CRP (mg/dl)	A	5.44 (2.26–7.03)	23.7 (12.5–26.5)	NA	NA	NA	NA	**0.005**
PCT (ng/ml)	A	0.14 (0.11–0.41)	0.21 (0.15–0.83)	NA	NA	NA	NA	0.440
Ferritin (mg/dl)	A	949 (344–1,374)	1,030 (435.3–1,998)	NA	NA	NA	NA	0.450
D-dimers (ng/ml)	A	0.43 (0.19–53)	0.23 (0.18–0.63)	NA	NA	NA	NA	0.712
LDH (U/L)	A	366 (222–417.5)	372 (293–393)	NA	NA	NA	NA	0.736
Lymphocytes/µl	A	1,390 (835–2,108)	870 (840–1,160)	1,940 (1,423–2,200)	**0.005**	**0.003**	0.152	0.146
	D	1,810 (1,675–1,995)	1,982 (1,269–2,680)		0.8464	0.710	0.661	0.898
Neutrophils/µl	A	3,923 (2,385–4,952)	7,447 (4,687–11,793)	3,228 (2,521–6,390)	**0.011**	**0.010**	0.924	**0.007**
	D	3,349 (2,792–4,891)	5,557 (4,303–9,620)		**0.067**	**0.045**	0.978	**0.**060
Lymphocytes/neutrophils	A	0.316 (0.26–0.65)	0.146 (0.086–0.380)	0.509 (0.47–0.605)	**0.013**	**0.008**	0.194	**0.038**
	D	0.588 (0.35–0.69)	0.264 (0.142–0.559)		0.098	**0.005**	0.892	**0.032**
Monocytes/µl	A	321.9 (228–503)	376.8 (210.6–658.5)	398 (274.8–732.8)	0.872	0.833	0.640	0.766
	D	397 (347–595)	636 (472–1,057)		0.099	0.055	0.890	0.112
Basophils/µl	A	15.09 (6.35–31.77)	31.2 (16.9–42.32)	31.6 (16.4–63)	0.150	0.550	0.077	0.152
	D	19.56 (10.1–26.8)	30.9 (15.86–54.2)		0.273	0.589	0.109	0.364
Eosinophils/µl	A	12.5 (5.5–40.88)	24.39 (6.85–60.18)	114.8 (96.48–297)	**<0.001**	**<0.001**	**<0.001**	0.602
	D	116 (36.95–142.7)	42 (23.21–58.41)		**0.008**	**<0.001**	0.364	0.190
Detectable SARS-Cov-2 Plasma viral Load, n (%)[c]	A	3 (33%)	10 (91%)	NA	**0.007**	NA	NA	**0.007**
	D	0 (0%)	0 (0%)					
SARS-Cov-2 Plasma viral Load in patients with detectable levels (cps/ml)	A	111.7 (33.91–563.5)	131 (36.1–713)	NA	NA	NA	NA	0.864
	D	NA	NA	NA	NA	NA	NA	NA
Treatment[c]:				NA		NA	NA	
Dexamethasone, n (%)		1 (11)	4 (36)		0.293			0.293
Other glucocorticoids, n (%)		1 (11)	5 (45)		0.619			0.619
Tocilizumab, n (%)		0 (0)	3 (27)		0.507			0.507
Lopinavir/Ritonavir, n (%)		6 (68)	2 (18)		0.123			0.123
Remdesivir, n (%)		2 (22)	4 (36)		0.632			0.632

Values expressed as medians (interquartile range) unless otherwise specified. P/F, Ratio of the partial pressure of arterial oxygen to the fraction of inspired oxygen; CRP, C reactive protein; PCT, procalcitonin; Ferritin: A, Admission; D, Discharge; NA, Not Applicable. Comparisons were done using [a]One way ANOVA unless otherwise stated; [b]Mann–Whitney U-test unless otherwise stated; [c]Chi-squared test.

Significant p values were shown in bold.

In this and other studies we confirmed that if rapid sample processing was performed in whole blood no significant amount of dead cells are reported, therefore a live/dead marker was not used for this evaluation. After erythrocyte bulk lysis, 10 million leukocytes were incubated with a panel of fluorochrome-labelled antibodies, for 30 min at room temperature. The cell populations were stained with the following antibodies: anti-Slan Ef450, anti-CD141 BV510, anti-CD45 BV605, anti-HLA-DR BV650, anti-CD86 BV711, anti-PD-L1 BV785, anti-CD3 FITC, anti-CD19 FITC, anti-CD66b FITC, anti-CD14 PerCP-Cy5.5, anti-CD80 PE, anti-CD163 PE-CF594, anti-CD206 PE-Cy5, anti-CD123 PE-Cy7, anti-CD204 APC, anti-CD16 AF700, anti-CD1c APC-Cy7 (**Supplementary Table 1**). After fixation, cells were resuspended in PBS and acquired in a Fortessa X20 flow cytometer. The data were analyzed with FlowJo software (Version 10.7; Tree Star, Inc., Ashland, OR, USA).

For flow cytometry data analysis, both supervised and unsupervised approaches were implemented. Traditional manual hierarchical gating was applied on 2D scatterplots starting on a large lymphocyte/monocyte including gate (**Supplementary Figure 1**). After cell debris and doublets exclusion, based on forward and side scatter, monocytes, macrophages, and DCs were defined by selection of CD45 antigen-expressing cells, negative for the lineage markers CD66b, CD19, and CD3 (CD45+Lin− cells). CD56 was not used among lineage markers in order to prevent the exclusion of possible myeloid cells expressing CD56 (13).

For the unsupervised analysis, CD45+Lin− cells were gated and dimensionality reduction was applied through the t-distributed Stochastic Neighbour Embedding (tSNE) in Flow-Jo version 10.7. on 79,688 events from each patient and HC. Firstly, to obtain the cluster number definition, both X-Shift and Phenograph were used on the same datasets, evaluating the best clustering resolution visualized on the t-SNE images. The Phenograph clustering was excluded because of the higher number of clusters defined, several of which representing single outliers. The X-Shift cluster definition of 16 clusters in CD45+Lin− concatenated events was applied (14). Afterwards, to confirm and visualize the results on a minimal spanning tree, the dataset was re-clustered using FlowSOM (15).

Bidimensional hierarchical gating strategy was also used to further define in a CD45+Lin− gate the plasmocytoid dendritic cell (pDC), and the CD141+ and CD1c+ myeloid dendritic cell (mDC) subpopulations.

Within the CD14 positive cells, in the CD45+Lin− population, a trapezoidal gating strategy was applied uniformly to all patients and control samples to define the monocyte subsets as CD14++CD16− classical, CD14++CD16+ intermediate, CD14lowCD16+ non-classical (16, 17). Slan was used for non-classical monocyte sub-setting.

In monocyte and DC cell populations, the levels of expression of CD163, CD204, and CD206 (for M2-like polarization), PD-L1 (immune-regulation/suppression), HLA-DR, CD80, CD86 (activation, antigen presentation, and M1-like phenotype), were assessed.

For each studied individual unstained cells were used as control for gating of the negative and positive populations.

For each patient and control a hemogram with complete white blood cell count was performed from the same blood sampling at Santa Maria Hospital clinical laboratory. Absolute numbers of monocyte subsets were calculated by multiplying their percentual representation by the absolute monocyte count obtained at the clinical laboratory.

Serum Proteins

Multiplex ELISA for 71 cytokines and chemokines was performed on the −80°C stored serum samples, from each time point, using a Multiplexing LASER Bead Assay (Human Cytokine Array/ Chemokine Array 71-Plex Panel, HD71, Eve Technologies, Canada) while CCL28, RAGE, SP-D, IL-22BP were determined by Sandwich ELISA kits, as specified by the manufacturer (RayBiotech, GA).

SARS-CoV-2 specific antibody responses were evaluated through quantitative tests for IgM, IgG, and IgA against spike protein or its receptor binding domain, as previously described (18).

SARS-CoV-2 Plasma Viral Load

Total RNA was extracted from collected plasma samples (560 µl) using QIAamp® Viral RNA Mini Kit (QIAGEN), according to manufacturer's instructions. SARS-CoV-2 viremia was quantified using the commercial RT-PCR amplification kit Bio-Rad SARS-CoV-2 ddPCR Test Kit (Bio-Rad) on QX200™ Droplet Digital PCR System (Bio-Rad), following manufacturer's instructions. Each 20 µl ddPCR reaction used 5 µl of extracted RNA with samples in duplicate to quantify copies/reaction. Plasma samples with one of the two N1 or N2 regions or both regions detected were considered as positive samples and results were analyzed on QuantaSoft Analysis Pro (1.0.596). SARS-CoV-2 RNA concentrations (cp/ml) were finally calculated considering the extracted volume of plasma.

Statistical Analysis

The statistical analysis was performed within and between different patient groups and in comparison to HCs. The Kruskal-Wallis and the Dunn's multiple comparison tests were used to compare variables with continuous distribution in more than two groups. Wilcoxon matched-pairs signed rank test and Mann–Whitney U-test were used for paired and unpaired analyses of continuous data, respectively. Spearman's Delta was done for hypothesis testing of correlations. Principal Component Analysis was performed for dimensionality reduction and evaluation of relevant analytes contributing to data variation, afterwards hierarchical clustering was applied. Ultimately, volcano plots were employed to quantify, in terms of fold changes and statistical significance, the most meaningful modifications in the variables analyzed. All values were presented as median (25^{th}–75^{th} percentiles). Data were analyzed with R version 4.0.2., using the packages *heatmaply, EnhancedVolcano*, and *ggplot2* for data visualization and GraphPad Prism version 8 (GraphPad Software, San Diego, CA, USA). A p value <0.05 was considered statistically significant.

RESULTS

In order to investigate myeloid cell phenotype contributing to the recovery of patients with severe COVID-19, we compared the

data obtained at admission and at discharge from the respiratory isolation units or the ICU, within patient group or between patient groups and HCs (**Table 1**). As expected, patients requiring ICU featured significantly longer hospital stay and lower ratio of the partial pressure of arterial oxygen to the fraction of inspired oxygen (P/f), both at admission and at discharge (**Table 1**). The use of steroids and other therapies with possible impact on the viral or immune response was comparable between the two patient groups (**Table 1**). Interestingly, SARS-CoV-2 was detectable in the plasma of all ICU patients at admission, but not at discharge. Although ICU patients had higher neutrophil counts and C reactive protein (CRP) serum levels, no difference was reported for procalcitonin (PCT), ferritin, and D-dimers in the two groups (**Table 1**).

Notably, both patient groups featured no significant changes in circulating monocyte counts (**Table 1**).

Monocytes, macrophages, and DCs were analyzed within the concatenated CD45+Lin− dataset (**Supplementary Figure 1**), through an unsupervised approach, starting with dimensionality reduction by tSNE (**Figure 1A**). Afterwards, X-Shift clustering was applied to obtain 16 different clusters (**Figures 1B, C**, **Supplementary Figure 2** and **Supplementary Table 2**). The CD45+Lin− dataset was then re-clustered with FlowSOM, to show the relative distribution of the populations in a self-organizing map defining a minimal spanning tree (**Figures 1D, E**).

Interestingly, all patients showed relevant changes in several cluster frequencies compared to HCs, but at different time points for No-ICU and ICU groups.

The Cluster (C) 8, having the characteristics of non-classical monocytes expressing high levels of Slan, HLA-DR, PD-L1, CD80, and CD86, and low CD163, was significantly and persistently reduced in both patient groups until discharge, in comparison to healthy subjects (**Figures 1B, C**, **Figure 2A**, **Supplementary Figure 2** and **Supplementary Table 2**). In the spanning tree, a complete shrinking of the Slan+ CD14lowCD16+ nodes was observed in No-ICU patients at HA, only partially re-appearing in the discharge time-point map. A reduction of this branch was also present in the ICU group, but more notably at discharge (**Figure 1E**).

On the other hand, the C15, with a classical monocyte phenotype, characterized by the highest CD163 levels, low/intermediate HLA-DR, CD86, and CD204, and low CD80 (CD163+++M2-like monocytes), was significantly expanded, especially in ICU patients at admission and discharge (**Figures 1B, C**, **Figure 2B**, **Supplementary Figure 2** and **Supplementary Table 2**).

Importantly, C16, a classical monocyte population with positivity for M2 markers, high HLA-DR, and PD-L1 levels (PD-L1+M2-like monocytes), showed the highest percentages in ICU patients at discharge (**Figures 1B, C**, **Figure 2C Supplementary Figure 2** and **Supplementary Table 2**).

In the FlowSOM maps, classical monocytes with higher expression of scavenger receptors, HLA-DR and PD-L1, as well as the HLA-DRlow classical monocytes, were mainly observable at discharge in ICU patients (**Figures 1D, E**).

No differences were found for less differentiated CD14++ CD16− monocytes (C5 and C14), as well as for other CD14lowCD16+ clusters (C9 and C13) (**Figures 1B, C**, **Supplementary Figure 2** and **Supplementary Table 2**).

The bidimensional hierarchical gating strategy confirmed the results of the unbiased analysis (**Figure 3**). A significant increase in classical monocyte count was observed reaching significance in ICU patients at discharge (ICU D = 599, 456–740; HC = 349, 253–519 cells/μl, p = 0.04). A global decrease in non-classical monocyte population counts was observed in comparison with HCs (34, 24–43 μ/ml) in all patients at both time points (No-ICU HA/D = 6, 0.7–8.6 cells/μl, p = 0.007/13, 5–15 cells/μl, p = 0.05; ICU A/D = 2.7, 1–4.6 cells/μl, p = 0.0005/7, 3–8 cells/μl, p < 0.0001). No significant alterations were reported in the intermediate monocyte subset counts (**Figure 3A**).

Concerning the M2-like/immuno-regulatory marker expression, in the ICU group at discharge, a significant increase in CD163 MFI (HCs = 8,142, 7,280–9,945; ICU D = 14,938, 12,035–15,700, p = 0.01) and a tendency to increase in the percentages of CD14++CD16− monocytes showing M2-like markers (CD204+CD206+ classical monocytes at ICU D = 27, 16–33% *vs* HCs = 13, 9–17%, p = 0.08) was observed, complemented by the expansion of a HLA-DRhighPD-L1+ cell population (ICU D = 1.7, 0.7–2.8%; HCs = 0.6, 0.1–0.8%) (**Figure 3B**).

Concerning non-classical monocytes, the most striking feature in all patients from admission was the persistent decline in the frequency of the non-classical monocytes expressing Slan (HCs = 16, 7–25%, No-ICU HA/D = 1.6, 1.3–2.1%, p = 0.002/0.1, 0.1–0.6, p = 0.0009; ICU A/D = 0.4, 0–2, p = 0.0005/0.6, 0.2–0.7, p = 0.001), and the expansion of cells lacking the co-stimulatory molecules CD80 and CD86 at discharge (ICU = 26, 8–30%, HCs = 4, 0.9–9%, p = 0.01) (**Figure 3C**).

Possible associations of relevant circulating myeloid cell populations with clinical variables and circulatory inflammatory or immune-regulatory mediators were evaluated. PD-L1+M2-like classical monocytes (C16) constituted the only population which frequency was positively correlated with the time elapsed from start of the symptoms and from hospital admission (**Figure 4A**). PD-L1+ M2-like classical monocyte cluster percentage was also directly correlated with the anti-SARS-CoV-2 IgM and IgG levels (**Figure 4B**). This finding suggests that specific humoral immunity is developed in parallel with the significant increase of myeloid cell subsets with immunoregulatory phenotype, raising the possibility that the emergence of M2-like phenotype and the development of specific antibodies might be sustained by common mechanisms. Given the previous data on the impact of SARS-CoV-2 on myeloid cell differentiation (10–12), we also sought to evaluate if viremia might be a factor underlying the expansion of PD-L1+ M2-like classical monocytes (C16) and observed that their levels at admission were higher in patients with detectable SARS-CoV-2 viral load (**Figure 4C**). No other cell population was affected by the viremic status of the patients.

Moreover, as displayed in **Figure 4D**, the expansion of PD-L1+ M2-like (C16) and CD163+++M2-like (C15) classical monocytes showed an inverse correlation with the levels of circulating inflammatory cytokines and chemokines related to the IFN pathway (IP-10, CXCL9, IL-12p40). Conversely, the non-classical

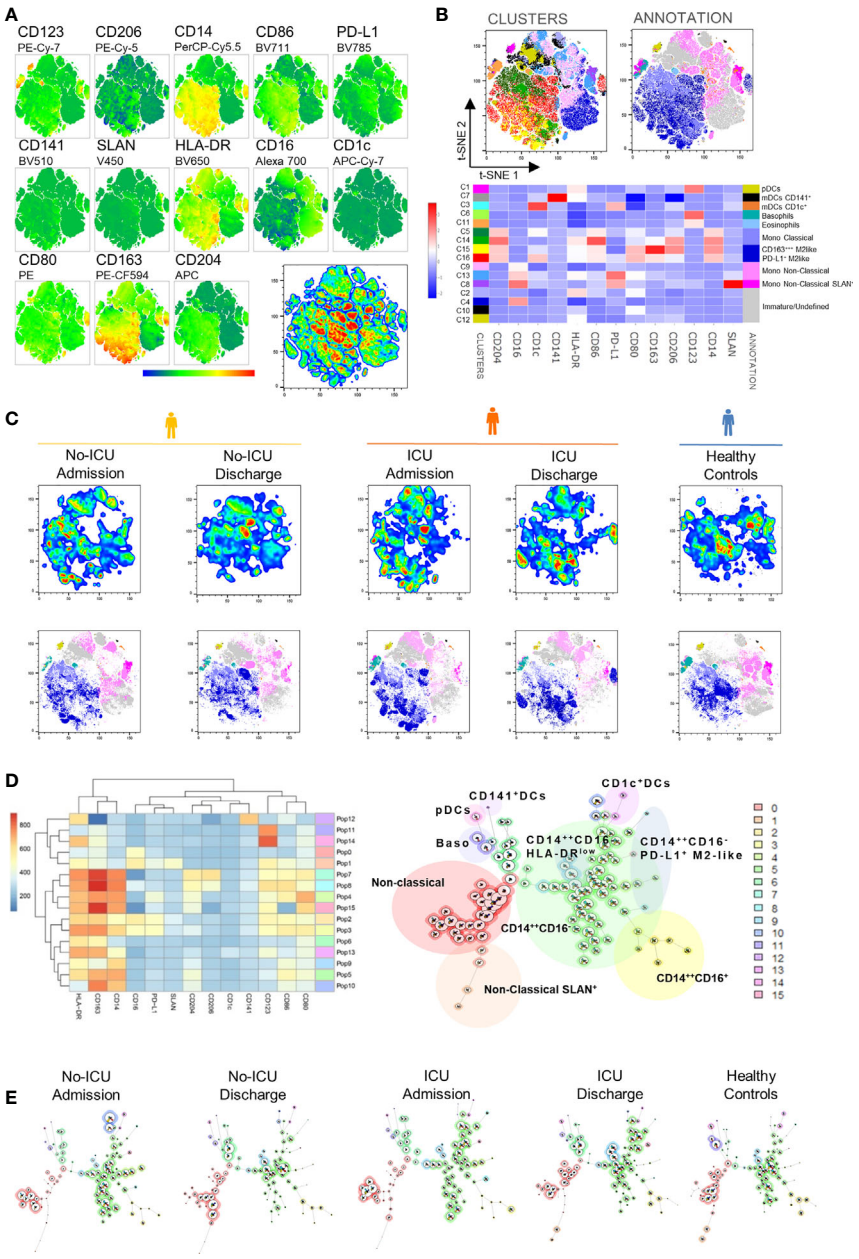

FIGURE 1 | Unsupervised analysis of myeloid cells in COVID-19 patients and healthy controls. **(A)** Dimensionality reduction performed by t-distributed Stochastic Neighbor Embedding (t-SNE) on concatenated CD45+Lin– cells from both time-points and from patient and control groups. Bi-dimensional plots of concatenated samples showing marker distribution. **(B)** Unsupervised clustering performed using X-shift. Bi-dimensional plots showing the 16 clusters obtained (left) and the manual annotation of the clusters (right). Heatmap showing the marker expression in the 16 X-shift clusters. **(C)** Cluster distribution in patients at admission/discharge and in healthy controls. Bi-dimensional plots showing event density using pseudo-color (top) and cluster manual annotation (bottom). **(D)** Unsupervised clustering using FlowSOM. Heatmap showing relative marker expression (left) and self-organizing map with the obtained clusters (right). **(E)** FlowSOM cluster distribution in patients at admission/discharge and in healthy controls. Healthy controls (blue), No-ICU patients (yellow), and ICU patients (orange).

monocyte populations (C8, C9, and C13) declined in parallel with several inflammatory cytokines, being correlated with the levels of MIG-CXCL-9, MCP-2, IFNα2, IFNγ, IL-1α, IP-10, IL-21, and MIP1-β (**Figure 4D**).

Concerning DC subsets, a persistent and marked contraction of pDCs (C1) and CD141+mDCs (C7) was observed in all patients, with a partial recovery at discharge in the No-ICU group (**Figures 5A, B**, respectively, and **Supplementary Table 2**).

A targeted analysis performed by manual gating, confirmed the contraction of all main DC populations (**Supplementary Figure 3**), and revealed a profile remarkably similar to the one observed in the monocyte compartment. Namely, an increase in

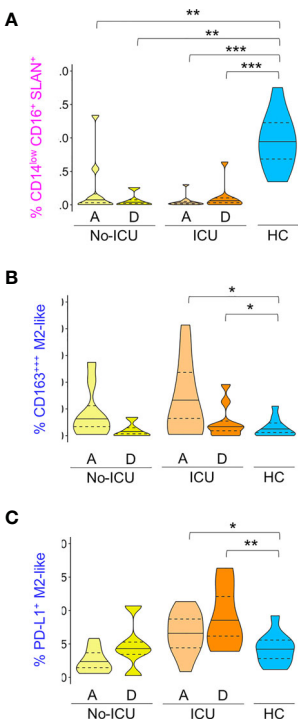

FIGURE 2 | *M2-like and Slan+ monocyte clusters in COVID-19*. Frequency of clusters, manually annotated, identified using X-Shift within total CD45+ Lin– cells: **(A)** In pink: CD14lowCD16+Slan+; **(B)** In dark blue: CD163+++ M2-like; **(C)** In dark blue: PD-L1+M2-like. Comparisons were performed between patient groups and healthy controls using Mann–Whitney U-test. p values are shown as $***p < 0{,}001$; $**p < 0{,}01$; $*p < 0{,}05$. No statistical differences were found between patient groups. ICU, Intensive care unit; A, admission; D, Discharge; HCs, Healthy controls.

the expression of scavenger receptors was observed in both CD141+ mDCs and pDCs from all patients, persisting until discharge in ICU patients (**Figures 5C, D**). ICU patients also featured an increased percentage of HLA-DRhighPD-L1+ cells in both DC populations at discharge, and a significant increase of CD163+ pDCs at ICU admission (**Figures 5C, D**).

If analyzing both patient groups and time points, the frequencies of HLA-DRhighPD-L1+ and CD204+CD206+ cells in pDCs and CD141+mDCs were inversely correlated with analytes related to IFN pathway, as well as to acute phase response proteins and TNF levels (**Figure 5E**), overall confirming the induction of an immune-modulatory signature also in DC sub-populations. No significant changes were reported for CD1c+ mDCs (**Supplementary Figure 4**).

For assessing the circulating cytokine environment, from the 71 inflammatory mediators analyzed, we selected 42 analytes showing significant changes between patients and HCs or within patient groups, or previously reported in literature as central for the hyperinflammatory syndrome pathogenesis (**Supplementary Table 3**) (5). Then, we evaluated using principal component analysis, the most relevant analytes for the segregation of patients from HCs (**Figure 6A**).

Subsequently, combining the analytes with higher loading scores in the principal components with the relevant myeloid cell populations described above, we were able to discriminate the admission and discharge datasets, as well as HCs, using unsupervised hierarchical clustering (**Figure 6B**).

Finally, using volcano plots, we showed that only ICU patients kept at discharge statistically significant increased levels of IL-1RA, IL-10, and IL-6 in comparison with HCs, in parallel with the expansion of myeloid cells expressing M2 markers and PDL-1 (**Figure 6C** and **Supplementary Table 3**).

Notably, in the present cohort, no significant increase was reported for IFN-γ, IL-1α, and IL-1β levels in all patients, in comparison to HCs. Moreover, although not significantly increased at admission, IFN-γ and IL-12p40 showed a negative correlation with time, declining from admission to discharge, in ICU patients (**Figure 6C** and **Supplementary Table 2**).

Altogether, our results show an immune-regulatory profile shift in myeloid cell populations in a cohort of severe patients surviving SARS-CoV-2. Moreover, the evolution towards recovery, in ICU patients, was linked to the expansion of a PD-L1+M2-like classical monocyte and DC subset, in parallel with control of SARS-CoV-2 plasma viral load, development of high titers of specific Ig, and a cytokine signature defined by persistently low IFN-γ, IL1-α, and IL1-β and high IL-1RA and IL10 levels (**Figure 6C**).

DISCUSSION

This longitudinal study revealed systemic immune-regulatory myeloid cell responses in all COVID-19 patients with respiratory insufficiency throughout the path to recovery.

Interestingly, our longitudinal data showed that the myeloid cell subpopulation modifications were associated with significant changes in the balance of pro-inflammatory and immune-regulatory cytokine/chemokine levels, in which low levels of IFN-α2, TNF-α, IL-1α, and IL-1β, decline of IFN-γ and IL-12p40, and persistence of significantly high IL-10, and IL-1RA were main features. Also, the evaluation of patients at admission and recovery allowed us to describe, in those admitted to ICU, the expression of immuno-regulatory elements, especially at discharge, whereas this profile was mainly present at admission to hospital in patients that did not require ICU. These findings support a contribution of the timely acquisition of a myeloid cell immune-regulatory phenotype to the recovery from respiratory insufficiency.

As already described in severe COVID-19, global reduction of pro-inflammatory myeloid cell subsets was observed in all patients in comparison to healthy subjects (10). It appears plausible that blunted type I interferon and IL-1 responses, together with high systemic levels of regulatory cytokines, support the M2-like differentiation observed in our COVID-19 patient cohort.

Circulating monocytes differentiate along a continuous gradient of phenotype states to macrophage-like cells and they are also precursors of myeloid DCs in tissues (19).

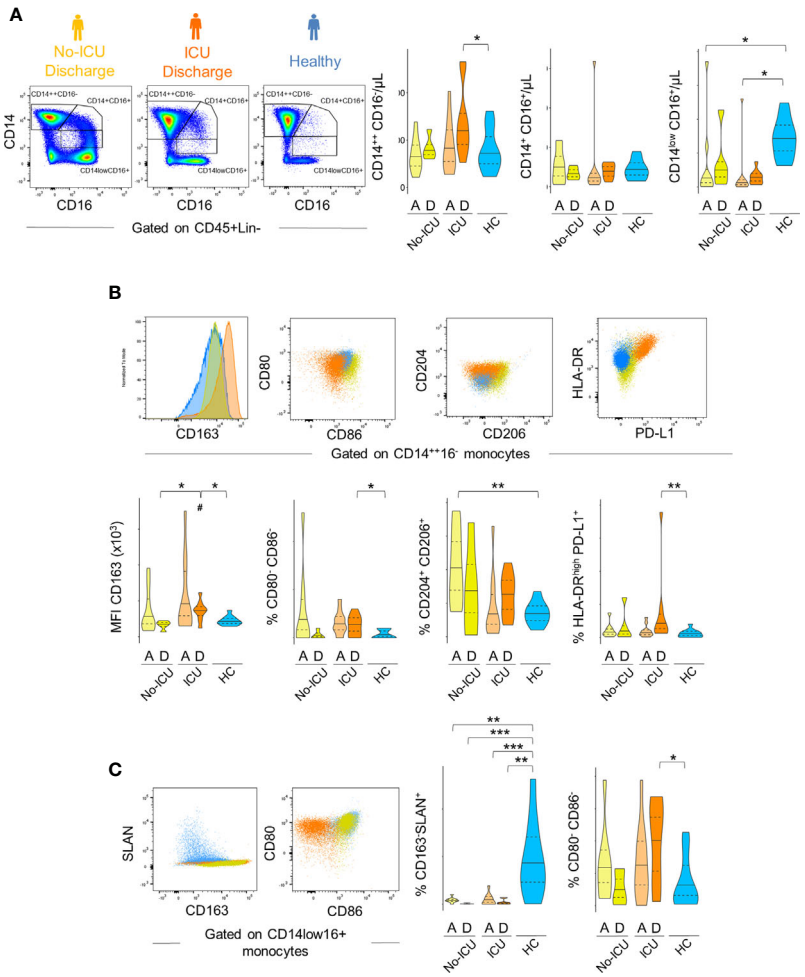

FIGURE 3 | Immune regulatory phenotype of monocytes in severe COVID-19 assessed by bi-dimensional hierarchical gating strategy. **(A–C)** Illustrative dot plots of the analysis performed in a representative No-ICU patient at discharge (yellow) and in an ICU patient at discharge (orange), as well as in a healthy control (blue) are shown; **(A)** Violin graphs show absolute counts of the main monocyte subsets; **(B)** CD163 MFI and proportion of $CD80^{-}CD86^{-}$, $CD204^{+}CD206^{+}$, and HLA-$DR^{high}PD\text{-}L1^{+}$ subsets within classical ($CD14^{++}CD16^{-}$) monocytes; **(C)** Proportion of $CD163^{-}Slan^{+}$ and $CD80^{-}CD86^{-}$ within non-classical ($CD14^{low}CD16^{+}$) monocytes. There were no significant differences between admission and discharge in both ICU and No-ICU patient groups (Wilcoxon matched-pairs signed rank test). Other comparisons were done using Mann–Whitney U-test and significant *P* values are shown: $^{***}p < 0{,}001$; $^{**}p < 0{,}01$; $^{*}p < 0{,}05$, as compared to healthy; $^{\#}p < 0{,}05$, as compared to No-ICU at the same time-point.

Notably, healthy resident alveolar macrophages show an immune-regulatory/M2-like phenotype, favoring the continuous non-inflammatory clearance of pathogens, debris, and apoptotic cells. However they also secrete the cytokines and chemokines that orchestrate the recruitment of inflammatory bone marrow derived cells in the course of infections (20). Regarding myeloid cell phenotype role in viral infection prognosis, a M1-like shift, correlated with secretion of cytokines like IFN-γ, TNF-α, IL-6, and IL-12, both in mucosal associated and in systemic myeloid cells, was considered determinant for worse outcomes in life-threatening viral infection (21, 22). However, viruses, *per se*, can also divert macrophage phenotype towards M2-like, for instance through increasing the production of cytokines like IL-4 or IL-10 (21).

In the context of an acute viral infection, it is particularly remarkable the extreme decline in the Slan+ subset. A very recent paper, performed on hospitalized COVID-19 patients, showed significantly increased sCD163 and sCD14 and a reduction of non-classical monocytes, mDCs and pDCs in COVID-19. However, in this study, the Slan positive population was classified within DCs, while our unbiased flow cytometry data analysis, as well as previous evaluations, performed through genome-wide transcriptional profiling, demonstrated that those cells cluster together with non-classical monocyte population (22–25).

The non-classical monocyte subset was shown to expand in several bacterial and viral infections (26–28). Nevertheless, there are reports of a reduction of this sub-population in viral infections and in inflammatory or auto-immune diseases, where the decrease in circulation was mainly attributed to tissue migration (29–31). Interestingly, inflammasome activation and pyroptotic cell death was described in circulating monocytes from severe COVID-19

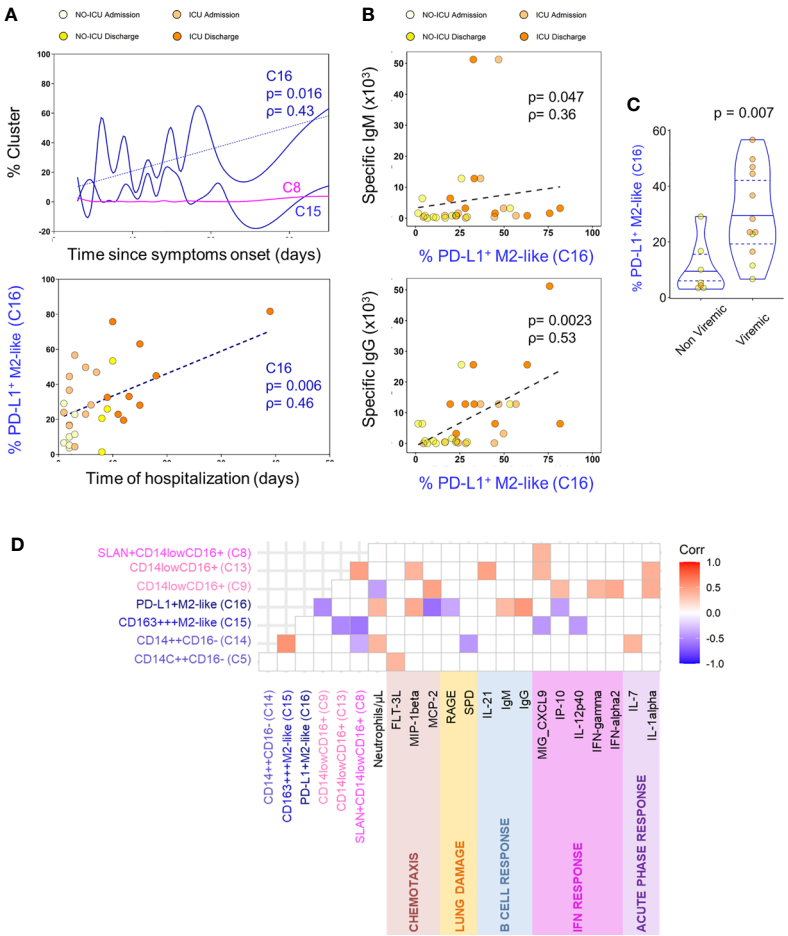

FIGURE 4 | M2-like monocytes expanded until discharge and correlated with the decrease of inflammatory analytes. **(A)** Correlation of indicated cluster frequencies with days since symptoms onset (top) and time of hospitalization (bottom). **(B)** Correlation between PD-L1+M2-like cluster frequency and anti-SARS-CoV-2 specific IgM (top) and IgG (bottom) titers. **(C)** Frequency of PD-L1+M2-like cluster at admission in viremic *versus* non-viremic patients; comparison done using Mann-Whitney U-test and P value are shown. **(D)** Correlation matrix identifying the relation between monocyte X-shift clusters and serum markers with only significant correlations showed (p-value <0.05); Spearman Rank correlation coefficient were used.

patients and non-classical monocytes might be among the first cells to undergo this lytic programmed cell death process, after inflammasome engagement (32).

Importantly, in our prospective cohort of patients surviving severe COVID-19, the significant reduction of Slan+ non-classical monocytes was associated to a contemporaneous general myeloid cell shift towards a M2-like phenotype. Indeed, a similar transition from a pro- to an anti-inflammatory status of human monocytes was described to enhance protective functions like phagocytosis, anti-microbial activity, and tissue remodeling, during sepsis (33).

In a recent *in-vitro* study, it was demonstrated that SARS-CoV-2 infection of monocytes and macrophages is abortive and associated with secretion of IL-10 and TGF-β immunoregulatory cytokines, inducing a transcriptional program characterized by the upregulation of M2 molecules (34).

In addition, a longitudinal study on cytokine and chemokine response signature in severe COVID-19 demonstrated an increase in multiple type 2 effectors, including IL-5, IL-13, IgE, with low expression of pro-inflammatory cytokines and enrichment in tissue repair genes in recovering patients, while higher interferons and pro-inflammatory cytokines and chemokines were observed in patients with worse prognosis (35).

It is relevant that we were able to quantify SARS-CoV-2 plasma viral load in a significant number of patients at admission, particularly in those that required ICU. Moreover, the presence of viral genes was associated with increased IL-10 levels and expansion of the PD-L1+M2-like monocytes, suggesting a role for SARS-CoV-2 viral load in induction of immune-regulatory changes in the innate immune system.

Besides M2-like polarization in myeloid cells, previous data on classical monocytes expressing several scavenger receptors and PD-L1 (PD-L1+M2-like) in viral infections are scarce. Similar subsets have been studied mainly in association with the immune-suppressive effects of neoplastic processes. Interestingly, they are considered to be induced by commensal bacteria with beneficial immunomodulatory properties in

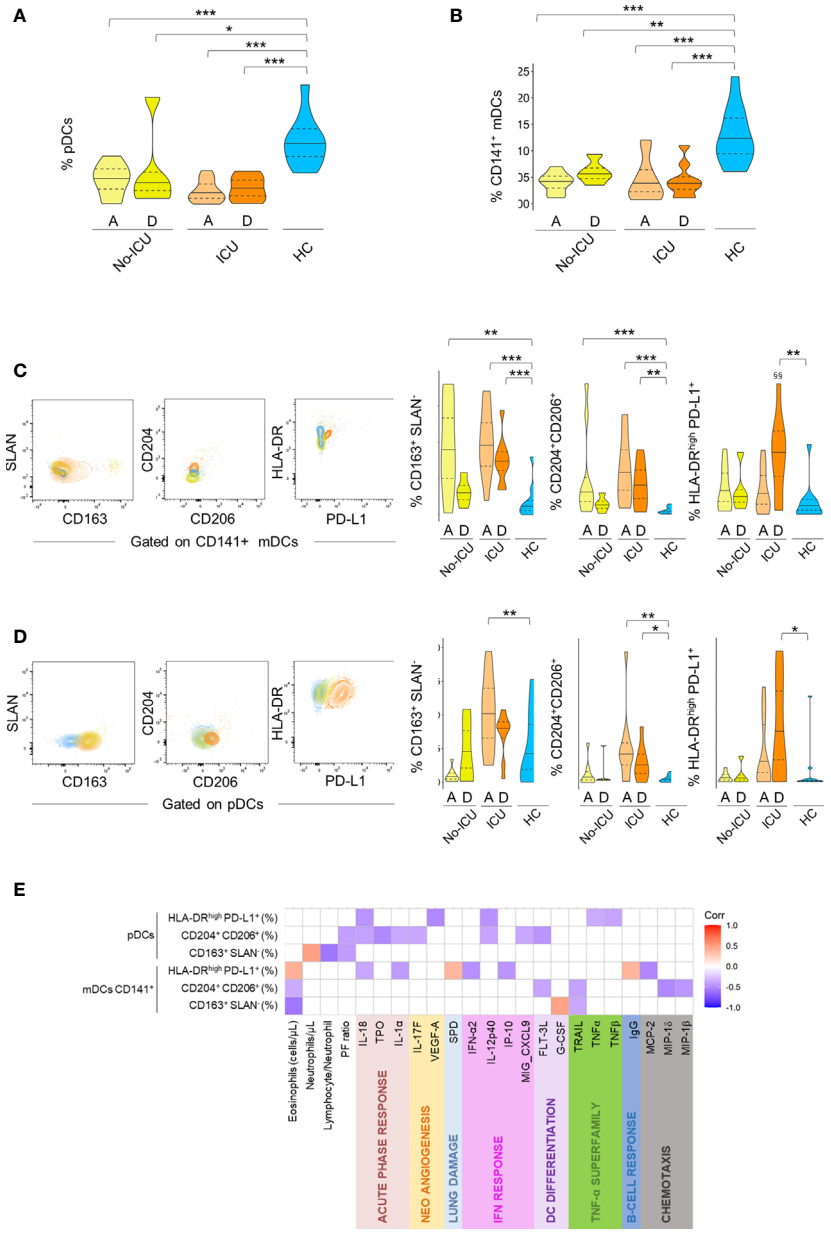

FIGURE 5 | Immune regulatory phenotype of dendritic cells in severe COVID-19. Frequency of pDC cluster **(A)** and CD141+mDC cluster **(B)** identified by X-Shift within total CD45+Lin– cells in the different groups. **(C–D)** Illustrative dot-plots (left) of bi-dimensional hierarchical gating strategy were used to further analyze the phenotype of CD141+mDCs **(C)** and pDCs **(D)** from No-ICU (yellow) and ICU (orange) patients at discharge and healthy control (blue) and the respective graphs (right). Wilcoxon matched-pairs signed rank test to the paired analysis of the two-time points and significant P values are shown: $^{§§}p < 0,01$. Mann–Whitney U-test were used for comparison with healthy controls: $^{***}p < 0,001$; $^{**}p < 0,01$; $^{*}p < 0,05$. **(E)** Correlation matrix identifying relations between frequency of the identified populations within pDCs and CD141+mDCs and serum markers from both time-points and from patient and control groups; Spearman Rank correlation coefficient was used and $p < 0.05$ are showed.

inflammatory diseases (36). Therefore, a favorable role for this particular cell subset in immune-regulation during viral infections should be further assessed.

Alterations attributable to immuno-regulatory/suppressive changes of myeloid cell compartment, such as reduction of HLA-DR or increase of CD163 in classical monocytes, and low levels of non-classical monocytes, were defined as characteristics of the pathogenic mechanism of immune-paralysis (37–40). On the other hand, a hyper-inflammatory syndrome associated with cytokine storm was shown to be linked with critical disease and fatality in severe viral infections such as Ebola, Dengue, or Influenza A H1N1 (41–43). Furthermore, in severe COVID-19, the increase in pro-inflammatory cytokines and chemoattractant proteins was associated with fatal outcome (44–50).

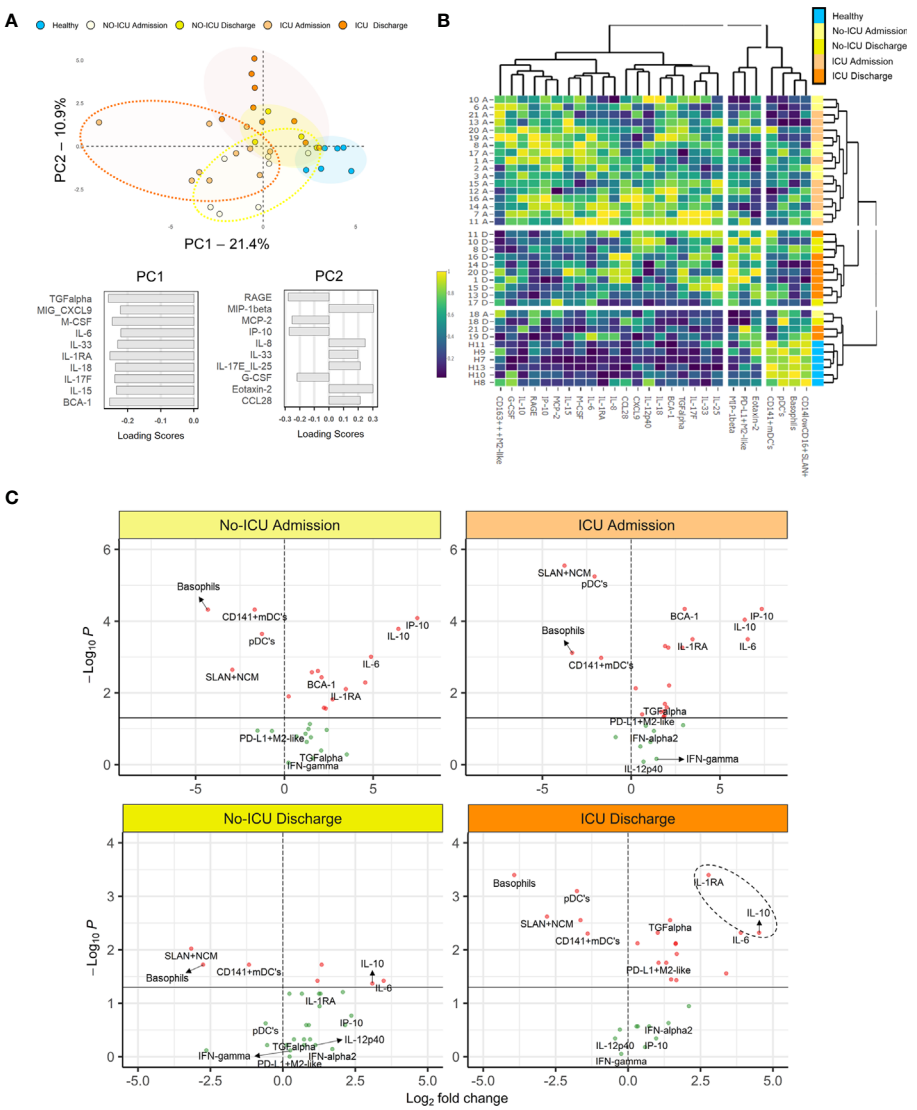

FIGURE 6 | Myeloid cell populations and inflammatory/immunoregulatory serum markers segregate COVID-19 stages. **(A)** Principal component analysis (PCA) of the 35 serum analytes showed to have significant different levels as compared to healthy or between the time-points analyzed; loading scores of principal component (PC)1 and PC2 showing the top 10 highest absolute values. **(B)** Heatmap performed using the top 10 parameters in the PC1 and PC2 of the PCA analysis showed in **(A)** and the frequencies of the X-shift clusters found to be significantly altered in COVID-19 patients; dendrograms illustrate the hierarchical clustering; a color code was added to identify individual groups. **(C)** Volcano plots comparing the variables used in the heatmap showed in **(B)** in patient groups and healthy controls; $p < 0.05$ were considered significant.

SARS-CoV-2 was demonstrated to influence innate immune responses in a complex way, inducing exuberant inflammatory cytokine production associated with weak type I and III IFN responses and reduced IFN stimulated gene (ISG) expression, as previously observed for SARS-CoV-1 and MERS-CoV (51). The function of all the 30 proteins encoded by the SARS-CoV-2 genome was recently studied, demonstrating that several non-structural proteins have a direct suppressive effect on IFN signaling (52).

A highly impaired IFN-α and β response was associated with persistent SARS-CoV-2 viremia and exacerbated inflammation in severe and critically ill patients (53). The importance of a reduced IFN response in SARS-CoV-2 infection was highlighted also by two studies showing that inborn errors of immunity involving IFN type I signaling pathways or auto-antibodies against type I IFNs have increased frequency in patients developing severe and critical disease (54, 55).

Conversely, strong/rapid type I IFN responses and distinctive myeloid cell signatures were described in early, mild, and moderate SARS-CoV-2 infection (11, 12, 56).

Our data supports the idea that IFN response or prophylactic treatment with recombinant IFN can have different roles

depending on the timing: an early and robust increase might be needed for a rapid viral clearance in the initial stage of SARS-CoV-2 infection (57, 58). The present patient cohort might be considered as representative of a late phase, characterized by persistent viral replication, inducing systemic spreading of the virus and high levels of numerous inflammatory mediators. In this disease stage, a coordinated action of low IFNs levels, high immune-regulatory cytokines/decoy receptors and immuno-suppressive/regulatory cell differentiation in circulation, might induce the interruption of the auto-amplifying inflammatory process. Immune-regulatory responses may re-establish an equilibrium in the host-pathogen interaction, favoring recovery from the respiratory insufficiency.

In this context, M2-like myeloid cells could represent potential cellular targets contributing the required negative feedback to the inflammatory response.

At the same time, our data raise concerns regarding evolution towards lung fibrosis in COVID-19, since the expression of M2 phenotype markers in macrophages was associated with pathogenesis of the fibro-proliferative process in lung fibrosis, both idiopathic and associated to auto-immune conditions (59, 60). Although early studies in severe COVID-19 patients linked extended lung fibrosis to the high pressure ventilation-related barotrauma, the last reports under protective ventilation still show presence of fibrotic abnormalities, reduced health-related quality of life, and persistent respiratory symptoms (61). Consequently, long-term studies are necessary for the evaluation of myeloid cell phenotype in circulation, broncoalveolar lavage, and lung tissue, to address the possible persistence of M2 signature and its relationship with long-term sequelae in severe COVID-19.

Some limitation of the study should be noted, mainly related to the relatively small sample size. In agreement with the gender bias in severe COVID-19, few female patients were admitted to hospital at the time of the study, precluding the evaluation of the effect of sex as a variable.

Additionally, it was not possible to evaluate the effect of the treatment, however it has to be considered that numerous severe COVID-19 patients were enrolled before the routine administration of steroids was implemented. In fact, a particular importance has to be given to the possible impact of a treatment with steroids on M2-like phenotype induction. Steroids were demonstrated to influence myeloid cell phenotype both *in-vivo* and *in-vitro* (62, 63). However, the results of those studies are not conclusive, and it was not the purpose of the present research to exclude an impact of immune-regulatory drugs on cell phenotype in patients surviving severe COVID-19. Steroids have been demonstrated to have a positive impact on severe disease outcome, and the induction of a M2-like phenotype in myeloid cells could possibly concur to this therapeutic effect (64). Nevertheless, the development of larger perspective studies, exploring the possible impact of a treatment with steroids on regulatory myeloid cell phenotype induction in recovery from symptomatic COVID-19, would be of critical significance.

Finally, even if high mortality is registered in critically ill COVID-19 patients, only two deaths were observed in the patient cohort, not providing statistical power for the evaluation of a possible effect of innate immune system signature on death rate.

In conclusion, the results of the present study support that severe COVID-19 recovery is associated with timely acquisition of a myeloid cell immune-regulatory phenotype. Consequently, the development and use of therapeutic agents, in addition to glucocorticoids, that would favor the immune-regulatory shift of innate immune system components would be the best strategy at this disease stage.

DATA AVAILABILITY STATEMENT

The raw data supporting the conclusions of this article will be made available by the authors, without undue reservation.

ETHICS STATEMENT

The studies involving human participants were reviewed and approved by the ethics committee at the CHULN/Faculdade de Medicina da Universidade de Lisboa. The patients/participants provided their written informed consent to participate in this study.

AUTHOR CONTRIBUTIONS

ACT, SMF, and AES designed the study. CM and SF enrolled and followed up the patients. ACT, GBF, AMCG, AG-S, PR, CMC, JL, DFS, and ARMA performed the experimental research. AG and MS performed the antibody assays. MV supervised specific antibody titers quantification. ACT and GBF performed the supervised and unsupervised analysis and the statistical analysis. ACT wrote the manuscript. All authors participated to data discussion and manuscript revision. All authors contributed to the article and approved the submitted version.

FUNDING

The Research was funded by Fundação para a Ciência e Tecnologia (FCT), "APOIO ESPECIAL RESEARCH 4COVID-19" projects 803, 125, 231_596873172, and 729. AMCG and GF received fellowships funded by FCT (DOCTORATES4COVID-19, 2020.10202.BD), and JANSSEN- CILAG FARMACÊUTICA, respectively. The funder was not involved in the study design, collection, analysis, interpretation of data, writing of the article or decision to submit it for publication. MV was supported by the European Union H2020 ERA project (No 667824 – EXCELLtoINNOV). This project has received funding from the European Union's Horizon 2020 research and innovation programme under grant agreement No 667824.

ACKNOWLEDGMENTS

We wish to acknowledge Ines Neiva, BSc and Alexandre Raposo, PhD, for their help for data analysis. Also we thank all the participating patients and clinicians.

SUPPLEMENTARY MATERIAL

The Supplementary Material for this article can be found online at: https://www.frontiersin.org/articles/10.3389/fimmu.2021.691725/full#supplementary-material

REFERENCES

1. Available at: https://covid19.who.int (Accessed March 19, 2021).
2. Guan WJ, Ni ZY, Hu Y, Liang WH, Ou CQ, He JX, et al. Clinical Characteristics of Coronavirus Disease 2019 in China. *N Engl J Med* (2020) 382(18):1708–20. doi: 10.1056/NEJMoa2002032
3. Cron RQ, Chatham WW. The Rheumatologist's Role in COVID-19. *J Rheumatol* (2020) 47:639–42. doi: 10.3899/jrheum.200334
4. Available at: https://clinicaltrials.gov/ct2/show/NCT04747574 (Accessed March 19, 2021).
5. Fajgenbaum DC, June CH. Cytokine Storm. *N Engl J Med* (2020) 383 (23):2255–73. doi: 10.1056/NEJMra2026131
6. Lee JS, Park S, Jeong HW, Ahn JY, Choi SJ, Lee H, et al. Immunophenotyping of COVID-19 and Influenza Highlights the Role of Type I Interferons in Development of Severe COVID-19. *Sci Immunol* (2020) 5(49):eabd1554. doi: 10.1126/sciimmunol.abd1554
7. Booz GW, Altara R, Eid AH, Wehbe Z, Fares S, Zaraket H, et al. Macrophage Responses Associated With COVID-19: A Pharmacological Perspective. *Eur J Pharmacol* (2020) 887:173547. doi: 10.1016/j.ejphar.2020.173547
8. Zhang D, Guo R, Lei L, Liu H, Wang Y, Wang Y, et al. Frontline Science: Covid-19 Infection Induces Readily Detectable Morphologic and Inflammation-Related Phenotypic Changes in Peripheral Blood Monocytes. *J Leukoc Biol* (2021) 109(1):13–22. doi: 10.1002/JLB.4HI0720-470R
9. Peruzzi B, Bencini S, Capone M, Mazzoni A, Maggi L, Salvati L, et al. Quantitative and Qualitative Alterations of Circulating Myeloid Cells and Plasmacytoid DC in SARS-CoV-2 Infection. *Immunology* (2020) 161(4):345–53. doi: 10.1111/imm.13254
10. Zhou R, To KK, Wong YC, Liu L, Zhou B, Li X, et al. Acute SARS-CoV-2 Infection Impairs Dendritic Cell and T Cell Responses. *Immunity* (2020) 53 (4):864–877.e5. doi: 10.1016/j.immuni.2020.07.026
11. Schulte-Schrepping J, Reusch N, Paclik D, Baßler K, Schlickeiser S, Zhang B, et al. Severe COVID-19 is Marked by a Dysregulated Myeloid Cell Compartment. *Cell* (2020) 182(6):1419–1440.e23. doi: 10.1016/j.cell.2020.08.001
12. Silvin A, Chapuis N, Dunsmore G, Goubet AG, Dubuisson A, Derosa L, et al. Elevated Calprotectin and Abnormal Myeloid Cell Subsets Discriminate Severe From Mild Covid-19. *Cell* (2020) 182(6):1401–18.e18. doi: 10.1016/j.cell.2020.08.002
13. Krasselt M, Baerwald C, Wagner U, Rossol M. CD56+ Monocytes Have a Dysregulated Cytokine Response to Lipopolysaccharide and Accumulate in Rheumatoid Arthritis and Immunosenescence. *Arthritis Res Ther* (2013) 15 (5):R139. doi: 10.1186/ar4321
14. Samusik N, Good Z, Spitzer MH, Davis KL, Nolan GP. Automated Mapping of Phenotype Space With Single-Cell Data. *Nat Methods* (2016) 13(6):493–6. doi: 10.1038/nmeth.3863
15. Van Gassen S, Callebaut B, Van Helden MJ, Lambrecht BN, Demeester P, Dhaene T, et al. Flowsom: Using Self-Organizing Maps for Visualization and Interpretation of Cytometry Data. *Cytometry A* (2015) 87(7):636–45. doi: 10.1002/cyto.a.22625
16. Ziegler-Heitbrock L, Hofer TP. Toward a Refined Definition of Monocyte Subsets. *Front Immunol* (2013) 4:23. doi: 10.3389/fimmu.2013.00023
17. Zawada AM, Fell LH, Untersteller K, Seiler S, Rogacev KS, Fliser D, et al. Comparison of Two Different Strategies for Human Monocyte Subsets Gating Within the Large-Scale Prospective CARE for HOMe Study. *Cytometry A* (2015) 87(8):750–8. doi: 10.1002/cyto.a.22703
18. Figueiredo-Campos P, Blankenhaus B, Mota C, Gomes A, Serrano M, Ariotti S, et al. Seroprevalence of anti-SARS-CoV-2 Antibodies in COVID-19 Patients and Healthy Volunteers Up to 6 Months Post Disease Onset. *Eur J Immunol* (2020) 50(12):2025–40. doi: 10.1002/eji.202048970
19. Specht H, Emmott E, Petelski AA, Huffman RG, Perlman DH, Serra M, et al. Single-Cell Proteomic and Transcriptomic Analysis of Macrophage Heterogeneity Using Scope2. *Genome Biol* (2021) 22(1):50. doi: 10.1186/s13059-021-02267-5
20. Guilliams M, Svedberg FR. Does Tissue Imprinting Restrict Macrophage Plasticity? *Nat Immunol* (2021) 22(2):118–27. doi: 10.1038/s41590-020-00849-2
21. Rojas JM, Avia M, Martín V, Sevilla N. Il-10: A Multifunctional Cytokine in Viral Infections. *J Immunol Res* (2017) 2017:6104054. doi: 10.1155/2017/6104054
22. Cole SL, Dunning J, Kok WL, Benam KH, Benlahrech A, Repapi E, et al. M1-Like Monocytes are a Major Immunological Determinant of Severity in Previously Healthy Adults With Life-Threatening Influenza. *JCI Insight* (2017) 2(7):e91868. doi: 10.1172/jci.insight.91868
23. Zingaropoli MA, Nijhawan P, Carraro A, Pasculli P, Zuccalà P, Perri V, et al. Increased sCD163 and Scd14 Plasmatic Levels and Depletion of Peripheral Blood Pro-Inflammatory Monocytes, Myeloid and Plasmacytoid Dendritic Cells in Patients With Severe Covid-19 Pneumonia. *Front Immunol* (2021) 12:627548. doi: 10.3389/fimmu.2021.627548
24. van Leeuwen-Kerkhoff N, Lundberg K, Westers TM, Kordasti S, Bontkes HJ, de Gruijl TD, et al. Transcriptional Profiling Reveals Functional Dichotomy Between Human Slan+ non-Classical Monocytes and Myeloid Dendritic Cells. *J Leukoc Biol* (2017) 102(4):1055–68. doi: 10.1189/jlb.3MA0117-037R
25. Hofer TP, van de Loosdrecht AA, Stahl-Hennig C, Cassatella MA, Ziegler-Heitbrock L. 6-Sulfo LacNAc (Slan) as a Marker for Non-classical Monocytes. *Front Immunol* (2019) 10:2052. doi: 10.3389/fimmu.2019.02052
26. Wang Z, Yang L, Ye J, Wang Y, Liu Y. Monocyte Subsets Study in Children With Mycoplasma Pneumoniae Pneumonia. *Immunol Res* (2019) 67(4-5):373–81. doi: 10.1007/s12026-019-09096-6
27. Thieblemont N, Weiss L, Sadeghi HM, Estcourt C, Haeffner-Cavaillon N. Cd14lowCD16high: A Cytokine-Producing Monocyte Subset Which Expands During Human Immunodeficiency Virus Infection. *Eur J Immunol* (1995) 25:3418–24. doi: 10.1002/eji.1830251232
28. Naim E, Paukovics G, Hocking J, Heinlein AC, Maslin CL, Sonza S, et al. Normal CD16 Expression and Phagocytosis of Mycobacterium Avium Complex by Monocytes From a Current Cohort of HIV-1–infected Patients. *J Infect Dis* (2006) 193:693–7. doi: 10.1086/500367
29. Naranjo-Gómez JS, Castillo JA, Rojas M, Restrepo BN, Diaz FJ, Velilla PA, et al. Different Phenotypes of non-Classical Monocytes Associated With Systemic Inflammation, Endothelial Alteration and Hepatic Compromise in Patients With Dengue. *Immunology* (2019) 156(2):147–63. doi: 10.1111/imm.13011
30. Tacke F, Alvarez D, Kaplan TJ, Jakubzick C, Spanbroek R, Llodra J, et al. Monocyte Subsets Differentially Employ CCR2, CCR5, and CX3CR1 to Accumulate Within Atherosclerotic Plaques. *J Clin Investig* (2007) 117:185–94. doi: 10.1172/JCI28549
31. Yoshimoto S, Nakatani K, Iwano M, Asai O, Samejima K, Sakan H, et al. Elevated Levels of Fractalkine Expression and Accumulation of CD16+ Monocytes in Glomeruli of Active Lupus Nephritis. *Am J Kidney Dis* (2007) 50:47–58. doi: 10.1053/j.ajkd.2007.04.012
32. Ferreira AC, Soares VC, de Azevedo-Quintanilha IG, Dias SDSG, Fintelman-Rodrigues N, Sacramento CQ, et al. Sars-CoV-2 Engages Inflammasome and Pyroptosis in Human Primary Monocytes. *Cell Death Discovery* (2021) 7 (1):43. doi: 10.1038/s41420-021-00428-w
33. Shalova IN, Lim JY, Chittezhath M, Zinkernagel AS, Beasley F, Hernández-Jiménez E, et al. Human Monocytes Undergo Functional Re-Programming During Sepsis Mediated by Hypoxia-Inducible Factor-1α. *Immunity* (2015) 42(3):484–98. doi: 10.1016/j.immuni.2015.02.001
34. Boumaza A, Gay L, Mezouar S, Bestion E, Diallo AB, Michel M, et al. Monocytes and Macrophages, Targets of SARS-CoV-2: The Clue for Covid-19 Immunoparalysis. *J Infect Dis* (2021) jiab044. doi: 10.1093/infdis/jiab044
35. Lucas C, Wong P, Klein J, Castro TBR, Silva J, Sundaram M, et al. Longitudinal Analyses Reveal Immunological Misfiring in Severe COVID-19. *Nature* (2020) 584(7821):463–9. doi: 10.1038/s41586-020-2588-y
36. Paynich ML, Jones-Burrage SE, Knight KL. Exopolysaccharide From Bacillus Subtilis Induces Anti-Inflammatory M2 Macrophages That Prevent T Cell-

Mediated Disease. *J Immunol* (2017) 198(7):2689–98. doi: 10.4049/jimmunol.1601641
37. Giamarellos-Bourboulis EJ, Netea MG, Rovina N, Akinosoglou K, Antoniadou A, Antonakos N, et al. Complex Immune Dysregulation in COVID-19 Patients With Severe Respiratory Failure. *Cell Host Microbe* (2020) 27(6):992–1000.e3. doi: 10.1016/j.chom.2020.04.009
38. Gatti A, Radrizzani D, Viganò P, Mazzone A, Brando B. Decrease of Non-Classical and Intermediate Monocyte Subsets in Severe Acute SARS-CoV-2 Infection. *Cytometry A* (2020) 97(9):887–90. doi: 10.1002/cyto.a.24188
39. Channappanavar R, Fehr AR, Vijay R, Mack M, Zhao J, Meyerholz DK, et al. Dysregulated Type I Interferon and Inflammatory Monocyte-Macrophage Responses Cause Lethal Pneumonia in SARS-CoV-infected Mice. *Cell Host Microbe* (2016) 19(2):181–93. doi: 10.1016/j.chom.2016.01.007
40. Sánchez-Cerrillo I, Landete P, Aldave B, Sánchez-Alonso S, Sánchez-Azofra A, Marcos-Jiménez A, et al. Covid-19 Severity Associates With Pulmonary Redistribution of CD1c+ Dcs and Inflammatory Transitional and Nonclassical Monocytes. *J Clin Invest* (2020) 130(12):6290–300. doi: 10.1172/JCI140335
41. Younan P, Iampietro M, Nishida A, Ramanathan P, Santos RI, Dutta M, et al. Ebola Virus Binding to Tim-1 on T Lymphocytes Induces a Cytokine Storm. *mBio* (2017) 8(5):e00845–17. doi: 10.1128/mBio.00845-17
42. Srikiatkhachorn A, Mathew A, Rothman AL. Immune-Mediated Cytokine Storm and its Role in Severe Dengue. *Semin Immunopathol* (2017) 39(5):563–74. doi: 10.1007/s00281-017-0625-1
43. Gao R, Bhatnagar J, Blau DM, Greer P, Rollin DC, Denison AM, et al. Cytokine and Chemokine Profiles in Lung Tissues From Fatal Cases of 2009 Pandemic Influenza A (H1N1): Role of the Host Immune Response in Pathogenesis. *Am J Pathol* (2013) 183(4):1258–68. doi: 10.1016/j.ajpath.2013.06.023
44. Huang C, Wang Y, Li X, Ren L, Zhao J, Hu Y, et al. Clinical Features of Patients Infected With 2019 Novel Coronavirus in Wuhan, China. *Lancet* (2020) 395:497–506. doi: 10.1016/S0140-6736(20)30183-5
45. Chen G, Wu D, Guo W, Cao Y, Huang D, Wang H, et al. Clinical and Immunological Features of Severe and Moderate Coronavirus Disease 2019. *J Clin Invest* (2020) 130:2620–9. doi: 10.1172/JCI137244
46. Gong J, Dong H, Xia SQ, Huang YZ, Wang D, Zhao Y, et al. Correlation Analysis Between Disease Severity and Inflammation-related Parameters in Patients With COVID-19 Pneumonia. *medRxiv* (2020) 20(1):963. doi: 10.1186/s12879-020-05681-5
47. Zhou F, Yu T, Du R, Fan G, Liu Y, Liu Z, et al. Clinical Course and Risk Factors for Mortality of Adult Inpatients With COVID-19 in Wuhan, China: A Retrospective Cohort Study. *Lancet* (2020) 395:1054–62. doi: 10.1016/S0140-6736(20)30566-3
48. Ruan Q, Yang K, Wang W, Jiang L, Song J. Clinical Predictors of Mortality Due to COVID-19 Based on an Analysis of Data of 150 Patients From Wuhan, China. *Intensive Care Med* (2020) 46:846–8. doi: 10.1007/s00134-020-05991-x
49. Merad M, Martin JC. Pathological Inflammation in Patients With COVID-19: A Key Role for Monocytes and Macrophages. *Nat Rev Immunol* (2020) 20:355–62. doi: 10.1038/s41577-020-0331-4
50. Li H, Liu L, Zhang D, Dai H, Tang N, Su X, et al. Sars-CoV-2 and Viral Sepsis: Observations and Hypotheses. *Lancet* (2020) 395:1517–20. doi: 10.1016/S0140-6736(20)30920-X
51. Blanco-Melo D, Nilsson-Payant BE, Liu WC, Uhl S, Hoagland D, Møller R, et al. Imbalanced Host Response to SARS-CoV-2 Drives Development of COVID-19. *Cell* (2020) 181(5):1036–1045.e9. doi: 10.1016/j.cell.2020.04.026
52. Thoms M, Buschauer R, Ameismeier M, Koepke L, Denk T, Hirschenberger M, et al. Structural Basis for Translational Shutdown and Immune Evasion by the Nsp1 Protein of SARS-Cov-2. *Science* (2020) 369(6508):1249–55. doi: 10.1126/science.abc8665
53. Hadjadj J, Yatim N, Barnabei L, Corneau A, Boussier J, Smith N, et al. Impaired Type I Interferon Activity and Inflammatory Responses in Severe COVID-19 Patients. *Science* (2020) 369(6504):718–24. doi: 10.1126/science.abc6027
54. Zhang Q, Bastard P, Liu Z, Le Pen J, Moncada-Velez M, Chen J, et al. Inborn Errors of Type I IFN Immunity in Patients With Life-Threatening COVID-19. *Science* (2020) 370(6515):eabd4570. doi: 10.1126/science.abd4570
55. Bastard P, Rosen LB, Zhang Q, Michailidis E, Hoffmann HH, Zhang Y, et al. Autoantibodies Against Type I Ifns in Patients With Life-Threatening COVID-19. *Science* (2020) 370(6515):eabd4585. doi: 10.1126/science.abd4585
56. Jamilloux Y, Henry T, Belot A, Viel S, Fauter M, El Jammal T, et al. Should We Stimulate or Suppress Immune Responses in COVID-19? Cytokine and Anti-Cytokine Interventions. *Autoimmun Rev* (2020) 19(7):102567. doi: 10.1016/j.autrev.2020.102567
57. King C, Sprent J. Dual Nature of Type I Interferons in SARS-CoV-2-Induced Inflammation. *Trends Immunol* (2021) S1471-4906(21):00027–2. doi: 10.1016/j.it.2021.02.003
58. Park A, Iwasaki A. Type I and Type Iii Interferons - Induction, Signaling, Evasion, and Application to Combat Covid-19. *Cell Host Microbe* (2020) 27(6):870–8. doi: 10.1016/j.chom.2020.05.008
59. Hou J, Shi J, Chen L, Lv Z, Chen X, Cao H, et al. M2 Macrophages Promote Myofibroblast Differentiation of LR-MSCs and are Associated With Pulmonary Fibrogenesis. *Cell Commun Signal* (2018) 16(1):89. doi: 10.1186/s12964-018-0300-8
60. Trombetta AC, Soldano S, Contini P, Tomatis V, Ruaro B, Paolino S, et al. A Circulating Cell Population Showing Both M1 and M2 Monocyte/Macrophage Surface Markers Characterizes Systemic Sclerosis Patients With Lung Involvement. *Respir Res* (2018) 19(1):186. doi: 10.1186/s12931-018-0891-z
61. Lindén VB, Lidegran MK, Frisén G, Dahlgren P, Frenckner BP, Larsen F. ECMO in ARDS: A Long-Term Follow-Up Study Regarding Pulmonary Morphology and Function and Health-Related Quality of Life. *Acta Anaesthesiol Scand* (2009) 53(4):489–95. doi: 10.1111/j.1399-6576.2008.01808.x
62. Liu B, Dhanda A, Hirani S, Williams EL, Sen HN, Martinez Estrada F, et al. Cd14++Cd16+ Monocytes are Enriched by Glucocorticoid Treatment and Are Functionally Attenuated in Driving Effector T Cell Responses. *J Immunol* (2015) 194(11):5150–60. doi: 10.4049/jimmunol
63. Zwadlo-Klarwasser G, Schmutzler W. The Effects of the Glucocorticoids Prednisolone, Deflazacort and Beclomethasone-Dipropionate on the RM 3/1 Macrophage in Human Peripheral Blood. *Skin Pharmacol Appl Skin Physiol* (1998) 11(4-5):227–31. doi: 10.1159/000029831
64. WHO and Rapid Evidence Appraisal for COVID-19 Therapies (REACT) Working Group, Sterne JAC, Murthy S, Diaz JV, Slutsky AS, et al. Association Between Administration of Systemic Corticosteroids and Mortality Among Critically Ill Patients With Covid-19: A Meta-Analysis. *JAMA* (2020) 324(13):1330–41. doi: 10.1001/jama.2020.17023

Conflict of Interest: The authors declare that the research was conducted in the absence of any commercial or financial relationships that could be construed as a potential conflict of interest.

frontiers in Immunology

ORIGINAL RESEARCH
published: 17 March 2022
doi: 10.3389/fimmu.2022.851497

Plasma Markers of Neutrophil Extracellular Trap Are Linked to Survival but Not to Pulmonary Embolism in COVID-19-Related ARDS Patients

Renaud Prével[1,2†], Annabelle Dupont[3†], Sylvie Labrouche-Colomer[4,5], Geoffrey Garcia[6], Antoine Dewitte[7,8], Antoine Rauch[3], Julien Goutay[9], Morgan Caplan[9], Elsa Jozefowicz[10], Jean-Philippe Lanoix[11,12], Julien Poissy[13], Etienne Rivière[4,14], Arthur Orieux[1], Denis Malvy[15], Didier Gruson[1,2], Loic Garçon[6], Sophie Susen[3] and Chloé James[4,5]*

[1] CHU Bordeaux, Medical Intensive Care Unit, Pessac, France, [2] Univ. Bordeaux, INSERM, U1045, Centre de Recherche Cardio-Thoracique de Bordeaux, Pessac, France, [3] Univ. Lille, INSERM, CHU Lille, Department of Hematology and Transfusion, Pôle de Biologie Pathologie Génétique, Institut Pasteur de Lille, UMR1011-EGID, Lille, France, [4] Univ. Bordeaux, INSERM, UMR1034, Biology of Cardiovascular Diseases, Pessac, France, [5] CHU Bordeaux, Laboratory of Hematology, Pessac, France, [6] Laboratoire d'Hématologie, CHU Amiens, EA4666 HEMATIM, UPJV, Amiens, France, [7] CHU Bordeaux, Department of Anaesthesia and Critical Care, Magellan Medico-Surgical Centre, Bordeaux, France, [8] Univ. Bordeaux, CNRS, UMR 5164, INSERM ERL1303, Immunology from Concept and Experiments to Translation (ImmunoConcEpT), Bordeaux, France, [9] Centre Hospitalier Universitaire Lille, Intensive Care Department, Pôle de Réanimation, Lille, France, [10] Centre Hospitalier Universitaire Lille, Surgical Critical Care, Department of Anesthesiology and Critical Care, Lille, France, [11] CHU Amiens-Picardie, Infectious Diseases Department, Amiens, France, [12] EA4294, Université Picardie Jules Verne, Amiens, France, [13] Univ. Lille, INSERM U1285, CHU Lille, Pôle de réanimation, CNRS, UMR 8576-UGSF-Unité de Glycobiologie Structurale et Fonctionnelle, Lille, France, [14] CHU Bordeaux, Internal Medicine and Infectious Diseases Unit, Pessac, France, [15] Department for Infectious and Tropical diseases, University Hospital Centre and INSERM 1219, University of Bordeaux, Bordeaux, France

OPEN ACCESS

Edited by:
Georges Michel Verjans,
Erasmus Medical Center, Netherlands

Reviewed by:
Werner Ouwendijk,
Erasmus Medical Center, Netherlands
Jessica G. Moreland,
University of Texas Southwestern Medical Center, United States

***Correspondence:**
Chloé James
chloe.james@inserm.fr

[†]These authors have contributed equally to this work

Specialty section:
This article was submitted to Viral Immunology, a section of the journal Frontiers in Immunology

Received: 11 January 2022
Accepted: 23 February 2022
Published: 17 March 2022

Citation:
Prével R, Dupont A, Labrouche-Colomer S, Garcia G, Dewitte A, Rauch A, Goutay J, Caplan M, Jozefowicz E, Lanoix J-P, Poissy J, Rivière E, Orieux A, Malvy D, Gruson D, Garçon L, Susen S and James C (2022) Plasma Markers of Neutrophil Extracellular Trap Are Linked to Survival but Not to Pulmonary Embolism in COVID-19-Related ARDS Patients. Front. Immunol. 13:851497. doi: 10.3389/fimmu.2022.851497

Introduction: Coronavirus disease 2019 (COVID-19) can cause life-threatening acute respiratory distress syndrome (ARDS). Recent data suggest a role for neutrophil extracellular traps (NETs) in COVID-19-related lung damage partly due to microthrombus formation. Besides, pulmonary embolism (PE) is frequent in severe COVID-19 patients, suggesting that immunothrombosis could also be responsible for increased PE occurrence in these patients. Here, we evaluate whether plasma levels of NET markers measured shorty after admission of hospitalized COVID-19 patients are associated with clinical outcomes in terms of clinical worsening, survival, and PE occurrence.

Patients and Methods: Ninety-six hospitalized COVID-19 patients were included, 50 with ARDS (severe disease) and 46 with moderate disease. We collected plasma early after admission and measured 3 NET markers: total DNA, myeloperoxidase (MPO)–DNA complexes, and citrullinated histone H3. Comparisons between survivors and non-survivors and patients developing PE and those not developing PE were assessed by Mann–Whitney test.

Results: Analysis in the whole population of hospitalized COVID-19 patients revealed increased circulating biomarkers of NETs in patients who will die from COVID-19 and in patients who will subsequently develop PE. Restriction of our analysis in the most severe

patients, i.e., the ones who enter the hospital for COVID-19-related ARDS, confirmed the link between NET biomarker levels and survival but not PE occurrence.

Conclusion: Our results strongly reinforce the hypothesis that NETosis is an attractive therapeutic target to prevent COVID-19 progression but that it does not seem to be linked to PE occurrence in patients hospitalized with COVID-19.

Keywords: neutrophil extracellular trap, acute respiratory distress syndrome, COVID-19, immunothrombosis, pulmonary embolism

INTRODUCTION

Coronavirus disease 2019 (COVID-19) is responsible for more than 4,550,00 deaths worldwide at the beginning of September 2021 according to the World Health Organization (WHO). The vast majority of the infected people have subclinical to moderate forms, but some of them develop respiratory failure with acute respiratory distress syndrome (ARDS) (1). *Postmortem* histological analysis from COVID-19-related ARDS non-survivor patients exhibited vascular microthrombi in lung capillaries that participate in lung damage (2). Moreover, about 20% of critically ill COVID-19 patients develop pulmonary embolism (PE), which can aggravate their pulmonary condition and impair oxygenation because of shunt effect (3). Immunothrombosis is a physiological innate immune response that leads to formation of thrombi inside blood vessels in order to contain and destroy pathogens such as bacteria, fungi, and viruses (4). It involves neutrophils, monocytes, platelets, and activation of hemostasis. Activation of neutrophils by pathogens causes the emission of neutrophil extracellular traps (NETs) that are DNA fragments decorated with proteins of neutrophil origin such as myeloperoxidase (MPO) (5). When uncontrolled, immunothrombosis becomes detrimental to the host. As NETs are procoagulant (6, 7) and cytotoxic for lung vascular endothelial cells (8, 9), increased NETosis has been found to participate in various pathological processes such as arterial and venous thrombosis (6), ARDS (10), and other critical conditions not linked to COVID-19 (11).

It is now well-admitted that circulating markers of NET formation are associated with COVID-19 severity (12–14). Whether measurement of NET biomarkers early after admission for COVID-19 can be of prognostic value is a major question, as it would strengthen the rationale to target NETs and may help in clinical decision-making. The aim of this study is thus to evaluate whether plasma levels of NET markers measured shorty after admission of hospitalized COVID-19 patients are associated with clinical outcomes in terms of clinical worsening, survival, and PE occurrence.

PATIENTS AND METHODS

Study Design and Participants

A prospective observational study was conducted in 3 French university hospitals from April to July 2020. We enrolled all patients with laboratory-confirmed COVID-19 admitted to conventional hospitalization ward (moderate, i.e., non-ARDS patients) and patients admitted to intensive care unit (ICU) for COVID-19-related ARDS (critical illness) defined according to National Institutes of Health treatment guidelines (15) with available samples. ARDS was defined according to Berlin's criteria (16), and criteria for admission to ICU were persistence of SpO_2 <92% and/or clinical respiratory failure despite conventional oxygen therapy. All ARDS patients required high-flow nasal cannula oxygen (flow between 30 and 60 L/min) or mechanical ventilation. Patients could only be included in the moderate or ARDS group for the subgroup analyses according to their clinical condition at admission to hospital. COVID-19 was defined as a positive result of real-time reverse transcriptase–polymerase chain reaction (RT-PCR) on nasal and pharyngeal swabs according to the WHO guidance. All patients received prophylactic heparin treatment according to the Groupe Français d'étude sur l'Hémostase et la Thrombose (GFHT) / Groupe d'Intérêt en Hémostase Périoperatoire (GIHP) proposals (17) or therapeutic treatment if indicated by their comorbidities, but patients with PE at the time of sampling were not included. PE was diagnosed by computerized tomography angiography performed at clinician's discretion according to routine care. Routine criteria for receiving a computerized tomography angiogram in patients with ARDS were hypoxemia not improving with positive end-expiratory pressure titration or PaO_2 worsening without lung compliance impairment or elevation of right heart pressure without lung compliance worsening. Ten non-hospitalized, non-COVID-19, healthy participants with no history of thromboembolic events, hemorrhagic events, or pneumonia were included as a control reference group.

Data Collection

Data were prospectively recorded by physicians in charge of the patient by questioning the patients, patients' family, and patients' general practitioners. Electronic worksheet was completed by physicians caring for the patients.

Sample Collection

Samples were collected early after admission to hospital for moderate COVID-19 patients and at admission to ICU for ARDS patients. Both non-ICU COVID-19 patients and COVID-19 ARDS patients were included at direct admission or after a short (<12 h) stay in the emergency room. It implies that hospitalized patients who were further admitted to ICU were not included again in the ARDS patient group. Plasma samples

were prepared from citrated blood after two 10-min centrifugations at 2,500g and stored at -80°C.

Quantification of Plasmatic Cell-Free DNA

The Quant-it™ PicoGreen assay kit (Invitrogen, San Diego, CA, USA) was used to quantify circulating cell-free double-strand DNA according to manufacturer's instructions. Fluorescence intensity was measured using a microplate photometer (Infinite® 200 PRO NanoQuant Multimode Microplate Reader, Tecan; 480 nm excitation wavelength/523 nm emission wavelength).

Quantification of Myeloperoxidase–DNA Complexes

MPO–DNA complexes were quantified by enzyme-linked immunosorbent assay (ELISA) using a modified approach of the Cell Death Detection ELISA kit (Roche, Basel, Switzerland) and the capture of anti-MPO antibody (Bio-Rad®) (7). To limit the inter-assay variability and because no international standard preparation is available to measure MPO–DNA complexes, we used a calibration range made from a stock solution of NETs, and results are expressed as standard NETs (ST) (18). The detailed protocol is available in the **Supplementary Material**.

Quantification of Citrullinated Histone H3

Citrullinated histone H3 (H3Cit) was quantified with a slight modification of the ELISA previously described by Thalin et al. (19) by using Cell Death detection kit without streptavidin-precoated wells. The optical densities (ODs) were measured at a wavelength of 450 nm with a reference correction wavelength at 620 nm using a microplate photometer (Infinite® 200 PRO NanoQuant Multimode Microplate Reader, Tecan).

Statistical Analyses

No statistical sample size calculation was performed *a priori*, and sample size was equal to the number of patients admitted for COVID-19 with available frozen plasma. Continuous variables are presented as median and interquartile range (IQR) and are compared using the Mann–Whitney test for comparison between two groups and Kruskal–Wallis test with Dunn's multiple comparison test for comparison between three groups. Categorical variables are expressed as the number of patients (percentage) and are compared using Fisher's exact test. Correlation analysis was performed using Pearson correlation test. All analyses were performed on Prism 6.0 software (GraphPad, La Jolla, CA) and R 3.6.1 statistical software (R Foundation for Statistical Computing, Vienna, Austria).

Ethics Statement

According to French law and the French Data Protection Authority, the handling of these data for research purposes was declared to the Data Protection Officer of the University Hospital of Bordeaux. Patients or relatives were notified about the anonymized use of their healthcare data *via* the departments' booklets, and non-opposition was recorded. All patients included in the study gave their written informed consent for the use of their plasma. The study complied with the Declaration of Helsinki of 1975, revised in 2000. This study was approved by the French institutional authority for personal data protection [Commission Nationale de l'Informatique et des Libertés (CNIL), registration number DEC20-086] and ethics committee (ID-CRB 2020-A00763-36) and by the institutional review board of the University Hospital of Bordeaux (declaration number CE-GP-2020-39). Samples from healthy controls were authorized by the Comité de Protection des Personnes Sud Ouest et Outre Mer III DC 2015/94.

RESULTS

Patients' Characteristics

Ninety-six COVID-19 patients were included, 50 (52%) with ARDS and 46 (48%) with moderate disease. Samples were collected with a median delay from admission of 2 days [1-3] for moderate COVID-19 patients and of 1 day [1-2] for critical COVID-19-related ARDS patients. Patients' characteristics are summarized in **Table 1**. Briefly, patients were mostly men (54% for moderate patients and 68% for ARDS patients) with a median age of 68 years for moderate patients and 61 for ARDS patients. Hypertension and diabetes were the main comorbidities (**Table 1**). PE occurred in 19 patients, one with moderate disease and 18 with ARDS. Death occurred in 29/96 patients (4/46 moderate patients and 25/50 ARDS patients). All patients were on heparin treatment at the time of blood sampling, and majority were on low-molecular weight heparin (LMWH) (66%). Compared to moderate patients, ARDS patients were more frequently treated with unfractionated heparin (UFH) than with LMWH (64% vs. 13%, p = 0.0001) and on therapeutic rather than prophylactic anticoagulant regimen (36% vs. 15%, p = 0.005). Median anti-Xa value for patients receiving UFH at therapeutic dose (n = 13) was 0.34 (IQR 0.195–0.515), with no difference between moderate and ARDS patients [respectively 0.35 (IQR 0.19–0.52) and 0.34 (IQR 0.21–0.49), p = 0.87). Indications for therapeutic anticoagulation at the time of sampling were atrial fibrillation (n = 9), history of phlebitis (n = 3), history of PE (n = 2), essential thrombocythemia with history of PE (n = 1), early initiation of veno-venous extracorporeal membrane oxygenation (ECMO) (n = 1), physicians' discretion in front of elevated fibrinogen and/or D-dimer levels (n = 6), and unknown (n = 3). Nine patients were treated with veno-venous ECMO during their stay in the ICU.

Plasma Levels of Neutrophil Extracellular Traps Increase With COVID-19 Clinical Severity

We quantified 3 NET markers in patients' plasma collected shortly after patients' admission: one unspecific, i.e., total cell-free DNA, and two more specific, i.e., MPO–DNA complexes and H3Cit. For all 3 markers, we observed that all COVID-19 patients (n = 96) have significantly more NETs than healthy donors (n = 10), respectively: total cell-free DNA concentrations [304 ng/ml (209–443) vs. 140 ng/ml (124–151), p < 0.0001], plasma MPO–DNA levels [0.63ST (0.15–3.10) vs. 0.044 ST (0.012–0.093), p < 0.0001], and plasma H3Cit levels [0.37

TABLE 1 | Patients' characteristics at the time of blood sampling.

	Moderate COVID-19 patients N = 46	COVID-19 ARDS patients N = 50	p-value
Age (years)	68 [62–78]	61 [54–68]	0.008
Sex (male)	25 (54%)	34 (68%)	0.18
Body mass index (kg/m²)	26 [24–30]	29 [26–36]	0.008
Hypertension	29 (63%)	29 (58%)	0.82
Diabetes mellitus	8 (17%)	16 (32%)	0.19
Chronic kidney disease	3 (7%)	0 (0%)	0.25
Chronic heart disease	8 (17%)	9 (18%)	1.00
Chronic obstructive pulmonary disease	5 (10%)	10 (20%)	0.35
Immunosuppressive drug before COVID-19	6 (14%)	10 (20%)	0.55
Respiratory rate (/min)	24 [18–22]	30 [24–35]	0.04
Oxygen flow (L/min)	4 [2–6]	–	–
FiO_2 (%)	–	60 [45–90]	–
Heart rate (/min)	97 [78–123]	105 [68–137]	0.90
Mean blood pressure (mmHg)	72 [64–91]	68 [59–94]	0.82
Temperature (°C)	37 [36.8–37.3]	38 [37–39]	0.08
Fibrinogen (g/L)	6 [5.45–6.5]	7.5 [5.8–8.5]	0.22
D-dimers (mg/L)	625 [513–838]	2,123 [1,230–6,308]	<0.001
Platelets (/mm³)	175,000 [111,250–252,500]	210,000 [130,000–320,000]	0.78
Neutrophils (/mm³)	3,300 [2,510–5,450]	6,300 [4,430–11,750]	0.02
Lymphocytes (/mm³)	1,000 [700–1,315]	820 [400–1,240]	0.07
C-reactive protein (mg/L)	49 [27–78]	132 [73–256]	<0.01
Anticoagulant treatment at the time of blood sampling			
Prophylactic vs. therapeutic anticoagulation regimen	39 (85%)/7 (15%)	32 (64%)/18 (36%)	0.05
Care during hospitalization			
Corticosteroids use	5 (11%)	16 (32%)	0.01
Immunomodulating agents	2 (5%)	8 (16%)	0.13
Tocilizumab	0	6	–
Anakinra	1	0	–
Interferon-β	1	0	–
Antiviral agents	3 (7%)	18 (36%)	0.001
Lopinavir-ritonavir	2	10	–
Remdesivir	1	1	–
Oseltamivir	0	2	–
Clinical evolution after blood sampling			
PE	1	18	
In-hospital mortality	4	25	

Continuous variables are presented as median and interquartile range and are compared using Mann–Whitney test. Categorical variables are expressed as the number of patients (percentage) and are compared using Fisher's exact test.
ARDS, acute respiratory distress syndrome; FiO2, fractional inspired oxygen; PE, pulmonary embolism.

(0.16–1.06) vs. 0.14 (0.088–0.18), p < 0.01]. The 3 NET markers were significantly higher in ARDS patients compared to patients with moderate COVID-19 disease (**Figures 1A–C**). Because one study reported that heparin can dismantle already formed NETs by removing histones from secreted DNA (20), we wondered whether heparin anticoagulation, either at prophylactic or therapeutic dose, modified NET dosages in COVID-19 patients. A first, analysis in all COVID-19 patients showed no difference in plasma levels of NET markers (total DNA, MPO—DNA, and H3Cit, respectively; **Figures 1D–F**) between patients treated with prophylactic or therapeutic anticoagulant treatment. As we were concerned that the more severe patients were the ones who received the most therapeutic anticoagulation, thereby inducing a bias in the analysis, we analyzed moderate and ARDS patients separately. We did not observe any difference of NET markers whether patients were under prophylactic or therapeutic heparin either for ARDS or moderate patients (respectively; **Figures 1G–L**).

Levels of Neutrophil Extracellular Trap Markers at the Time of Admission Are Not Higher in Moderate COVID-19 Patients Who Will Later Worsen Their Respiratory Condition Compared With Those Who Will Not

We did not find any significant difference between patients initially hospitalized for moderate COVID-19 disease (n = 46) who later developed ARDS (n = 9) and those who did not (n = 37) [respectively, cell-free total DNA concentrations of 193 ng/ml (177–226) vs. 240 ng/ml (191–290), p = 0.14; MPO–DNA: 0.60 ST (0.40–2.2) vs. 1.2 ST (0.60–2.3), p = 0.58; and H3Cit OD

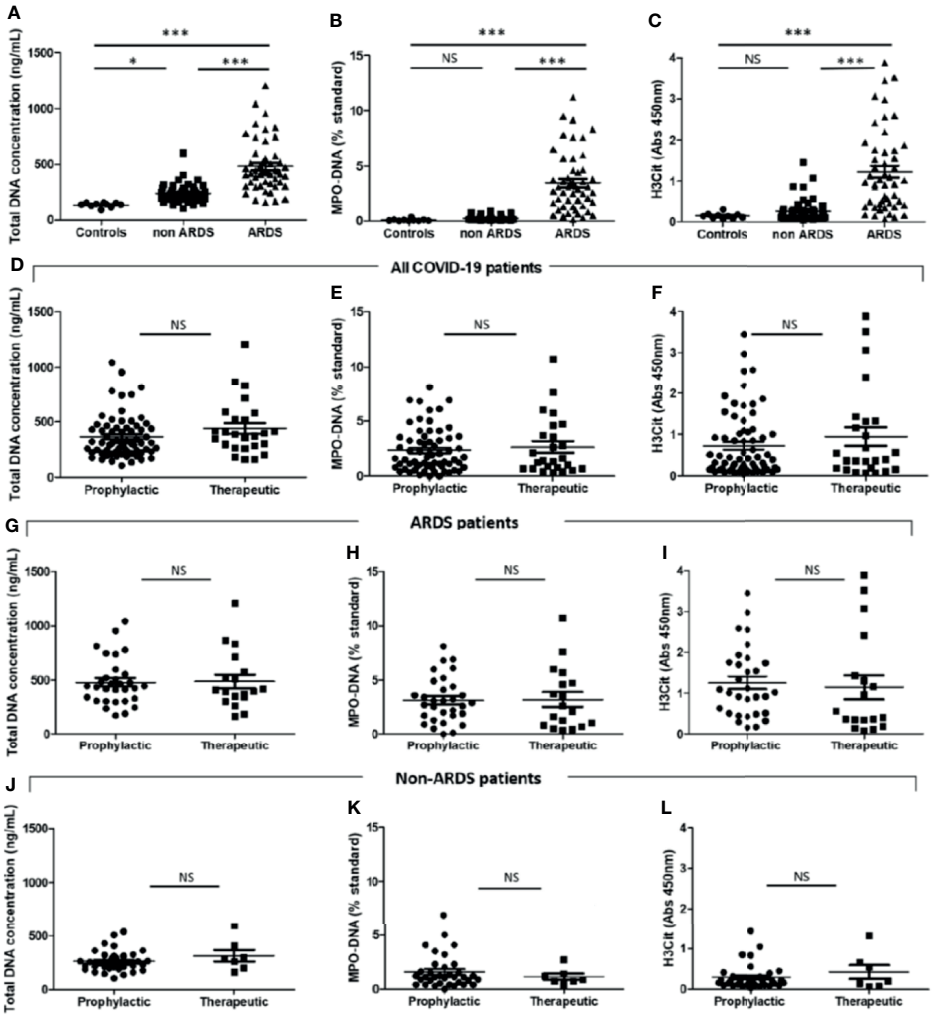

FIGURE 1 | Critically ill COVID-19 patients have higher plasma neutrophil extracellular trap (NET) levels than those of moderate COVID-19 patients and controls. Plasma NET levels were compared between healthy donors ("controls", n = 10), moderate [without acute respiratory distress syndrome (ARDS) "non-ARDS"] COVID-19 patients (n = 46), and patients with ARDS (n = 50) admitted to the intensive care unit. Levels of NET markers were as follows: plasma total DNA concentrations [140 ng/ml (124–151) vs. 220 ng/ml (188–271) vs. 428 ng/ml (324–560), $p < 0.0001$], plasma MPO–DNA levels [0.044 ST (0.012–0.093) vs. 10.15 ST (0.10–0.31) vs. 3.00 (1.38–4.63), $p < 0.0001$] and plasma H3Cit levels [0.14 (0.088–0.18) vs. 0.17 (0.10–0.30) vs. 0.97 (0.41–1.75), $p < 0.0001$]. **(A)** Total DNA concentration (ng/ml). **(B)** Myeloperoxidase–DNA levels (% standard NETs). **(C)** Histone H3 citrullinated (absorbance 450 nm). Plasma NET levels were compared between COVID-19 patients treated with prophylactic (n = 71) or therapeutic (n = 25) heparin treatment. **(D)** Total DNA concentration (ng/ml). **(E)** Myeloperoxidase–DNA levels (% standard NETs). **(F)** Histone H3 citrullinated (absorbance 450 nm). Plasma NET levels were compared between COVID-19-related ARDS patients treated with prophylactic (n = 32) or therapeutic (n = 18) heparin treatment. **(G)** Total DNA concentration (ng/ml). **(H)** Myeloperoxidase–DNA levels (% standard NETs). **(I)** Histone H3 citrullinated (absorbance 450 nm). Plasma NET levels were compared between COVID-19 moderate patients treated with prophylactic (n = 39) or therapeutic (n = 7) heparin treatment. **(I)** Total DNA concentration (ng/ml). **(J)** Myeloperoxidase–DNA levels (% standard NETs). **(K)** Histone H3 citrullinated (absorbance 450 nm). Threshold for statistical significance was a p-value of 0.05. *$p < 0.05$, ***$p < 0.0001$. NS, statistically non-significant.

measures: 0.21 (0.081–0.23) vs. 0.16 (0.10–0.31), $p = 0.78$] (**Figures 2A–C**).

Levels of Neutrophil Extracellular Trap Markers Are Higher in COVID-19 Patients Who Will Not Survive, Even in the Subgroup of Patients Admitted With ARDS

We found that the plasma levels of the 3 NET markers were higher in non-survivor COVID-19 patients than those in survivors [respectively, cell-free total DNA concentration: 437 ng/ml (362–600) vs. 264 ng/ml (200–382), $p < 0.0001$; MPO–DNA: 3.60 ST (1.65–5.85) vs. 1.20 ST (0.68–2.52), $p < 0.001$; and H3Cit OD: 0.91 (0.33–1.43) vs. 0.30 (0.14–0.85), $p < 0.01$] (**Figures 3A–C**). Given that our population of COVID patients includes patients who arrive at the hospital with either moderate or severe disease, we were concerned that analysis of the whole population induces a bias, as the patients who arrive at the hospital with a severe form have *de facto* a

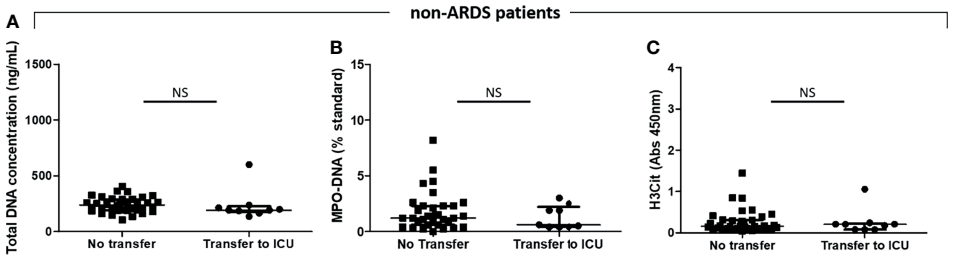

FIGURE 2 | Plasma NET levels are not different between COVID-19 moderate patients who will subsequently need a transfer to the ICU than those who will not. Plasma NET levels were compared between moderate COVID-19 patients who will subsequently have a worsened respiratory condition needing a transfer to the intensive care unit because of acute respiratory distress syndrome (ARDS) (n = 9) and those who will not (n = 37). **(A)** Total DNA concentration (ng/ml). **(B)** Myeloperoxidase–DNA levels (% standard NETs). **(C)** Histone H3 citrullinated (absorbance 450 nm). NS, non-significant.

worse prognosis than the ones who arrive with a moderate disease. We thus analyzed both populations separately.

In COVID-19 moderate patients, only total DNA concentration, but not MPO-DNA nor H3Cit levels, was higher in non-survivors than that in survivors (**Supplementary Figure S1**), but the low number of events deters from firm conclusions.

We then focused on the more severe patients with the higher mortality rate, i.e., COVID-19-related ARDS patients (n = 50). Cell-free total DNA concentrations and MPO–DNA complex levels measured within the first 3 days after ICU admission were significantly higher in non-survivors (n = 25) than those in survivors (n = 25) (respectively, cell-free total DNA concentration: 475 ng/ml (391–760) vs. 393 ng/ml (303–460), p = 0.03; MPO–DNA: 3.70 ST (2.25–6.25) vs. 2.00 ST (0.70–3.10), p < 0.001] but not plasma H3Cit levels [H3Cit OD: 0.97 (0.41–1.66) vs. 0.97 (0.39–1.81), p = 0.91] (**Table 2** and **Figures 3D–F**). Median time between dosage of NET markers and death was 5 days [3-13]. We did not observe any correlation between plasma levels of NET markers and time to death (**Supplementary Figure S2**).

When going back to the clinical and biological characteristics of non-survivor and survivor ARDS patients at inclusion, we did not observe major significant differences except a higher proportion of patients with chronic obstructive pulmonary disease (COPD) and higher levels of plasmatic d-dimers in non-survivors compared to survivors (**Table 2**).

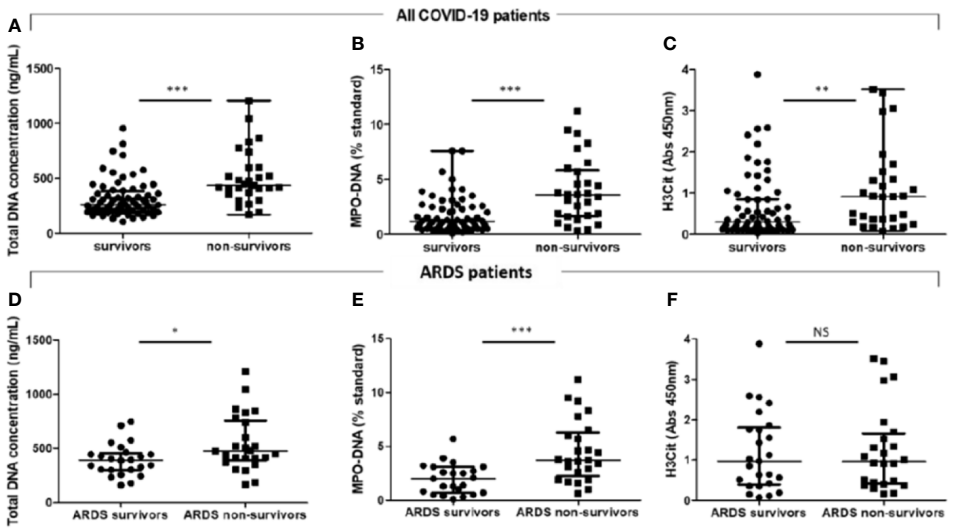

FIGURE 3 | COVID-19 acute respiratory distress syndrome non-survivors have higher plasma total DNA concentrations and myeloperoxidase–DNA levels than survivors. Plasma NET levels were compared in all COVID-19 patients between survivors (n = 67) and non-survivors (n = 29). **(A)** Total DNA concentration (ng/ml). **(B)** Myeloperoxidase–DNA levels (% standard NETs). **(C)** Histone H3 citrullinated (absorbance 450 nm). Plasma NET levels were compared between COVID-19-related acute respiratory distress syndrome (ARDS) survivors (n = 25) and non-survivors (n = 25). **(D)** Total DNA concentration (ng/ml). **(E)** Myeloperoxidase–DNA levels (% standard NETs). **(F)** Histone H3 citrullinated (absorbance 450 nm). Threshold for statistical significance was a p-value of 0.05. *p < 0.05, **p < 0.01, ***p < 0.001. NS, statistically non-significant.

Levels of Neutrophil Extracellular Trap Markers Are Higher in COVID-19 Patients Who Will Subsequently Develop Pulmonary Embolism Compared With Those Who Will Not, but Not When Assessed in the Subset Group of ARDS Patients

Besides being implicated in microthrombus formation leading to lung damage, NETs are also involved in thrombosis in the macrocirculation, especially in veins (21, 22). Consistent with data in conditions other than COVID-19, we found that cell-free total DNA in plasma and H3Cit levels were higher in COVID-19 patients who subsequently developed PE (n = 19) than those who did not (n = 73) [respectively, cell-free DNA concentrations: 437 ng/ml (333–529) vs. 263 ng/ml (198–409), $p < 0.01$; H3Cit OD: 1.09 (0.72–1.55) vs. 0.26 (0.14–0.85), $p < 0.0001$] (**Figures 4A, C**). Plasma MPO–DNA levels were not different [2.60 ST (1.30–3.90) vs. 1.90 ST (0.73–3.50), p = 0.27] (**Figure 4B**). PE occurred 4 days (3–6) after the time of sampling [8 days (6–11) after admission].

PE is of particular concern in COVID-19 ARDS patients, as it occurs in about 20% of them (23) vs. only in 3.1% of non-critically ill patients (24). Consistent with these data, only 1 patient in the moderate COVID-19 group subsequently developed PE, 5 days before he died. We thus focused our analysis on those patients (n = 50), and neither plasma cell-free DNA concentrations, MPO–DNA, nor H3Cit levels were different between ARDS patients who later developed PE (n = 18) and those who did not (n = 32) (**Figures 4D–F**). The occurrence of PE did not seem to be associated with death in this subset of critical patients, as 7/25 (28%) non-survivors developed PE vs. 11/25 (44%) in survivors (p = 0.38). No patient died from severe gas exchange impairment or circulatory failure attributed to PE. As D-dimers are a classical biomarker of venous thrombosis, we assessed the correlation between plasma levels of NET markers and D-dimers. Interestingly, only MPO–DNA, but not plasma total DNA concentration nor H3Cit, correlated with D-dimer levels in ARDS patients but with a poor correlation coefficient (r = 0.43) (**Supplementary Figure S3**).

DISCUSSION

The prediction of disease evolution is a challenge among COVID-19 patients and especially among the most severe ones, i.e., with COVID-19-related ARDS. Our study was designed to assess the involvement of circulating markers of NETs for COVID-19 evolution among inpatients who were admitted at the hospital for moderate and severe COVID-19. We thus included 46 COVID-19 patients with moderate disease and 50 with ARDS. We studied the association between 3 circulating markers of NETs measured shortly after hospital admission and disease evolution in terms of survival, aggravation (for patients with moderate disease only), and PE occurrence. Our findings confirm previous reports showing that circulating markers of NETs correlate with the clinical severity at the time of blood sampling (12–14), but we also report an association between circulating markers of NETs and later survival within the subgroup of patients admitted to the hospital for severe COVID-19 (ARDS patients). The study of Ng et al. (14) previously reported an association between

TABLE 2 | COVID-19-related ARDS patients' characteristics at the time of blood sampling.

	Survivors N = 25	Non-survivors N = 25	p-value
Age (years)	60 [54–70]	62 [52–69]	0.99
Sex (male)	17 (68%)	17 (68%)	1.00
Body mass index (kg/m²)	28 [25–38]	31 [27–36]	0.65
Hypertension	13 (52%)	18 (72%)	0.48
Diabetes mellitus	5 (20%)	11 (44%)	0.15
Chronic kidney disease	0 (0%)	0 (0%)	1.00
Chronic heart disease	5 (20%)	2 (8%)	0.39
Chronic obstructive pulmonary disease	1 (4%)	11 (44%)	<0.01
Immunosuppressive drug before COVID-19	3 (12%)	8 (32%)	0.39
SOFA	4 [2–9]	5 [2–8]	0.99
PaO_2/FiO_2 (mmHg)	149 [115–275]	160 [86–212]	0.39
Fibrinogen (g/L)	7.6 [6.7–9]	7.5 [5.1–8.5]	0.39
D-dimers (mg/L)	1,342 [751–3,760]	3,450 [1,930–8,850]	0.05
Platelets (/mm^3)	294,000 [178,000–393,000]	166,000 [107,000–297,000]	0.06
Neutrophils (/mm^3)	5,240 [4,100–9,000]	7,850 [4,430–13,980]	0.26
Lymphocytes (/mm^3)	840 [680–1,400]	750 [325–1,025]	0.12
Albumin (g/L)	23 [18–26.8]	25 [18–28.5]	0.64
C-reactive protein (mg/L)	137 [77–229]	118 [69–267]	0.88
Invasive ventilation	19 (83%)	25 (100%)	0.27
ECMO	1 (4%)	8 (32%)	0.005
Corticosteroids	8 (32%)	10 (40%)	0.72
Immunomodulating agents	4 (16%)	4 (16%)	1.00
Antiviral agents	8 (32%)	9 (36%)	1.00

Continuous variables are presented as median and interquartile range and are compared using Mann–Whitney test. Categorical variables are expressed as the number of patients (percentage) and are compared using Fisher's exact test. ARDS, acute respiratory distress syndrome; ECMO, extracorporeal membrane oxygenation; MPO–DNA, myeloperoxidase–DNA; SOFA, sequential organ failure assessment score; %ST, % Standard NETs.

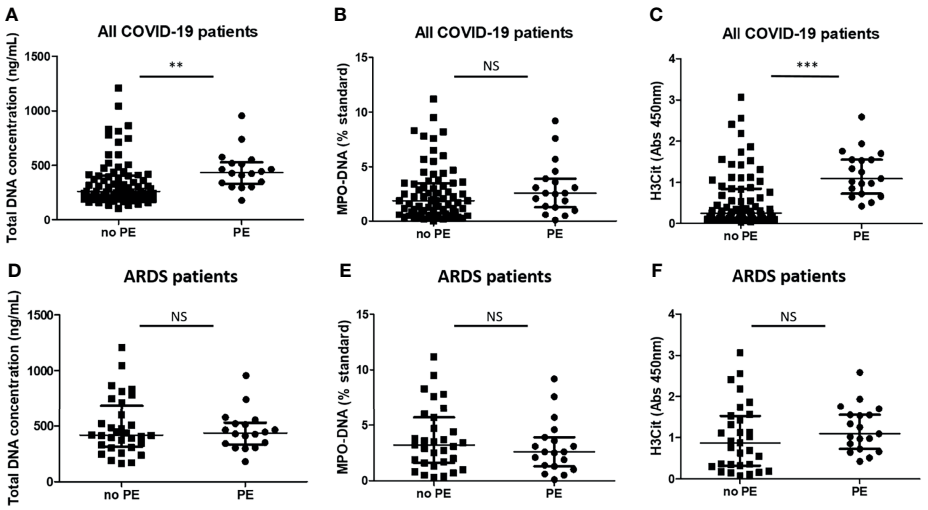

FIGURE 4 | Plasma total DNA concentrations and myeloperoxidase–DNA levels are higher in COVID-19 patients who will subsequently have pulmonary embolism but not when assessed by comparable severity. Plasma NET levels were compared between COVID-19 patients who will subsequently develop pulmonary embolism (PE) (n = 19) and those who will not (n = 77). **(A)** Total DNA concentration (ng/ml). **(B)** Myeloperoxidase–DNA levels (standard NETs). **(C)** Histone H3 citrullinated (absorbance 450 nm). Plasma NET levels were compared between COVID-19-related acute respiratory distress syndrome patients who will subsequently develop pulmonary embolism (PE) (n = 18) and those who will not (n = 32). **(D)** Total DNA concentration (ng/ml). **(E)** Myeloperoxidase–DNA levels (standard NETs). **(F)** Histone H3 citrullinated (absorbance 450 nm). $^{**}p < 0.01$, $^{***}p < 0.001$, NS, statistically non-significant.

circulating markers of NETs and clinical outcome in a cohort of 106 patients with moderate to severe COVID-19 patients, but this study did not analyze the prognostic value of circulating markers of NETs specifically in each group of patients. Here we did not report any significant association between circulating markers of NETs and disease evolution in the moderate COVID-19 patients in terms of clinical aggravation (i.e., transfer to ICU, PE occurrence, or death). On the contrary, we did find an association between plasma levels of NET markers and survival in ARDS patients.

These results reinforce the hypothesis that immunothrombosis and in particular NETosis are involved in the complications of COVID-19, especially in the most severe forms (13, 25–27). Only experiments in animal models could definitely prove the pathogenic role of NETosis in COVID-19 progression but, at present, several lines of evidence show a link between severe acute respiratory syndrome coronavirus 2 (SARS-CoV-2) infection and NET formation. First of all, several studies reported induction of NET release during COVID-19 either by the virus itself (28), plasma and serum from severe COVID-19 patients (probably through the hyperinflammation typical of severe forms of COVID-19), activated platelets from severe patients (12, 13, 29), and anti-phospholipid antibodies (30). Second, a recent study compared lung specimens from four patients who died from COVID-19 and four from a COVID-19-unrelated cause. The authors reported that NETs infiltrated the lung airways and interstitial and vascular compartments only in severe COVID-19 patients but not in controls, supporting the hypothesis that NETs may drive severe pulmonary complications of COVID-19 (31). The third range of evidence comes from the known role of NETs in thrombosis (32) and the observation that severe SARS-CoV-2 infection induces a prothrombotic state manifesting especially with microthrombosis (33). In line with that, a consortium of authors recently proposed that exaggerated immunothrombosis, occurring for the most part within lung microvessels, drives the clinical manifestations of COVID-19 (32), with the atypical ARDS of COVID-19 being summarized as "microvascular COVID-19 lung vessels obstructive thromboinflammatory syndrome" (MicroCLOTS) (34).

It may look contradictory that we observe an association between circulating NET markers and survival in patients who arrive at the hospital for an already severe form of COVID-19 but that we do not find any association with transfer to ICU in the moderate ones. Part of the explanation could be that host response is still regulated in moderate patients but not in ARDS patients, causing the accumulation of NETs. Another plausible explanation is that NETosis generation could occur mostly within the lung tissue (31, 35) and not the circulation. Lung biopsies are not available in these patients for ethical reasons, as their complications are frequent and possibly lethal.

From a therapeutic point of view, as our results show that NETosis is already highly activated in severe patients who will die, we wonder whether targeting NETosis in severe patients is not already too late. In our opinion, our results suggest that NETosis should be targeted to prevent COVID-19 aggravation, before ARDS occurrence. There are ongoing clinical trials that aim to either prevent NET formation or degrade already-formed NETs. The first ones use anti-inflammatory drugs such as the Janus Kinases 1/2 (JAK1/2) inhibitor ruxolitinib (NCT04338958), dipyridamole (NCT 04391179), and ticagrelor (NCT02735707, NCT04518735). We suspect that these drugs should be more efficient in the less severe patients. DNase I (dornase alpha) can degrade already formed NETs and is currently tested by inhalation

in patients with COVID-19 (NCT04402944, NCT04355364, NCT04432987, NCT04359654, NCT04445285, NCT04402970). A major issue with the nebulizing administration route in severe COVID-19 is that there is concern that it will not reach the perialveolar vessels due to the high amounts of platelet factor 4 (PF4) (13) that compacts NETs and decrease their susceptibility to DNase degradation (36).

Thrombosis, and especially PE, is a frequent feature in COVID-19 patients and is an independent risk factor for death (37). It should be noted that the embolic origin of the pulmonary vessel occlusions is questionable, and it may be that the so-called PEs are rather pulmonary thrombi that occur directly in pulmonary arteries (38, 39). Given the known role of NETs in venous thrombosis, we looked for differences in circulating markers of NETs. We found that 2 markers were higher in hospitalized COVID-19 patients who subsequently developed PE than those who did not. But when we restricted our analysis within the specific subgroup of COVID-19-related ARDS patients, who are the ones at more risk to develop PE, we did not find any difference between patients who will develop PE or not. This suggests, if confirmed in a larger cohort, that NETosis in itself is not a major driver for PE (venous thromboembolic event in the macrocirculation). Whereas there is an abundant literature to search for biological markers of clinical aggravation, there are only very few studies that report an association between a biological marker or a clinical parameter that is associated with occurrence of thrombosis among severe COVID-19 patients. D-dimers, which are reported to have a significant predictive value for mortality both in non-critical and critical COVID-19 patients (40, 41), have a limited predictive value for venous thromboembolism (VTE) occurrence, with an area under the curve (AUC) of 0.565 (42).

Our study has several limitations. First, we observe, as others in COVID-19 patients (12), dichotomies between the three circulating NET markers. This could be due to the relatively small number of samples we analyzed and also to the lack of standardization for NET marker measurement. We used 3 different plasma markers to measure NETs. Indeed, despite the discovery of the process of NETosis in 2004 (5), there is still no reference test for NET quantification (6). NETs can be visualized and quantified with conventional fluorescence microscopy, but this assay is hardly reproducible and time-consuming and is better when performed right after blood sampling. To overcome this issue and quantify NETosis that occurs *in vivo*, various plasmatic tests, and mostly ELISAs, have been developed. Given the large amount of tests available and the lack of homogeneity between them, we decided to perform 3 of them: total DNA, MPO–DNA complexes, and H3Cit. Total DNA dosage is not specific for NETs, as it also measures DNA coming from necrotic cells. MPO–DNA complexes are more specific, as it measures DNA together with MPO that specifically comes from neutrophils, but this assay is often not standardized in publications. Here we used a standardized method, with a calibration curve, to allow precise measurement and reproducibility. Lastly, H3Cit measurement can appear to be the most reliable marker, as it directly measures histone H3 that has been citrullinated, a process that is specific from NETosis. But currently, all available ELISAs lack reproducibility and standardization (43). A Scientific and Standardization Subcommittee of the International Society of Thrombosis and Haemostasis is currently running a study aiming at providing recommendation for NETs' dosage standardization.

Second, computerized tomography pulmonary angiograms were not systematically performed because of in-hospital transport issues regarding these critically ill patients. We only considered here clinically relevant PE. PE occurrence might have been underestimated, as the pretest probability and clinical likelihood of PE could have presumably been lower in patients treated with therapeutic heparin, especially in the ARDS subgroup. Moreover, transportation to CT scan may have been avoided in the more severe patients because of the risks of transferring patients with critical respiratory failure. As catheter-related thrombosis and limb deep-vein thrombosis screening strategy was heterogeneous among centers, we did not analyze those outcomes.

CONCLUSION

Taken together, our data demonstrate that circulating markers of NETs are linked to survival but not to PE occurrence in patients with COVID-19 and especially among the most severe ones. Even if measuring NET markers could not be easily implemented in clinical practice to become prognostic biomarkers, our findings are important, as they strengthen the fact that NETosis is a proper therapeutic target in COVID-19 disease, but, more specifically, they argue that NETosis should be targeted before COVID-19 aggravation and ARDS occurrence to be the most efficient.

DATA AVAILABILITY STATEMENT

The raw data supporting the conclusions of this article will be made available by the authors without undue reservation.

ETHICS STATEMENT

According to French law and the French Data Protection Authority, the handling of these data for research purposes was declared to the Data Protection Officer of the University Hospital of Bordeaux. Patients or relatives were notified about the anonymized use of their healthcare data *via* the departments' booklets, and non-opposition was recorded. This study was approved by the French institutional authority for personal data protection [Commission Nationale de l'Informatique et des Libertés (CNIL), registration number DEC20-086] and ethics committee (ID-CRB 2020-A00763-36) and by the institutional review board of the University Hospital of Bordeaux (declaration number CE-GP-2020-39). Samples from healthy controls were authorized by the Comité de Protection des Personnes Sud Ouest et Outre Mer III DC 2015/94.

AUTHOR CONTRIBUTIONS

RP and CJ designed the study. ADe, ADu, DG, AO, AR, SS, JG, MC, EJ, JP, and GG included the patients and collected the data. SL-C, AD, LG, SS, GG, CJ, and AR collected the samples. SC performed NET measurements. RP, AD, CJ, SC, AD, AR, and SS analyzed the data. RP, AD, and CJ wrote the article. All the authors read and substantially improved the article.

FUNDING

This work was funded by a COVID-19 grant from the University of Bordeaux and an ANR-COVID (CORONET R21025GG).

ACKNOWLEDGMENTS

We would like to acknowledge P. Blanco, A. Godier, J. Goret, and F. Philippart for helpful discussions. We are grateful to CHU de Bordeaux and Université de Bordeaux for research grants dedicated to COVID-19. We are also grateful to I. Pellegrin and the "Centre de Ressources Biologiques" of CHU de Bordeaux.

SUPPLEMENTARY MATERIAL

The Supplementary Material for this article can be found online at: https://www.frontiersin.org/articles/10.3389/fimmu.2022.851497/full#supplementary-material

REFERENCES

1. Wu C, Chen X, Cai Y, Xia J, Zhou X, Xu S, et al. Risk Factors Associated With Acute Respiratory Distress Syndrome and Death in Patients With Coronavirus Disease 2019 Pneumonia in Wuhan, China. *JAMA Internal Med* (2020) 180(7):934–43. doi: 10.1001/jamainternmed.2020.0994
2. Ackermann M, Verleden SE, Kuehnel M, Haverich A, Welte T, Laenger F, et al. Pulmonary Vascular Endothelialitis, Thrombosis, and Angiogenesis in Covid-19. *N Engl J Med* (2020) 383:120–8. doi: 10.1056/NEJMoa2015432
3. Helms J, Tacquard C, Severac F, Leonard-Lorant I, Ohana M, Delabranche X, et al. High Risk of Thrombosis in Patients With Severe SARS-CoV-2 Infection: A Multicenter Prospective Cohort Study. *Intensive Care Med* (2020) 46:1089–98. doi: 10.1007/s00134-020-06062-x
4. Engelmann B, Massberg S. Thrombosis as an Intravascular Effector of Innate Immunity. *Nat Rev Immunol* (2013) 13:34–45. doi: 10.1038/nri3345
5. Brinkmann V. Neutrophil Extracellular Traps Kill Bacteria. *Science* (2004) 303:1532–5. doi: 10.1126/science.1092385
6. Thålin C, Hisada Y, Lundström S, Mackman N, Wallén H. Neutrophil Extracellular Traps: Villains and Targets in Arterial, Venous, and Cancer-Associated Thrombosis. *Arterioscler Thromb Vasc Biol* (2019) 39:1724–38. doi: 10.1161/ATVBAHA.119.312463
7. Guy A, Favre S, Labrouche-Colomer S, Deloison L, Gourdou-Latyszenok V, Renault M-A, et al. High Circulating Levels of MPO-DNA are Associated With Thrombosis in Patients With MPN. *Leukemia* (2019) 33:2544–8. doi: 10.1038/s41375-019-0500-2
8. Grégoire M, Uhel F, Lesouhaitier M, Gacouin A, Guirriec M, Mourcin F, et al. Impaired Efferocytosis and Neutrophil Extracellular Trap Clearance by Macrophages in ARDS. *Eur Respir J* (2018) 52(2):1702590. doi: 10.1183/13993003.02590-2017
9. Zhang YL, Zhao J, Guan L, Zheng YM, Chen M, Guo LX, et al. Activation of Lung Endothelial Cells by Extracellular Histone in Mice With Acute Respiratory Distress Syndrome. *Zhonghua Lao Dong Wei Sheng Zhi Ye Bing Za Zhi* (2019) 37:732–6. doi: 10.3760/cma.j.issn.1001-9391.2019.10.004
10. Lefrançais E, Mallavia B, Zhuo H, Calfee CS, Looney MR. Maladaptive Role of Neutrophil Extracellular Traps in Pathogen-Induced Lung Injury. *JCI Insight* (2018) 3(3):e98178. doi: 10.1172/jci.insight.98178
11. Abrams ST, Morton B, Alhamdi Y, Alsabani M, Lane S, Welters ID, et al. A Novel Assay for Neutrophil Extracellular Trap Formation Independently Predicts Disseminated Intravascular Coagulation and Mortality in Critically Ill Patients. *Am J Respir Crit Care Med* (2019) 200:869–80. doi: 10.1164/rccm.201811-2111OC
12. Zuo Y, Yalavarthi S, Shi H, Gockman K, Zuo M, Madison JA, et al. Neutrophil Extracellular Traps in COVID-19. *JCI Insight* (2020) 5(11):e138999. doi: 10.1172/jci.insight.138999
13. Middleton EA, He X-Y, Denorme F, Campbell RA, Ng D, Salvatore SP, et al. Neutrophil Extracellular Traps (NETs) Contribute to Immunothrombosis in COVID-19 Acute Respiratory Distress Syndrome. *Blood* (2020) 136 (10):1169–79. doi: 10.1182/blood.2020007008
14. Ng H, Havervall S, Rosell A, Aguilera K, Parv K, von Meijenfeldt FA, et al. Circulating Markers of Neutrophil Extracellular Traps are of Prognostic Value in Patients With COVID-19. *Arterioscler Thromb Vasc Biol* (2021) 41:988–94. doi: 10.1161/ATVBAHA.120.315267
15. COVID-19 Treatment Guidelines Panel. *Coronavirus Disease 2019 (COVID-19) Treatment Guidelines*. National Institutes of Health. Available at: https://www.covid19treatmentguidelines.nih.gov/.
16. ARDS Definition Task Force, Ranieri VM, Rubenfeld GD, Thompson BT, Ferguson ND, Caldwell E, et al. Acute Respiratory Distress Syndrome: The Berlin Definition. *JAMA* (2012) 307:2526–33. doi: 10.1001/jama.2012.5669
17. Susen S, Tacquard CA, Godon A, Mansour A, Garrigue D, Nguyen P, et al. Prevention of Thrombotic Risk in Hospitalized Patients With COVID-19 and Hemostasis Monitoring. *Crit Care* (2020) 24:364. doi: 10.1186/s13054-020-03000-7
18. Sil P, Yoo D-G, Floyd M, Gingerich A, Rada B. High Throughput Measurement of Extracellular DNA Release and Quantitative NET Formation in Human Neutrophils *In Vitro*. *J Vis Exp* (2016) 18(112):52779. doi: 10.3791/52779
19. Thålin C, Daleskog M, Göransson SP, Schatzberg D, Lasselin J, Laska A-C, et al. Validation of an Enzyme-Linked Immunosorbent Assay for the Quantification of Citrullinated Histone H3 as a Marker for Neutrophil Extracellular Traps in Human Plasma. *Immunol Res* (2017) 65:706–12. doi: 10.1007/s12026-017-8905-3
20. Fuchs TA, Brill A, Duerschmied D, Schatzberg D, Monestier M, Myers DD, et al. Extracellular DNA Traps Promote Thrombosis. *Proc Natl Acad Sci USA* (2010) 107:15880–5. doi: 10.1073/pnas.1005743107
21. von Brühl M-L, Stark K, Steinhart A, Chandraratne S, Konrad I, Lorenz M, et al. Monocytes, Neutrophils, and Platelets Cooperate to Initiate and Propagate Venous Thrombosis in Mice in Vivo. *J Exp Med* (2012) 209:819–35. doi: 10.1084/jem.20112322
22. Martinod K, Demers M, Fuchs TA, Wong SL, Brill A, Gallant M, et al. Neutrophil Histone Modification by Peptidylarginine Deiminase 4 is Critical for Deep Vein Thrombosis in Mice. *Proc Natl Acad Sci USA* (2013) 110:8674–9. doi: 10.1073/pnas.1301059110
23. Klok FA, Kruip MJHA, van der Meer NJM, Arbous MS, Gommers D a MPJ, Kant KM, et al. Incidence of Thrombotic Complications in Critically Ill ICU Patients With COVID-19. *Thromb Res* (2020) 191:145–7. doi: 10.1016/j.thromres.2020.04.013
24. Al-Samkari H, Karp Leaf RS, Dzik WH, Carlson JCT, Fogerty AE, Waheed A, et al. COVID-19 and Coagulation: Bleeding and Thrombotic Manifestations of SARS-CoV-2 Infection. *Blood* (2020) 136:489–500. doi: 10.1182/blood.2020006520
25. Barnes BJ, Adrover JM, Baxter-Stoltzfus A, Borczuk A, Cools-Lartigue J, Crawford JM, et al. Targeting Potential Drivers of COVID-19: Neutrophil Extracellular Traps. *J Exp Med* (2020) 217(6):e20200652. doi: 10.1084/jem.20200652
26. Tomar B, Anders H-J, Desai J, Mulay SR. Neutrophils and Neutrophil Extracellular Traps Drive Necroinflammation in COVID-19. *Cells* (2020) 9 (6):1383. doi: 10.3390/cells9061383

27. Skendros P, Mitsios A, Chrysanthopoulou A, Mastellos DC, Metallidis S, Rafailidis P, et al. Complement and Tissue Factor-Enriched Neutrophil Extracellular Traps are Key Drivers in COVID-19 Immunothrombosis. *J Clin Invest* (2020) 6:141374. doi: 10.1101/2020.06.15.20131029
28. Veras FP, Pontelli MC, Silva CM, Toller-Kawahisa JE, de Lima M, Nascimento DC, et al. SARS-CoV-2-Triggered Neutrophil Extracellular Traps Mediate COVID-19 Pathology. *J Exp Med* (2020) 217(12):e20201129. doi: 10.1084/jem.20201129
29. Nicolai L, Leunig A, Brambs S, Kaiser R, Weinberger T, Weigand M, et al. Immunothrombotic Dysregulation in COVID-19 Pneumonia is Associated With Respiratory Failure and Coagulopathy. *Circulation* (2020) 142 (12):1176–89. doi: 10.1161/CIRCULATIONAHA.120.048488
30. Zuo Y, Estes SK, Ali RA, Gandhi AA, Yalavarthi S, Shi H, et al. Prothrombotic Autoantibodies in Serum From Patients Hospitalized With COVID-19. *Sci Transl Med* (2020) 12:eabd3876. doi: 10.1126/scitranslmed.abd3876
31. Radermecker C, Detrembleur N, Guiot J, Cavalier E, Henket M, d'Emal C, et al. Neutrophil Extracellular Traps Infiltrate the Lung Airway, Interstitial, and Vascular Compartments in Severe COVID-19. *J Exp Med* (2020) 217(12): e20201012. doi: 10.1084/jem.20201012
32. Bonaventura A, Vecchié A, Dagna L, Martinod K, Dixon DL, Van Tassell BW, et al. Endothelial Dysfunction and Immunothrombosis as Key Pathogenic Mechanisms in COVID-19. *Nat Rev Immunol* (2021) 21:319–29. doi: 10.1038/s41577-021-00536-9
33. McFadyen JD, Stevens H, Peter K. The Emerging Threat of (Micro) Thrombosis in COVID-19 and Its Therapeutic Implications. *Circ Res* (2020) 127:571–87. doi: 10.1161/CIRCRESAHA.120.317447
34. Ciceri F, Beretta L, Scandroglio AM, Colombo S, Landoni G, Ruggeri A, et al. Microvascular COVID-19 Lung Vessels Obstructive Thromboinflammatory Syndrome (MicroCLOTS): An Atypical Acute Respiratory Distress Syndrome Working Hypothesis. *Crit Care Resusc* (2020) 22:95–7. doi: 10.51893/2020.2.pov2
35. Leppkes M, Knopf J, Naschberger E, Lindemann A, Singh J, Herrmann I, et al. Vascular Occlusion by Neutrophil Extracellular Traps in COVID-19. *EBioMedicine* (2020) 58:102925. doi: 10.1016/j.ebiom.2020.102925
36. Gollomp K, Kim M, Johnston I, Hayes V, Welsh J, Arepally GM, et al. Neutrophil Accumulation and NET Release Contribute to Thrombosis in HIT. *JCI Insight* (2018) 3:99445. doi: 10.1172/jci.insight.99445
37. Bilaloglu S, Aphinyanaphongs Y, Jones S, Iturrate E, Hochman J, Berger JS. Thrombosis in Hospitalized Patients With COVID-19 in a New York City Health System. *JAMA* (2020) 324(8):799–801. doi: 10.1001/jama.2020.13372
38. Cattaneo M, Bertinato EM, Birocchi S, Brizio C, Malavolta D, Manzoni M, et al. Pulmonary Embolism or Pulmonary Thrombosis in COVID-19? Is the Recommendation to Use High-Dose Heparin for Thromboprophylaxis Justified? *Thromb Haemost* (2020) 120:1230–2. doi: 10.1055/s-0040-1712097
39. Patel BV, Arachchillage DJ, Ridge CA, Bianchi P, Doyle JF, Garfield B, et al. Pulmonary Angiopathy in Severe COVID-19: Physiologic, Imaging, and Hematologic Observations. *Am J Respir Crit Care Med* (2020) 202:690–9. doi: 10.1164/rccm.202004-1412OC
40. Yao Y, Cao J, Wang Q, Shi Q, Liu K, Luo Z, et al. D-Dimer as a Biomarker for Disease Severity and Mortality in COVID-19 Patients: A Case Control Study. *J Intensive Care* (2020) 8:49. doi: 10.1186/s40560-020-00466-z
41. Xie J, Wu W, Li S, Hu Y, Hu M, Li J, et al. Clinical Characteristics and Outcomes of Critically Ill Patients With Novel Coronavirus Infectious Disease (COVID-19) in China: A Retrospective Multicenter Study. *Intensive Care Med* (2020) 46(10):1863–72. doi: 10.1007/s00134-020-06211-2
42. Naymagon L, Zubizarreta N, Feld J, van Gerwen M, Alsen M, Thibaud S, et al. Admission D-Dimer Levels, D-Dimer Trends, and Outcomes in COVID-19. *Thromb Res* (2020) 196:99–105. doi: 10.1016/j.thromres.2020.08.032
43. Thålin C, Aguilera K, Hall NW, Marunde MR, Burg JM, Rosell A, et al. Quantification of Citrullinated Histones: Development of an Improved Assay to Reliably Quantify Nucleosomal H3Cit in Human Plasma. *J Thromb Haemost* (2020) 18(10):2732–43. doi: 10.1111/jth.15003

Conflict of Interest: The authors declare that the research was conducted in the absence of any commercial or financial relationships that could be construed as a potential conflict of interest.

Publisher's Note: All claims expressed in this article are solely those of the authors and do not necessarily represent those of their affiliated organizations, or those of the publisher, the editors and the reviewers. Any product that may be evaluated in this article, or claim that may be made by its manufacturer, is not guaranteed or endorsed by the publisher.

frontiers in Immunology

ORIGINAL RESEARCH
published: 22 March 2022
doi: 10.3389/fimmu.2022.831763

The S1 Subunit of the SARS-CoV-2 Spike Protein Activates Human Monocytes to Produce Cytokines Linked to COVID-19: Relevance to Galectin-3

John T. Schroeder and Anja P. Bieneman*

The Department of Medicine, Division of Allergy and Clinical Immunology, Johns Hopkins Asthma and Allergy Center, Johns Hopkins University, Baltimore, MD, United States

Coronavirus disease 2019 (COVID-19), caused by the severe acute respiratory syndrome coronavirus 2 (SARS-CoV-2), rapidly evolved into a pandemic –the likes of which has not been experienced in 100 years. While novel vaccines show great efficacy, and therapeutics continue to be developed, the persistence of disease, with the concomitant threat of emergent variants, continues to impose massive health and socioeconomic issues worldwide. Studies show that in susceptible individuals, SARS-CoV-2 infection can rapidly progress toward lung injury and acute respiratory distress syndrome (ARDS), with evidence for an underlying dysregulated innate immune response or cytokine release syndrome (CRS). The mechanisms responsible for this CRS remain poorly understood, yet hyper-inflammatory features were also evident with predecessor viruses within the β-coronaviridae family, namely SARS-CoV-1 and the Middle East Respiratory Syndrome (MERS)-CoV. It is further known that the spike protein (S) of SARS-CoV-2 (as first reported for other β-coronaviruses) possesses a so-called *galectin-fold* within the N-terminal domain of the S1 subunit (S1-NTD). This fold (or pocket) shows structural homology nearly identical to that of human galectin-3 (Gal-3). In this respect, we have recently shown that Gal-3, when associated with epithelial cells or anchored to a solid phase matrix, facilitates the activation of innate immune cells, including basophils, DC, and monocytes. A synthesis of these findings prompted us to test whether segments of the SARS-CoV-2 spike protein might also activate innate immune cells in a manner similar to that observed in our Gal-3 studies. Indeed, by immobilizing S components onto microtiter wells, we show that only the S1 subunit (with the NTD) activates human monocytes to produce a near identical pattern of cytokines as those reported in COVID-19-related CRS. In contrast, both the S1-CTD/RBD, which binds ACE2, and the S2 subunit (stalk), failed to mediate the same effect. Overall, these findings provide evidence that the SARS-CoV-2 spike protein can activate monocytes for cytokines central to COVID-19, thus providing insight into the innate immune mechanisms underlying the CRS and the potential for therapeutic interventions.

Keywords: inflammation, lectin, cytokine, virus, innate immunity, dendritic cell, basophil

OPEN ACCESS

Edited by:
Daniela Novick,
Weizmann Institute of Science, Israel

Reviewed by:
Sharvan Sehrawat,
Indian Institute of Science Education and Research Mohali, India
Michelle Gill,
University of Texas Southwestern Medical Center, United States

****Correspondence:***
John T. Schroeder
schray@jhmi.edu

Specialty section:
This article was submitted to Inflammation, a section of the journal Frontiers in Immunology

Received: *08 December 2021*
Accepted: *02 March 2022*
Published: *22 March 2022*

Citation:
Schroeder JT and Bieneman AP (2022) The S1 Subunit of the SARS-CoV-2 Spike Protein Activates Human Monocytes to Produce Cytokines Linked to COVID-19: Relevance to Galectin-3. Front. Immunol. 13:831763. doi: 10.3389/fimmu.2022.831763

INTRODUCTION

The Coronavirus disease 2019 (COVID-19) pandemic, caused by the severe acute respiratory syndrome coronavirus 2 (SARS-CoV-2), has caused devastation worldwide with massive health consequences that continue to spawn enormous socioeconomic and political issues. While vaccines have had clear beneficial impact, COVID-19 cases, and a proportional number of deaths, continue to swell. And, as variants of the virus concurrently arise, so likely the need for updated vaccines and/or other preventative measures.

As with its predecessors within the Coronaviridae family, including SARS-CoV and the Middle East Respiratory Syndrome (MERS)-CoV, infection with SARS-CoV-2 is commonly linked to the development of acute respiratory distressed syndrome (ARDS) (1, 2). ARDS is the life-threatening condition involving a leakage of fluid into the lung that is most often responsible for the mortality seen in severe COVID. In addition, studies continue to reveal evidence for a dysregulated hyper-inflammation, or cytokine release syndrome (CRS) that is thought to contribute to acute lung injury and development of ARDS (3, 4). Among the cytokines over-expressed in COVID-19 are those generally linked to innate immunity, including pro-inflammatory cytokines (e.g. IL-6, TNF-α, IL-1β), chemokines (e.g. CXCL10/IP-10, CCL2/MCP-1, CCL3/MIP-1α, CCL4/MIP-1β, and IL-8), immunoregulatory cytokines (e.g. IL-10, TGF-β), and growth factors (G-CSF) (5–11). Studies are also emerging with evidence that several of these cytokines associate with and/or are predictive of severe COVID, with IL-6, CXCL10/IP-10, and IL-10 most often cited (7, 9, 10, 12, 13). Likewise, several studies point to various innate immune cells – many of which are well known for producing these cytokines– to be hallmark in the lung inflammation associated with COVID, with monocytes and macrophages most often implicated in the underlying pathogenesis of the disease (14–17). Yet, despite the mounting reports, there remains a poor understanding of the exact mechanism(s) underlying the dysregulated innate immune response and CRS associated with COVID-19.

Like SARS-CoV-1, SARS-CoV-2 uses Angiotensin-converting enzyme 2 (ACE2) as its major receptor to infect host cells (namely epithelial cells), which is mediated *via* the virus' envelope-anchored spike glycoprotein (S). The mature S glycoprotein is a heavily glycosylated trimer, with each protomer composed of 1260 amino acids (residues 14-1273). The S1 subunit is composed of 672 amino acids (residues 14-685) and organized into four domains: an N-terminal domain (NTD), a C-terminal domain (CTD), which is also known as the receptor-binding domain (RBD), and two subdomains (SD1 & SD2). A transmembrane S2 subunit forms the stalk and is composed of 588 amino acids (residues 686-1273) (18, 19).

Within the NTD of SARS-CoV-2 (and other β-coronaviruses) is a region often referred to as the "galectin-fold", given its high degree of structural homology to that of human galectin-3 (Gal-3) (20, 21). Because of this remarkable similarity, it has been proposed that the S1-NTD of SARS-CoV-2 may very well act like Gal-3 and that this might explain, in part, the immunological sequelae observed in COVID-19 (22, 23). Indeed, intracellular Gal-3 has been linked to immune cell activation, namely that of monocytes/macrophages (24). We also recently reported evidence that epithelial cell-associated Gal-3 (EC-Gal-3) can activate a variety of innate immune cells to produce pro-inflammatory cytokines (25–27). In particular, we showed the activation of human dendritic cells (DC) and monocytes, demonstrating that these cells produced high levels of IL-6 and TNF-α –two hallmark cytokines in COVID-19-associated CRS (27).

A synthesis of the above observations prompted us to test whether portions of the SARS-CoV-2 spike protein might also activate innate immune cells in a manner similar to that observed in our Gal-3 studies. Indeed, by immobilizing subunit components onto microtiter wells, we show that the S1 subunit (and likely the NTD portion) activates human monocytes to produce a near identical pattern of cytokines to that observed in COVID-19-related CRS. Other regions of the spike protein, such as S1-CTD/RBD, which binds ACE2, or the S2 subunit (stalk), failed to activate monocytes. Overall, these findings provide novel evidence that the S1 subunit of the SARS-CoV-2 spike protein directly activates monocytes for cytokines central to COVID-19-related CRS, with mechanistic implications fundamental to the pathogenesis of the disease.

MATERIALS AND METHODS

Special Reagents, Buffers, and Media

The following reagents were purchased: crystallized human serum albumin (Calbiochem-Behring Corp, La Jolla, CA); PIPES, FCS, and crystallized BSA (Sigma-Aldrich, Allentown, PA); gentamicin, IMDM, and nonessential amino acids (Life Technologies, Inc, Grand Island, NY); Percoll (Pharmacia Biotec, Inc., Piscataway, NJ); rhIL-3 and the following recombinant SARS-CoV-2 Spike protein subunits: 1) S1/S2 "active trimer" (cat. # 10549-CV) consisting of a.a. 16-1211 and made resistant to Furin cleavage, yet capable of binding ACE2; 2) S1-RBD (cat. # 10500-CV) consisting of a.a. 319-541 and capable of binding ACE2; S1 (cat. # 10569-CV) consisting of a.a. 16-681, and S2 (cat. # 10594-CV) consisting of a.a. 686-1211. All were c-terminal His-tagged, HEK cell-derived, and contained no detectable endotoxin (R&D Systems, Minneapolis, MN). Some experiments used another S1 subunit (cat. # REC31806) containing a.a. 1-674) –also HEK cell-derived and with no detectable endotoxin yet Fc-tagged (The NativeAntigen Co., Oxfordshire, UK). All PIPES-containing buffers used in this study (e.g. 1x PIPES, PIPES/albumin/glucose –PAG, and PAG-EDTA) were made from a 10x solution, as previously described (27, 28). C-IMDM consisted of IMDM supplemented with 5% FCS, non-essential amino acids, L-glutamine, 10 μg/ml gentamicin, pH 7.2-7.4.

Coupling of Recombinant SARS-CoV-2 Spike Protein Components to Microtiter Plate Wells

Recombinant SARS-CoV-2 spike protein components were coupled to polystyrene microtiter plate wells (ThermoFisher, Grand Island, NY). In brief, wells immediately received 0.100 ml

of a 5 μg/ml solution after preparing in carbonate buffer (ThermoFisher, Grand Island, NY). Plates were covered and placed at 4°C for overnight. Within ~30 min. of initiating cell culture, the contents of each well was aspirated, with wells then washed three times using 0.250 ml 1x PIPES per wash. After the final wash, each well immediately received 0.100 ml C-IMDM before adding cells and stimuli for cell culture, as described in detail below. In the experiments using galectin-3-binding protein (LGALS3BP) as a reagent to block S1-induced monocyte activation, washed wells first received 0.200 ml PAG buffer to which 0.050 ml of serially-diluted solutions of 5x LGALS3BP (also in PAG) were immediately added. These plates were then incubated at 37°C, 5% CO_2 for 1 hr. before transferring to 4°C until used for cell culture (~3h total). At that time, each well was again washed 3x with 1x PIPES (0.250 ml per wash) before adding 0.100ml C-IMDM to initiate set-up for cell culture.

Isolation of Basophils, Monocytes and DC Subtypes From Blood

Basophils, monocytes and DC subtypes were prepared from residual TRIMA cassettes from anonymous subjects undergoing platelet pheresis. In some instances, venipuncture was performed on consenting adults (age range, 21-65 years) using a protocol approved by the Johns Hopkins University Institutional Review Board. Subjects were selected regardless of allergic status. Buffy-coats from both specimen sources were subjected to double-Percoll density centrifugation, which produces both basophil-depleted cell (BDC) and basophil-enriched cell (BEC) suspensions, as described (28). Basophils were purified from BEC suspensions by negative selection using an antibody cocktail & microbeads (StemCell Technologies, Vancouver, Canada, cat# 14309-A01P), and collecting the flow-thru from magnetized LS columns (Miltenyi Biotec, Gaithersburg, MD), as described in detail (28). Basophil purities ranged between 98% and >99%, as assessed by Alcian blue staining. The BDC suspensions were washed 4x to remove platelets before preparing monocytes and DC subtypes. Monocytes were prepared using $CD14^+$ selection by collecting those binding to magnetized LS columns (Miltenyi), Monocyte suspensions regularly exceed 95% purity when prepared in this manner, as assessed by flow cytometry. The monocyte-depleted flow-thru cells were then partitioned to separately isolate pDC and mDC using negative selection protocols (StemCell Technologies, Vancouver, Canada). The few numbers of DCs isolated did not always allow for flow cytometric analysis, but previous studies indicate purities in the range of 50-90%, based on $CD123^+BDCA2^+$ (pDC) and $BDCA1^+$ (mDC) staining (27).

Co-Culture Conditions

All cultures to induce cytokine production by basophils, monocytes and DC subtypes were done in a manner similar to that previously described (26, 27). In brief, cells were suspended in C-IMDM such that $2x10^4$ (DC and monocytes) and $1x10^5$ (basophils) were added in 0.050 ml volumes to flat-bottom wells (96-well plates) pre-coated with spike protein components, and with all wells containing 0.100 ml C-IMDM. Immediately after adding cells, 0.050 ml of 4x the final IL-3 concentration (or medium alone) was added and the cultures incubated as indicated at 37°C, 5% CO_2. Supernatants were harvested after 20h unless otherwise indicated and tested for cytokine secretion.

Cytokine Measurements

Supernatants were analyzed for cytokine content using Bio-Plex plates capable of simultaneously measuring 27 cytokines in a 0.050 ml volume using Luminex technology (Bio-Rad, Hercules, CA). Assays were performed according to the manufacturer's specifications and included standard curves for each cytokine. Plates were analyzed using a Bio-Plex 200 instrument (Bio-Rad, Hercules, CA). Supernatants were additionally analyzed for IL-6 protein by ELISA (ThermoFisher. Grand Island, NY).

Statistical Analysis

Statistical analyses were performed with Prism 7.0 software (GraphPad, Software, LaJolla, Calif.) Analyses were performed using multiple paired t-test analyses unless otherwise specified. Differences were considered statistically significant at a P value <0.05.

RESULTS

S1 Subunit of SARS-CoV-2 Activates Human Blood Monocytes to Secrete Cytokines Linked to COVID-19

In testing whether recombinant components of the SARS-CoV-2 spike protein activate innate immune cells for cytokine production, we focused on the effects potentially seen with basophils, monocytes, and dendritic cell subtypes (pDC and mDC) –all freshly isolated from blood. These cell types were chosen because we have shown that all are activated by EC-Gal-3. And, since the S1-NTD of the spike protein expresses a "galectin-fold", we hypothesized that each might likewise be stimulated. Two additional approaches were done for these experiments: 1) cultures were performed in microtiter plates pre-coated with spike protein components, since preliminary results indicated that proteins used in solution showed no to little capacity to stimulate cells (data not shown); and 2) we investigated the effects of co-stimulation with IL-3. Importantly, both *in vitro* culture strategies had proved instrumental is establishing the role of Gal-3 in activating these cells types (26, 27).

We first investigated the effects on those pro-inflammatory cytokines that are hallmark in COVID-19. As shown in **Figure 1A**, effects were most evident with IL-6 production by monocytes. In particular, culture wells pre-coated with S1 induced 194 ± 64 pg/10^6 monocytes vs. 41 ± 20 seen with medium alone. For comparison, monocytes averaged less IL-6 secretion in culture wells coated with either the S2 or the S1/S2 "active Trimer" components, with levels just 20 ± 8 and 21 ± 9 pg/10^6, respectively. These amounts, however, were not significantly different from the IL-6 secreted in control cultures with medium alone. As predicted, the addition of IL-3 (10 ng/ml) augmented all responses and most significantly in culture wells

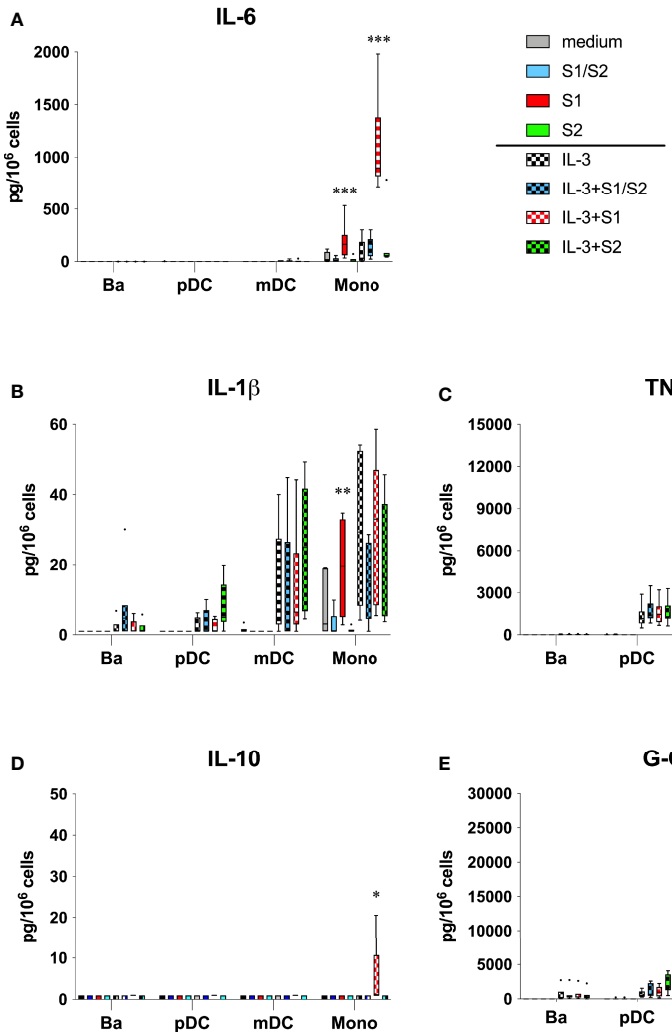

FIGURE 1 | **(A–E)** Cytokines linked to COVID-19 are induced by the S1 subunit of the SARS-CoV-2 spike protein. Subunit components of the SARS-CoV-2 spike protein were passively absorbed onto polystyrene culture wells, as described in the Materials & Methods section. After overnight incubation at 4°C followed with 3x washes, basophils (Ba), pDC, mDC, and monocytes (Mono) were then cultured as indicated in medium alone or with IL-3 added to 10 ng/ml. After 20h incubation, cell-free supernatants were harvested for analysis of the indicated cytokines using multiplex analysis. Box-Whisker plots (Tukey's method) represent results from different donor cell preparations (n=7). Responses to spike protein components were tested for significance by comparing to medium/IL-3 controls. ***P<0.001, **P<0.01, *P<0.05.

coated with S1, where IL-6 levels averaged 12.5-fold more than those detected in the IL-3 controls (1104 ± 167 vs. 88 ± 48 pg/106, respectively). In contrast, IL-6 levels averaged just ~2-fold above the IL-3 controls for wells coated with S2 or the active Trimer (163 ± 104 and 148 ± 38 pg/10^6, respectively), with neither significantly different. These IL-6 responses were not seen with any of the other cell types tested (basophils, pDC, or mDC), where levels mostly went undetected.

With results signifying that the S1 component of the spike protein activates monocytes for IL-6 secretion, additional analyses revealed a comparable pattern for other COVD-19 relevant cytokines produced in the same monocyte cultures. For example, IL-1β and TNF-α were both induced in culture wells coated with the S1 subunit, which were significantly higher than those measured in uncoated wells or wells containing either the S2 or S1/S2 components (**Figures 1B, C**). The addition of IL-3 did not augment these responses as it did for IL-6. Instead, IL-3 itself triggered monocytes to produce IL-1β and TNF-α. Whereas pDC and mDC also produced these cytokines, they primarily did so in response to IL-3 alone, with no evidence that any of the spike protein components directly acted on these DC subtypes. The S1 subunit also induced IL-10 in a couple of the monocyte cultures, although the levels were generally much lower and only evident when IL-3 was included. In contrast, none of the other spike protein components acted in a similar capacity to induce this cytokine (**Figure 1D**).

Several growth factors were among the panel of cytokines assayed by the multiplex analysis. As shown in **Figure 1E**, only the S1 unit mediated any significant affect by directly inducing

G-CSF secretion by monocytes. There was a trend for increased production of G-CSF by mDC when cultured with S2 and in the presence of IL-3, yet this did not reach statistical significance. None of the spike protein components significantly impacted any other cell type for the production of the other growth factors investigated, which included FGF, PDGF, CM-CSF, or VEGF (**Figure S1**, online supplemental data).

As shown in **Figures S2**, **S3** of the online supplemental data, the spike protein components mediated little to no effect on most of the Th1 and Th2 interleukins analyzed, despite some predictable responses that lent validation to the multiplex analysis. For example, basophils cultured in IL-3 were clearly the predominant source of interleukin-13 among the four cell types investigated, as expected. However, these responses were not affected by any of the spike protein components analyzed (**Figure S3A**). Interestingly, the secretion of both IL-1ra and IL-15 was significantly affected, but not specifically by the S1 subunit. For example, IL-1ra was spontaneously secreted by monocytes in medium alone, yet this response was significantly reduced in culture wells coated with each of the three spike protein components (**Figure S2S**). Likewise, IL-15 was secreted by monocytes in response to IL-3, yet all three components significantly suppressed this response (**Figure S3E**).

S1 Subunit of SARS-CoV-2 Activates Human Blood Monocytes to Secrete Chemokines Linked to COVID-19

The S1 subunit also acted on monocytes to produce several chemokines that are prominent in severe COVID-19 (**Figures 2A–E**). In particular, CXCL10/IP-10, CCL3/MIP-1α, and CCL4/MIP-1β were all significantly induced in culture wells coated with S1, but not in culture wells containing S2 or the S1/S2 component. IL-3 augmented these responses for the latter two chemokines, although this was only significant for CCL4/MIP-1β. Oddly, both the S2 and S1/S2 components appeared to inhibit monocytes from producing these chemokines when compared to the controls, although levels were not significantly different. Likewise, a similar pattern was evident for CCL2/MCP-1, where S1 showed only a trend for inducing this chemokine vs. the medium control, yet significantly induced this this cytokine compared to the other spike protein components (**Figure 2B**). When used alone, the S1 subunit showed no capacity to induce any of these chemokines from the other cell types (basophils, pDC, or mDC). However, when combined with IL-3, the S2 subunit significantly induced both CCL3/MIP-1α and CCL/MIP-1β from mDC, but not from any other cell type. None of the spike protein components acted on the other chemokines measured in the multiplex analysis, including IL-8 (**Figure 2E**), CCL5/RANTES (**Figure S1E**), or CCL11/eotaxin (**Figure S3D**).

An overall summary of the monocyte cytokines significantly induced and/or affected by the S1 subunit is shown in **Table S1** of the online supplemental data. Included in these analyses are comparisons between values observed with S1 vs. those made in response to the S1/S2 and S2 components. In general, the latter two showed a trend to induce less cytokine, even when comparing to the medium and IL-3 controls.

Activation of Monocytes by the S1 Subunit Does Not Track With the CTD/RBD Region Known to Bind ACE2

Structural analyses indicate that the so-called galectin-fold lies within the NTD of the S1 subunit (20). However, the S1 subunit used in the above cytokine experiments consisted of both the NTD and CTD/RBD (i.e. a.a. residues 1-681). Hence, it remained possible that the capacity of S1 to activate monocytes for cytokine secretion might still be attributed to the CTD/RBD region, and if confirmed, then a potential role for ACE2 despite this enzyme not typically found on immune cells. Therefore, additional experiments were conducted using another recombinant protein consisting of only the CTD/RBD region of S1 (a.a. residues 319-541). This component retains the capacity to bind ACE 2, as indicated by the data sheets provided by R&D Systems yet lacks the NTD region. For these experiments, we focused only on the capacity to induce IL-6, since this cytokine was readily secreted by the S1 subunit alone. However, cultures co-stimulated with IL-3 were also included with the goal of maximizing the IL-6 response. Measurements were performed using ELISA and included several of the previously analyzed specimens simply to lend validation of the IL-6 findings using the multiplex analysis. **Figure 3** shows that the same pattern of IL-6 was indeed detected as in the multiplex analysis and with comparable levels. However, the added experiments indicated little to no capacity for the CTD/RBD component to induce IL-6 from monocytes (used alone or with IL-3), despite robust responses from the same donor cells when using the full length S1 subunit that additionally contains the NTD.

Galectin-3 Binding Protein Suppresses IL-6 Secretion by Monocytes Activated by the S1 Subunit

In a recent study conducted with the purpose of identifying novel serum proteins that bind/interact with the SARS-CoV-2 spike protein, the authors reported evidence that galectin-3 binding protein (LGALS3BP) was the top contender detected (29). Therefore, in a final set of experiments, we tested whether LGALS3BP might suppress the S1 subunit from activating monocytes for IL-6 secretion. To conduct these experiments, various concentrations of LGALS3BP were added to culture wells pre-coated with the S1 component. After incubating, the wells were then washed 3 times to remove any excess LGALS3BP. Again, IL-3 was added to maximize the S1-induced response. As shown in **Figure 4**, a consistent dose response suppression of the IL-6 produced by monocytes was observed with increasing amounts of LGALS3BP for an average inhibition of 59% (range 50-70%) observed at the 1μg/ml concentration (P=0.012).

DISCUSSION

The motivation for conducting this study evolved from two independent observations. The first originated from our work prior to the COVID-19 pandemic in which we showed evidence

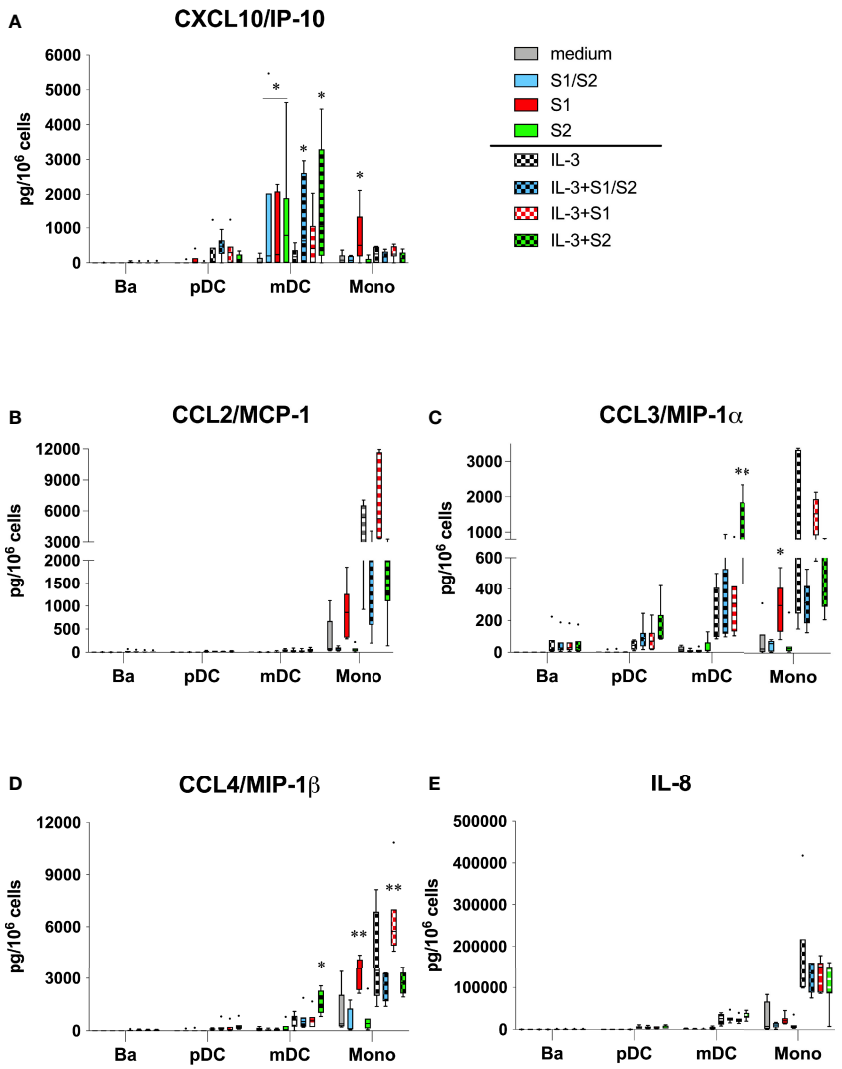

FIGURE 2 | **(A–E)** Chemokines linked to COVID-19 are induced by the S1 subunit of the SARS-CoV-2 spike protein. The same culture supernatants described in **Figure 1** were also assayed for the indicated chemokines using multiplex analysis. Box-Whisker plots (Tukey's method) represent results from different donor cell preparations (n=7). Responses to spike protein components were tested for significance by comparing to medium/IL-3 controls. **P<0.01, *P<0.05.

that epithelial cell-associated Gal-3 (EC-Gal-3) can effectively activate various innate immune cells for cytokine production (25–27). The second arose after the start of the pandemic upon learning that the SARS-CoV-2 virus contains a structurally relevant "galectin-fold" or pocket within the NTD of the S1 subunit of its spike protein –a structural feature first identified in the spike proteins of its predecessors (SARS-CoV-1 and MERS-Co) (20, 21). A synthesis of the two led us to hypothesize that the innate immune cytokine response (or CRS), which is most prominent in severe COVID-19, results, in part, from the S1-NTD of the spike protein mimicking the cytokine-inducing potential we had observed with EC-Gal-3. For further context, we have recently demonstrated that monocytes, and to a lesser extent DC subtypes, secrete IL-6 and TNF-α when co-cultured with A549 epithelial cells. However, these cytokine responses were eliminated upon knocking down Gal-3 expression in this adenocarcinoma cell line (27). We had also shown in earlier reports that IgE-expressing basophils produced IL-4 and IL-13 when co-cultured with EC-Gal-3 (26). Moreover, many of these EC-Gal-3-dependent cytokine responses were similarly replicated by culturing basophils, monocytes, and DC with microspheres coupled with rhGal-3 (MS-Gal-3). And, that IL-3 augmented Gal-3 dependent cytokine production by several of the innate immune cells, in particular basophils and pDC –those that bear the highest levels of IL-3R (CD123).

To address the belief that S1-NTD acts similarly to Gal-3 in promoting cytokine responses, we took the approach of using recombinant and endotoxin-free proteins that encompass various regions of the SARS-CoV-2 spike protein and that collectively span the entire ~1211 amino acid sequence.

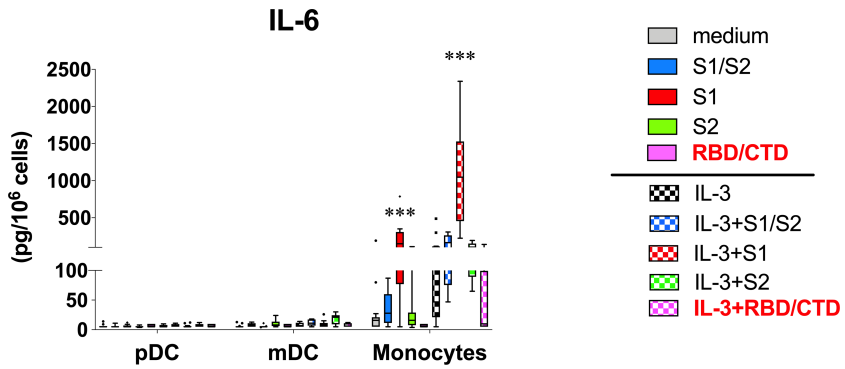

FIGURE 3 | Capacity for S1 to activate monocytes for IL-6 secretion is lost using only the CTD/RBD region known to bind ACE2. Additional experiments (n = 5) were conducted like those described in **Figure 1** to test whether the S1-CTD/RBD region, which lacks the NTD, is capable of activating monocytes and DC. These experiments included using the full length S1 as a positive control. Since IL-6 measurements were made using ELISA, several supernatants from the multiplex analysis (**Figure 1**) were included for added validation. Box-Whisker plots (Tukey's method) represent results from different donor cell preparations (n = 5-14). Responses to spike protein components were tested for significance by comparing to medium/IL-3 controls. ***P < 0.00001.

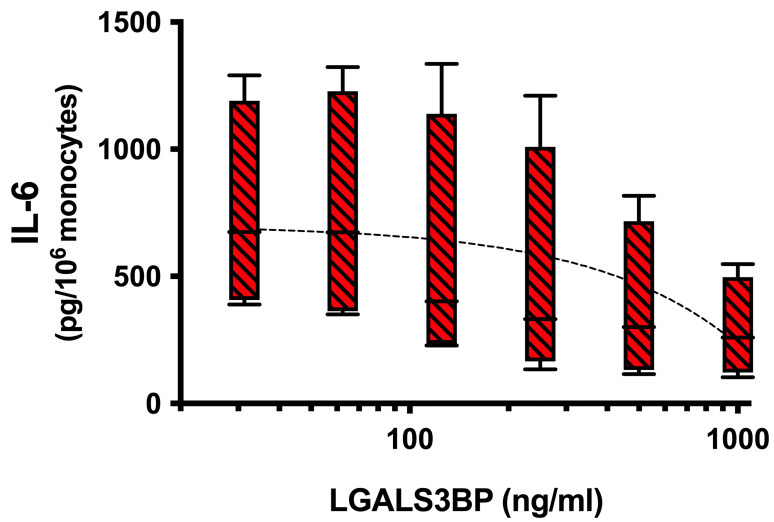

FIGURE 4 | Galectin-3 binding protein (LGALS3BP) suppresses IL-6 secretion by monocytes activated by the S1 subunit. Increasing concentrations of LGALS3BP were added to wells pre-coated with the S1 subunit, as described in the *Materials & Methods*. After incubating, plate wells were washed 3x to remove excess LGALS3BP before adding monocytes and IL-3 for cell culture. Supernatants were harvested after 20h incubation and assayed for IL-6 by ELISA. Box-Whisker plots represent results from different cell preparations (n = 4), with a linear regression line shown (P = 0.012). IL-6 levels induced by S1 alone without LGALS3BP averaged 713 ± 258 pg/10^6 monocytes (n = 4).

Importantly, with the exception of the S2 subunit (stalk), all of the recombinant proteins investigated possess the CTD/RBD, which, according to data sheets supplied by R&D Systems, enables functional binding to ACE2. Unfortunately, none of the proteins consisted only of the NTD. Nonetheless, of those investigated, only the S1 subunit, comprising the first ~615 amino acids and containing both the NTD and CTD, showed the capacity to induce cytokines from monocytes. In fact, this activity was observed using recombinant S1 proteins made by two different companies (see *Materials & Methods*). In contrast, both the CTD/RBD alone (a.a. 319-541) and the S2 subunit (a.a. 686-1211) failed to activate monocytes, thus implying the importance of the NTD –the region showing structural homology to Gal-3 (20, 21).

Most unexpectantly, the so-called S1/S2 "active trimer", which encompasses nearly the entire spike protein sequence (a.a. 16-1211), failed to induce significant cytokine levels, despite including the S1-NTD. Exactly why this full-length spike protein lacked the capacity to activate monocytes remains unknown. However, we propose that in this form, the S1-NTD may not be properly exposed, perhaps even hidden, and thus unable to activate monocytes, as did the S1 subunit. In fact,

R&D Systems specifies modifications to this protein making it resistant to furin (and perhaps other serine proteases), which means cleavage at the S1/S2 junction site is not possible. Accordingly, we further propose herein that a similar mechanism seems possible with the spike protein of live SARS-CoV-2 virus, at least during the course of infecting host cells. For instance, the virus attaches to ACE2 molecules expressed on host airway epithelial cells by utilizing the S1-CTD/RBD portion of its spike protein. However, it is known that viral entry is mediated by the S2 subunit, which is only primed and exposed after cleavage at the S1/S2 linkage site by the transmembrane serine protease 2 (TMPRSS2) and possibly by other host cell-associated proteases (30, 31). As a consequence, this cleavage event may serve to unmask the S1-NTD on the surfaces of infected cells, especially if the S1-CTD portion remains bound/anchored to ACE2, as conceptualized in **Figure 5**. If this mechanism is correct, it's logical to hypothesize that the S1-NTD of the spike protein can then act in a manner similar to EC-Gal-3 and thus activate innate immune cells such as monocytes/macrophages that infiltrate virally infected lesion sites. Whether such a mechanism contributes to the CRS often seen in severe COVID-19 disease remains speculative at this time, yet the hypothesis is logical and thus requires further investigation.

Importantly, the mechanism proposed above (and in **Figure 5**) eliminates the prerequisite that immune cells express ACE2, which seems necessary if the virus was to promote cytokine production and dysregulation by directly infecting monocytes/macrophages *via* this receptor. However, there is currently little evidence in the literature to support ACE2 expression on human immune cells. Moreover, with the exception of the S2 protein, all the other spike protein components used in this study reportedly bind ACE 2. It therefore seems probable that all would have activated monocytes for cytokine production if binding to ACE 2 is critical for this response. In contrast, only the S1 subunit containing the NTD showed a capacity to activate monocytes. Naturally, our study did not use live virus, let alone test its capacity to bind ACE2, nor did we test whether it uses a variety of other receptors that have been proposed to facilitate its capacity to directly infect monocytes for induction of cytokines (14, 32–34). Therefore, we are not dismissing these possibilities yet only suggesting the above as another potential mechanism based on our findings using recombinant spike protein components and the resemblance of the S1-NTD region to that of human Gal-3.

Interestingly, of the innate immune cells co-cultured with plate bound S1 protein, only monocytes reacted by producing relevant cytokines. Basophils, pDC and mDC did not react to this

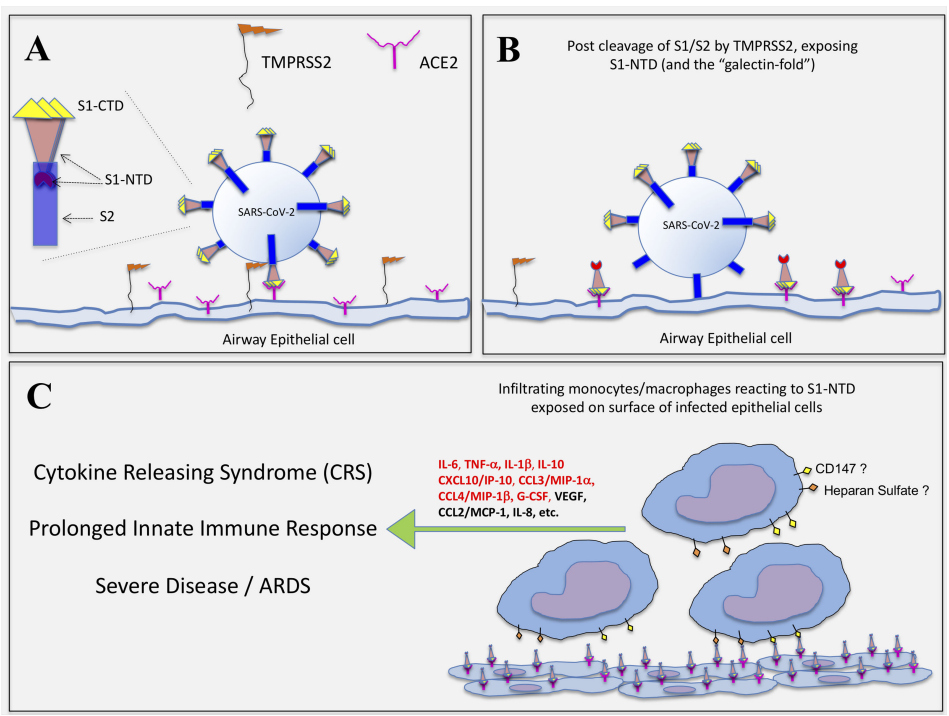

FIGURE 5 | Hypothetical representation of how SARS-CoV-2 infection exposes the S1-NTD (and "galectin-fold") on epithelial cells for potential activation of infiltrating monocytes. **(A)** SARS-CoV-2 infection of epithelial cells is initiated with the binding of S1-CTD/RBD to ACE2. The serine protease, TMPRSS2, expressed on host cells then cleaves the spike protein at the S1/S2 linkage. **(B)** The S2 subunit undergoes structural changes, serving first to anchor the virus and then facilitating its entry into the cell. It is proposed that the S1/S2 cleavage event simultaneously exposes the S1-NTD, which extends outward as the S1-CTD/RBD remains bound to ACE2. **(C)** Infiltrating monocytes/macrophages are then activated to produce COVID-related cytokines *via* cell surface glycoproteins (e.g. CD147) and/or polysaccharides (e.g. Heparan Sulfate) interacting with S1-NTD, which mimics EC-Gal-3. Those cytokines indicated in red type were significantly impacted by the S1 subunit in this study.

spike protein subunit, as was predicted based on our prior work showing EC-Gal-3-dependent activation. While there is currently no precise explanation for these findings, one could argue that the S1-NTD, while closely resembling Gal-3, may not function to the full range of this lectin, especially given that we only tested recombinant protein. Moreover, Gal-3 is somewhat unique among the known mammalian galectins in that it can exist in many forms, ranging in structure from monomers to multivalent pentamers, each potentially having different binding affinities for many kinds of glycoproteins that contain the β-galactosides required for binding this lectin (35). For example, studies conducted ~30 years ago were among the first to show that Gal-3 binds IgE (hence, the early name of epsilon binding protein, ϵBP) (36). In fact, this partly explained its capacity to activate RBL cells (a mast cell line) for serotonin release (37), and more recently why basophils were required to express this immunoglublin when activated by EC-Gal-3 (26). However, Gal-3 has since been shown to bind many other non-IgE glycoproteins, including those for which the SARS-CoV-2 spike protein reportedly interact with, such as heparan sulfate (38) and CD147 (39). Although we did not explore the ligand(s) or receptor(s) on monocytes potentially binding the S1 subunit, it's reasonable to hypothesize involvement of heparan sulfate and/or CD147 since both are reportedly expressed on monocytes (40, 41). Moreover, it seems possible that IL-3 may modulate expression of the putative receptor, since this factor generally augmented S1-induced cytokine secretion. Whether it acts *in vivo* to impact severe COVID-19 is presently unknown. Nonetheless, IL-3 is reported to promote the alternative activation of monocytes *in vitro*, thus it seemingly affects the plasticity of these cells (42). Future studies are required to determine the exact molecule/receptor on monocytes responsible for interacting with the S1 subunit to trigger cytokine secretion and whether IL-3 modulates its expression. Of particular importance, monocytes and macrophages are currently regarded to be the primary innate immune cells contributing to the CRS associated with COVID-19 (15–17). Therefore, the observation that monocytes were the only cells reactive to S1-NTD among those tested is consistent with this line of thought.

The pattern of monocyte-derived cytokines induced by the S1 subunit is among the more striking observations revealed in this study because the profile is remarkably similar to that implicated in the CRS associated with severe COVID-19. Again, IL-6 was the cytokine most consistently induced by the S1 subunit, which occurred regardless of whether IL-3 was added to augment the response. Likewise, IL-6 is perhaps the most consistently elevated cytokine associated with COVID-19 (7, 10, 13), which was the impetus for early trials testing whether blocking the activity of this cytokine (e.g. with anti-IL-6 receptor antibodies such as tocilizumab and sarilumab) might be useful in treating or preventing severe pneumonia in critically ill COVID-19 patients (43). Indeed, several studies have reported some efficacy in combating COVID-19 by blocking IL-6 activity (44, 45). To a lesser extent, TNF-α and IL-1β were other pro-inflammatory cytokines significantly induced by the S1 subunit and they too are cytokines that are generally increased in COVID-19. Interestingly, IL-10 has been linked to the CRS, but may play a pathological role by suppressing otherwise beneficial DC and T cell activity (46). While levels of this cytokine were generally low and detected in just a few of our experiments, its secretion was only evident when S1 was included in the culture (**Figure 1D**).

Several chemokines linked to COVID-19 were also significantly induced by the S1 subunit, including CCL3/MIP-1α, CCL4MIP-1β, and CXCL10/IP-10. All are implicated in playing a role in monocyte recruitment and are reportedly secreted by monocytes. Several studies, in fact, have reported CXCL10/IP-10 as a key marker of severe disease (9, 12). While our study also showed DC to be a source of this chemokine, only monocytes produced it in response to S1. In contrast, we observed no significant induction of CCL2/MCP-1 (only a trend) or IL-8 by S1, even though several studies report these chemokines increased in COVID-19 (47, 48). The same was true for VEGF (8). However, G-CSF was the only growth factor among those included on our multiplex panel that was significantly induced by S1 alone –it too is linked to COVID-19 (8).

As expected, no Th1/Th2 cytokines were induced by S1 or any of the spike protein components. Indeed, we know of no studies that consistently report increased level of any Th1/Th2 cytokines occurring with COVID-19. IL-2R levels are reported increased in the disease, but this cytokine was not among those investigated in our multiplex panel. Interestingly, our results showed that both IL-15 and IL-1ra, which were produced by monocytes when cultured in medium alone or with IL-3, were significantly decreased by all of the spike protein components tested. The bases for these latter findings remain unclear. Although, IL-1ra has been implicated in immune homeostasis, its suppression by the spike protein may thus help to promote dysregulation (1). Obviously, our *in vitro* cytokine findings do not definitively prove that the S1 subunit of the spike protein is responsible for inducing these in actual COVID-19 disease, but the comparison is quite striking and thus warrants further investigation.

To further support the notion that S1-NTD mimics Gal-3 in its capacity to activate immune cells, we demonstrated that Gal-3 binding protein, LGALS3BP, blocked (up to ~70%) the ability of the S1 subunit to activate monocytes. The rationale for conducting this set of experiments was two-fold. First, LGALS3BP is long known to interact with Gal-3, hence the name given to this 90kD protein. Therefore, we reasoned that it should also interact with S1-NTD, given the high degree of structural homology of this component with that of Gal-3. Second, a recent study reported evidence that recombinant SARS-CoV-2 spike protein, when added to serum/plasma specimens, specifically interacted with LGALS3BP, as determined by analysis using mass-spectrometry (29). Importantly, in conducting the experiments herein, we added increasing concentrations of LGALS3BP to wells pre-coated with the S1 subunit. After incubating, the wells were then washed extensively to remove any unbound LGALS3BP. Thus, not only was residual unbound protein removed prior to cell culture, which seemingly reduced any chances of LGALS3BP directly interacting with monocyte, its apparent interaction with plate bound S1 seemed stable enough to suppress monocyte activation. Overall, these results support the concept that the S1-NTD of the SARS-CoV-2 spike protein does, indeed, act like Gal-3.

In conclusion, the COVID-19 pandemic caused by the SARS-CoV-2 virus has to date claimed the lives of some 5.7 million worldwide, with over 900,000 of those occurring here in the United States alone (based on the JHU COVID-19 Dashboard). While vaccines continue to show remarkable efficacy in slowing these numbers and novel therapeutics continue to emerge, a better understanding of how this virus mediates immune dysfunction and the development of ARDS, remains poorly understood. Therefore, we propose that the findings presented herein provide insight into a potentially relevant mechanism – one in which the S1-NTD of the viruses' spike protein (and likely that of other β-coronaviruses) mimics Gal-3 and the capacity of this lectin to modulate activation of innate immune cells, namely monocytes. Therefore, the development of therapeutics, such as Gal-3-like antagonists or neutralizing antibodies that target the S1-NTD of the spike protein, cannot be overstated in that they could prove efficacious in preventing prolonged innate immune dysfunction and onset of CRS leading to ARDS.

DATA AVAILABILITY STATEMENT

The raw data supporting the conclusions of this article will be made available by the authors, without undue reservation.

ETHICS STATEMENT

The studies involving human participants were reviewed and approved by Johns Hopkins University IRB. Participants provided their written informed consent to participate in this study.

AUTHOR CONTRIBUTIONS

JS conceived the study, helped conduct experiments and wrote the manuscript. AB provided input regarding experimental design and conducted many of the experiments. All authors contributed to manuscript revision, read and approved the submitted version.

FUNDING

Supported, in part, by Public Health Services Research Grants R01AI115703 and R01AI141486 to JS from the National Institute of Allergy and Infectious Diseases, National Institutes of Health (NIAID, NIH).

ACKNOWLEDGMENTS

The authors wish to acknowledge colleagues: Dr. Pei-Song Gao for helpful discussions, Dr. Robert G. Hamilton in allowing access to the Bio-Plex 200 instrument and Charles Bronzert for assisting in the reading/analyses of the multiplex cytokine plates.

SUPPLEMENTARY MATERIAL

The Supplementary Material for this article can be found online at: https://www.frontiersin.org/articles/10.3389/fimmu.2022.831763/full#supplementary-material

REFERENCES

1. Zhou T, Su TT, Mudianto T, Wang J. Immune Asynchrony in COVID-19 Pathogenesis and Potential Immunotherapies. *J Exp Med* (2020) 217(10):1–8. doi: 10.1084/jem.20200674
2. Giamarellos-Bourboulis EJ. Complex Immune Deregulation in Severe COVID-19: More Than a Mechanism of Pathogenesis. *EBioMedicine* (2021) 73:103673. doi: 10.1016/j.ebiom.2021.103673
3. Lin SH, Zhao YS, Zhou DX, Zhou FC, Xu F. Coronavirus Disease 2019 (COVID-19): Cytokine Storms, Hyper-Inflammatory Phenotypes, and Acute Respiratory Distress Syndrome. *Genes Dis* (2020) 7(4):520–7. doi: 10.1016/j.gendis.2020.06.009
4. Schultze JL, Aschenbrenner AC. COVID-19 and the Human Innate Immune System. *Cell* (2021) 184(7):1671–92. doi: 10.1016/j.cell.2021.02.029
5. Blanco-Melo D, Nilsson-Payant BE, Liu WC, Uhl S, Hoagland D, Moller R, et al. Imbalanced Host Response to SARS-CoV-2 Drives Development of COVID-19. *Cell* (2020) 181(5):1036–45 e9. doi: 10.1016/j.cell.2020.04.026
6. Chen G, Wu D, Guo W, Cao Y, Huang D, Wang H, et al. Clinical and Immunological Features of Severe and Moderate Coronavirus Disease 2019. *J Clin Invest* (2020) 130(5):2620–9. doi: 10.1172/JCI137244
7. Chen X, Zhao B, Qu Y, Chen Y, Xiong J, Feng Y, et al. Detectable Serum Severe Acute Respiratory Syndrome Coronavirus 2 Viral Load (RNAemia) Is Closely Correlated With Drastically Elevated Interleukin 6 Level in Critically Ill Patients With Coronavirus Disease 2019. *Clin Infect Dis* (2020) 71 (8):1937–42. doi: 10.1093/cid/ciaa449
8. Chi Y, Ge Y, Wu B, Zhang W, Wu T, Wen T, et al. Serum Cytokine and Chemokine Profile in Relation to the Severity of Coronavirus Disease 2019 in China. *J Infect Dis* (2020) 222(5):746–54. doi: 10.1093/infdis/jiaa363
9. Guo J, Wang S, Xia H, Shi D, Chen Y, Zheng S, et al. Cytokine Signature Associated With Disease Severity in COVID-19. *Front Immunol* (2021) 12:681516. doi: 10.3389/fimmu.2021.681516
10. Han H, Ma Q, Li C, Liu R, Zhao L, Wang W, et al. Profiling Serum Cytokines in COVID-19 Patients Reveals IL-6 and IL-10 are Disease Severity Predictors. *Emerg Microbes Infect* (2020) 9(1):1123–30. doi: 10.1080/22221751.2020.1770129
11. Liu Y, Zhang C, Huang F, Yang Y, Wang F, Yuan J, et al. Elevated Plasma Levels of Selective Cytokines in COVID-19 Patients Reflect Viral Load and Lung Injury. *Natl Sci Rev* (2020) 7(6):1003–11. doi: 10.1093/nsr/nwaa037
12. Chen Y, Wang J, Liu C, Su L, Zhang D, Fan J, et al. IP-10 and MCP-1 as Biomarkers Associated With Disease Severity of COVID-19. *Mol Med* (2020) 26(1):97. doi: 10.1186/s10020-020-00230-x
13. Santa Cruz A, Mendes-Frias A, Oliveira AI, Dias L, Matos AR, Carvalho A, et al. Interleukin-6 Is a Biomarker for the Development of Fatal Severe Acute Respiratory Syndrome Coronavirus 2 Pneumonia. *Front Immunol* (2021) 12:613422. doi: 10.3389/fimmu.2021.613422
14. Lu Q, Liu J, Zhao S, Gomez Castro MF, Laurent-Rolle M, Dong J, et al. SARS-CoV-2 Exacerbates Proinflammatory Responses in Myeloid Cells Through C-Type Lectin Receptors and Tweety Family Member 2. *Immunity* (2021) 54 (6):1304–19 e9. doi: 10.1016/j.immuni.2021.05.006
15. Melms JC, Biermann J, Huang H, Wang Y, Nair A, Tagore S, et al. A Molecular Single-Cell Lung Atlas of Lethal COVID-19. *Nature* (2021) 595 (7865):114–9. doi: 10.1038/s41586-021-03569-1
16. Merad M, Martin JC. Pathological Inflammation in Patients With COVID-19: A Key Role for Monocytes and Macrophages. *Nat Rev Immunol* (2020) 20 (6):355–62. doi: 10.1038/s41577-020-0331-4
17. Knoll R, Schultze JL, Schulte-Schrepping J. Monocytes and Macrophages in COVID-19. *Front Immunol* (2021) 12:720109. doi: 10.3389/fimmu.2021.720109

18. Duan L, Zheng Q, Zhang H, Niu Y, Lou Y, Wang H. The SARS-CoV-2 Spike Glycoprotein Biosynthesis, Structure, Function, and Antigenicity: Implications for the Design of Spike-Based Vaccine Immunogens. *Front Immunol* (2020) 11:576622. doi: 10.3389/fimmu.2020.576622
19. Seyran M, Takayama K, Uversky VN, Lundstrom K, Palu G, Sherchan SP, et al. The Structural Basis of Accelerated Host Cell Entry by SARS-CoV-2dagger. *FEBS J* (2021) 288(17):5010–20. doi: 10.1111/febs.15651
20. Li F. Structure, Function, and Evolution of Coronavirus Spike Proteins. *Annu Rev Virol* (2016) 3(1):237–61. doi: 10.1146/annurev-virology-110615-042301
21. Behloul N, Baha S, Shi R, Meng J. Role of the GTNGTKR Motif in the N-Terminal Receptor-Binding Domain of the SARS-CoV-2 Spike Protein. *Virus Res* (2020) 286:198058. doi: 10.1016/j.virusres.2020.198058
22. Caniglia JL, Asuthkar S, Tsung AJ, Guda MR, Velpula KK. Immunopathology of Galectin-3: An Increasingly Promising Target in COVID-19. *F1000Res* (2020) 9:1078. doi: 10.12688/f1000research.25979.2
23. Garcia-Revilla J, Deierborg T, Venero JL, Boza-Serrano A. Hyperinflammation and Fibrosis in Severe COVID-19 Patients: Galectin-3, a Target Molecule to Consider. *Front Immunol* (2020) 11:2069. doi: 10.3389/fimmu.2020.02069
24. Chen SS, Sun LW, Brickner H, Sun PQ. Downregulating Galectin-3 Inhibits Proinflammatory Cytokine Production by Human Monocyte-Derived Dendritic Cells *via* RNA Interference. *Cell Immunol* (2015) 294(1):44–53. doi: 10.1016/j.cellimm.2015.01.017
25. Schroeder JT, Bieneman AP. Activation of Human Basophils by A549 Lung Epithelial Cells Reveals a Novel IgE-Dependent Response Independent of Allergen. *J Immunol* (2017) 199(3):855–65. doi: 10.4049/jimmunol.1700055
26. Schroeder JT, Adeosun AA, Do D, Bieneman AP. Galectin-3 Is Essential for IgE-Dependent Activation of Human Basophils by A549 Lung Epithelial Cells. *J Allergy Clin Immunol* (2019) 144(1):312–5.e1. doi: 10.1016/j.jaci.2019.03.001
27. Schroeder JT, Adeosun AA, Bieneman AP. Epithelial Cell-Associated Galectin-3 Activates Human Dendritic Cell Subtypes for Pro-Inflammatory Cytokines. *Front Immunol* (2020) 11:524826. doi: 10.3389/fimmu.2020.524826
28. Schroeder JT, Bieneman AP. Isolation of Human Basophils. *Curr Protoc Immunol* (2016) 112:7 24 1–7 8. doi: 10.1002/0471142735.im0724s112
29. Gutmann C, Takov K, Burnap SA, Singh B, Ali H, Theofilatos K, et al. SARS-CoV-2 RNAemia and Proteomic Trajectories Inform Prognostication in COVID-19 Patients Admitted to Intensive Care. *Nat Commun* (2021) 12(1):3406. doi: 10.1038/s41467-021-23494-1
30. Hoffmann M, Kleine-Weber H, Schroeder S, Kruger N, Herrler T, Erichsen S, et al. SARS-CoV-2 Cell Entry Depends on ACE2 and TMPRSS2 and Is Blocked by a Clinically Proven Protease Inhibitor. *Cell* (2020) 181(2):271–80 e8. doi: 10.1016/j.cell.2020.02.052
31. Hirano T, Murakami M. COVID-19: A New Virus, But a Familiar Receptor and Cytokine Release Syndrome. *Immunity* (2020) 52(5):731–3. doi: 10.1016/j.immuni.2020.04.003
32. Thepaut M, Luczkowiak J, Vives C, Labiod N, Bally I, Lasala F, et al. Dc/L-SIGN Recognition of Spike Glycoprotein Promotes SARS-CoV-2 Trans-Infection and Can Be Inhibited by a Glycomimetic Antagonist. *PloS Pathog* (2021) 17(5):e1009576. doi: 10.1371/journal.ppat.1009576
33. Daly JL, Simonetti B, Klein K, Chen KE, Williamson MK, Anton-Plagaro C, et al. Neuropilin-1 Is a Host Factor for SARS-CoV-2 Infection. *Science* (2020) 370(6518):861–5. doi: 10.1126/science.abd3072
34. Cantuti-Castelvetri L, Ojha R, Pedro LD, Djannatian M, Franz J, Kuivanen S, et al. Neuropilin-1 Facilitates SARS-CoV-2 Cell Entry and Infectivity. *Science* (2020) 370(6518):856–60. doi: 10.1126/science.abd2985
35. Nabi IR, Shankar J, Dennis JW. The Galectin Lattice at a Glance. *J Cell Sci* (2015) 128(13):2213–9. doi: 10.1242/jcs.151159
36. Liu FT, Frigeri LG, Gritzmacher CA, Hsu DK, Robertson MW, Zuberi RI. Expression and Function of an IgE-Binding Animal Lectin (Epsilon BP) in Mast Cells. *Immunopharmacology* (1993) 26(3):187–95. doi: 10.1016/0162-3109(93)90034-n
37. Zuberi RI, Frigeri LG, Liu FT. Activation of Rat Basophilic Leukemia Cells by Epsilon BP, an IgE-Binding Endogenous Lectin. *Cell Immunol* (1994) 156(1):1–12. doi: 10.1006/cimm.1994.1148
38. Clausen TM, Sandoval DR, Spliid CB, Pihl J, Perrett HR, Painter CD, et al. SARS-CoV-2 Infection Depends on Cellular Heparan Sulfate and ACE2. *Cell* (2020) 183(4):1043–57 e15. doi: 10.1016/j.cell.2020.09.033
39. Wang K, Chen W, Zhang Z, Deng Y, Lian JQ, Du P, et al. CD147-Spike Protein Is a Novel Route for SARS-CoV-2 Infection to Host Cells. *Signal Transduct Target Ther* (2020) 5(1):283. doi: 10.1038/s41392-020-00426-x
40. Sikora AS, Delos M, Martinez P, Carpentier M, Allain F, Denys A. Regulation of the Expression of Heparan Sulfate 3-O-Sulfotransferase 3b (HS3ST3B) by Inflammatory Stimuli in Human Monocytes. *J Cell Biochem* (2016) 117(7):1529–42. doi: 10.1002/jcb.25444
41. Sturhan H, Ungern-Sternberg SN, Langer H, Gawaz M, Geisler T, May AE, et al. Regulation of EMMPRIN (CD147) on Monocyte Subsets in Patients With Symptomatic Coronary Artery Disease. *Thromb Res* (2015) 135(6):1160–4. doi: 10.1016/j.thromres.2015.03.022
42. Borriello F, Longo M, Spinelli R, Pecoraro A, Granata F, Staiano RI, et al. IL-3 Synergizes With Basophil-Derived IL-4 and IL-13 to Promote the Alternative Activation of Human Monocytes. *Eur J Immunol* (2015) 45(7):2042–51. doi: 10.1002/eji.201445303
43. Atal S, Fatima Z. IL-6 Inhibitors in the Treatment of Serious COVID-19: A Promising Therapy? *Pharmaceut Med* (2020) 34(4):223–31. doi: 10.1007/s40290-020-00342-z
44. Antwi-Amoabeng D, Kanji Z, Ford B, Beutler BD, Riddle MS, Siddiqui F. Clinical Outcomes in COVID-19 Patients Treated With Tocilizumab: An Individual Patient Data Systematic Review. *J Med Virol* (2020) 92(11):2516–22. doi: 10.1002/jmv.26038
45. Soin AS, Kumar K, Choudhary NS, Sharma P, Mehta Y, Kataria S, et al. Tocilizumab Plus Standard Care Versus Standard Care in Patients in India With Moderate to Severe COVID-19-Associated Cytokine Release Syndrome (COVINTOC): An Open-Label, Multicentre, Randomised, Controlled, Phase 3 Trial. *Lancet Respir Med* (2021) 9(5):511–21. doi: 10.1016/S2213-2600(21)00081-3
46. Lu L, Zhang H, Dauphars DJ, He YW. A Potential Role of Interleukin 10 in COVID-19 Pathogenesis. *Trends Immunol* (2021) 42(1):3–5. doi: 10.1016/j.it.2020.10.012
47. Mulchandani R, Lyngdoh T, Kakkar AK. Deciphering the COVID-19 Cytokine Storm: Systematic Review and Meta-Analysis. *Eur J Clin Invest* (2021) 51(1):e13429. doi: 10.1111/eci.13429
48. Zawawi A, Naser AY, Alwafi H, Minshawi F. Profile of Circulatory Cytokines and Chemokines in Human Coronaviruses: A Systematic Review and Meta-Analysis. *Front Immunol* (2021) 12:666223. doi: 10.3389/fimmu.2021.666223

Conflict of Interest: The authors declare that the research was conducted in the absence of any commercial or financial relationships that could be construed as a potential conflict of interest.

Publisher's Note: All claims expressed in this article are solely those of the authors and do not necessarily represent those of their affiliated organizations, or those of the publisher, the editors and the reviewers. Any product that may be evaluated in this article, or claim that may be made by its manufacturer, is not guaranteed or endorsed by the publisher.

frontiers | Frontiers in Immunology

REVIEW
published: 01 June 2022
doi: 10.3389/fimmu.2022.864387

Neutrophils in COVID-19: Not Innocent Bystanders

*Ellen McKenna[1,2], Richard Wubben[3], Johana M. Isaza-Correa[1,2], Ashanty M. Melo[1,2], Aisling Ui Mhaonaigh[4], Niall Conlon[5], James S. O'Donnell[6], Clíona Ní Cheallaigh[7,8], Tim Hurley[1,2,9,10], Nigel J. Stevenson[3,11], Mark A. Little[4,6] and Eleanor J. Molloy[1,2,9,10,12,13]**

[1] Discipline of Paediatrics, Dublin Trinity College, The University of Dublin, Dublin, Ireland, [2] Paediatric Research Laboratory, Trinity Translational Medicine Institute (TTMI), St James' Hospital, Dublin, Ireland, [3] Viral Immunology Group, School of Biochemistry and Immunology, Trinity Biomedical Sciences Institute, Dublin, Ireland, [4] Trinity Health Kidney Centre, Trinity Translational Medicine Institute (TTMI), Trinity College Dublin, Dublin, Ireland, [5] Department of Immunology, St James' Hospital, Trinity College Dublin, Dublin, Ireland, [6] Irish Centre for Vascular Biology, Dublin, Ireland, [7] Department of Clinical Medicine, Trinity Centre for Health Science, Trinity College Dublin, Dublin, Ireland, [8] Department of Infectious Diseases, St James's Hospital, Dublin, Ireland, [9] Neonatology, Coombe Women and Infant's University Hospital, Dublin, Ireland, [10] National Children's Research Centre, Children's Hospital Ireland (CHI) at Crumlin, Dublin, Ireland, [11] Viral Immunology Group, Royal College of Surgeons in Ireland - Medical College of Bahrain, Al Muharraq, Bahrain, [12] Neonatology, Children's Hospital Ireland (CHI) at Crumlin, Dublin, Ireland, [13] Paediatrics, Children's Hospital Ireland (CHI) at Tallaght, Tallaght University Hospital, Dublin, Ireland

OPEN ACCESS

Edited by:
Antonio Condino-Neto, University of São Paulo, Brazil

Reviewed by:
José Jiram Torres-Ruiz, Instituto Nacional de Ciencias Médicas y Nutrición Salvador Zubirán (INCMNSZ), Mexico
Jorge Masso-Silva, University of California, San Diego, United States

***Correspondence:**
Eleanor J. Molloy
eleanor.molloy@tcd.ie

Specialty section:
This article was submitted to Viral Immunology, a section of the journal Frontiers in Immunology

Received: *28 January 2022*
Accepted: *29 April 2022*
Published: *01 June 2022*

Citation:
McKenna E, Wubben R, Isaza-Correa JM, Melo AM, Mhaonaigh AU, Conlon N, O'Donnell JS, Ní Cheallaigh C, Hurley T, Stevenson NJ, Little MA and Molloy EJ (2022) Neutrophils in COVID-19: Not Innocent Bystanders. Front. Immunol. 13:864387. doi: 10.3389/fimmu.2022.864387

Unusually for a viral infection, the immunological phenotype of severe COVID-19 is characterised by a depleted lymphocyte and elevated neutrophil count, with the neutrophil-to-lymphocyte ratio correlating with disease severity. Neutrophils are the most abundant immune cell in the bloodstream and comprise different subpopulations with pleiotropic actions that are vital for host immunity. Unique neutrophil subpopulations vary in their capacity to mount antimicrobial responses, including NETosis (the generation of neutrophil extracellular traps), degranulation and *de novo* production of cytokines and chemokines. These processes play a role in antiviral immunity, but may also contribute to the local and systemic tissue damage seen in acute SARS-CoV-2 infection. Neutrophils also contribute to complications of COVID-19 such as thrombosis, acute respiratory distress syndrome and multisystem inflammatory disease in children. In this Progress review, we discuss the anti-viral and pathological roles of neutrophils in SARS-CoV-2 infection, and potential therapeutic strategies for COVID-19 that target neutrophil-mediated inflammatory responses.

Keywords: neutrophil, COVID-19, SARS-CoV-2, innate immunity, inflammation

INTRODUCTION

Neutrophils are the first responders to infection and extravasate rapidly from the blood vessels into tissue. They are the most abundant leukocyte in blood, with about 10^{11} neutrophils produced by the bone marrow each day, representing 40-60% of circulating immune cells in healthy adults (1). Neutrophils kill pathogens using oxidative burst, degranulation, phagocytosis and the release of neutrophil extracellular traps (NETs) (2, 3). Their role is most prominent in bacterial infection but they can also contribute to antiviral immunity.

Severe disease in COVID-19 is associated to increased neutrophil-to-lymphocyte ratio and high expression of neutrophil-related cytokines IL-8 and IL-6 in serum, and neutrophilia has been described as a predictor of poor outcome (4–14). Peripheral blood neutrophil counts in patients with COVID-19, although not as elevated as bacterial pneumonia, are higher in severe COVID-19 compared with mild cases and most other viral infections (4, 15). Neutrophils are associated with the development of thrombosis and pulmonary infiltrates found in post-mortem samples following severe acute respiratory syndrome coronavirus 2 (SARS-CoV-2) (16–18). In this Progress review, we focus on emerging data on the roles of neutrophils in the pathogenesis and response to SARS-CoV-2.

NEUTROPHILS IN COVID-19

An altered neutrophil-to-lymphocyte ratio occurs in many conditions such as cancer, cardiovascular disease, sepsis and inflammatory disorders, including Systemic lupus erythematosus (SLE) and psoriasis (19). Patients with COVID-19 with severe disease had significantly higher absolute neutrophil counts (8) similar to the neutrophilia in both Severe Acute Respiratory Syndrome (SARS) and Middle East Respiratory Syndrome (MERS) (20). The limited antiviral response in COVID-19 may exacerbate neutrophil infiltration, resulting in exuberant inflammation (21).

A small gene ontology (GO) analysis of COVID-19 infected cells indicated that neutrophil activation and degranulation are the most activated cellular immune processes in COVID-19, but did not play a role in the antibody-mediated elimination of SARS-CoV-2 in a passive immunisation model (22). Neutrophils contribute to hypersensitivity pneumonitis in SARS-CoV-2 infection and altered neutrophil immunometabolism, with accumulation of succinate correlating with disease severity (21). A rat coronavirus (RCoV) model demonstrated that neutrophils produce cytokines and chemokines in response to alveolar epithelial cell infection with SARS-CoV-2, resulting in an inflammatory response which contributes to lung injury (23).

NEUTROPHIL EXTRACELLULAR TRAPS

Neutrophil extracellular traps (NETs) are web-like chromatin structures released by neutrophils to degrade virulence factors and kill bacteria. Once unregulated in sepsis or severe COVID-19, they induce multiple organ damage, including arterial hypotension, hypoxemia, coagulopathy, renal, neurological, and hepatic dysfunction as consequence of a NETs-associated cytokine storm (24–26). Silva et al. found that gasdermin inhibition with disulfiram or genic deletion decreases NETs formation with reduced multiple organ dysfunction and mortality in a sepsis model (27). NETs concentration was markedly increased in the tracheal aspirate and plasma of patients hospitalised with COVID-19 as well as in SARS-CoV-2-infected lung airways and alveoli, with spontaneous NETs production from their neutrophils (13, 28–32). SARS-CoV-2 can directly induce healthy neutrophils to release NETs *in vitro*, which increase pulmonary epithelium cell death (28). NETs also appear to drive neuroinflammation in Ischemic Brain Damage (IBD) and IBD following COVID-19, by affecting the blood-brain barrier, promoting thrombosis, and by inducing neuronal damage through extruded NETs components, NETs-IL-1 loop and IL-17 cascades (33, 34), making them a promising target for therapy.

The first step in NETosis is cellular activation *via* pattern recognition receptors (PRR) such as Toll-like receptors 4 (TLR4), TLR7 and TLR8 in viral infections (24, 35, 36). Reactive oxygen species (ROS) are subsequently produced, resulting in the activation of protein arginase deiminase 4 (PAD4) which is responsible for chromatin decondensation (24, 37). Neutrophil elastase (NE), a granule protein, induces neutrophil nuclear membrane break down while granule protein gasdermin D facilitates pore formation in the cell membrane and mediates release of NETs into the extracellular space (**Figure 1**) (24, 31). NETs do play a role in viral clearance, but excessive NETs production exacerbates inflammation in acute respiratory distress syndrome (ARDS) and contributes to microvascular thrombosis (**Figure 1**) (38). These is potentially related to over-activation of the Stimulator of interferon genes (STING) pathway through cyclic GMP-AMP synthase (cGAS) in phagosomes, and by SARS-CoV-2 infection itself through Angiotensin-Converting Enzyme 2 (ACE2)-angiotensin II (39, 40). Pharmacological activation of the STING pathway may also regulate the effects of SARS-CoV-2 infection (41). NETs can also have different proteins cargo associated to their deoxyribonucleic acid (DNA), citrullinated histone 3 (cit-H3), NE, and myeloperoxidase (MPO) structure which can influence the type of immune response triggered (42). Severe COVID-19 patients were shown to have higher expression of the alarmin nuclear protein High mobility group box 1 (HMGB1), antiviral molecules like ISG-15 and LL-37, or functionally active tissue factor (TF) as protein cargo in NETs, produced mostly by normal density granulocytes (NDG) (43, 44). These cargo molecules induced thrombogenic activity and differential cytokines expression (43, 44).

INFLAMMASOME ACTIVATION IN COVID-19

COVID-19 is characterised by a cytokine storm and the Pyrin domain containing 3 (NLRP3) inflammasome has been implicated. The inflammasomes are molecular mechanism involving multiprotein complexes which regulate the production of pro-inflammatory cytokines. NLRP3, a member of the nucleotide oligomerization domain (NOD)-like receptor (NLR) family, is present in neutrophils (17). After NLRP3 activation, pro-caspase 1 is cleaved to the active form caspase 1, leading to the cleavage of pro-inflammatory pro-IL-1β and pro-IL-18 into the active forms (**Figure 2**) (45). Single-stranded ribonucleic acid (ssRNA) viruses, such as SARS-CoV-2, induce Nuclear factor kappa B (NF-κB)

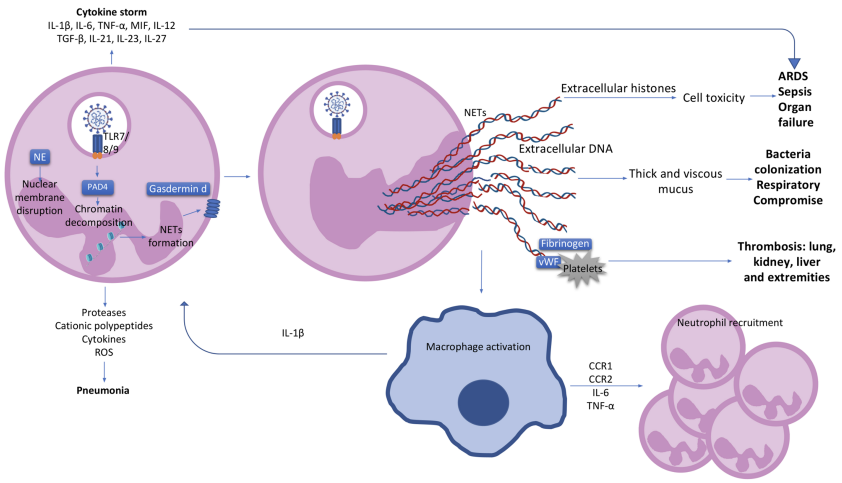

FIGURE 1 | The neutrophil and clinical characteristics of COVID-19 patients. Activated neutrophils can produce cytokines such as IL-1β, IL-6, TNF-α, MIF, IL-12, TGF-β, IL-21, IL-23 and IL-27, contributing to a cytokine storm and the further development of ARDS and organ failure in COVID-19 patients. Pneumonia in COVID-19 patients is most likely to be caused by the production of proteases, cationic polypeptides, cytokines and ROS by neutrophils. Upon SARS-CoV-2 recognition by TLR7/8/9, protein arginase deiminase 4 (PAD4) is activated, which induces chromatin decondensation through histones citrullination and consequently NETs formation. Neutrophil nuclear membrane is disrupted by neutrophil elastase (NE) and gasdermin D which facilitates the formation of a pore in the neutrophil cell membrane and mediates release of the contents of NETs into the extracellular space. NETs induce macrophage activation and IL-1β production resulting in a positive loop with neutrophils and NETs formation. Macrophages also secrete CCR1, CCR2, IL-6 and TNF-α leading to further neutrophil recruitment. Extracellular histones presented in NETs causes cell cytotoxicity contributing with ARDS, sepsis and organ failure observed in COVID-19 patients. Extracellular DNA induces thick and viscous mucus production allowing bacteria colonization and respiratory failure. NETs also interact with fibrinogen, VWF and platelets causing thrombosis in several organs such as lung, kidney, liver and extremities. IL, interleukin; TNF, tumour necrosis factor; MIF, macrophage migration inhibitory factor; ARDS, acute respiratory distress syndrome; ROS, reactive oxygen species; PAD4, protein arginase deiminase 4; NETs, neutrophil extracellular trap; NE, neutrophil elastase; CCR, chemokine receptor; DNA, deoxyribonucleic acid; VWF, von Willebrand factor.

activation and the further production of pro-IL-1β and pro-IL-18 (45, 46). Simultaneously, ROS and Adenosine 5'-triphosphate (ATP) produced by mitochondria trigger NLRP3 inflammasome assembly (46). Active NLRP3 inflammasome is present in peripheral blood mononuclear cells (PBMCs) and post-mortem tissues of COVID-19 patients, and high expression of its derived products such as Casp1p20 and IL-18 were seen to correlate with disease severity and poor clinical outcome (47). NLRP3 inflammasome activation has also been described in neutrophils of severe COVID-19 patients (48). Aymonnier et al. found that neutrophils from COVID-19 patients with respiratory failure demonstrated NLRP3 inflammasome molecule Apoptosis-associated speck-like protein containing a CARD (ASC) specks, and their early formation in NETosis. In patients with severe COVID-19 neutrophils with intact multilobulated nuclei, ASC specks formation and histone H3 citrullination was elevated (48). In a murine model they also showed transient presence of ASC specks at the microtubule organizing center, before nuclear rounding, early in NETosis (48). In addition, SARS-CoV-2 has been shown to directly activate the NLRP3 inflammasome through viroporin protein 3a, which most likely acts by the formation of K^+ and Ca^+ channels (49). Such direct activation of the inflammasome leads to the production of IL-1β and IL-18, perpetuating inflammation and resulting in further neutrophil activation (50). NLRP3 inflammasome activation in the blood of patients reveals an impaired immature neutrophil response in severe COVID-19. Inflammasome signature analysis in circulating myeloid cells allows COVID-19 patients to be stratified and predicts evolution of disease severity (51).

NEUTROPHIL SUBSETS IN COVID-19

Heterogeneity within the neutrophil population during infection has been demonstrated in multiple diseases, and different subsets have defined roles in influencing the inflammatory response (38, 52). Neutrophil subsets varying in their density, maturity and expression of surface markers have been reported in COVID-19 (53, 54). Classically, in sepsis, immature neutrophils are released from the bone marrow and Carissimo et al. found increased immature neutrophils in whole blood that correlated with increased IL-6 and IP-10, and COVID-19 disease severity (55). The ratio of immature neutrophils to gamma delta (Vδ)2 T cells could predict severe COVID-19 (55). Additionally, a shift toward immature neutrophils as the driver of hyperinflammation is associated with severe COVID-19 disease (56).

Recently there has been a renewed interest in immunomodulatory neutrophil subsets, specifically in the field of cancer, SLE and sepsis, including low density granulocytes (LDGs) and myeloid derived suppressor cells (MDSCs) (38), but there is not a consensus on nomenclature and classification (57). MDSCs are a mixed population of mature and immature cells with differing immunomodulatory roles (58). There is a lack of clarity on the phenotypical and functional characteristics of MDSCs and their relationship to LDGs but their

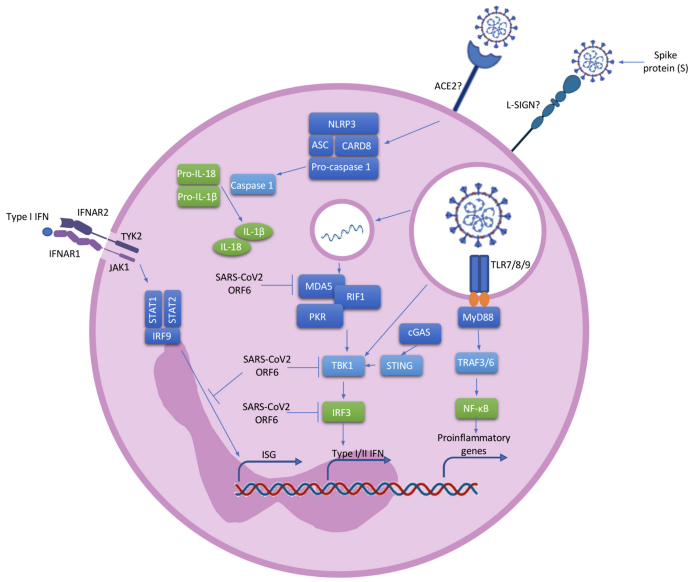

FIGURE 2 | Neutrophil activation. ACE2 or L-SING receptors on neutrophils most likely recognise SARS-CoV2 *via* a spike (S) protein on its surface. Once the virus enters the cell, ssRNA viruses such as SARS-CoV-2 are recognised by TLR 7/8/9 which induce the activation of the MyD88 pathway. MyD88 activates TRAF3 and TRAF6 which result in the transcription of NF-κB and IRF7 associated genes. The activated NF-κB pathway leads to the transcriptional induction of proinflammatory cytokines, chemokines and additional inflammatory mediators in neutrophils. In addition, cytosolic viral RNA recruiting MDA5, RIF1 and PKR lead to the activation of TBK1 and the further activation of IRF3 resulting in the transcription of type I/II IFN genes. The positive stimulatory loop by type I IFN induces the production of more IFNs through the JAK/STAT pathway and the induction of Interferon Stimulated Genes (ISG). At the same time, SARS-CoV-2 possess ORF6, an accessory protein antagonist of IFNs by the inhibition of MDA5, TBK1, IRF3 and IRF9. ssRNA viruses also cause the recruitment of the NLRP3 inflammasome complex and the further activation of pro-caspase-1 resulting in the cleavage of pro-IL-1β and pro-IL-18 into the active forms. ACE2, angiotensin-Converting Enzyme 2; L-SING, L-Specific Intercellular adhesion molecule-3-Grabbing Non-integrin/CD209L; RNA, ribonucleic acid; ssRNA, Single-stranded RNA; TLR, toll-like receptor; MyD88, myeloid differentiation primary response 88; TRAF, tumor necrosis factor receptor (TNF-R)-associated factor; NF-κB, nuclear factor kappa B; IRF, Interferon Regulatory Factor; MDA, melanoma differentiation-associated protein; RIF, Replication Timing Regulatory Factor; PKR, protein kinase R; TBK, TANK Binding Kinase; IFN, interferon; ISG, Interferon Stimulated Genes; JAK-STAT, janus kinase; ORF, open Reading Frame; NLRP3, nod like receptor family, pyrin domain containing 3; IL, interleukin.

defining characteristic is suppression of the adaptive immune response (59). MDSC expansion is linked to G-CSF, a cytokine increased in the lungs of COVID-19 patients (60) and almost 90% of mononuclear cells in the severe disease cohort were MDSCs. Proportion of LDGs increases with disease severity in COVID-19 patients, as well as their production of NETs when compared to healthy controls (43, 61).

Morrisey et al. described a population of LDGs correlating with disease severity and hypercoagulable state in COVID-19 patients (53). A population of $CD45^{+}CD66b^{+}CD16^{Int}CD44^{low}CD11b^{Int}$ LDGs was found in patients with severe disease, which displayed enhanced phagocytic capacity, spontaneous NETs formation and elevated cytokine production. Similarly, an immune-suppressive $CD16^{bright}/CD62L^{dim}$ neutrophil subtype was increased in patients developing pulmonary embolism (PE) on the day of ICU admission (54). Using whole blood transcriptomics analysis, increased NLRP3 inflammasome, monocytes and LDGs were found in the lungs of COVID-19 patients, and neutrophil activation-associated signatures correlated to disease severity (62). In COVID-19, immature neutrophils are expanded and show increased programmed death ligand (PD-L) 1, which suppresses T cells, and reduced oxidative burst functions with no change in phagocytosis in severe COVID-19 (63). Chevrier et al. found higher LDGs were present in COVID-19 patients early in the course of the disease and decreased in convalescence using mass cytometry and serum proteomics, but $CD16^{low}$ neutrophil population remained expanded over the disease course (64). COVID-19 induced-ARDS is associated with MDSC expansion, reduced lymphocyte function and arginine shortage, through increased arginase activity, therefore arginase supplementation may be therapeutic (65). Further study into the role of neutrophil subsets in COVID-19 is warranted, potentially as biomarkers of disease severity, or as new targets for therapeutic approaches.

NEUTROPHIL RESPONSE TO SARS-COV-2

Does SARS-CoV-2 Actively Infect Neutrophils?

Although neutrophils express the L-SIGN and DC-SIGN C-type lectins receptors that have been suggested to act as entry receptors for SARS-CoV-2, there is conflicting evidence about active infection of neutrophils with the virus. In other ssRNA viruses such as West Nile and influenza virus neutrophils serve as

an important viral reservoir and contain actively replicating virus, and studies with human immunodeficiency virus (HIV) and Respiratory syncytial virus (RSV) viral models suggest that neutrophils can internalise virus without productive infection (66). Neutrophils are important for viral detection and initiation of downstream effector immune pathways but the replicative ability of ssRNA virus SARS-CoV-2 within neutrophils is not known.

ACE2 is the primary cell entry receptor for SARS-CoV-2 and ACE2 deficiency is associated with worse outcomes in COVID-19 (67). Entry of SARS-CoV2 into the cells following membrane fusion majorly down-regulates ACE2 receptors, with loss of the catalytic effect of these receptors at the external site of the membrane (68). This induces increased pulmonary inflammation and coagulation due to enhanced and unopposed angiotensin II effects. ACE2 down-regulation induced by viral invasion may be especially detrimental in people with baseline ACE2 deficiency (68). Following viral entry, the additional ACE2 deficiency may exacerbate the dysregulation between ACE→Angiotensin II→AT1 receptor axis (potentially adverse) and the ACE2→Angiotensin→Mas receptor axis (negative regulator of angiotensin II activity, potentially protective recombinant ACE2) (68). Therefore, angiotensin and angiotensin II type 1 receptor blockers may be beneficial in patients with severe SARS-CoV-2 (68). However, two large cohort studies showed that angiotensin-converting enzyme inhibitors (ACEIs)/angiotensin receptor blockers (ARBs) use was not associated with increased SARS-CoV-2 infection, but was in fact associated with a lower risk of all-cause mortality in hospitalized patients (69, 70). Further studies are needed to test the protective effects of ACEIs/ARBs in COVID-19 (69, 70). NETs triggered by SARS-CoV-2 depend on ACE2, serine protease TMPRSS2, virus replication, and PAD-4 (28). ACE is important in neutrophil antibacterial activity. Veras at al found that NETosis was facilitated in neutrophils in patients with COVID-19 (28). Neutrophils express ACE2 similar to other immune cells and it is postulated that allows the virus-triggered cell activation and NETosis (28). Knockout of this gene in mice or treatment with an ACE inhibitor increased susceptible to bacterial infection by methicillin-resistant *Staphylococcus aureus* (MRSA). Mice overexpressing ACE in neutrophils have increased killing of MRSA *Pseudomonas aeruginosa*, and *Klebsiella pneumoniae*, with increased neutrophil production of reactive oxygen species (ROS) independent of the angiotensin II AT1 receptor (71).

DYSFUNCTIONAL NEUTROPHIL ACTIVATION IN COVID-19

Neutrophils express all known Toll-like receptors (TLRs) with the exception of TLR3 (72). TLR7, TLR8 and TLR9 are involved in the detection of ssRNA viruses such as SARS-COV-2 (73). Activation of these receptors leads to downstream activation of NF-κB and interferon regulatory factor (IRF7), and the subsequent production of pro-inflammatory cytokines and chemokines in neutrophils (**Figure 2**) (74). In conjunction with neutrophils, these pro-inflammatory cytokines and chemokines drive the characteristic hyperinflammation and pulmonary infiltration seen in severe COVID-19 (74). Neutrophils also produce type 1 interferons (IFN-α/IFNβ) through the activation of IRF proteins (75) and this broad, but dysregulated, pro-inflammatory and antiviral response puts selective pressure on these highly pathogenic respiratory viruses. The host response to SARS-CoV-2 has also been broadly defined as a significantly depleted type 1 IFN response, with a consistent upregulation of chemotactic signals (CCL8, CCL2, CXCL2, CXCL8 and CXCL9), most of which are key mediators of neutrophil recruitment. Liao et al. found that in the lungs of patients with severe COVID-19, macrophages exacerbate inflammation by producing chemokines that recruit neutrophils to the site of infection through chemokine receptors CC-chemokine receptor 1 (CCR1) and C-X-C chemokine receptor type 2 (CXCR2) (57). Using a SARS-CoV-2 animal model early induction of CXCL9 and CCL8 was found consistent with observations in primary human bronchial epithelial cells infected with SARS-CoV-2. At day 7, despite waning levels of virus, elevated CCR5, CCL2, CXCL9 and IL-6 were found in the animal model, suggesting neutrophil-mediated inflammation may persist after the virus has been cleared (76). This may correlate with the clinical findings of persistent symptoms and fatigue with post-viral infection complications in some patients.

The loss of IFN signalling is vital to understanding why SARS-CoV-2 elicits such a potent inflammatory and neutrophilic chemotactic response. For instance, bats appear to limit the inflammatory and neutrophilic chemotactic response when infected with coronaviruses endemic in the bat population (77). Banerjee et al. have proposed that bats possess repressors of NF-κB signalling, a potent inductor of pro-inflammatory and chemotactic responses, allowing these strains of the viruses to become endemic in the population. However, unlike bats, humans lack this repressor activity rendering us susceptible to this uncontrollable neutrophil-mediated inflammatory response following viral infection (77).

NEUTROPHILS AND THROMBOSIS

Coagulation cascade activation is a common finding in patients with COVID-19 and is associated with disease severity (78). Elevated levels of fibrin D-dimer degradation products, a marker of fibrin degradation indicating overactive coagulation, correlates with a worse clinical outcome (79). High plasma levels of plasminogen activator (tPA) and plasminogen activator inhibitor-1 (PAI-1) in hospitalised COVID-19 patients had strong correlations with neutrophil counts and activation, and extremely high levels of tPA increasing fibrinolysis (80). Plasmatic matrix metalloproteinase-9 (MMP-9) was likewise increased in COVID-19 patients which induced platelet and neutrophil activation, and NETs formation *in vitro* (81). Post-mortem studies have consistently shown that micro-thrombi are present throughout the pulmonary vasculature (82). Collectively,

these data suggest that coagulation activation and vasculopathy within the lungs (pulmonary intravascular coagulopathy [PIC]) plays a role in modulating COVID-19 pathogenesis (78). The biological mechanisms through which SARS-CoV-2 infection causes PIC within the lung blood vessels remain poorly understood (83). However, recent autopsy studies have reported significant endothelial cell (EC) damage, apoptosis, loss of tight junctions and separation from the basement membrane (84). Local inflammation and dysregulated pro-inflammatory cytokine generation within the lungs are a major factor as well as local hypoxia and complement activation, which significantly enhance procoagulant pathways and downregulate anticoagulant pathways *in vivo*. Moreover, ECs express the ACE2 receptor through which SARS-CoV-2 gains entry into cells, and electron microscopy studies have reported viral inclusion bodies within ECs.

Neutrophils and platelets are key modulators of thrombosis. Significant NETosis is found in patients with severe COVID-19 and is important in thrombus aetiology (85). NETs can bind to platelets, triggering platelet activation, and through their citrullinated histone H3 (citH3) they can also interact with procoagulant von Willebrand factor (VWF) (85). In addition to their effects on primary hemostasis, NETs also enhance local thrombin generation. In particular, NETs initiate coagulation activation through the alternative contact pathway and trigger thrombin generation by enhancing the intrinsic tissue-factor dependent pathway. NETs have also been described to over-activate the STING pathway through the cGAS sensor in phagosomes (40). The over-activation of the STING-pathway increases hyper-coagulability *via* interferon-β and tissue factor, released by monocytes-macrophages, and can be inhibited upstream the STING-pathway by aspirin, intravenous immunoglobulins and Vitamin-D (40). NETs histones can activate platelets by stimulating platelet TLR4 and TLR2; neutrophils can bind to these active platelets through surface glycoprotein Ib to induce NETosis and, consequently, result in thrombosis (85). Platelet activation is associated with disease severity in COVID-19 (86). Finally, NETosis has potent pro-inflammatory effects on ECs, which serve to attenuate the normal ability of ECs to regulate procoagulant pathways (87, 88). NETs and thrombosis have been implicated in several disorders including cancer, SLE, rheumatoid arthritis (RA), atherosclerosis and ischemic stroke. NETs have been shown to invade microthrombi in septic patients and contribute to organ damage, hence it is likely that neutrophils are a mediator of organ dysfunction in COVID-19 (31).

NEUTROPHILS AND COVID-19 IN CHILDREN

The severity of COVID-19 differs between age-groups, and children, especially neonates, exhibit milder disease with only a small proportion require intensive care with acute respiratory illness. There are many theories about this discrepancy, which is also seen with other similar viral illnesses, and the decreased expression of ACE2 and NETs formation may be contributory (89). However, a multisystem inflammatory disease in children (MIS-C) or paediatric multisystem inflammatory syndrome temporally associated with COVID-19 (PIMS-TS) has emerged in children, occurring weeks after the primary infection with SARS-Cov-2, that can lead to serious and life-threatening illness in previously healthy children (90). There is no internationally accepted single definition of MIS-C/PIMS-TS, but most case definitions require multi-organ dysfunction, systemic inflammation evidence of recent a SARS-CoV-2 infection, and the exclusion of other causes. The clinical presentation and laboratory findings in MIS-C are similar to Kawasaki's disease and toxic shock syndrome, and considered to be a spectrum of disease (90).

Similar to adults with COVID-19, neutrophilia and lymphocytopenia are common in MIS-C. Neutrophils play a key functional role in Kawasaki disease with recent descriptions of NETosis and neutrophil activation in the form of CD11b and CD64 production (91). Neutrophil counts predict responsiveness of patients with Kawasaki disease to intravenous immunoglobulin therapy, also used in MIS-C (92, 93). Neutrophils activation marker Fc γ receptor I (FcγRI; CD64) was described to be highly expressed on neutrophils of treatment-naive MIS-C patients in acute phase compared with healthy controls (94). These patients also showed increase levels of the neutrophils chemoattractant cytokine IL-8 (94). Ramaswamy et al. talk of a potential myeloid dysfunction in MIS-C patients based on the high expression of alarmin-related S100A genes in neutrophils and monocytes, and the significant reduction in key antigen-presentation molecules such as HLA class II and CD86 (95). Additional research is required to fully understand the role of neutrophils in MIS-C and to determine whether treatments used in Kawasaki disease such as intravenous immunoglobulin therapy could also be used with MIS-C patients.

THERAPEUTIC TARGETING OF NEUTROPHILS

Targeting Cytokines

The efficacy of targeting cytokines produced by various immune cells, including neutrophils, is being explored in ongoing clinical trials. Neutrophils produce IL-6, and IL-6 inhibitor tocilizumab has been shown to decreases neutrophil survival and lipopolysaccharides (LPS)-induced oxidative burst, as well as neutrophil release from the bone marrow and lung demargination (96, 97). Tocilizumab has been approved by the United States Food and Drug Administration (FDA) for use in COVID-19 patients and decreased mortality, poor outcome and mechanical ventilation (98, 99). Clazakizumab also targets IL-6 and is currently being evaluated for safety in several clinical trials of patients with life-threatening COVID-19 (**Table 1**). The interleukin-6 receptor inhibitors (IL6ri) sarilumab or tocilizumab decreased intubation and mortality in a study including 255 patients with COVID-19 (100). Doxycycline (a

TABLE 1 | Clinical trials therapeutically targeting neutrophils.

Therapeutic target	Type of drug	Drug name	Effect on Neutrophils	Reference number
IL-6	Anti-IL-6	Clazakimumab	Reduces inflammation produced by neutrophils and other immune cells	NCT04363502 NCT04381052 NCT04343989
	Anti-IL-6	Tocilizumab		NCT04403685
	Anti-IL-6	Siltuximab		NCT04329650
	Anti-IL-6	Olokizumab		NCT04452474
	Anti-IL-6R	Sarilumab		NCT04357860
GM-CSF	Monoclonal antibody-anti-GM-CSF	Lenzilumab	Blocks neutrophils recruitment	NCT04351152
	Monoclonal antibody-anti-GM-CSF	Mavrilimumab		NCT04397497
	Monoclonal antibody-anti-GM-CSF	TJ003234		NCT04341116
	Monoclonal antibody-anti-GM-CSF	Gimsilumab		NCT04351243
	GM-CSF	Sargramostim	Recruits neutrophils	NCT04400929 NCT04411680 NCT04326920 NCT04400929
NLRP3 inflammasome	Inhibitor of NLRP3 inflammasome	Colchicine	Reduces NLRP3 inflammasome activated by neutrophils	NCT04322682 NCT04350320 NCT04322565 NCT04326790 NCT04367168 NCT04381936
	Inhibitor of NLRP3 inflammasome	Tranilast	Reduces hyperinflammation and organ damage	ChiCTR2000030002
NLRP3 inflammasome	Inhibitor of NLRP3 inflammasome	Dapansutrile	Reduces hyperinflammation and organ damage	NCT04540120
IL-1β	Anti-IL-1β monoclonal antibody	Canakinumab	Reduces hyperinflammation and organ damage	NCT04365153 NCT04348448 NCT04362813
IL-1	IL-1 receptor antagonist	Anakinra	Reduces hyperinflammation and organ damage	NCT04339712 NCT04324021 NCT04341584
IFN-y	Anti-IFN-y	Emapalumab	Inhibits activation of neutrophils	NCT04324021
TLR4	TLR4 inhibitor	EB05	Reduces hyperinflammation and organ damage	NCT04401475
NETs	rhDNase1	Dornase alfa	Promotes clearance of NETs	NCT04432987 NCT04359654 NCT04355364 NCT04409925 NCT04402970 NCT04402944
	NE inhibitor	13 cis retinoic acid	Promotes clearance of NETs	NCT04396067
	NE inhibitor	Alvelestat		NCT04539795
	NE inhibitor	Brensocatib		NCT04817332
JAK-STAT	JAK1/2 inhibitor	Ruxolitinib	Reduces inflammation produced by neutrophils and other immune cells.	NCT04334044 NCT04348071 NCT04355793 NCT04366232 NCT04362137
JAK-STAT	JAK1/2 inhibitor	Baricitinib Tofacitinib	Reduces inflammation produced by neutrophils and other immune cells.	NCT04320277 NCT04340232 NCT04321993 NCT04401579 NCT04469114 NCT04750317
Angiotensin receptor	Angiotensin receptor blocker	Telmisartan	Reduces oxidative stress. Inhibits NADPH oxidase in neutrophils.	NCT04360551 NCT04355936
	Angiotensin II receptor antagonist	Losartan	Blocks neutrophils recruitment	NCT04340557 NCT04328012
	Angiotensin II receptor antagonist	Valsartan	Reduces oxidative stress. Inhibits NADPH oxidase in neutrophils.	NCT04335786
	Inhibitor of the spike protein serine proteases	Alpha-1 antitrypsin	Blocks neutrophils recruitment	NCT04385836
Neutrophil	Calcium-release activated calcium (CRAC) channel inhibitor	CM4620-IE	Blocks neutrophils recruitment	NCT04345614
	Neutrophil viability modulator	Intravenous immunoglobulin (IVIG)	Neutrophil viability modulator	NCT04432324 NCT04411667

(Continued)

TABLE 1 | Continued

Therapeutic target	Type of drug	Drug name	Effect on Neutrophils	Reference number
				NCT04383548
				NCT04403269
		L-MOD	Neutrophil viability modulator	NCT04353674
	Neutrophil chemotaxis inhibitor	Lenalidomide	Blocks neutrophils recruitment	NCT04361643
		Dexamethasone		NCT04325061
				NCT04395105
				NCT04360876
				NCT04344730
IL-6, IL-8, IL-1β and TNF-α	Modulates IL-8, TNF-α, IL-1β and IL-6 gene expression	Doxycycline	Reduces inflammation produced by neutrophils and other immune cells	NCT04371952
IL-17A	Binds interleukin 17A and neutralizes it	Ixekizumab	Reduces inflammation produced by neutrophils and other immune cells	NCT04724629
Anti-inflammatory and anti-fibrotic agent	Monoclonal antibody	TB006	Reduces inflammation produced by neutrophils and other immune cells	NCT04801056

IL, interleukin; GM-CSF, granulocyte-macrophage colony-stimulating factor; NLRP3, nod like receptor family, pyrin domain containing 3; IFN, interferon; TLR, toll-like receptor; NET, neutrophil extracellular trap; JAK-STAT, janus kinase; TNF, tumour necrosis factor.

tetracycline) reduces IL-6, IL-1β and TNF-α levels, however, doxycycline treatment did not have a significant clinical impact on time to recovery, hospital admissions or deaths related to COVID-19 in patients with high risk to adverse outcomes (101).

Granulocyte-macrophage colony-stimulating factor (GM-CSF) is involved in neutrophil recruitment, survival, IL-6 release and priming for NETosis (102, 103). Mavrilimumab, an anti-GM-CSF receptor-α monoclonal antibody, improved clinical outcomes in patients with COVID-19 pneumonia and systemic hyperinflammation (104). In contrast, sargramostim, a recombinant human GM-CSF is under investigation, to improve the immune response by recruiting neutrophils, dendritic cells and macrophages to fight the virus and to repair tissue damage (**Table 1**), although there may be significant risks including neurotoxicity (103). GM-CSF also induces the expansion of immunosuppressive MDSCs, which impair NK cells, CD8+ T cells and increase proliferation of immunosuppressive T regulatory (Treg) cells (105, 106). GM-CSF stimulates the expression of IL-1β, IL-6, TNFα and other pro-inflammatory cytokines and chemokines, therefore, its inhibition would more broadly dampen hyperinflammation than therapy for IL-6 alone. In patients with rheumatoid arthritis this strategy is used for those unresponsive to anti-TNF therapy or tocilizumab (106). Cytokine signalling pathways are targeted by using inhibitors of JAK1/JAK2, to potentially reduce inflammation (**Table 1**). Clinical trials using JAK1/JAKK2 inhibitor Baricitinib showed reduction in 30-day mortality in over 70s with moderate-to-severe COVID-19 pneumonia, and combined with Remdesivir decreased recovery time and reduced 28-day mortality, serious events and new infections (107, 108). Reduction in the risk of death or respiratory failure was also described in a clinical trial including 289 COVID-19 patients when comparing the effects of JAK inhibitor Tofacitinib with a placebo (109).

NLRP3 inflammasome activation in neutrophils is implicated with pulmonary inflammation and inhibition with MCC950 inhibited IL-1β in the lungs of cystic fibrosis mice (110). Tranilast is the first NLRP3 inflammasome inhibitor in clinical trials in the Chinese Clinical Trial Registry. Interleukin-1 blockade with canakinumab treatment increases neutrophil apoptosis and decreases pro-inflammatory signalling in the IL-1β pathway using gene expression and pathway data (111). Canakinumab, is another FDA approved drug under investigation in clinical trials, and may help reduce respiratory and cardiac damage. Colchicine targets the neutrophil and monocyte NLRP3 inflammasome, hence attenuating activation of IL-1β (112). However, no significant differences were seen in primary (disease progression or mortality) or secondary (time to discharge, proportion of patients discharged, time in Intensive Care unit (ICU) or duration of hospitalisation) outcomes in two separated clinical trials comparing patients who were given colchicine to placebo/usual care treated patients (113, 114). Anakinra (commercially known as Kineret) is an FDA approved human IL-1RA (inflammasome-regulated immune response inhibitor of IL-1) which may reduce hyperinflammation and organ damage (**Table 1**) (112). Clinical trials using anakinra as treatment for COVID-19 have reported conflicting results. One study described lower risk of clinical progression in patients who received anakinra compared to placebo, while other study reports no effect of anakinra treatment on in-hospital mortality or days of organ support (115–117). However, the European Medicines Agency (EMA) recommended the use of anakinra in December 2021, specifically for COVID-19 adult patients at risk of developing severe respiratory failure or with pneumonia requiring supplemental oxygen (118).

Intravenous Immunoglobulin (IVIG) and Corticosteroids

IVIG are purified IgG made from a pool of plasma from healthy donors (119) and modulate neutrophil viability through agonistic antibodies anti-Fas and Siglec-9 (120). It may also decrease neutrophil activation and NETs formation and mitigate vascular injury (121). IVIG has been tested in clinical trials in patients with COVID-19 (**Table 1**) and has shown to have therapeutic value (121). Similar positive effects of IVIG have been described in children with Kawasaki's disease and MIS-C. However, ambiguity exists about dose dependent pro/anti-inflammatory effects as high dose IVIG is anti-inflammatory while a lower dose is considered pro-inflammatory (122). The widespread utility of this therapy may be precluded by plasma

shortage, as it is also use as treatment in immunodeficiencies and inflammatory disorders. Treatment of healthy neutrophils with IVIG decreased NETosis and ROS production but enhanced phagocytosis (122).

The efficacy of treating COVID-19 patients with corticosteroids remains controversial. Lomas et al. have demonstrated that dexamethasone can inhibit neutrophil chemotaxis *in vitro* and *in vivo* (123). A variety of studies hypothesise that this anti-inflammatory drug may be effective in reducing ARDS and respiratory failure in COVID-19 patients (**Table 1**). The randomised evaluation of COVID-19 therapy (RECOVERY) trial in hospitalized COVID-19 patients found that treatment with dexamethasone results in a lower 28-day mortality for patients receiving oxygen only or ventilation, though no explanation of the mechanism for this was provided (124). Neutrophil-to-Lymphocyte ratio was reduced in patients treated with corticosteroids for COVID-19.

Targeting NETs

The targeting of neutrophil extracellular traps with dornase alfa, a human recombinant deoxyribonuclease (DNAse) enzyme, degrades DNA and promotes the clearance of NETs and has been used in patients with cystic fibrosis (125). Several studies are investigating the use of dornase alfa to improve pulmonary function in severe COVID-19 with ARDS (**Table 1**) (125). Similarly, all-trans retinoic acid, an inhibitor of NE (granular component involved in NETosis), is also being explored to improve lung injury in COVID-19 patients. COVID-19 is associated with a significant neutrophil NETs burden and targeting NETs-driven IL-1 signalling, using the IL-1 receptor antagonist, decreased NETosis and may modulate inflammation.

CONCLUSION

The clinical syndrome of severe COVID-19 has several unique features, including, unusually for a viral infection, an increased neutrophil-lymphocyte ratio. Neutrophils play a role in viral clearance in terms of NETs and the production of IFN. However, neutrophils can have detrimental effects by aiding the pathogenesis of SARS-CoV-2 and exacerbating complications of COVID-19 such as ARDS, thrombosis and MIS-C. Understanding the role of neutrophils in the pathogenesis of severe COVID-19 may lead to identification of key therapeutic targets and/or biomarkers for early identification of patients who may benefit from immunomodulatory agents to control hyperinflammation and reduce mortality rates.

AUTHOR CONTRIBUTIONS

EM and AMM have performed literature research, designed the review layout, wrote, and revised the review. RW, AUM, NC, JO'D, CNC, TH, and NS have performed literature research, wrote, and revised the review. JI-C designed the review layout, and revised the review. ML has performed literature research, designed the review layout, wrote, and revised the review. EJM has performed literature research, designed the review layout, wrote, and revised the review. All authors agree to be accountable for the content of the work. All authors contributed to the article and approved the submitted version.

REFERENCES

1. Rosales C. Neutrophil: A Cell With Many Roles in Inflammation or Several Cell Types? *Front Physiol* (2018) 9:113. doi: 10.3389/fphys.2018.00113
2. Lacy P. Mechanisms of Degranulation in Neutrophils. *Allergy Asthma Clin Immunol* (2006) 2:98–108. doi: 10.1186/1710-1492-2-3-98
3. Brinkmann V, Reichard U, Goosmann C, Fauler B, Uhlemann Y, Weiss D, et al. Neutrophil Extracellular Traps Kill Bacteria. *Science* (2004) 303:1532–5. doi: 10.1126/science.1092385
4. Wan S, Xiang Y, Fang W, Zheng Y, Li B, Hu Y, et al. Clinical Features and Treatment of COVID-19 Patients in Northeast Chongqing. *J Med Virol* (2020) 92:797–806. doi: 10.1002/jmv.25783
5. Huang C, Wang Y, Li X, Ren L, Zhao J, Hu Y, et al. Clinical Features of Patients Infected With 2019 Novel Coronavirus in Wuhan, China. *Lancet* (2020) 395:497–506. doi: 10.1016/S0140-6736(20)30183-5
6. Liu J, Liu Y, Xiang P, Pu L, Xiong H, Li C, et al. Neutrophil-To-Lymphocyte Ratio Predicts Critical Illness Patients With 2019 Coronavirus Disease in the Early Stage. *J Transl Med* (2020) 18:206. doi: 10.1186/s12967-020-02374-0
7. Wang D, Hu B, Hu C, Zhu F, Liu X, Zhang J, et al. Clinical Characteristics of 138 Hospitalized Patients With 2019 Novel Coronavirus-Infected Pneumonia in Wuhan, China. *JAMA* (2020) 323:1061–9. doi: 10.1001/jama.2020.1585
8. Itelman E, Wasserstrum Y, Segev A, Avaky C, Negru L, Cohen D, et al. Clinical Characterization of 162 COVID-19 Patients in Israel: Preliminary Report From a Large Tertiary Center. *Isr Med Assoc J* (2020) 22:271–4.
9. Zeng Z, Feng S, Chen G, Wu J. Predictive Value of the Neutrophil to Lymphocyte Ratio for Disease Deterioration and Serious Adverse Outcomes in Patients With COVID-19: A Prospective Cohort Study. *BMC Infect Dis* (2021) 21:80. doi: 10.1186/s12879-021-05796-3
10. Seyit M, Avci E, Nar R, Senol H, Yilmaz A, Ozen M, et al. Neutrophil to Lymphocyte Ratio, Lymphocyte to Monocyte Ratio and Platelet to Lymphocyte Ratio to Predict the Severity of COVID-19. *Am J Emerg Med* (2021) 40:110–4. doi: 10.1016/j.ajem.2020.11.058
11. Moradi E, Teimouri A, Rezaee R, Morovatdar N, Foroughian M, Layegh P. Increased Age, Neutrophil-to-Lymphocyte Ratio (NLR) and White Blood Cells Count Are Associated With Higher COVID-19 Mortality. *Am J Emerg Med* (2021) 40:11–4. doi: 10.1016/j.ajem.2020.12.003
12. Li L, Li J, Gao M, Fan H, Wang Y, Xu X, et al. Interleukin-8 as a Biomarker for Disease Prognosis of Coronavirus Disease-2019 Patients. *Front Immunol* (2021) 11:602395. doi: 10.3389/fimmu.2020.602395
13. Masso-Silva J, Moshensky A, Lam M, Odish M, Patel A, Xu L, et al. Increased Peripheral Blood Neutrophil Activation Phenotypes and Neutrophil Extracellular Trap Formation in Critically Ill Coronavirus Disease 2019 (COVID-19) Patients: A Case Series and Review of the Literature. *Clin Infect Dis* (2022) 74:479–89. doi: 10.1093/cid/ciab437
14. Ma A, Zhang L, Ye X, Chen J, Yu J, Zhuang L, et al. High Levels of Circulating IL-8 and Soluble IL-2r Are Associated With Prolonged Illness in Patients With Severe COVID-19. *Front Immunol* (2021) 12:626235. doi: 10.3389/fimmu.2021.626235
15. Zhao Y, Nie H, Hu K, Wu X, Zhang Y, Wang M, et al. Abnormal Immunity of Non-Survivors With COVID-19: Predictors for Mortality. *Infect Dis Poverty* (2020) 9:108. doi: 10.1186/s40249-020-00723-1
16. Zuo Y, Zuo M, Yalavarthi S, Gockman K, Madison J, Shi H, et al. Neutrophil Extracellular Traps and Thrombosis in COVID-19. *J Thromb Thrombolysis* (2021) 51:446–53. doi: 10.1007/s11239-020-02324-z
17. Blasco A, Coronado M, Hernández-Terciado F, Martín P, Royuela A, Ramil E, et al. Assessment of Neutrophil Extracellular Traps in Coronary

Thrombus of a Case Series of Patients With COVID-19 and Myocardial Infarction. *JAMA Cardiol* (2020) 6:1–6. doi: 10.1001/jamacardio.2020.7308
18. Calabrese F, Pezzuto F, Fortarezza F, Hofman P, Kern I, Panizo A, et al. Pulmonary Pathology and COVID-19: Lessons From Autopsy. The Experience of European Pulmonary Pathologists. *Virchows Arch* (2020) 477:359–72. doi: 10.1007/s00428-020-02886-6
19. Soliman W, Sherif N, Ghanima I, El-Badawy M. Neutrophil to Lymphocyte and Platelet to Lymphocyte Ratios in Systemic Lupus Erythematosus: Relation With Disease Activity and Lupus Nephritis. *Reumatol Clin* (2020) 16:255–61. doi: 10.1016/j.reuma.2018.07.008
20. Leist S, Jensen K, Baric R, Sheahan T. Increasing the Translation of Mouse Models of MERS Coronavirus Pathogenesis Through Kinetic Hematological Analysis. *PloS One* (2019) 14:e0220126–e. doi: 10.1371/journal.pone.0220126
21. McElvaney O, McEvoy N, McElvaney O, Carroll T, Murphy M, Dunlea D, et al. Characterization of the Inflammatory Response to Severe COVID-19 Illness. *Am J Respir Crit Care Med* (2020) 202:812–21. doi: 10.1164/rccm.202005-1583OC
22. Hemmat N, Derakhshani A, Baghi H, Silvestris N, Baradaran B, De Summa S. Neutrophils, Crucial, or Harmful Immune Cells Involved in Coronavirus Infection: A Bioinformatics Study. *Front Genet* (2020) 11:641. doi: 10.3389/fgene.2020.00641
23. Haick A, Rzepka J, Brandon E, Balemba O, Miura T. Neutrophils are Needed for an Effective Immune Response Against Pulmonary Rat Coronavirus Infection, But Also Contribute to Pathology. *J Gen Virol* (2014) 95:578–90. doi: 10.1099/vir.0.061986-0
24. Thiam H, Wong S, Wagner D, Waterman C. Cellular Mechanisms of NETosis. *Annu Rev Cell Dev Biol* (2020) 36:191–218. doi: 10.1146/annurev-cellbio-020520-111016
25. Kumar S, Payal N, Srivastava V, Kaushik S, Saxena J, Jyoti A. Neutrophil Extracellular Traps and Organ Dysfunction in Sepsis. *Clin Chim Acta* (2021) 523:152–62. doi: 10.1016/j.cca.2021.09.012
26. Kumar S, Gupta E, Kaushik S, Srivastava V, Saxena J, Mehta S, et al. Quantification of NETs Formation in Neutrophil and its Correlation With the Severity of Sepsis and Organ Dysfunction. *Clin Chim Acta* (2019) 495:606–10. doi: 10.1016/j.cca.2019.06.008
27. Silva C, Wanderley C, Veras F, Sonego F, Nascimento D, Gonçalves A, et al. Gasdermin D Inhibition Prevents Multiple Organ Dysfunction During Sepsis by Blocking NET Formation. *Blood* (2021) 138:2702–13. doi: 10.1182/blood.2021011525
28. Veras F, Cornejo Pontelli M, Meirelles Silva C, Toller-Kawahisa J, de Lima M, Carvalho Nascimento D, et al. SARS-CoV-2-Triggered Neutrophil Extracellular Traps Mediate COVID-19 Pathology. *J Exp Med* (2020) 217: e20201129. doi: 10.1084/jem.20201129
29. Radermecker C, Detrembleur N, Guiot J, Cavalier E, Henket M, d'Emal C, et al. Neutrophil Extracellular Traps Infiltrate the Lung Airway, Interstitial, and Vascular Compartments in Severe COVID-19. *J Exp Med* (2020) 217: e20201012. doi: 10.1084/jem.20201012
30. Middleton E, He X, Denorme F, Campbell R, Ng D, Salvatore S, et al. Neutrophil Extracellular Traps Contribute to Immunothrombosis in COVID-19 Acute Respiratory Distress Syndrome. *Blood* (2020) 136:1169–79. doi: 10.1182/blood.2020007008
31. Barnes B, Adrover J, Baxter-Stoltzfus A, Borczuk A, Cools-Lartigue J, Crawford J, et al. Targeting Potential Drivers of COVID-19: Neutrophil Extracellular Traps. *J Exp Med* (2020) 217:e20200652. doi: 10.1084/jem.20200652
32. Ouwendijk W, Raadsen M, Kampen J, Verdijk R, von der Thusen J, Guo L, et al. Neutrophil Extracellular Traps Persist at High Levels in the Lower Respiratory Tract of Critically Ill COVID-19 Patients. *J Infect Dis* (2021) 223: jiab053. doi: 10.1093/infdis/jiab053
33. Li C, Xing Y, Zhang Y, Hua Y, Hu J, Bai Y. Neutrophil Extracellular Traps Exacerbate Ischemic Brain Damage. *Mol Neurobiol* (2022) 59:643–56. doi: 10.1007/s12035-021-02635-z
34. Pramitasuri T, Laksmidewi A, Putra I, Dalimartha F. Neutrophil Extracellular Traps in Coronavirus Disease-19-Associated Ischemic Stroke: A Novel Avenue in Neuroscience. *Exp Neurobiol* (2021) 30:1–12. doi: 10.5607/en20048
35. Drescher B, Bai F. Neutrophil in Viral Infections, Friend or Foe? *Virus Res* (2013) 171:1–7. doi: 10.1016/j.virusres.2012.11.002
36. Naumenko V, Turk M, Jenne C, Kim S. Neutrophils in Viral Infection. *Cell Tissue Res* (2018) 371:505–16. doi: 10.1007/s00441-017-2763-0
37. Hiroki C, Toller-Kawahisa J, Fumagalli M, Colon D, Figueiredo L, Fonseca B, et al. Neutrophil Extracellular Traps Effectively Control Acute Chikungunya Virus Infection. *Front Immunol* (2020) 10:3108. doi: 10.3389/fimmu.2019.03108
38. Darcy C, Minigo G, Piera K, Davis J, McNeil Y, Chen Y, et al. Neutrophils With Myeloid Derived Suppressor Function Deplete Arginine and Constrain T Cell Function in Septic Shock Patients. *Crit Care* (2014) 18:R163. doi: 10.1186/cc14003
39. Apel F, Andreeva L, Knackstedt L, Streeck R, Frese C, Goosmann C, et al. The Cytosolic DNA Sensor cGAS Recognizes Neutrophil Extracellular Traps. *Sci Signal* (2021) 14:eaax7942. doi: 10.1126/scisignal.aax7942
40. Berthelot J, Drouet L, Lioté F. Kawasaki-Like Diseases and Thrombotic Coagulopathy in COVID-19: Delayed Over-Activation of the STING Pathway? *Emerg Microbes Infect* (2020) 9:1514–22. doi: 10.1080/22221751.2020.1785336
41. Li M, Ferretti M, Ying B, Descamps H, Lee E, Dittmar M, et al. Pharmacological Activation of STING Blocks SARS-CoV-2 Infection. *Sci Immunol* (2021) 6:eabi9007. doi: 10.1126/sciimmunol.abi9007
42. Mitsios A, Arampatzioglou A, Arelaki S, Mitroulis I, Ritis K. NETopathies? Unraveling the Dark Side of Old Diseases Through Neutrophils. *Front Immunol* (2017) 7:678. doi: 10.3389/fimmu.2016.00678
43. Torres-Ruiz J, Absalón-Aguilar A, Nuñez-Aguirre M, Pérez-Fragoso A, Carrillo-Vázquez D, Maravillas-Montero J, et al. Neutrophil Extracellular Traps Contribute to COVID-19 Hyperinflammation and Humoral Autoimmunity. *Cells* (2021) 10:2545. doi: 10.3390/cells10102545
44. Skendros P, Mitsios A, Chrysanthopoulou A, Mastellos D, Metallidis S, Rafailidis P, et al. Complement and Tissue Factor-Enriched Neutrophil Extracellular Traps Are Key Drivers in COVID-19 Immunothrombosis. *J Clin Invest* (2020) 130:6151–7. doi: 10.1172/JCI141374
45. Mankan A, Dau T, Jenne D, Hornung V. The NLRP3/ASC/Caspase-1 Axis Regulates IL-1β Processing in Neutrophils. *Eur J Immunol* (2012) 42:710–5. doi: 10.1002/eji.201141921
46. Hayward J, Mathur A, Ngo C, Man S. Cytosolic Recognition of Microbes and Pathogens: Inflammasomes in Action. *Microbiol Mol Biol Rev* (2018) 82: e00015–18. doi: 10.1128/mmbr.00015-18
47. Rodrigues T, de Sá K, Ishimoto A, Becerra A, Oliveira S, Almeida L, et al. Inflammasomes are Activated in Response to SARS-CoV-2 Infection and are Associated With COVID-19 Severity in Patients. *J Exp Med* (2021) 218: e20201707. doi: 10.1084/jem.20201707
48. Aymonnier K, Ng J, Fredenburgh L, Zambrano-Vera K, Münzer P, Gutch S, et al. Inflammasome Activation in Neutrophils of Patients With Severe COVID-19. *Blood Adv* (2022) 6:2001–13. doi: 10.1182/bloodadvances.2021005949
49. Chen I, Moriyama M, Chang M, Ichinohe T. Severe Acute Respiratory Syndrome Coronavirus Viroporin 3a Activates the NLRP3 Inflammasome. *Front Microbiol* (2019) 10:50. doi: 10.3389/fmicb.2019.00050
50. Mousavizadeh L, Ghasemi S. Genotype and Phenotype of COVID-19: Their Roles in Pathogenesis. *J Microbiol Immunol Infect* (2021) 54:159–63. doi: 10.1016/j.jmii.2020.03.022
51. Courjon J, Dufies O, Robert A, Bailly L, Torre C, Chirio D, et al. Heterogeneous NLRP3 Inflammasome Signature in Circulating Myeloid Cells as a Biomarker of COVID-19 Severity. *Blood Adv* (2021) 5:1523–34. doi: 10.1182/bloodadvances.2020003918
52. Ui Mhaonaigh A, Coughlan A, Dwivedi A, Hartnett J, Cabral J, Moran B, et al. Low Density Granulocytes in ANCA Vasculitis Are Heterogenous and Hypo-Responsive to Anti-Myeloperoxidase Antibodies. *Front Immunol* (2019) 10:2603. doi: 10.3389/fimmu.2019.02603
53. Morrissey S, Geller A, Hu X, Tier D, Cooke E, Ding C, et al. Emergence of Low-Density Inflammatory Neutrophils Correlates With Hypercoagulable State and Disease Severity in COVID-19 Patients. *MedRxiv* (2020), 20106724. doi: 10.1101/2020.05.22.20106724
54. Spijkerman R, Jorritsma N, Bongers S, Bindels B, Jukema B, Hesselink L, et al. An Increase in CD62Ldim Neutrophils Precedes the Development of Pulmonary Embolisms in COVID- 19 Patients. *Scand J Immunol* (2021) 93: e13023. doi: 10.1111/sji.13023
55. Carissimo G, Xu W, Kwok I, Abdad M, Chan Y, Fong S, et al. Whole Blood Immunophenotyping Uncovers Immature Neutrophil-to-VD2 T-Cell Ratio as an Early Marker for Severe COVID-19. *Nat Commun* (2020) 11:5243. doi: 10.1038/s41467-020-19080-6

56. Parackova Z, Zentsova I, Bloomfield M, Vrabcova P, Smetanova J, Klocperk A, et al. Disharmonic Inflammatory Signatures in COVID-19: Augmented Neutrophils' But Impaired Monocytes' and Dendritic Cells' Responsiveness. *Cells* (2020) 9:2206. doi: 10.3390/cells9102206
57. Liao M, Liu Y, Yuan J, Wen Y, Xu G, Zhao J, et al. Single-Cell Landscape of Bronchoalveolar Immune Cells in Patients With COVID-19. *Nat Med* (2020) 26:842–4. doi: 10.1038/s41591-020-0901-9
58. Sagiv J, Michaeli J, Assi S, Mishalian I, Kisos H, Levy L, et al. Phenotypic Diversity and Plasticity in Circulating Neutrophil Subpopulations in Cancer. *Cell Rep* (2015) 10:562–73. doi: 10.1016/j.celrep.2014.12.039
59. Bronte V, Brandau S, Chen S, Colombo M, Frey A, Greten T, et al. Recommendations for Myeloid-Derived Suppressor Cell Nomenclature and Characterization Standards. *Nat Commun* (2016) 7:12150. doi: 10.1038/ncomms12150
60. Wu D, Yang X. TH17 Responses in Cytokine Storm of COVID-19: An Emerging Target of JAK2 Inhibitor Fedratinib. *J Microbiol Immunol Infect* (2020) 53:368–70. doi: 10.1016/j.jmii.2020.03.005
61. Torres-Ruiz J, Pérez-Fragoso A, Maravillas-Montero J, Llorente L, Mejía-Domínguez N, Páez-Franco J, et al. Redefining COVID-19 Severity and Prognosis: The Role of Clinical and Immunobiotypes. *Front Immunol* (2021) 12:689966. doi: 10.3389/fimmu.2021.689966
62. Aschenbrenner A, Mouktaroudi M, Krämer B, Oestreich M, Antonakos N, Nuesch-Germano M, et al. Disease Severity-Specific Neutrophil Signatures in Blood Transcriptomes Stratify COVID-19 Patients. *Genome Med* (2021) 13:7. doi: 10.1186/s13073-020-00823-5
63. Schulte-Schrepping J, Reusch N, Paclik D, Baßler K, Schlickeiser S, Zhang B, et al. Severe COVID-19 Is Marked by a Dysregulated Myeloid Cell Compartment. *Cell* (2020) 182:1419–40.e23. doi: 10.1016/j.cell.2020.08.001
64. Chevrier S, Zurbuchen Y, Cervia C, Adamo S, Raeber M, de Souza N, et al. A Distinct Innate Immune Signature Marks Progression From Mild to Severe COVID-19. *Cell Rep Med* (2020) 2:100166. doi: 10.1016/j.xcrm.2020.100166
65. Reizine F, Lesouhaitier M, Gregoire M, Pinceaux K, Gacouin A, Maamar A, et al. SARS-CoV-2-Induced ARDS Associates With MDSC Expansion, Lymphocyte Dysfunction, and Arginine Shortage. *J Clin Immunol* (2021) 41:515–25. doi: 10.1007/s10875-020-00920-5
66. Muralidharan A, Reid S. Complex Roles of Neutrophils During Arboviral Infections. *Cells* (2021) 10:1324. doi: 10.3390/cells10061324
67. Ni W, Yang X, Yang D, Bao J, Li R, Xiao Y, et al. Role of Angiotensin-Converting Enzyme 2 (ACE2) in COVID-19. *Crit Care* (2020) 24:422. doi: 10.1186/s13054-020-03120-0
68. Verdecchia P, Cavallini C, Spanevello A, Angeli F. The Pivotal Link Between ACE2 Deficiency and SARS-CoV-2 Infection. *Eur J Intern Med* (2020) 76:14–20. doi: 10.1016/j.ejim.2020.04.037
69. Mehta N, Kalra A, Nowacki AS, Anjewierden S, Han Z, Bhat P, et al. Association of Use of Angiotensin-Converting Enzyme Inhibitors and Angiotensin II Receptor Blockers With Testing Positive for Coronavirus Disease 2019 (COVID-19). *JAMA Cardiol* (2020) 5:1020–6. doi: 10.1001/jamacardio.2020.1855
70. Zhang P, Zhu L, Cai J, Lei F, Qin JJ, Xie J, et al. Association of Inpatient Use of Angiotensin-Converting Enzyme Inhibitors and Angiotensin II Receptor Blockers With Mortality Among Patients With Hypertension Hospitalized With COVID-19. *Circ Res* (2020) 126:1671–81. doi: 10.1161/CIRCRESAHA.120.317134
71. Khan Z, Shen XZ, Bernstein EA, Giani JF, Eriguchi M, Zhao TV, et al. Angiotensin-Converting Enzyme Enhances the Oxidative Response and Bactericidal Activity of Neutrophils. *Blood* (2017) 130:328–39. doi: 10.1182/blood-2016-11-752006
72. Hayashi F, Means T, Luster A. Toll-Like Receptors Stimulate Human Neutrophil Function. *Blood* (2003) 102:2660–9. doi: 10.1182/blood-2003-04-1078
73. Vaure C, Liu Y. Comparative Review of Toll-Like Receptor 4 Expression and Functionality in Different Animal Species. *Front Immunol* (2014) 5:316. doi: 10.3389/fimmu.2014.00316
74. Kawasaki T, Kawai T. Toll-Like Receptor Signaling Pathways. *Front Immunol* (2014) 5:461. doi: 10.3389/fimmu.2014.00461
75. Rocha B, Marques P, de Souza Leoratti F, Caroline Junqueira C, Batista Pereira D, do Valle Antonelli L, et al. Type I Interferon Transcriptional Signature in Neutrophils and Low-Density Granulocytes Are Associated With Tissue Damage in Malaria. *Cell Rep* (2015) 13:2829–41. doi: 10.1016/j.celrep.2015.11.055
76. Blanco-Melo D, Nilsson-Payant B, Liu W, Uhl S, Hoagland D, Møller R, et al. Imbalanced Host Response to SARS-CoV-2 Drives Development of COVID-19. *Cell* (2020) 181:1036–45.e9. doi: 10.1016/j.cell.2020.04.026
77. Banerjee A, Rapin N, Bollinger T, Misra V. Lack of Inflammatory Gene Expression in Bats: A Unique Role for a Transcription Repressor. *Sci Rep* (2017) 7:2232. doi: 10.1038/s41598-017-01513-w
78. Fogarty H, Townsend L, Ni Cheallaigh C, Bergin C, Martin-Loeches I, Browne P, et al. COVID19 Coagulopathy in Caucasian Patients. *Br J Haematol* (2020) 189:1044–9. doi: 10.1111/bjh.16749
79. Zhou F, Yu T, Du R, Fan G, Liu Y, Liu Z, et al. Clinical Course and Risk Factors for Mortality of Adult Inpatients With COVID-19 in Wuhan, China: A Retrospective Cohort Study. *Lancet* (2020) 395:1054–62. doi: 10.1016/s0140-6736(20)30566-3
80. Zuo Y, Warnock M, Harbaugh A, Yalavarthi S, Gockman K, Zuo M, et al. Plasma Tissue Plasminogen Activator and Plasminogen Activator Inhibitor-1 in Hospitalized COVID-19 Patients. *Sci Rep* (2021) 11:1580. doi: 10.1038/s41598-020-80010-z
81. Petito E, Falcinelli E, Paliani U, Cesari E, Vaudo G, Sebastiano M, et al. Neutrophil More Than Platelet Activation Associates With Thrombotic Complications in COVID-19 Patients. *J Infect Dis* (2020) 223:jiaa756. doi: 10.1093/infdis/jiaa756
82. Wichmann D, Sperhake J, Lütgehetmann M, Steurer S, Edler C, Heinemann A, et al. Autopsy Findings and Venous Thromboembolism in Patients With COVID-19: A Prospective Cohort Study. *Ann Intern Med* (2020) 173:268–77. doi: 10.7326/m20-2003
83. McGonagle D, O'Donnell J, Sharif K, Emery P, Bridgewood C. Immune Mechanisms of Pulmonary Intravascular Coagulopathy in COVID-19 Pneumonia. *Lancet Rheumatol* (2020) 2:e437–e45. doi: 10.1016/s2665-9913(20)30121-1
84. Ackermann M, Verleden S, Kuehnel M, Haverich A, Welte T, Laenger F, et al. Pulmonary Vascular Endothelialitis, Thrombosis, and Angiogenesis in Covid-19. *N Engl J Med* (2020) 383:120–8. doi: 10.1056/NEJMoa2015432
85. Kapoor S, Opneja A, Nayak L. The Role of Neutrophils in Thrombosis. *Thromb Res* (2018) 170:87–96. doi: 10.1016/j.thromres.2018.08.005
86. Comer S, Cullivan S, Szklanna P, Weiss L, Cullen S, Kelliher S, et al. COVID-19 Induces a Hyperactive Phenotype in Circulating Platelets. *PloS Biol* (2021) 19:e3001109. doi: 10.1371/journal.pbio.3001109
87. Folco E, Mawson T, Vromman A, Bernardes-Souza B, Franck G, Persson O, et al. Neutrophil Extracellular Traps Induce Endothelial Cell Activation and Tissue Factor Production Through Interleukin-1α and Cathepsin G. *Arterioscler Thromb Vasc Biol* (2018) 38:1901–12. doi: 10.1161/ATVBAHA.118.311150
88. Qi H, Yang S, Zhang L. Neutrophil Extracellular Traps and Endothelial Dysfunction in Atherosclerosis and Thrombosis. *Front Immunol* (2017) 8:928. doi: 10.3389/fimmu.2017.00928
89. Yost CC, Cody MJ, Harris ES, Thornton NL, McInturff AM, Martinez ML, et al. Impaired Neutrophil Extracellular Trap (NET) Formation: A Novel Innate Immune Deficiency of Human Neonates. *Blood* (2009) 113:6419–27. doi: 10.1182/blood-2008-07-171629
90. Feldstein L, Rose E, Horwitz S, Collins J, Newhams M, Son M, et al. Multisystem Inflammatory Syndrome in U.S. Children and Adolescents. *N Engl J Med* (2020) 383:334–46. doi: 10.1056/NEJMoa2021680
91. Yoshida Y, Takeshita S, Kawamura Y, Kanai T, Tsujita Y, Nonoyama S, et al. Enhanced Formation of Neutrophil Extracellular Traps in Kawasaki Disease. *Pediatr Res* (2020) 87:998–1004. doi: 10.1038/s41390-019-0710-3
92. Muto T, Masuda Y, Numoto S, Kodama S, Yamakawa K, Takasu M, et al. White Blood Cell and Neutrophil Counts and Response to Intravenous Immunoglobulin in Kawasaki Disease. *Global Pediatr Health* (2019) 6:2333794X19884826. doi: 10.1177/2333794X19884826
93. Pouletty M, Borocco C, Ouldali N, Caseris M, Basmaci R, Lachaume N, et al. Paediatric Multisystem Inflammatory Syndrome Temporally Associated With SARS-CoV-2 Mimicking Kawasaki Disease (Kawa-COVID-19): A Multicentre Cohort. *Ann Rheum Dis* (2020) 79:999–1006. doi: 10.1136/annrheumdis-2020-217960
94. Carter M, Fish M, Jennings A, Doores K, Wellman P, Seow J, et al. Peripheral Immunophenotypes in Children With Multisystem Inflammatory Syndrome Associated With SARS-CoV-2 Infection. *Nat Med* (2020) 26:1701–7. doi: 10.1038/s41591-020-1054-6

95. Ramaswamy A, Brodsky N, Sumida T, Comi M, Asashima H, Hoehn K, et al. Immune Dysregulation and Autoreactivity Correlate With Disease Severity in SARS-CoV-2-Associated Multisystem Inflammatory Syndrome in Children. *Immunity* (2021) 54:1083–95. doi: 10.1016/j.immuni.2021.04.003
96. Gaber T, Hahne M, Strehl C, Hoff P, Dörffel Y, Feist E, et al. Disentangling the Effects of Tocilizumab on Neutrophil Survival and Function. *Immunol Res* (2016) 64:665–76. doi: 10.1007/s12026-015-8770-x
97. Lok LSC, Farahi N, Juss JK, Loutsios C, Solanki CK, Peters AM, et al. Effects of Tocilizumab on Neutrophil Function and Kinetics. *Eur J Clin Invest* (2017) 47:736–45. doi: 10.1111/eci.12799
98. Molloy EJ, Bearer CF. COVID-19 in Children and Altered Inflammatory Responses. *Pediatr Res* (2020) 88:340–1. doi: 10.1038/s41390-020-0881-y
99. Molloy EJ, Lavizzari A, Klingenberg C, Profit J, Zupancic JAF, Davis AS, et al. Neonates in the COVID-19 Pandemic. *Pediatr Res* (2021) 89:1038–40. doi: 10.1038/s41390-020-1096-y
100. Sinha P, Mostaghim A, Bielick CG, McLaughlin A, Hamer DH, Wetzler LM, et al. Early Administration of Interleukin-6 Inhibitors for Patients With Severe COVID-19 Disease is Associated With Decreased Intubation, Reduced Mortality, and Increased Discharge. *Int J Infect Dis* (2020) 99:28–33. doi: 10.1016/j.ijid.2020.07.023
101. Butler C, Yu L, Dorward J, Gbinigie O, Hayward G, Saville B, et al. Doxycycline for Community Treatment of Suspected COVID-19 in People at High Risk of Adverse Outcomes in the UK (PRINCIPLE): A Randomised, Controlled, Open-Label, Adaptive Platform Trial. *Lancet Respir Med* (2021) 9:1010–20. doi: 10.1016/S2213-2600(21)00310-6
102. Castellani S, D'Oria S, Diana A, Polizzi A, Di Gioia S, Mariggiò M, et al. G-CSF and GM-CSF Modify Neutrophil Functions at Concentrations Found in Cystic Fibrosis. *Sci Rep* (2019) 9:12937. doi: 10.1038/s41598-019-49419-z
103. Mehta P, Porter J, Manson J, Isaacs J, Openshaw P, McInnes I, et al. Therapeutic Blockade of Granulocyte Macrophage Colony-Stimulating Factor in COVID-19-Associated Hyperinflammation: Challenges and Opportunities. *Lancet Respir Med* (2020) 8:822–30. doi: 10.1016/s2213-2600(20)30267-8
104. De Luca G, Cavalli G, Campochiaro C, Della-Torre E, Angelillo P, Tomelleri A, et al. GM-CSF Blockade With Mavrilimumab in Severe COVID-19 Pneumonia and Systemic Hyperinflammation: A Single-Centre, Prospective Cohort Study. *Lancet Rheumatol* (2020) 2:e465–e73. doi: 10.1016/S2665-9913(20)30170-3
105. Tavakkoli M, Wilkins C, Mones J, Mauro M. A Novel Paradigm Between Leukocytosis, G-CSF Secretion, Neutrophil-To-Lymphocyte Ratio, Myeloid-Derived Suppressor Cells, and Prognosis in Non-Small Cell Lung Cancer. *Front Oncol* (2019) 9:295. doi: 10.3389/fonc.2019.00295
106. Lang FM, Lee KMC, Teijaro JR, Becher B, Hamilton JA. GM-CSF-Based Treatments in COVID-19: Reconciling Opposing Therapeutic Approaches. *Nat Rev Immunol* (2020) 20:507–14. doi: 10.1038/s41577-020-0357-7
107. Kalil A, Patterson T, Mehta A, Tomashek K, Wolfe C, Ghazaryan V, et al. Baricitinib Plus Remdesivir for Hospitalized Adults With Covid-19. *N Engl J Med* (2021) 384:795–807. doi: 10.1056/NEJMoa2031994
108. Abizanda P, Calbo Mayo J, Mas Romero M, Cortés Zamora E, Tabernero Sahuquillo M, Romero Rizos L, et al. Baricitinib Reduces 30-Day Mortality in Older Adults With Moderate-to-Severe COVID-19 Pneumonia. *J Am Geriatr Soc* (2021) 69:2752–8. doi: 10.1111/jgs.17357
109. Guimarães P, Quirk D, Furtado R, Maia L, Saraiva J, Antunes M, et al. Tofacitinib in Patients Hospitalized With Covid-19 Pneumonia. *N Engl J Med* (2021) 385:406–15. doi: 10.1056/NEJMoa2101643
110. McElvaney OJ, Zaslona Z, Becker-Flegler K, Palsson-McDermott EM, Boland F, Gunaratnam C, et al. Specific Inhibition of the NLRP3 Inflammasome as an Antiinflammatory Strategy in Cystic Fibrosis. *Am J Respir Crit Care Med* (2019) 200:1381–91. doi: 10.1164/rccm.201905-1013OC
111. Torene R, Nirmala N, Obici L, Cattalini M, Tormey V, Caorsi R, et al. Canakinumab Reverses Overexpression of Inflammatory Response Genes in Tumour Necrosis Factor Receptor-Associated Periodic Syndrome. *Ann Rheum Dis* (2017) 76:303–9. doi: 10.1136/annrheumdis-2016-209335
112. Wu R, Wang L, Kuo H, Shannar A, Peter R, Chou P, et al. An Update on Current Therapeutic Drugs Treating COVID-19. *Curr Pharmacol Rep* (2020) 6:56–70. doi: 10.1007/s40495-020-00216-7
113. Absalón-Aguilar A, Rull-Gabayet M, Pérez-Fragoso A, Mejía-Domínguez N, Núñez-Álvarez C, Kershenobich-Stalnikowitz D, et al. Colchicine Is Safe Though Ineffective in the Treatment of Severe COVID-19: A Randomized Clinical Trial (COLCHIVID). *J Gen Intern Med* (2022) 37:4–14. doi: 10.1007/s11606-021-07203-8
114. RECOVERY CG. Colchicine in Patients Admitted to Hospital With COVID-19 (RECOVERY): A Randomised, Controlled, Open-Label, Platform Trial. *Lancet Respir Med* (2021) 9:1419–26. doi: 10.1016/S2213-2600(21)00435-5
115. Kyriazopoulou E, Huet T, Cavalli G, Gori A, Kyprianou M, Pickkers P, et al. Effect of Anakinra on Mortality in Patients With COVID-19: A Systematic Review and Patient-Level Meta-Analysis. *Lancet Rheumatol* (2021) 3:e690–e7. doi: 10.1016/S2665-9913(21)00216-2
116. Kyriazopoulou E, Poulakou G, Milionis H, Metallidis S, Adamis G, Tsiakos K, et al. Early Treatment of COVID-19 With Anakinra Guided by Soluble Urokinase Plasminogen Receptor Plasma Levels: A Double-Blind, Randomized Controlled Phase 3 Trial. *Nat Med* (2021) 27:1752–60. doi: 10.1038/s41591-021-01499-z
117. Derde L, Gordon A, Mouncey P, Al-Beidh F, Rowan K, Nichol A, et al. Effectiveness of Tocilizumab, Sarilumab, and Anakinra for Critically Ill Patients With COVID-19 The REMAP-CAP COVID-19 Immune Modulation Therapy Domain Randomized Clinical Trial. *medRxiv* (2021). doi: 10.1101/2021.06.18.21259133
118. European Medicines Agency. *EMA Recommends Approval for Use of Kineret in Adults With COVID-19* (2021). Available at: https://www.ema.europa.eu/en/news/ema-recommends-approval-use-kineret-adults-covid-19 (Accessed April 26, 2022).
119. Molloy E. The Doctor's Dilemma: Lessons From GB Shaw in a Modern Pandemic COVID-19. *Pediatr Res* (2021) 89:701–3. doi: 10.1038/s41390-020-0927-1
120. Schneider C, Wicki S, Graeter S, Timcheva T, Keller C, Quast I, et al. IVIG Regulates the Survival of Human But Not Mouse Neutrophils. *Sci Rep* (2017) 7:1296. doi: 10.1038/s41598-017-01404-0
121. Sakoulas G, Geriak M, Kullar R, Greenwood K, Habib M, Vyas A, et al. Intravenous Immunoglobulin Plus Methylprednisolone Mitigate Respiratory Morbidity in Coronavirus Disease 2019. *Crit Care Explor* (2020) 2:e0280. doi: 10.1097/CCE.0000000000000280
122. Liu X, Cao W, Li T. High-Dose Intravenous Immunoglobulins in the Treatment of Severe Acute Viral Pneumonia: The Known Mechanisms and Clinical Effects. *Front Immunol* (2020) 11:1660. doi: 10.3389/fimmu.2020.01660
123. Lomas D, Ip M, Chamba A, Stockley R. The Effect Of*In Vitro* And*In Vivo* Dexamethasone on Human Neutrophil Function. *Agents Actions* (1991) 33:279–85. doi: 10.1007/BF01986574
124. RECOVERY Collaborative Group, Horby P, Pessoa-Amorim G, Peto L, Brightling C, Sarkar R, et al. Tocilizumab in Patients Admitted to Hospital With COVID-19 (RECOVERY): Preliminary Results of a Randomised, Controlled, Open-Label, Platform Trial. *Lancet* (2021) 397:1637–45. doi: 10.1016/S0140-6736(21)00676-0
125. Earhart A, Holliday Z, Hofmann H, Schrum A. Consideration of Dornase Alfa for the Treatment of Severe COVID-19 Acute Respiratory Distress Syndrome. *New Microbes New Infect* (2020) 35:100689. doi: 10.1016/j.nmni.2020.100689

Conflict of Interest: The authors declare that the research was conducted in the absence of any commercial or financial relationships that could be construed as a potential conflict of interest.

frontiers | Frontiers in Immunology

REVIEW
published: 10 June 2022
doi: 10.3389/fimmu.2022.902206

Neutrophil Extracellular Traps, Sepsis and COVID-19 – A Tripod Stand

Esmeiry Ventura-Santana, Joshua R. Ninan, Caitlin M. Snyder and Emeka B. Okeke *

Department of Biology, State University of New York at Fredonia, Fredonia, NY, United States

The novel severe acute respiratory syndrome coronavirus 2 (SARS-CoV-2) is responsible for the current coronavirus disease 2019 (COVID-19) pandemic. Majority of COVID-19 patients have mild disease but about 20% of COVID-19 patients progress to severe disease. These patients end up in the intensive care unit (ICU) with clinical manifestations of acute respiratory distress syndrome (ARDS) and sepsis. The formation of neutrophil extracellular traps (NETs) has also been associated with severe COVID-19. Understanding of the immunopathology of COVID-19 is critical for the development of effective therapeutics. In this article, we discuss evidence indicating that severe COVID-19 has clinical presentations consistent with the definitions of viral sepsis. We highlight the role of neutrophils and NETs formation in the pathogenesis of severe COVID-19. Finally, we highlight the potential of therapies inhibiting NETs formation for the treatment of COVID-19.

Keywords: cytokines, inflammation, lymphocyte, septic shock, homeostasis, acute respiratory distress syndrome, pneumonia, cytokine storm

OPEN ACCESS

Edited by:
Vijay Kumar,
Duke University, United States

Reviewed by:
Marko Radic,
University of Tennessee College of Medicine, United States
Ahmed Yaqinuddin,
Alfaisal University, Saudi Arabia

***Correspondence:**
Emeka B. Okeke
okeke@fredonia.edu

Specialty section:
This article was submitted to Inflammation, a section of the journal Frontiers in Immunology

Received: *22 March 2022*
Accepted: *11 May 2022*
Published: *10 June 2022*

Citation:
Ventura-Santana E, Ninan JR, Snyder CM and Okeke EB (2022) Neutrophil Extracellular Traps, Sepsis and COVID-19 – A Tripod Stand. Front. Immunol. 13:902206. doi: 10.3389/fimmu.2022.902206

INTRODUCTION

Coronavirus disease 2019 (COVID-19) was first reported in the city of Wuhan, Hubei province in mainland China in late 2019. The disease spread rapidly around the globe and was declared a pandemic by the World Health Organization on March 11, 2020 (1). In 2021, at the peak of the surge, COVID-19 was the number one cause of death in the United States (US) surpassing heart disease and cancer with an average of more than 3000 deaths per day (2). In fact, COVID-19 has led to the biggest drop in life expectancy in the US in more than seven decades (3). The successful rollout of vaccines has significantly halted mortality from the disease in the US. However, the emergence of more virulent strains of the virus remains a public health concern. As of January 2022, COVID-19 resulted in more than 800,000 deaths in the US and more than five million deaths globally with experts suggesting the number is significantly higher (4).

The causative agent is severe acute respiratory syndrome coronavirus-2 (SARS-CoV-2), whose origin is unknown. The closest human coronavirus related to SARS-CoV-2 is SARS-CoV which caused the SARS outbreak from 2002-2004 with 79% genetic similarity (5). However, SARS-CoV-2 bears the greatest genetic similarity to bat coronavirus RaTG13, with 96% similarity (6), fueling a suspicion that the virus originated from bats.

Most patients with COVID-19 have mild disease. Roughly 20% of patients exhibit exaggerated immune responses, including a hyper-inflammatory state and cytokine storm that leads to acute

respiratory distress syndrome (ARDS) and eventually resulting in multi-organ damage and death. Several clinical observations indicate that severe COVID-19 meets the criteria to be classified as viral sepsis (7).

Although the cause of aberrant host immune response in severe COVID-19 is not completely understood, accumulating evidence indicates that immune dysfunction contributes to disease severity. The adaptive immune system plays a crucial role in host defense following SARS-CoV-2 infection. Antigen presenting cells (APCs) present viral antigens to CD4+ T cells which induce robust neutralizing antibody responses by B cells (8). In addition, CD8+ Cytotoxic T lymphocytes (CTLs) produce perforins and granzymes which mediate killing of virally infected cells and are important for antiviral immunity (9). Studies have shown that severe COVID-19 is associated with significant decrease in numbers of CD4+ T cells, CD8+ T cells and B cells (10, 11). Severe SARS-CoV-2 infection is also associated with an overwhelming inflammatory phenotype (12, 13). Inflammatory CD4+ Th17 cells have been shown to mediate lung damage in COVID-19 patients (14). Likewise, innate immune cells like macrophages and neutrophils have been shown to be skewed towards an inflammatory phenotype in SARS-CoV-2 infection (15, 16). In particular, the production of neutrophil extracellular traps has been shown to propagate severe COVID-19 (17–19). The role of T and B cells in COVID-19 has been extensively reviewed (8, 20, 21) and we will focus on the role of neutrophils in the pathology of severe COVID-19.

In this article, we highlight important observations which indicate that severe COVID-19 has clinical presentations consistent with the definitions of viral sepsis. We discuss the significant contribution of neutrophils in driving disease pathology following infection with SARS-CoV-2 *via* formation of neutrophil extracellular traps (NETs). Furthermore, we highlight the potential of therapies inhibiting NETs formation for the treatment of severe COVID-19.

NETS AND INFLAMMATION

Polymorphonuclear neutrophils (PMNs) are the most abundant white blood cells in circulation and are rapidly deployed to the site of bacterial, fungal or viral infection as a critical part of host defense (22, 23). The role of neutrophils in host defense is widely appreciated and defective neutrophil function is associated with recurrent infections or occurrence of rare diseases (24). For several decades, neutrophils have been known to kill pathogens through phagocytosis and oxidative burst accompanied by granular release of potent antimicrobials (25). Recently, neutrophils were shown to kill microbes through the release of neutrophil extracellular traps (NETs). NETs are web-like extrusions, composed of a DNA framework and decorated with granular proteins like neutrophil elastase (NE) and myeloperoxidase (MPO) (26).

The molecular mechanisms involved in NET formation is incompletely understood and the processes that lead to the release of DNA by neutrophils is still a subject of debate. It has been reported that neutrophils form NETs through a tightly regulated cell death pathway called NETosis that involves collapse of the nuclear envelope and rupture of the cytoplasmic membrane (27). Studies have also shown that neutrophils release NETs in the absence of cell death (28, 29). These discrepancies may be due to the use of different stimulants for NET induction. Nevertheless, the critical role of certain enzymes and molecules in NET formation including NE, NADPH oxidase complex, peptidylarginine deiminase 4 (PAD4) and the protein kinase C (PKC) pathway have been highlighted and reviewed elsewhere (30–32). NETs have been shown to kill bacteria, fungi, viruses, and parasites (26, 33–35) and there is significant interest in the role of NETs in SARS-CoV-2 infection.

Although NET formation is a mechanism of host defense, excessive NET formation or defective clearance of NETs triggers sustained inflammatory response that can lead to organ damage and drive disease pathology. For example, histones released during NET formation have been shown to be cytotoxic and damage endothelial cells (36). NET formation leads to the production of autoantibodies that damage important organs (37) and inhibition of NETs formation has been shown to be protective in several models of inflammatory diseases (38, 39). Accumulating evidence indicates that NETs contributes to the pathophysiology of severe COVID-19 (18, 19). The role of NETs in the pathophysiology of COVID-19 constitutes a major focus of this review and will be discussed in later sections.

VIRAL SEPSIS

Despite decades of research and treatment, sepsis still constitutes a major challenge in modern medicine and is a leading cause of death in the intensive care unit (ICU). Sepsis is a heterogeneous and dynamic syndrome, due to a complex interplay between the host immune response and the invading microbe. The Third International Consensus Definitions Task Force defined sepsis as life-threatening organ dysfunction caused by a dysregulated host response to infection (40). This definition implies the general notion that bacteria, fungi and viruses can equally cause sepsis. However, there has been concerns that physicians are reluctant to designate viral infections as a case of sepsis (7). Although, bacteria accounts for more than 70% of documented sepsis (41, 42), the role of viruses in sepsis should not be ignored and this knowledge is important to tailor adequate treatment to culture negative patients.

The global burden of viral sepsis is huge with an estimated occurrence of 200 million cases of viral community-acquired pneumonia (CAP) each year (43). Pneumonia is the most common clinical syndrome in patients with sepsis (41, 42). Interestingly, studies have shown that viruses are the most common causes of CAP (44, 45). Therefore, the strict association of sepsis with bacterial infection can be costly given that early antiviral therapy is associated with better outcome in viral sepsis (46). It is also concerning that antibiotics have been administered in culture negative cases of pneumonia (47) indicating the bias of physicians to ignore viruses as a veritable

cause of sepsis. It must be stated that the presence of a virus is not sufficient for the diagnosis of viral sepsis. This is due to the possibility of bacterial co-infection or bacterial sepsis resulting from virus-induced immunosuppression. However, among patients with a diagnosis of pure viral CAP, 61% and 7% presented with sepsis and septic shock respectively upon admission to the clinic (47).

Several viruses have been reported to cause sepsis including influenza viruses, rhinoviruses, respiratory syncytial viruses, adenoviruses, herpes simplex viruses, human enteroviruses, dengue viruses and coronaviruses (7, 47). Importantly, the betacoronaviruses – Middle East respiratory syndrome coronavirus (MERS-CoV), SARS-CoV, and SARS-CoV-2 that threaten global health have also been known to cause sepsis. For example, patients with severe COVID-19 have clinical symptoms of viral sepsis. In one study, 59% of patients with COVID-19 were diagnosed with sepsis (48). Importantly, 76% of COVID-19 patients diagnosed with sepsis were negative for bacterial or fungal infections (48). Another study diagnosed sepsis in 100% of patients who died of COVID-19 (49). More studies are required for the diagnosis of sepsis in critically ill patients with COVID-19. However, taking into consideration several clinical observations and the above definition of sepsis, the authors agree that severe COVID-19 is a typical case of dysregulated host response to infection and therefore qualifies as sepsis caused by SARS-CoV-2 infection.

PATHOPHYSIOLOGY OF SEPSIS

The normal immune response to microbial invasion leads to the activation of host defense mechanisms to counter the microbe and prevent colonization of the host by the microbe. This involves cellular activation, vasodilation, leukocyte recruitment and increased endothelial permeability (50, 51). This complex and well-choreographed mechanism of immune activation describes the inflammatory response. Overwhelming infection caused by a virulent microbe or dysregulated immune response to an infection can lead to an overtly exaggerated immune activation or hyper-inflammatory state causing tissue injury and collateral damage to the host.

Innate immune cells like neutrophils and macrophages express molecular receptors called pattern recognition receptors (PRRs) that recognize pathogen-associated molecular patterns (PAMPs) on microbes (52). Several PRRs have been described and among them, TLRs are the most studied.

SARS-CoV-2 is an enveloped virus, with a single-stranded, positive-sense RNA genome (53). During replication, RNA viruses produce double-stranded RNA (dsRNA) as an intermediate (53). Both ssRNA and dsRNA can activate TLRs leading to the production of proinflammatory cytokines *via* MyD88 and NFk-B activation (54, 55).

Innate immune cells also play a role in the maintenance of antiviral state by the activation of Stimulator of Interferon Genes (STING) pathway (56–58). Upon activation, STING recruits TANK binding kinase 1 (TBK1) and the STING-TBK1 complex subsequently phosphorylates Interferon Regulatory Factor 3 (IRF3) (58). STING can also stimulate IKK leading to NF-κB activation (58). The transcription factors, IRF3 and NF-κB induce the production of type I IFNs and other pro-inflammatory cytokines important for antiviral immunity (58). For example, activation of STING pathway has been shown to block human coronavirus infection (59) and defective type I IFN production is associated with severe COVID-19 (60, 61).

The production of cytokines *via* NF-κB activation is an important step for the recruitment of neutrophils and other immune cells. However, a major hallmark of sepsis and severe COVID-19 is the excessive production of pro-inflammatory cytokines termed cytokine storm (CS) (7, 49). Cytokines like tumor necrosis factor (TNF), Interleukin (IL)-1, IL-6, IL-8, IL-12 and IL-17 propagate the inflammatory response through leukocyte recruitment, release of secondary inflammatory mediators, endothelial dysfunction and NETs formation (7, 18). For example, TNF and IL-1 induce vasodilation, facilitate the release of secondary mediators such as nitric oxide (NO), platelet activation factor (PAF), prostaglandins, leukotrienes and the activation of the complement system (62). Indeed, CS has been implicated in the pathogenesis of sepsis, viral diseases, autoimmune diseases, cancer and COVID-19 (18, 62–65).

CS also promotes leukocyte recruitment and endothelial permeability in the pulmonary capillaries resulting in lung injury and acute respiratory distress syndrome (ARDS) (64). Microbes associated with pulmonary infection will induce neutrophil migration to the lungs. The lumen of the pulmonary capillaries are more narrow and this leads to extended transit time along the pulmonary endothelium. Neutrophil accumulation and sequestration in the lungs leads to prolonged release of proteolytic enzymes that results in acute lung injury (ALI) and ARDS (66). Sepsis is the most common cause of ARDS and sepsis-related ARDS is associated with overall higher disease severity, longer ICU stays and mortality (67, 68).

Additionally, cytokine activity also activates the coagulation pathway, which can lead to disseminated intravascular coagulation (DIC) and/or coagulopathy which is a hallmark of sepsis (62). Aberrant activation of the coagulation pathway leads to capillary microthrombi, tissue hypoperfusion and end-organ ischemia (69).

Overall, there is consensus that sepsis is driven by the host immune response to infection rather than the pathogen itself (63). However, several clinical trials of therapies targeting important steps in the host immune response during sepsis have not been successful (62). We anticipate that advances in technology will increase our knowledge of sepsis pathogenesis leading to more novel therapeutic interventions.

NETs, SEPSIS AND SEVERE COVID-19

Neutrophils are the first immune cells to arrive at the site of bacterial infection and play an important role in host defense. These cells are equipped with antimicrobial granular content that

is rapidly deployed to eliminate the invading microbe. However, there is unequivocal experimental evidence that neutrophils contribute to sepsis pathology by release of cytolytic granular content, vaso-occlusion, and NET formation (66, 70).

The discovery of the process of NET formation by neutrophils highlighted a novel mechanism of innate immune defense against microbes. NETs have been shown to trap and kill a wide range of microbes including bacteria, fungi and viruses (26, 33–35). NETs formation can be beneficial during sepsis because NETs spatially restrict the dissemination of microbes during infection (26). To prevent physical containment by NETs, some bacteria have evolved to degrade NETs and NET degradation promotes bacterial virulence (71). Patients with chronic granulomatous disease (CGD) caused by mutations in genes encoding NADPH oxidase subunits do not make NETs and are susceptible to recurrent life-threatening infections (72). Gene therapy in a CGD patient restored NET forming ability of neutrophils resulting in clearance of refractory fungal infection (72). Additionally, NET proteins like histones, NE, MPO and proteinase 3 (PR3) have potent antimicrobial properties and help in bacterial killing (73).

However, accumulating evidence suggests that NETs formation is a double-edged sword (74) that contributes to the pathogenesis of several diseases including sepsis (70), rheumatoid arthritis (75), vasculitis (76), diabetes (77), lupus (78), cancer (79) and COVID-19 (18, 80). For example, studies have shown that levels of circulating cell-free DNA that are released during NET formation is a strong predictor of sepsis mortality (81). Also, histones which are the most abundant proteins in NETs (82) are cytotoxic towards epithelial and endothelial cells (36, 83). Histone administration to mice resulted in neutrophil accumulation in the lungs, microvascular thrombosis and death (83). Additionally, in non-human primates challenged with lethal concentration of *E. coli*, histone levels correlate with onset of renal failure. Furthermore, using three different models of sepsis: injection of LPS, injection of TNF, and CLP, the authors showed that antibodies against H4 improved animal survival (83). Consistent with this, we recently showed that inhibition of NE produced during NET formation reduced lung neutrophil accumulation, systemic levels of proinflammatory cytokines and improved survival in a mouse model of endotoxic shock (38).

A major complication attributed to NETs formation is thrombosis resulting in multi-organ failure (84–87). Due to their ability to form scaffolds, NETs can occlude blood vessels and cause thrombosis. NET scaffolds also promote adhesion of platelets leading to thrombus formation (85, 86). Importantly, serine proteases released by NETs like neutrophil elastase enhance tissue factor and factor XII dependent coagulation thereby leading to intravascular thrombus formation (88). Histones produced by NETs can promote platelet aggregation and thrombin generation *via* toll-like receptor (TLR) 2 and 4 (89). Interestingly, activated platelets have been shown to induce *de novo* NETs formation thereby propagating the vicious circle of platelet-neutrophil interaction in coagulopathy (90–92). Indeed, dysregulated NETs formation is associated with coagulopathy in sepsis and severe COVID-19 (80, 92–95).

We have drawn comparisons between sepsis and severe COVID-19 and conclude that the clinical presentations of sepsis and severe COVID-19 intersect at so many levels. Sepsis and severe COVID-19 commonly affect the pulmonary, cardiovascular, and renal systems. Many patients with severe COVID-19 exhibited clinical manifestations of shock-like cold extremities, weak peripheral pulses, dysfunction in microcirculation and organ damage notably in the lungs, kidney and liver (96). Like sepsis, ARDS and respiratory failure is the most common cause of death in COVID-19 patients (49, 97). Additionally, like sepsis, mortality in severe COVID-19 is driven by risk factors like age and presence of predisposing conditions (49). Severe COVID-19 is also characterized by excessive inflammatory cytokine production (19, 98, 99). Moreover, C-reactive protein, a biomarker for sepsis severity has also been shown to predict poor prognosis in COVID-19 (100). Furthermore, similar to sepsis, patients with severe COVID-19 show evidence of coagulopathy and dysregulated thrombus formation (80, 101). Indeed, one study showed that 100% of patients who died from COVID-19 were diagnosed with sepsis (49). In line with the evidence given above, we argue that severe COVID-19 is a typical case of viral sepsis.

Since NETs have been shown to contribute to sepsis pathology, it is conceivable that NETs may contribute to the pathogenesis of severe COVID-19 (**Figure 1**). Indeed, several studies have implicated NETs in the pathogenesis of severe COVID-19. For example, it was shown that SARS-CoV-2 replicates in neutrophils and triggers NETosis which contributes to COVID-19 pathology by killing lung epithelial cells (102). Sera from patients with COVID-19 have elevated levels of markers of NET formation including cell-free DNA, MPO-DNA, citrullinated histone H3, and neutrophil elastase (**Table 1**) and these markers are associated with disease severity (18, 111–113). Neutrophilia and NETosis is a major cause of ARDS and lung injury in severe COVID-19 (80, 114, 115). NETs formation is associated with systemic inflammation and cytokine storm which contributes to mortality in severe COVID-19 (116, 117). Additionally, dysregulated thrombus formation which contributes to mortality in severe COVID-19 has been associated with NET formation (80, 118, 119). Furthermore, COVID-19 has been shown to induce the production of autoantibodies associated with NET production (101). These observations have led to an overwhelming scientific support for targeting NETs formation as a veritable approach for the treatment of severe COVID-19 (19, 120, 121).

TARGETING NETs IN COVID-19

Recently, there has been concerted efforts to develop therapies targeting NETs in several diseases. Therapies targeting NETs have shown excellent success in mitigating lung inflammation and ARDS in preclinical models (19, 38). Since ARDS is the major cause of death in COVID-19, we advocate for the investigation of NET therapies in the treatment of COVID-19 patients. Different approaches to targeting NETs have shown remarkable success in preclinical models. Such approaches include dissolving NET

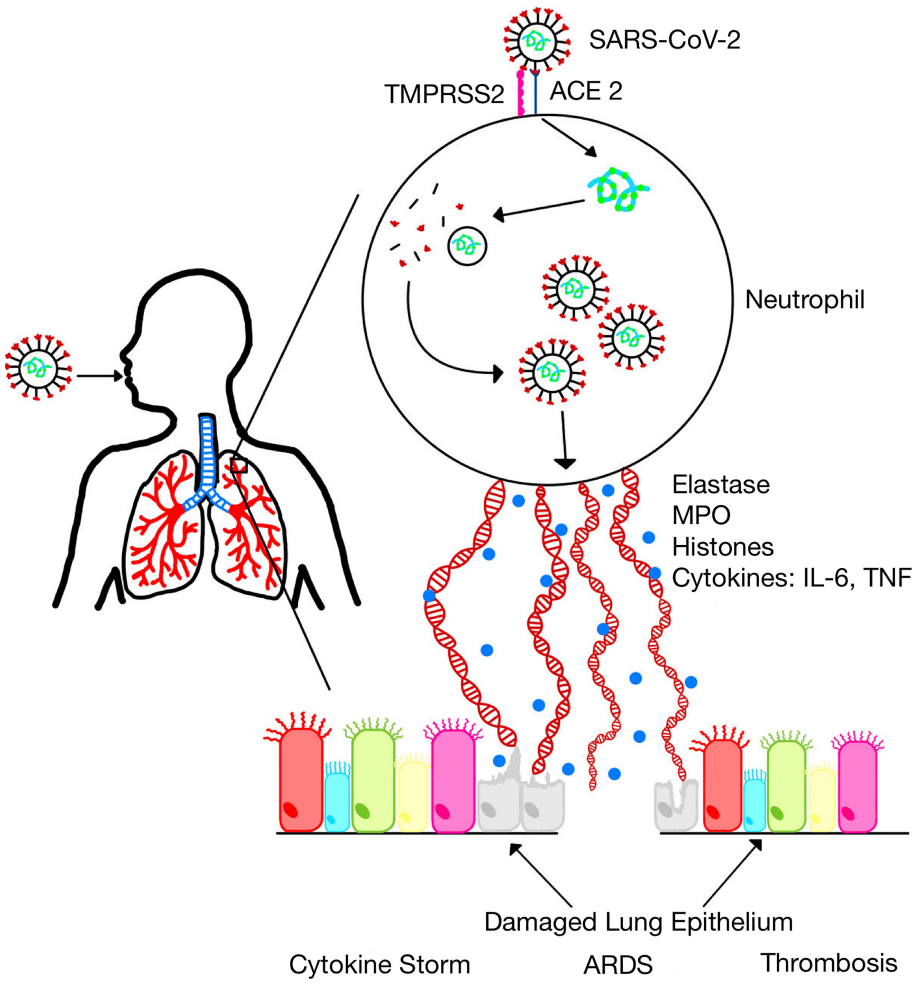

FIGURE 1 | SARS-CoV-2 infection induces neutrophil extracellular traps. SARS-CoV-2 replicates in neutrophils and induces the formation of NETs which leads to the release of inflammatory cytokines and several proteins that damage lung epithelium resulting in acute lung injury and acute respiratory distress syndrome (ARDS).

backbone, for example using DNAse (122), blocking molecules relevant in NET formation for example ROS, PAD4 and gasdermin D (39, 123) or blocking the activity of NET proteins like neutrophil elastase (38). Some of these NET therapeutics are currently available in the clinic and should be considered for the treatment of patients critically ill with COVID-19. For example, DNAse treatment is used in the clinic for patients with cystic fibrosis and the NE inhibitor sivelestat is clinically approved for the treatment of ARDS in Japan and South Korea (124, 125). Indeed, clinical trials of several NET inhibitors are underway for the treatment of COVID-19 (**Table 2**) and some of them have already been adopted as the standard of care for COVID-19 patients. For example, glucocorticoid therapy which is one of the earliest anti-inflammatory treatments available for sepsis patients has been shown to be beneficial for COVID-19 patients and dexamethasone is routinely given to COVID-19 patients (133). Importantly, dexamethasone has been shown to reduce NETs formation (134). Heparin, another NET inhibitor has also been shown to be beneficial for the treatment of COVID-19 patients (135, 136).

Anti-inflammatory therapies and anti-cytokine therapies can also be beneficial in reducing neutrophilia, NETs formation and NET-induced thrombosis. For example, elevated levels of IL-6 has been associated with severe COVID-19 thereby highlighting IL-6

TABLE 1 | NET proteins associated with severe COVID-19.

NET COMPONENT	REFERENCE
DNA	(18, 103)
Elastase	(104)
Myeloperoxidase	(18, 105)
Proteinase 3	(105, 106)
Histone 3	(18, 103)
Cathepsin G	(104, 107)
Azurocidin	(108)
Transketolase	(104, 109)
Alpha-defensins	(110)
Calprotectin	(110)

as a therapeutic target. IL-6 signaling has been shown to promote NET formation and lung inflammation (137). We recently showed that inhibition of NETs formation led to decrease in systemic levels of IL-6 and improved survival in a mouse model of endotoxic shock (38). Indeed, Tocilizumab, a recombinant humanized monoclonal anti-IL-6 antibody targeting the human IL-6 receptor was recently approved for the treatment of COVID-19 (138). Previous studies showed that Tocilizumab is also associated with decrease in NET formation (139).

As our understanding of the molecular mechanisms of NET formation increases, more therapies targeting NETs will become available and may hold promise for the effective treatment of severe COVID-19.

CONCLUDING REMARKS

The management of sepsis has been a challenge in modern medicine and the launch of surviving sepsis campaign was aimed to curtail the unacceptably high mortality of sepsis patients in the ICU (40). The mortality induced by the novel SARS-CoV-2 responsible for the current global pandemic has been attributed to sepsis (49). In this regard, biomarkers used for sepsis can be used for the early identification of COVID-19 patients that are at risk of progressing to severe disease. There is consensus that mortality in sepsis and COVID-19 is due to host immune response. Hence, modulating dysfunctional immune response in COVID-19 is critical for improving survival.

The formation of neutrophil extracellular traps has emerged as a contributing factor to the pathogenesis of COVID-19 (102). Importantly, SARS-CoV-2 has been shown to infect neutrophils and promote NETosis (102). Understanding of the role of NETs in the pathogenesis of severe COVID-19 holds potential for improving survival of patients. NET biomarkers can be easily detected in the blood and has been shown to indicate disease severity in COVID-19 (18). Hence, biomarkers of NET formation can be used to stratify COVID-19 patients at risk of progressing to severe disease. Since therapies targeting NETs have shown success in experimental models of ARDS, we propose that therapies targeting NETs have great potential for the treatment of COVID-19.

While we have focused on the role of extracellular traps produced by neutrophils in this review, macrophages also produce macrophage extracellular traps (METs) which propagate inflammation (140, 141). Interestingly, macrophages have been shown to contribute to inflammation in COVID-19 (12). Moreover, neutrophil extracellular traps from COVID-19 patients induce a proinflammatory response in monocyte-derived macrophages thereby linking NET formation to inflammatory macrophage activity (17). It is worthy of note that similar to neutrophils, macrophages also release elastase, histones and MPO during MET formation (142, 143). Hence, it is conceivable that mechanisms inhibiting the formation of NETs as highlighted here will also inhibit the formation of METs. Studies investigating the role of macrophage extracellular traps in severe COVID-19 will help unravel its role in the condition.

As with the case in sepsis, it is likely that one drug may not be sufficient to improve survival in COVID-19. Rather, a combinatorial approach may be necessary to reverse mortality in COVID-19. For example, the recently approved Tocilizumab showed benefit for COVID-19 patients who received it in conjunction with corticosteroids (144). We advocate for clinical trials investigating such combinations of NET therapeutics for the treatment of COVID-19. As another example, although sivelestat did not improve mortality in patients with ARDS (145), combination of sivelestat with antiviral therapy or another NET inhibitor may be beneficial for COVID-19 patients.

The intelligent design of clinical trials of therapies targeting NETs is essential and several factors including timing of intervention is critical for success. For example, there are concerns that DNase may enhance the dispersal of free histones and promote inflammation thereby leading to worse outcome in sepsis. In line with this, Meng et al, showed that early administration of DNase led to hyper-susceptibility to polymicrobial sepsis in mice (146). In a follow-up study, Mai et al showed that delayed administration of DNase is necessary for improved outcome in sepsis (147).

More research is needed to understand neutrophil behavior during SARS-CoV-2 infection. For example, an interesting question is whether different viral strains that have varying degrees of immunogenicity differ in their degree of NET induction, and this remains an important subject of investigation in our laboratory. Increase in our knowledge and understanding of the pathogenesis of COVID-19 will widen the

TABLE 2 | Clinical trials of NET inhibitors for COVID-19 Treatment.

NET INHIBITOR	MOLECULAR TARGET/FUNCTION	COVID TRIAL
Pulmozyme (dornase alfa) (126)	Recombinant DNase that improves lung function by thinning sputum.	NCT04359654 NCT04409925
Brensocatib (127)	Inhibits dipeptidyl peptidase 1 and neutrophil proteases	NCT04817332
Anakinra (128)	Interleukin-1 Receptor antagonist	NCT04594356
Glucocorticoid (methylprednisolone) (129)	Immunosuppressive treatment	NCT04244591
Hydroxychloroquine (130)	Reduces activity of immune system by disrupting lysosomal stability	NCT04332991
Colchicine (131)	Anti-inflammatory	NCT04326790
Alvelestat (132)	Neutrophil Elastase inhibitor	NCT00769119

availability of molecular targets that will yield the desired therapeutic benefit. With concerted research efforts, the menace of severe COVID-19 in the ICU will be curtailed.

AUTHOR CONTRIBUTIONS

EV did literature search and wrote portions of the manuscript. JN also did literature search and wrote portions of the manuscript. EO corrected and edited the manuscript for publication. CS did literature review and table for manuscript revision. All authors contributed to the article and approved the submitted version.

FUNDING

Funding for this work was provided by the State University of New York at Fredonia.

REFERENCES

1. Cucinotta D, Vanelli M. WHO Declares COVID-19 a Pandemic. *Acta BioMed* (2020) 91:157–60. doi: 10.23750/ABM.V91I1.9397
2. Woolf SH, Chapman DA, Lee JH. COVID-19 as the Leading Cause of Death in the United States. *JAMA* (2021) 325:123–4. doi: 10.1001/JAMA.2020.24865
3. Dyer O. US Life Expectancy Plunged in 2020, Especially in Hispanic and African Americans. *BMJ* (2021) 374:n1873. doi: 10.1136/BMJ.N1873
4. CDC COVID Data Tracker. Available at: https://covid.cdc.gov/covid-data-tracker/#datatracker-home (Accessed August 9, 2021).
5. Gorbalenya AE, Baker SC, Baric RS, de Groot RJ, Drosten C, Gulyaeva AA, et al. The Species Severe Acute Respiratory Syndrome-Related Coronavirus: Classifying 2019-Ncov and Naming it SARS-CoV-2. *Nat Microbiol* (2020) 5:536–44. doi: 10.1038/S41564-020-0695-Z
6. Zhou P, Yang XL, Wang XG, Hu B, Zhang L, Zhang W, et al. A Pneumonia Outbreak Associated With a New Coronavirus of Probable Bat Origin. *Nature* (2020) 579:270–3. doi: 10.1038/S41586-020-2012-7
7. Lin GL, McGinley JP, Drysdale SB, Pollard AJ. Epidemiology and Immune Pathogenesis of Viral Sepsis. *Front Immunol* (2018) 9:2147. doi: 10.3389/FIMMU.2018.02147
8. Cox RJ, Brokstad KA. Not Just Antibodies: B Cells and T Cells Mediate Immunity to COVID-19. *Nat Rev Immunol 2020 2010* (2020) 20:581–2. doi: 10.1038/s41577-020-00436-4
9. Mallajosyula V, Ganjavi C, Chakraborty S, McSween AM, Pavlovitch-Bedzyk AJ, Wilhelmy J, et al. Cd8+T Cells Specific for Conserved Coronavirus Epitopes Correlate With Milder Disease in COVID-19 Patients. *Sci Immunol* (2021) 6:5669. doi: 10.1126/SCIIMMUNOL.ABG5669/SUPPL_FILE/SCIIMMUNOL.ABG5669_MDAR_CHECKLIST.ZIP
10. Chen G, Wu D, Guo W, Cao Y, Huang D, Wang H, et al. Clinical and Immunological Features of Severe and Moderate Coronavirus Disease 2019. *J Clin Invest* (2020) 130:2620–9. doi: 10.1172/JCI137244
11. Diao B, Wang C, Tan Y, Chen X, Liu Y, Ning L, et al. Reduction and Functional Exhaustion of T Cells in Patients With Coronavirus Disease 2019 (COVID-19). *Front Immunol* (2020) 11:827. doi: 10.3389/FIMMU.2020.00827
12. Merad M, Martin JC. Author Correction: Pathological Inflammation in Patients With COVID-19: A Key Role for Monocytes and Macrophages (Nature Reviews Immunology, (2020), 20, 6, (355-362), 10.1038/S41577-020-0331-4). *Nat Rev Immunol* (2020) 20:448. doi: 10.1038/S41577-020-0353-Y
13. Bhaskar S, Sinha A, Banach M, Mittoo S, Weissert R, Kass JS, et al. Cytokine Storm in COVID-19—Immunopathological Mechanisms, Clinical Considerations, and Therapeutic Approaches: The REPROGRAM Consortium Position Paper. *Front Immunol* (2020) 11:1648/BIBTEX. doi: 10.3389/FIMMU.2020.01648/BIBTEX
14. Zhao Y, Kilian C, Turner JE, Bosurgi L, Roedl K, Bartsch P, et al. Clonal Expansion and Activation of Tissue-Resident Memory-Like Th17 Cells Expressing GM-CSF in the Lungs of Severe COVID-19 Patients. *Sci Immunol* (2021) 6:eabf6692. doi: 10.1126/SCIIMMUNOL.ABF6692
15. Wen W, Su W, Tang H, Le W, Zhang X, Zheng Y, et al. Immune Cell Profiling of COVID-19 Patients in the Recovery Stage by Single-Cell Sequencing. *Cell Discovery* (2020) 6:31. doi: 10.1038/S41421-020-0168-9
16. Shaath H, Vishnubalaji R, Elkord E, Alajez NM. Single-Cell Transcriptome Analysis Highlights a Role for Neutrophils and Inflammatory Macrophages in the Pathogenesis of Severe COVID-19. *Cells* (2020) 9:2374. doi: 10.3390/CELLS9112374
17. Torres-Ruiz J, Absalón-Aguilar A, Nuñez-Aguirre M, Pérez-Fragoso A, Carrillo-Vázquez DA, Maravillas-Montero JL, et al. Neutrophil Extracellular Traps Contribute to COVID-19 Hyperinflammation and Humoral Autoimmunity. *Cells* (2021) 10:2545. doi: 10.3390/CELLS10102545/S1
18. Zuo Y, Yalavarthi S, Shi H, Gockman K, Zuo M, Madison JA, et al. Neutrophil Extracellular Traps in COVID-19. *JCI Insight* (2020) 5:e138999. doi: 10.1172/JCI.INSIGHT.138999
19. Barnes BJ, Adrover JM, Baxter-Stoltzfus A, Borczuk A, Cools-Lartigue J, Crawford JM, et al. Targeting Potential Drivers of COVID-19: Neutrophil Extracellular Traps. *J Exp Med* (2020) 217:e20200652. doi: 10.1084/JEM.20200652/151683
20. Sette A, Crotty S. Adaptive Immunity to SARS-CoV-2 and COVID-19. *Cell* (2021) 184:861. doi: 10.1016/J.CELL.2021.01.007
21. Chen Z, John Wherry E. T Cell Responses in Patients With COVID-19. *Nat Rev Immunol* (2020) 20:529–36. doi: 10.1038/s41577-020-0402-6
22. Bardoel BW, Kenny EF, Sollberger G, Zychlinsky A. The Balancing Act of Neutrophils. *Cell Host Microbe* (2014) 15:526–36. doi: 10.1016/j.chom.2014.04.011
23. Ley K, Hoffman HM, Kubes P, Cassatella MA, Zychlinsky A, Hedrick CC, et al. Neutrophils: New Insights and Open Questions. *Sci Immunol* (2018) 3:eaat4579. doi: 10.1126/SCIIMMUNOL.AAT4579
24. Klein C. Genetic Defects in Severe Congenital Neutropenia: Emerging Insights Into Life and Death of Human Neutrophil Granulocytes. *Annu Rev Immunol* (2011) 29:399–413. doi: 10.1146/ANNUREV-IMMUNOL-030409-101259
25. Nathan C. Neutrophils and Immunity: Challenges and Opportunities. *Nat Rev Immunol* (2006) 6:173–82. doi: 10.1038/nri1785
26. Brinkmann V, Reichard U, Goosmann C, Fauler B, Uhlemann Y, Weiss DS, et al. Neutrophil Extracellular Traps Kill Bacteria. *Science* (2004) 303:1532–5. doi: 10.1126/science.1092385
27. Fuchs TA, Abed U, Goosmann C, Hurwitz R, Schulze I, Wahn V, et al. Novel Cell Death Program Leads to Neutrophil Extracellular Traps. *J Cell Biol* (2007) 176:231–41. doi: 10.1083/JCB.200606027
28. Yousefi S, Mihalache C, Kozlowski E, Schmid I, Simon HU. Viable Neutrophils Release Mitochondrial DNA to Form Neutrophil Extracellular Traps. *Cell Death Differ* (2009) 16:1438–44. doi: 10.1038/cdd.2009.96
29. Amini P, Stojkov D, Felser A, Jackson CB, Courage C, Schaller A, et al. Neutrophil Extracellular Trap Formation Requires OPA1-Dependent Glycolytic ATP Production. *Nat Commun* (2018) 9:2958. doi: 10.1038/S41467-018-05387-Y
30. Brinkmann V, Zychlinsky A. Neutrophil Extracellular Traps: Is Immunity the Second Function of Chromatin? *J Cell Biol* (2012) 198:773–83. doi: 10.1083/JCB.201203170
31. Papayannopoulos V, Metzler KD, Hakkim A, Zychlinsky A. Neutrophil Elastase and Myeloperoxidase Regulate the Formation of Neutrophil Extracellular Traps. *J Cell Biol* (2010) 191:677–91. doi: 10.1083/jcb.201006052
32. Hakkim A, Fuchs TA, Martinez NE, Hess S, Prinz H, Zychlinsky A, et al. Activation of the Raf-MEK-ERK Pathway is Required for Neutrophil

Extracellular Trap Formation. *Nat Chem Biol* (2011) 7:75–7. doi: 10.1038/nchembio.496
33. Urban CF, Reichard U, Brinkmann V, Zychlinsky A. Neutrophil Extracellular Traps Capture and Kill Candida Albicans Yeast and Hyphal Forms. *Cell Microbiol* (2006) 8:668–76. doi: 10.1111/J.1462-5822.2005.00659.X
34. Guimarães-Costa AB, Nascimento MTC, Froment GS, Soares RPP, Morgado FN, Conceição-Silva F, et al. Leishmania Amazonensis Promastigotes Induce and are Killed by Neutrophil Extracellular Traps. *Proc Natl Acad Sci USA* (2009) 106:6748–53. doi: 10.1073/PNAS.0900226106
35. Saitoh T, Komano J, Saitoh Y, Misawa T, Takahama M, Kozaki T, et al. Neutrophil Extracellular Traps Mediate a Host Defense Response to Human Immunodeficiency Virus-1. *Cell Host Microbe* (2012) 12:109–16. doi: 10.1016/J.CHOM.2012.05.015
36. Saffarzadeh M, Juenemann C, Queisser MA, Lochnit G, Barreto G, Galuska SP, et al. Neutrophil Extracellular Traps Directly Induce Epithelial and Endothelial Cell Death: A Predominant Role of Histones. *PLoS One* (2012) 7:e32366. doi: 10.1371/journal.pone.0032366
37. Khandpur R, Carmona-Rivera C, Vivekanandan-Giri A, Gizinski A, Yalavarthi S, Knight JS, et al. NETs are a Source of Citrullinated Autoantigens and Stimulate Inflammatory Responses in Rheumatoid Arthritis. *Sci Transl Med* (2013) 5:178ra40. doi: 10.1126/scitranslmed.3005580
38. Okeke EB, Louttit C, Fry C, Najafabadi AH, Han K, Nemzek J, et al. Inhibition of Neutrophil Elastase Prevents Neutrophil Extracellular Trap Formation and Rescues Mice From Endotoxic Shock. *Biomaterials* (2020) 238:119836. doi: 10.1016/j.biomaterials.2020.119836
39. Knight JS, Zhao W, Luo W, Subramanian V, O'Dell AA, Yalavarthi S, et al. Peptidylarginine Deiminase Inhibition is Immunomodulatory and Vasculoprotective in Murine Lupus. *J Clin Invest* (2013) 123:2981–93. doi: 10.1172/JCI67390
40. Singer M, Deutschman CS, Seymour C, Shankar-Hari M, Annane D, Bauer M, et al. The Third International Consensus Definitions for Sepsis and Septic Shock (Sepsis-3). *JAMA* (2016) 315:801–10. doi: 10.1001/JAMA.2016.0287
41. Zahar JR, Timsit JF, Garrouste-Orgeas M, Français A, Vesim A, Descorps-Declere A, et al. Outcomes in Severe Sepsis and Patients With Septic Shock: Pathogen Species and Infection Sites are Not Associated With Mortality. *Crit Care Med* (2011) 39:1886–95. doi: 10.1097/CCM.0B013E31821B827C
42. Phua J, Ngerng WJ, See KC, Tay CK, Kiong T, Lim HF, et al. Characteristics and Outcomes of Culture-Negative Versus Culture-Positive Severe Sepsis. *Crit Care* (2013) 17:R202. doi: 10.1186/CC12896
43. Ruuskanen O, Lahti E, Jennings LC, Murdoch DR. Viral Pneumonia. *Lancet (London England)* (2011) 377:1264–75. doi: 10.1016/S0140-6736(10)61459-6
44. Jain S, Self WH, Wunderink RG, Fakhran S, Balk R, Bramley AM, et al. Community-Acquired Pneumonia Requiring Hospitalization Among U.S. Adults. *N Engl J Med* (2015) 373:415–27. doi: 10.1056/NEJMOA1500245
45. Cilla G, Oñate E, Perez-Yarza EG, Montes M, Vicente D, Perez-Trallero E. Viruses in Community-Acquired Pneumonia in Children Aged Less Than 3 Years Old: High Rate of Viral Coinfection. *J Med Virol* (2008) 80:1843–9. doi: 10.1002/JMV.21271
46. Gu X, Zhou F, Wang Y, Fan G, Cao B. Respiratory Viral Sepsis: Epidemiology, Pathophysiology, Diagnosis and Treatment. *Eur Respir Rev* (2020) 29:1–12. doi: 10.1183/16000617.0038-2020
47. Cillóniz C, Dominedò C, Magdaleno D, Ferrer M, Gabarrús A, Torres A. Pure Viral Sepsis Secondary to Community-Acquired Pneumonia in Adults: Risk and Prognostic Factors. *J Infect Dis* (2019) 220:1166–71. doi: 10.1093/INFDIS/JIZ257
48. Zhou F, Yu T, Du R, Fan G, Liu Y, Liu Z, et al. Clinical Course and Risk Factors for Mortality of Adult Inpatients With COVID-19 in Wuhan, China: A Retrospective Cohort Study. *Lancet (London England)* (2020) 395:1054–62. doi: 10.1016/S0140-6736(20)30566-3
49. Chen T, Wu D, Chen H, Yan W, Yang D, Chen G, et al. Clinical Characteristics of 113 Deceased Patients With Coronavirus Disease 2019: Retrospective Study. *BMJ* (2020) 368:m1091. doi: 10.1136/BMJ.M1091
50. Sommers MS. The Cellular Basis of Septic Shock. *Crit Care Nurs Clin North Am* (2003) 15:13–25. doi: 10.1016/S0899-5885(02)00046-1
51. Brodsky IE, Medzhitov R. Targeting of Immune Signalling Networks by Bacterial Pathogens. *Nat Cell Biol* (2009) 11:521–6. doi: 10.1038/NCB0509-521
52. Aderem A, Ulevitch RJ. Toll-Like Receptors in the Induction of the Innate Immune Response. *Nature* (2000) 406:782–7. doi: 10.1038/35021228
53. V'kovski P, Kratzel A, Steiner S, Stalder H, Thiel V. Coronavirus Biology and Replication: Implications for SARS-CoV-2. *Nat Rev Microbiol 2020 193* (2020) 19:155–70. doi: 10.1038/s41579-020-00468-6
54. Lund JM, Alexopoulou L, Sato A, Karow M, Adams NC, Gale NW, et al. Recognition of Single-Stranded RNA Viruses by Toll-Like Receptor 7. *Proc Natl Acad Sci* (2004) 101:5598–603. doi: 10.1073/PNAS.0400937101
55. Lee SMY, Yip TF, Yan S, Jin DY, Wei HL, Guo RT, et al. Recognition of Double-Stranded RNA and Regulation of Interferon Pathway by Toll-Like Receptor 10. *Front Immunol* (2018) 9:516/BIBTEX. doi: 10.3389/FIMMU.2018.00516/BIBTEX
56. Schoggins JW, MacDuff DA, Imanaka N, Gainey MD, Shrestha B, Eitson JL, et al. Pan-Viral Specificity of IFN-Induced Genes Reveals New Roles for cGAS in Innate Immunity. *Nature* (2014) 505:691–5. doi: 10.1038/nature12862
57. Glück S, Guey B, Gulen MF, Wolter K, Kang TW, Schmacke NA, et al. Innate Immune Sensing of Cytosolic Chromatin Fragments Through cGAS Promotes Senescence. *Nat Cell Biol* (2017) 19:1061–70. doi: 10.1038/ncb3586
58. Li T, Chen ZJ. The cGAS–cGAMP–STING Pathway Connects DNA Damage to Inflammation, Senescence, and Cancer. *J Exp Med* (2018) 215:1287–99. doi: 10.1084/JEM.20180139
59. Liu W, Reyes HM, Yang JF, Li Y, Stewart KM, Basil MC, et al. Activation of STING Signaling Pathway Effectively Blocks Human Coronavirus Infection. *J Virol* (2021) 95: e00490–21. doi: 10.1128/JVI.00490-21
60. Zhang Q, Liu Z, Moncada-Velez M, Chen J, Ogishi M, Bigio B, et al. Inborn Errors of Type I IFN Immunity in Patients With Life-Threatening COVID-19. *Science* (2020) 370:eabd4570. doi: 10.1126/SCIENCE.ABD4570
61. Hadjadj J, Yatim N, Barnabei L, Corneau A, Boussier J, Smith N, et al. Impaired Type I Interferon Activity and Inflammatory Responses in Severe COVID-19 Patients. *Science* (2020) 369:718–24. doi: 10.1126/SCIENCE.ABC6027
62. Okeke EB, Uzonna JE. In Search of a Cure for Sepsis: Taming the Monster in Critical Care Medicine. *J Innate Immun* (2016) 8:156–70. doi: 10.1159/000442469
63. Chousterman BG, Swirski FK, Weber GF. Cytokine Storm and Sepsis Disease Pathogenesis. *Semin Immunopathol* (2017) 39:517–28. doi: 10.1007/S00281-017-0639-8
64. Fajgenbaum DC, June CH. Cytokine Storm. *N Engl J Med* (2020) 383:2255–73. doi: 10.1056/NEJMRA2026131/SUPPL_FILE/NEJMRA2026131_DISCLOSURES.PDF
65. Díelia RV, Harrison K, Oyston PC, Lukaszewski RA, Clark GC. Targeting the "Cytokine Storm" for Therapeutic Benefit. *Clin Vaccine Immunol* (2013) 20:319–27. doi: 10.1128/CVI.00636-12/ASSET/C6C0D2AB-72D5-4549-8FED-F8B5A53D7B36/ASSETS/GRAPHIC/ZCD9990946740002.JPEG
66. Grommes J, Soehnlein O. Contribution of Neutrophils to Acute Lung Injury. *Mol Med* (2010) 17:293–307. doi: 10.2119/MOLMED.2010.00138
67. Sheu CC, Gong MN, Zhai R, Chen F, Bajwa EK, Clardy PF, et al. Clinical Characteristics and Outcomes of Sepsis-Related vs non-Sepsis-Related ARDS. *Chest* (2010) 138:559–67. doi: 10.1378/CHEST.09-2933
68. Kim WY, Hong SB. Sepsis and Acute Respiratory Distress Syndrome: Recent Update. *Tuberc Respir Dis (Seoul)* (2016) 79:53–7. doi: 10.4046/TRD.2016.79.2.53
69. Gando S, Kameue T, Matsuda N, Sawamura A, Hayakawa M, Kato H. Systemic Inflammation and Disseminated Intravascular Coagulation in Early Stage of ALI and ARDS: Role of Neutrophil and Endothelial Activation. *Inflammation 2004 284* (2004) 28:237–44. doi: 10.1023/B:IFLA.0000049049.81688.FE
70. Czaikoski PG, Mota JMSC, Nascimento DC, Sônego F, Castanheira FV e S, Melo PH, et al. Neutrophil Extracellular Traps Induce Organ Damage During Experimental and Clinical Sepsis. *PLoS One* (2016) 11:e0148142. doi: 10.1371/journal.pone.0148142
71. Buchanan JT, Simpson AJ, Aziz RK, Liu GY, Kristian SA, Kotb M, et al. DNase Expression Allows the Pathogen Group A Streptococcus to Escape Killing in Neutrophil Extracellular Traps. *Curr Biol* (2006) 16:396–400. doi: 10.1016/J.CUB.2005.12.039

72. Bianchi M, Niemiec MJ, Siler U, Urban CF, Reichenbach J. Restoration of Anti-Aspergillus Defense by Neutrophil Extracellular Traps in Human Chronic Granulomatous Disease After Gene Therapy is Calprotectin-Dependent. *J Allergy Clin Immunol* (2011) 127:1243–52.e7. doi: 10.1016/J.JACI.2011.01.021
73. Korkmaz B, Moreau T, Gauthier F. Neutrophil Elastase, Proteinase 3 and Cathepsin G: Physicochemical Properties, Activity and Physiopathological Functions. *Biochimie* (2008) 90:227–42. doi: 10.1016/j.biochi.2007.10.009
74. Kaplan MJ, Radic M. Neutrophil Extracellular Traps: Double-Edged Swords of Innate Immunity. *J Immunol* (2012) 189:2689–95. doi: 10.4049/jimmunol.1201719
75. Sur Chowdhury C, Giaglis S, Walker UA, Buser A, Hahn S, Hasler P. Enhanced Neutrophil Extracellular Trap Generation in Rheumatoid Arthritis: Analysis of Underlying Signal Transduction Pathways and Potential Diagnostic Utility. *Arthritis Res Ther* (2014) 16:R122. doi: 10.1186/ar4579
76. Kambas K, Chrysanthopoulou A, Vassilopoulos D, Apostolidou E, Skendros P, Girod A, et al. Tissue Factor Expression in Neutrophil Extracellular Traps and Neutrophil Derived Microparticles in Antineutrophil Cytoplasmic Antibody Associated Vasculitis may Promote Thromboinflammation and the Thrombophilic State Associated With the Disease. *Ann Rheum Dis* (2014) 73:1854–63. doi: 10.1136/annrheumdis-2013-203430
77. Wong SL, Demers M, Martinod K, Gallant M, Wang Y, Goldfine AB, et al. Diabetes Primes Neutrophils to Undergo NETosis, Which Impairs Wound Healing. *Nat Med* (2015) 21:815–9. doi: 10.1038/nm.3887
78. Hakkim A, Fürnrohr BG, Amann K, Laube B, Abed UA, Brinkmann V, et al. Impairment of Neutrophil Extracellular Trap Degradation is Associated With Lupus Nephritis. *Proc Natl Acad Sci U S A* (2010) 107:9813–8. doi: 10.1073/pnas.0909927107
79. Albrengues J, Shields MA, Ng D, Park CG, Ambrico A, Poindexter ME, et al. Neutrophil Extracellular Traps Produced During Inflammation Awaken Dormant Cancer Cells in Mice. *Science* (2018) 361:eaao4227. doi: 10.1126/science.aao4227
80. Middleton EA, He XY, Denorme F, Campbell RA, Ng D, Salvatore SP, et al. Neutrophil Extracellular Traps Contribute to Immunothrombosis in COVID-19 Acute Respiratory Distress Syndrome. *Blood* (2020) 136:1169–79. doi: 10.1182/blood.2020007008
81. Dwivedi DJ, Toltl LJ, Swystun LL, Pogue J, Liaw KL, Weitz JI, et al. Prognostic Utility and Characterization of Cell-Free DNA in Patients With Severe Sepsis. *Crit Care* (2012) 16:R151. doi: 10.1186/CC11466
82. Urban CF, Ermert D, Schmid M, Abu-Abed U, Goosmann C, Nacken W, et al. Neutrophil Extracellular Traps Contain Calprotectin, a Cytosolic Protein Complex Involved in Host Defense Against Candida Albicans. *PLoS Pathog* (2009) 5:e1000639. doi: 10.1371/JOURNAL.PPAT.1000639
83. Xu J, Zhang X, Pelayo R, Monestier M, Ammollo CT, Semeraro F, et al. Extracellular Histones are Major Mediators of Death in Sepsis. *Nat Med* (2009) 15:1318–21. doi: 10.1038/NM.2053
84. Brill A, Fuchs TA, Savchenko AS, Thomas GM, Martinod K, De Meyer SF, et al. Neutrophil Extracellular Traps Promote Deep Vein Thrombosis in Mice. *J Thromb Haemost* (2012) 10:136–44. doi: 10.1111/j.1538-7836.2011.04544.x
85. Fuchs TA, Brill A, Duerschmied D, Schatzberg D, Monestier M, Myers DD, et al. Extracellular DNA Traps Promote Thrombosis. *Proc Natl Acad Sci U S A* (2010) 107:15880–5. doi: 10.1073/PNAS.1005743107
86. Laridan E, Martinod K, De Meyer SF. Neutrophil Extracellular Traps in Arterial and Venous Thrombosis. *Semin Thromb Hemost* (2019) 45:86–93. doi: 10.1055/S-0038-1677040/ID/JR02600-32
87. Gould TJ, Vu TT, Swystun LL, Dwivedi DJ, Mai SHC, Weitz JI, et al. Neutrophil Extracellular Traps Promote Thrombin Generation Through Platelet-Dependent and Platelet-Independent Mechanisms. *Arterioscler Thromb Vasc Biol* (2014) 34:1977–84. doi: 10.1161/ATVBAHA.114.304114
88. Massberg S, Grahl L, Von Bruehl ML, Manukyan D, Pfeiler S, Goosmann C, et al. Reciprocal Coupling of Coagulation and Innate Immunity *via* Neutrophil Serine Proteases. *Nat Med* (2010) 16:887–96. doi: 10.1038/NM.2184
89. Semeraro F, Ammollo CT, Morrissey JH, Dale GL, Friese P, Esmon NL, et al. Extracellular Histones Promote Thrombin Generation Through Platelet-Dependent Mechanisms: Involvement of Platelet TLR2 and TLR4. *Blood* (2011) 118:1952–61. doi: 10.1182/BLOOD-2011-03-343061
90. Maugeri N, Campana L, Gavina M, Covino C, De Metrio M, Panciroli C, et al. Activated Platelets Present High Mobility Group Box 1 to Neutrophils, Inducing Autophagy and Promoting the Extrusion of Neutrophil Extracellular Traps. *J Thromb Haemost* (2014) 12:2074–88. doi: 10.1111/JTH.12710
91. Dyer MR, Chen Q, Haldeman S, Yazdani H, Hoffman R, Loughran P, et al. Deep Vein Thrombosis in Mice is Regulated by Platelet HMGB1 Through Release of Neutrophil-Extracellular Traps and DNA. *Sci Rep* (2018) 8:2068. doi: 10.1038/S41598-018-20479-X
92. Clark SR, Ma AC, Tavener SA, McDonald B, Goodarzi Z, Kelly MM, et al. Platelet TLR4 Activates Neutrophil Extracellular Traps to Ensnare Bacteria in Septic Blood. *Nat Med* (2007) 13:463–9. doi: 10.1038/NM1565
93. McDonald B, Davis RP, Kim S-J, Tse M, Esmon CT, Kolaczkowska E, et al. Platelets and Neutrophil Extracellular Traps Collaborate to Promote Intravascular Coagulation During Sepsis in Mice. *Blood* (2017) 129:1357–67. doi: 10.1182/blood-2016-09-741298
94. Blasco A, Coronado MJ, Hernández-Terciado F, Martín P, Royuela A, Ramil E, et al. Assessment of Neutrophil Extracellular Traps in Coronary Thrombus of a Case Series of Patients With COVID-19 and Myocardial Infarction. *JAMA Cardiol* (2021) 6:469–74. doi: 10.1001/JAMACARDIO.2020.7308
95. Bautista-Becerril B, Campi-Caballero R, Sevilla-Fuentes S, Hernández-Regino LM, Hanono A, Flores-Bustamante A, et al. Immunothrombosis in COVID-19: Implications of Neutrophil Extracellular Traps. *Biomol* (2021) 11:694. doi: 10.3390/BIOM11050694
96. Li H, Liu L, Zhang D, Xu J, Dai H, Tang N, et al. SARS-CoV-2 and Viral Sepsis: Observations and Hypotheses. *Lancet (London England)* (2020) 395:1517–20. doi: 10.1016/S0140-6736(20)30920-X
97. Contou D, Cally R, Sarfati F, Desaint P, Fraissé M, Plantefève G. Causes and Timing of Death in Critically Ill COVID-19 Patients. *Crit Care* (2021) 25:79. doi: 10.1186/S13054-021-03492-X
98. Liu J, Li S, Liu J, Liang B, Wang X, Wang H, et al. Longitudinal Characteristics of Lymphocyte Responses and Cytokine Profiles in the Peripheral Blood of SARS-CoV-2 Infected Patients. *EBioMedicine* (2020) 55:102763. doi: 10.1016/J.EBIOM.2020.102763
99. Hu B, Huang S, Yin L. The Cytokine Storm and COVID-19. *J Med Virol* (2021) 93:250–6. doi: 10.1002/JMV.26232
100. Sahu BR, Kampa RK, Padhi A, Panda AK. C-Reactive Protein: A Promising Biomarker for Poor Prognosis in COVID-19 Infection. *Clin Chim Acta* (2020) 509:91–4. doi: 10.1016/J.CCA.2020.06.013
101. Zuo Y, Estes SK, Ali RA, Gandhi AA, Yalavarthi S, Shi H, et al. Prothrombotic Autoantibodies in Serum From Patients Hospitalized With COVID-19. *Sci Transl Med* (2020) 12:eabd3876. doi: 10.1126/SCITRANSLMED.ABD3876
102. Veras FP, Pontelli MC, Silva CM, Toller-Kawahisa JE, de Lima M, Nascimento DC, et al. SARS-CoV-2-Triggered Neutrophil Extracellular Traps Mediate COVID-19 Pathology. *J Exp Med* (2020) 217:e20201129. doi: 10.1084/JEM.20201129
103. Huckriede J, de Vries F, Hultström M, Wichapong K, Reutelingsperger C, Lipcsey M, et al. Histone H3 Cleavage in Severe COVID-19 ICU Patients. *Front Cell Infect Microbiol* (2021) 11:694186. doi: 10.3389/FCIMB.2021.694186
104. Akgun E, Tuzuner MB, Sahin B, Kilercik M, Kulah C, Cakiroglu HN, et al. Proteins Associated With Neutrophil Degranulation are Upregulated in Nasopharyngeal Swabs From SARS-CoV-2 Patients. *PloS One* (2020) 15:e0240012. doi: 10.1371/JOURNAL.PONE.0240012
105. Uppal NN, Kello N, Shah HH, Khanin Y, De Oleo IR, Epstein E, et al. *De Novo* ANCA-Associated Vasculitis With Glomerulonephritis in COVID-19. *Kidney Int Rep* (2020) 5:2079. doi: 10.1016/J.EKIR.2020.08.012
106. Felzer JR, Fogwe DT, Samrah S, Michet CJ, Specks U, Baqir M, et al. Association of COVID-19 Antigenicity With the Development of Antineutrophilic Cytoplasmic Antibody Vasculitis. *Respirol Case Rep* (2022) 10:e0894. doi: 10.1002/RCR2.894
107. Beloglazov V, Yatskov I, Nikolaeva A, Lavrenchuk E, DuBuske L. Cathepsin G in Patients With SARS-Cov-2 Infection of Various Degrees of Severity. *J Allergy Clin Immunol* (2022) 149:AB59. doi: 10.1016/J.JACI.2021.12.223

108. Mellhammar L, Thelaus L, Elen S, Fisher J, Linder A. Heparin Binding Protein in Severe COVID-19-A Prospective Observational Cohort Study. *PloS One* (2021) 16:e0249570. doi: 10.1371/JOURNAL.PONE.0249570
109. Bojkova D, Costa R, Reus P, Bechtel M, Jaboreck MC, Olmer R, et al. Targeting the Pentose Phosphate Pathway for SARS-CoV-2 Therapy. *Metabolites* (2021) 11:699. doi: 10.3390/METABO11100699
110. Shrivastava S, Chelluboina S, Jedge P, Doke P, Palkar S, Mishra AC, et al. Elevated Levels of Neutrophil Activated Proteins, Alpha-Defensins (DEFA1), Calprotectin (S100A8/A9) and Myeloperoxidase (MPO) Are Associated With Disease Severity in COVID-19 Patients. *Front Cell Infect Microbiol* (2021) 11:751232. doi: 10.3389/FCIMB.2021.751232
111. Leppkes M, Knopf J, Naschberger E, Lindemann A, Singh J, Herrmann I, et al. Vascular Occlusion by Neutrophil Extracellular Traps in COVID-19. *EBioMedicine* (2020) 58:102925. doi: 10.1016/J.EBIOM.2020.102925
112. Wang J, Li Q, Yin Y, Zhang Y, Cao Y, Lin X, et al. Excessive Neutrophils and Neutrophil Extracellular Traps in COVID-19. *Front Immunol* (2020) 11:2063. doi: 10.3389/FIMMU.2020.02063
113. Karampoor S, Hesamizadeh K, Maleki F, Farahmand M, Zahednasab H, Mirzaei R, et al. A Possible Pathogenic Correlation Between Neutrophil Elastase (NE) Enzyme and Inflammation in the Pathogenesis of Coronavirus Disease 2019 (COVID-19). *Int Immunopharmacol* (2021) 100:108137. doi: 10.1016/J.INTIMP.2021.108137
114. Radermecker C, Detrembleur N, Guiot J, Cavalier E, Henket M, d'Emal C, et al. Neutrophil Extracellular Traps Infiltrate the Lung Airway, Interstitial, and Vascular Compartments in Severe COVID-19. *J Exp Med* (2020) 217: e20201012. doi: 10.1084/JEM.20201012
115. Narasaraju T, Tang BM, Herrmann M, Muller S, Chow VTK, Radic M. Neutrophilia and NETopathy as Key Pathologic Drivers of Progressive Lung Impairment in Patients With COVID-19. *Front Pharmacol* (2020) 11:870. doi: 10.3389/FPHAR.2020.00870
116. Ng H, Havervall S, Rosell A, Aguilera K, Parv K, Von Meijenfeldt FA, et al. Circulating Markers of Neutrophil Extracellular Traps Are of Prognostic Value in Patients With COVID-19. *Arterioscler Thromb Vasc Biol* (2021) 41:988–94. doi: 10.1161/ATVBAHA.120.315267
117. Arcanjo A, Logullo J, Menezes CCB, de Souza Carvalho Giangiarulo TC, dos Reis MC, de Castro GMM, et al. The Emerging Role of Neutrophil Extracellular Traps in Severe Acute Respiratory Syndrome Coronavirus 2 (COVID-19). *Sci Rep* (2020) 10:19630. doi: 10.1038/S41598-020-76781-0
118. Zuo Y, Zuo M, Yalavarthi S, Gockman K, Madison JA, Shi H, et al. Neutrophil Extracellular Traps and Thrombosis in COVID-19. *J Thromb Thrombolysis* (2021) 51:446–53. doi: 10.1007/S11239-020-02324-Z
119. Skendros P, Mitsios A, Chrysanthopoulou A, Mastellos DC, Metallidis S, Rafailidis P, et al. Complement and Tissue Factor-Enriched Neutrophil Extracellular Traps are Key Drivers in COVID-19 Immunothrombosis. *J Clin Invest* (2020) 130:6151–7. doi: 10.1172/JCI141374
120. Zuo Y, Kanthi Y, Knight JS, Kim AHJ. The Interplay Between Neutrophils, Complement, and Microthrombi in COVID-19. *Best Pract Res Clin Rheumatol* (2021) 35:101661. doi: 10.1016/J.BERH.2021.101661
121. Ackermann M, Anders HJ, Bilyy R, Bowlin GL, Daniel C, De Lorenzo R, et al. Patients With COVID-19: In the Dark-NETs of Neutrophils. *Cell Death Differ* (2021) 28:3125–39. doi: 10.1038/s41418-021-00805-z
122. Park J, Wysocki RW, Amoozgar Z, Maiorino L, Fein MR, Jorns J, et al. Cancer Cells Induce Metastasis-Supporting Neutrophil Extracellular DNA Traps. *Sci Transl Med* (2016) 8:361ra138–361ra138. doi: 10.1126/scitranslmed.aag1711
123. Sollberger G, Choidas A, Burn GL, Habenberger P, Di Lucrezia R, Kordes S, et al. Gasdermin D Plays a Vital Role in the Generation of Neutrophil Extracellular Traps. *Sci Immunol* (2018) 3:eaar6689. doi: 10.1126/sciimmunol.aar6689
124. Papayannopoulos V, Staab D, Zychlinsky A. Neutrophil Elastase Enhances Sputum Solubilization in Cystic Fibrosis Patients Receiving DNase Therapy. *PloS One* (2011) 6:e28526. doi: 10.1371/journal.pone.0028526
125. Aikawa N, Ishizaka A, Hirasawa H, Shimazaki S, Yamamoto Y, Sugimoto H, et al. Reevaluation of the Efficacy and Safety of the Neutrophil Elastase Inhibitor, Sivelestat, for the Treatment of Acute Lung Injury Associated With Systemic Inflammatory Response Syndrome; a Phase IV Study. *Pulm Pharmacol Ther* (2011) 24:549–54. doi: 10.1016/j.pupt.2011.03.001
126. Fisher J, Mohanty T, Karlsson CAQ, Khademi SMH, Malmström E, Frigyesi A, et al. Proteome Profiling of Recombinant DNase Therapy in Reducing NETs and Aiding Recovery in COVID-19 Patients. *Mol Cell Proteomics* (2021) 20:100113. doi: 10.1016/J.MCPRO.2021.100113
127. Korkmaz B, Lesner A, Marchand-Adam S, Moss C, Jenne DE. Lung Protection by Cathepsin C Inhibition: A New Hope for COVID-19 and ARDS? *J Med Chem* (2020) 63:13258–65. doi: 10.1021/ACS.JMEDCHEM.0C00776
128. Huet T, Beaussier H, Voisin O, Jouveshomme S, Dauriat G, Lazareth I, et al. Anakinra for Severe Forms of COVID-19: A Cohort Study. *Lancet Rheumatol* (2020) 2:e393–400. doi: 10.1016/S2665-9913(20)30164-8
129. Edalatifard M, Akhtari M, Salehi M, Naderi Z, Jamshidi A, Mostafaei S, et al. Intravenous Methylprednisolone Pulse as a Treatment for Hospitalised Severe COVID-19 Patients: Results From a Randomised Controlled Clinical Trial. *Eur Respir J* (2020) 56:2002808. doi: 10.1183/13993003.02808-2020
130. Kashour Z, Riaz M, Garbati MA, AlDosary O, Tlayjeh H, Gerberi D, et al. Efficacy of Chloroquine or Hydroxychloroquine in COVID-19 Patients: A Systematic Review and Meta-Analysis. *J Antimicrob Chemother* (2021) 76:30–42. doi: 10.1093/JAC/DKAA403
131. Mikolajewska A, Fischer AL, Piechotta V, Mueller A, Metzendorf MI, Becker M, et al. Colchicine for the Treatment of COVID-19. *Cochrane Database Syst Rev* (2021) 10:CD015045. doi: 10.1002/14651858.CD015045
132. *Mereo BioPharma Sees Positive Results in Trial for Covid-19 Treatment - MarketWatch* . Available at: https://www.marketwatch.com/story/mereo-biopharma-sees-positive-results-in-trial-for-covid-19-treatment-271640175318 (Accessed January 17, 2022).
133. Horby P, Lim WS, Emberson JR, Mafham M, Bell JL, Linsell L, et al. Dexamethasone in Hospitalized Patients With Covid-19. *N Engl J Med* (2021) 384:693–704. doi: 10.1056/NEJMOA2021436
134. Vargas A, Boivin R, Cano P, Murcia Y, Bazin I, Lavoie JP. Neutrophil Extracellular Traps are Downregulated by Glucocorticosteroids in Lungs in an Equine Model of Asthma. *Respir Res* (2017) 18:207. doi: 10.1186/S12931-017-0689-4
135. Sun Y, Chen C, Zhang X, Wang S, Zhu R, Zhou A, et al. Heparin Improves Alveolarization and Vascular Development in Hyperoxia-Induced Bronchopulmonary Dysplasia by Inhibiting Neutrophil Extracellular Traps. *Biochem Biophys Res Commun* (2020) 522:33–9. doi: 10.1016/J.BBRC.2019.11.041
136. Nadkarni GN, Lala A, Bagiella E, Chang HL, Moreno PR, Pujadas E, et al. Anticoagulation, Bleeding, Mortality, and Pathology in Hospitalized Patients With COVID-19. *J Am Coll Cardiol* (2020) 76:1815–26. doi: 10.1016/J.JACC.2020.08.041
137. Keir HR, Chalmers JD. IL-6 Trans-Signalling: How Haemophilus Surfs the NET to Amplify Inflammation in COPD. *Eur Respir J* (2021) 58:2102143. doi: 10.1183/13993003.02143-2021
138. *FDA Approves Actemra for Hospitalised COVID-19 Patients* . Available at: https://www.europeanpharmaceuticalreview.com/news/157399/fda-approves-actemra-for-emergency-use-in-hospitalised-covid-19-patients/ (Accessed January 16, 2022).
139. Ruiz-Limón P, Ortega R, Arias de la Rosa I, Abalos-Aguilera M del C, Perez-Sanchez C, Jimenez- Gomez Y, et al. Tocilizumab Improves the Proatherothrombotic Profile of Rheumatoid Arthritis Patients Modulating Endothelial Dysfunction, NETosis, and Inflammation. *Transl Res* (2017) 183:87–103. doi: 10.1016/J.TRSL.2016.12.003
140. Rasmussen KH, Hawkins CL. Role of Macrophage Extracellular Traps in Innate Immunity and Inflammatory Disease. *Biochem Soc Trans* (2022) 50:21–32. doi: 10.1042/BST20210962
141. Doster RS, Rogers LM, Gaddy JA, Aronoff DM. Macrophage Extracellular Traps: A Scoping Review. *J Innate Immun* (2018) 10:3–13. doi: 10.1159/000480373
142. Halder LD, Abdelfatah MA, Jo EAH, Jacobsen ID, Westermann M, Beyersdorf N, et al. Factor H Binds to Extracellular DNA Traps Released From Human Blood Monocytes in Response to Candida Albicans. *Front Immunol* (2017) 7:671. doi: 10.3389/FIMMU.2016.00671
143. Je S, Quan H, Yoon Y, Na Y, Kim BJ, Seok SH. Mycobacterium Massiliense Induces Macrophage Extracellular Traps With Facilitating Bacterial Growth. *PLoS One* (2016) 11:e0155685. doi: 10.1371/JOURNAL.PONE.0155685

144. Abani O, Abbas A, Abbas F, Abbas M, Abbasi S, Abbass H, et al. Tocilizumab in Patients Admitted to Hospital With COVID-19 (RECOVERY): A Randomised, Controlled, Open-Label, Platform Trial. *Lancet (London England)* (2021) 397:1637–45. doi: 10.1016/S0140-6736(21)00676-0
145. Tagami T, Tosa R, Omura M, Fukushima H, Kaneko T, Endo T, et al. Effect of a Selective Neutrophil Elastase Inhibitor on Mortality and Ventilator-Free Days in Patients With Increased Extravascular Lung Water: A *Post Hoc* Analysis of the PiCCO Pulmonary Edema Study. *J Intensive Care* (2014) 2:67. doi: 10.1186/S40560-014-0067-Y
146. Meng W, Paunel-Görgülü A, Flohé S, Hoffmann A, Witte I, MacKenzie C, et al. Depletion of Neutrophil Extracellular Traps *In Vivo* Results in Hypersusceptibility to Polymicrobial Sepsis in Mice. *Crit Care* (2012) 16:R137. doi: 10.1186/CC11442
147. Mai SHC, Khan M, Dwivedi DJ, Ross CA, Zhou J, Gould TJ, et al. Delayed But Not Early Treatment With Dnase Reduces Organ Damage and Improves Outcome in a Murine Model of Sepsis. *Shock* (2015) 44:166–72. doi: 10.1097/SHK.0000000000000396

Conflict of Interest: The authors declare that the research was conducted in the absence of any commercial or financial relationships that could be construed as a potential conflict of interest.

frontiers | Frontiers in Immunology

TYPE Original Research
PUBLISHED 08 September 2022
DOI 10.3389/fimmu.2022.995886

OPEN ACCESS

EDITED BY
James Cheng-Chung Wei,
Chung Shan Medical University Hospital, Taiwan

REVIEWED BY
Ken-Pen Weng,
Kaohsiung Veterans General Hospital, Taiwan
Hsiao-Chen Lin,
Chung Shan Medical University, Taiwan

*CORRESPONDENCE
Ho-Chang Kuo
erickuo48@yahoo.com.tw
dr.hckuo@gmail.com

†These authors have contributed equally to this work

SPECIALTY SECTION
This article was submitted to Inflammation, a section of the journal Frontiers in Immunology

RECEIVED 16 July 2022
ACCEPTED 18 August 2022
PUBLISHED 08 September 2022

CITATION
Chen K-D, Huang Y-H, Wu W-S, Chang L-S, Chu C-L and Kuo H-C (2022) Comparable bidirectional neutrophil immune dysregulation between Kawasaki disease and severe COVID-19. *Front. Immunol.* 13:995886. doi: 10.3389/fimmu.2022.995886

Comparable bidirectional neutrophil immune dysregulation between Kawasaki disease and severe COVID-19

Kuang-Den Chen[1,2,3†], Ying-Hsien Huang[1,2,4†], Wei-Sheng Wu[5], Ling-Sai Chang[1,2,4], Chiao-Lun Chu[1,2] and Ho-Chang Kuo[1,2,4,6*]

[1]Kawasaki Disease Center, Kaohsiung Chang Gung Memorial Hospital, Kaohsiung, Taiwan, [2]Department of Pediatrics, Kaohsiung Chang Gung Memorial Hospital, Kaohsiung, Taiwan, [3]nstitute for Translational Research in Biomedicine, Kaohsiung Chang Gung Memorial Hospital, Kaohsiung, Taiwan, [4]College of Medicine, Chang Gung University, Taoyuan, Taiwan, [5]Department of Electrical Engineering, National Cheng Kung University, Tainan, Taiwan, [6]Department of Respiratory Therapy, Kaohsiung Chang Gung Memorial Hospital, Kaohsiung, Taiwan

Kawasaki disease (KD), a multisystem inflammatory syndrome that occurs in children, and severe acute respiratory syndrome coronavirus 2 (SARS-CoV-2 or COVID-19) may share some overlapping mechanisms. The purpose of this study was to analyze the differences in single-cell RNA sequencing between KD and COVID-19. We performed single-cell RNA sequencing in KD patients (within 24 hours before IVIG treatment) and age-matched fever controls. The single-cell RNA sequencing data of COVID-19, influenza, and health controls were downloaded from the Sequence Read Archive (GSE149689/PRJNA629752). In total, 22 single-cell RNA sequencing data with 102,355 nuclei were enrolled in this study. After performing hierarchical and functional clustering analyses, two enriched gene clusters demonstrated similar patterns in severe COVID-19 and KD, heightened neutrophil activation, and decreased MHC class II expression. Furthermore, comparable dysregulation of neutrophilic granulopoiesis representing two pronounced hyperinflammatory states was demonstrated, which play a critical role in the overactivated and defective aging program of granulocytes, in patients with KD as well as those with severe COVID-19. In conclusion, both neutrophil activation and MHC class II reduction play a crucial role and thus may provide potential treatment targets for KD and severe COVID-19.

KEYWORDS

kawasaki disease, COVID-19, aged neutrophils, overactivation, single-cell RNA sequencing

Introduction

Kawasaki disease (KD) was first reported with an unknown etiology more than 50 years ago by Dr. Kawasaki in Japan. The five major clinical diagnosis criteria of KD (1) include oral mucosa changes (fissure lips, strawberry tongue, and oral mucosal inflammation), bilateral conjunctivitis, enlarged neck lymph nodes, limb induration (subsequent desquamation), and polymorphic skin rash (2). However, the detailed mechanisms underlying the pathogenesis of KD is complex and remains inconclusive (3).

Recent outbreaks of the SARS-CoV-2 pandemic in 2019-2021 (COVID-19) have been associated with a sharp increase in the incidence of multisystemic inflammatory syndrome in children (MIS-C), suggesting a common etiology and pathophysiology with KD (4–6). Certain signs or symptoms are specific to KD and go beyond the five major symptoms, such as induration over the bacillus Calmette-Guérin (BCG) vaccination site and coronary arteritis, dilatation, or aneurysm formation. Coronary artery involvement has also been found in rheumatologic or infectious diseases but are primarily (more than 95%) found in KD patients, MIS-C patients and now also experience of COVID-19 vaccine-related adverse events among adolescents and youth (7–9). Meanwhile, BCG vaccination has also been reported to have some protective role in COVID-19 (10, 11). BCG induration in patients with KD was considered a T cell immune response, much like the type 4 hypersensitivity of the tuberculin skin test (PPD skin test), while T cell response has also been reported in COVID-19 (12, 13).

Hypercytokinemia, or "cytokine storm," refers to a set of clinical conditions caused by excessive immune reactions and has been recognized as a leading cause of both Kawasaki disease (KD) (14) and severe COVID-19 (15, 16). A recent study profiled MIS-C, adult COVID-19, and healthy individuals using single-cell RNA sequencing and found elevated alarmins and decreased antigen presentation signatures, thus indicating myeloid dysfunction in both MIS-C and COVID-19 patients (17). Currently, a study revealed that MIS-C and KD shared same fundamental nature of the host immune response continuum as COVID-19 which was found to be predominantly IL15/IL15RA-centric cytokine storm (18). Thus, we determined to characterize the cytokine responses in COVID-19, focusing on the impact of disease severity by comparing those in KD, as such may provide important clues regarding the underlying pathogenesis of both diseases. Monocyte/macrophage-derived interleukin (IL)-1β and epithelial cell-derived IL-6 were unique features of SARS-CoV-2 infection compared to the viral and bacterial causes of pneumonia. Despite having no evidence of active infection, MIS-C patients displayed elevated S100A-family alarmins and decreased antigen presentation signatures, which indicated myeloid dysfunction (17). Therefore, COVID-19 and KD may share some innate inflammatory or immune responses and thus need to be analyzed together. In this study, we aimed to analyze the shared innate immune characteristics between COVID-19 and KD using single-cell RNA sequencing profiling. To unravel the complexity of immune response in COVID-19 and KD, we performed a detailed immune cell phenotyping and transcriptomics analyzed at the single-cell level on whole blood cells. We compared data from children with KD during acute phase and patients with SARS-CoV-2 acute infection, and then analyzed the hyperinflammatory cell types and their associated molecular signatures.

Results

Comparing single-cell transcriptomes of peripheral immune cells between Kawasaki disease and COVID-19 patients

To characterize the immunological properties of patients with Kawasaki disease, we performed droplet-based single-cell transcriptomic profiling of whole blood cell (WBC) specimens from three patients (KD) and two febrile controls (FC) at Kaohsiung Chang Gung Memorial Hospital. Furthermore, we obtained the COVID-19 datasets were obtained from the Sequence Read Archive (SRA) public repository (five data sets for severe influenza (FLU), nine datasets for COVID-19 (four for mild COVID-19, five for severe COVID-19), and four datasets for healthy controls (HC) in BioProject PRJNA629752 according to GSE149689 in the GEO database).

After completing the unified single-cell analysis procedure with stringent quality control (see Methods), we obtained approximately 625 million unique transcripts from 107,387 nuclei from the immune cells of all samples. Among these cells, 16,973 cells (15.8%) came from KD patients, 14,773 cells (13.8%) came from FC, 17,327 cells (16.1%) came from severe COVID-19, 24,672 cells (23%) came from mild COVID-19, 8,718 cells (8.1%) came from FLU, and 24,924 cells (23.2%) came from HC subjects. We performed integrative analysis to harmonize all 23 datasets, followed by graph-based clustering and non-linear dimensionality reduction using t-Distributed Stochastic Neighbor Embedding (t-SNE) in order to visualize communities of similar cells by reducing dimensionality based on highly variable genes using the Loupe® browser (Figure 1A). We resolved 14 distinct cell types (Figure 1B) assigned from 45 t-SNE-identified different clusters, unbiased by datasets from all the experimental batches of scRNA-seq studies based on well-known marker genes (Figure S1).

We performed the first direct comparison of cytokine profiles in both diseases. Genes were considered differentially expressed when the false discovery rate (FDR) ≤ 0.05. Seven out of the 16 known cytokine markers (including IL1A, IL1R1, CCL2, IL6, IL10, CXCL10, and VEGFA) were less pronounced in KD than in severe COVID-19 patients compared to FC and

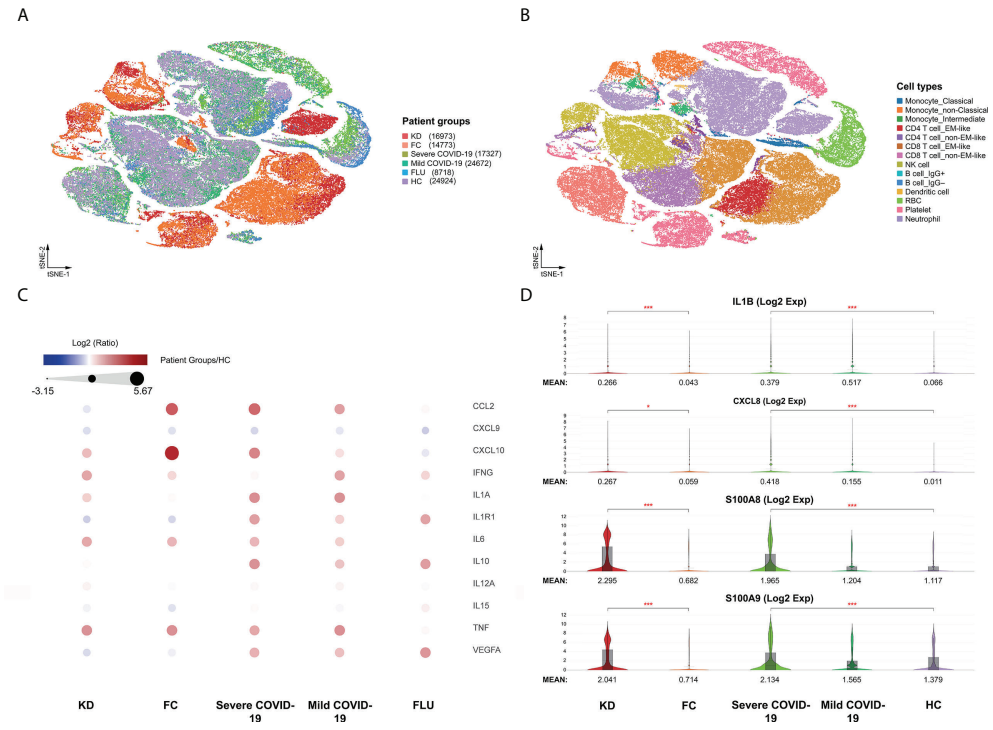

FIGURE 1
Immunological characterization of blood cells from Kawasaki disease and COVID-19 patients. **(A)** t-SNE projection of the blood cells from patients with Kawasaki disease (KD) (three samples), febrile controls (FC) (two samples), patients with COVID-19 (four samples for mild COVID-19, five samples for severe COVID-19), and healthy controls (HC) (four samples). Each dot corresponds to a single cell, colored according to group information. **(B)** t-SNE projection colored by cell types. Canonical cell markers were used to label clusters by cell identity as represented in the t-SNE plots of Figure S1. **(C)** Direct comparison of known cytokines among single-cell datasets that may be involved in hypercytokinemia of both KD and severe COVID-19 diseases. **(D)** Violin plots showing the comparable expression of canonical hypercytokinemia markers IL1B, CXCL8, S100A8, and S100A9 under different conditions. Genes were considered differentially expressed according to the *P* values from the Mann-Whitney *U* test with a false discovery rate (FDR) < 0.05 (*), or < 0.0005 (***).

HC, respectively (Figure 1C). Levels of the inflammasome cytokine IL1B, the neutrophil chemotaxis factor CXCL8, and alarmins S100A8 and S100A9 were comparably elevated in KD and severe COVID-19 compared to FC and HC, respectively (Figure 1D). However, IL15, CXCL9 and IL12A levels were not significantly altered in KD or severe COVID-19 compared to FC or HC, respectively. TNF levels did not differ between KD and its febrile controls. Furthermore, IFN-γ (IFNG) levels were more than three-fold higher in KD compared to severe COVID-19, a key observation that differentiates KD hypercytokinemia from the cytokine storm in severe COVID-19. Nevertheless, we found markedly lower levels of IFNG-induced chemokine CXCL10 in KD and CXCL9 and IL15 in both KD and severe COVID-19, suggesting blunted type II interferon signaling in both KD and severe COVID-19 conditions. Therefore, we linked comparably elevated IL1B and CXCL8 values to the emerging role of neutrophil activation in both KD and severe COVID-19. Interestingly, the four highly increased markers of IL1B, CXCL8, S100A8, and A100A9 were mainly expressed by neutrophils (Figure 2), so we specifically focused on neutrophils in downstream analysis.

Features of neutrophil subsets in both KD and severe COVID-19 patients

We compared the expression patterns of the KD or severe COVID-19 condition with that of the FC or HC condition, respectively, in 15,428 neutrophils. Genes were considered differentially expressed when FDR ≤ 0.05. In the KD patient group, 474 genes were differentially expressed when compared with the FC group, while 2,265 differentially expressed genes (DEGs) appeared in the severe COVID-19 group when compared with the HC group. Figure S2 shows 219 overlapped DEGs between the KD group and the severe COVID-19 group. Next, we aimed to identify relevant biological functions in clustered genes in terms of the ontological categorization. We found that the overlapping DEGs were highly associated with immune response,

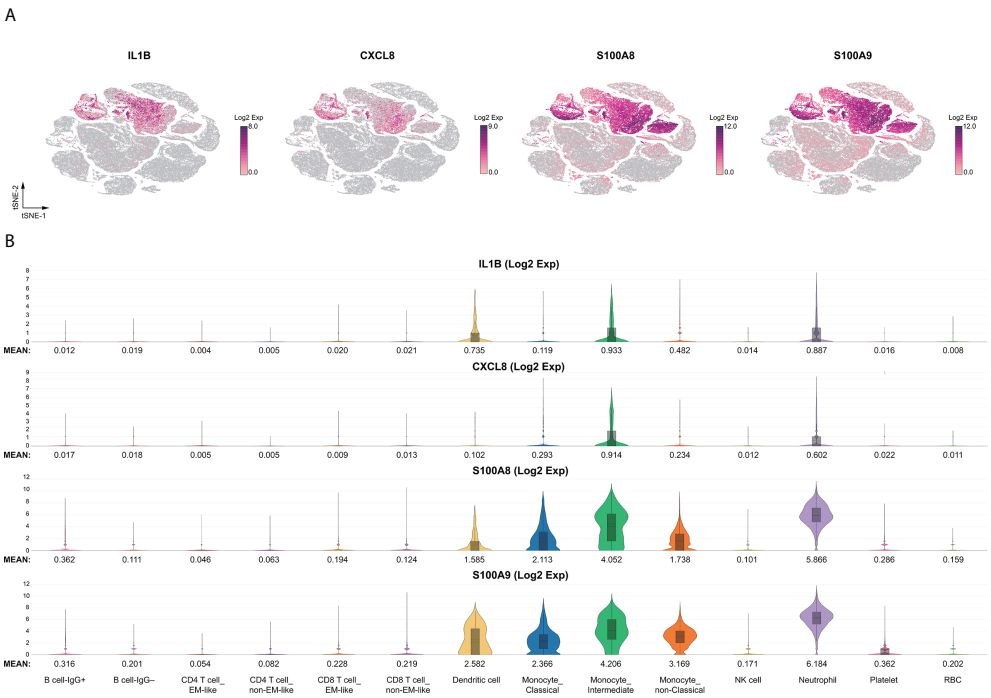

FIGURE 2
Immune landscape of the comparable myeloid inflammatory markers. The comparable innate inflammatory response between KD and severe COVID-19 with elevated myeloid IL1B, CXCL8, and alarmins of the S100A family were heightened in neutrophils. **(A)** t-SNE projection of representative gene expression patterns for IL1B, CXCL8, S100A8, and S100A9. **(B)** Violin plots of normalized log2 expression of the selected activation genes across the 14 different cell types.

MHC class II protein complex, T cell co-stimulation, interferon-γ-mediated signaling pathway, inflammatory response, and neutrophil chemotaxis as the top-ranked biological and cellular functions (Table 1). Interestingly, the three functional categories of MHC class II protein complex, T cell co-simulation, and interferon-γ-mediated signaling pathway share nine MHC class II genes, while the two functional categories of inflammatory response and neutrophil chemotaxis share 11 genes involved in neutrophil activation (Figure S3).

Furthermore, the hierarchical cluster analysis results of the 219 DEGs represented two clusters with comparably up-regulated and down-regulated genes in both KD and severe COVID-19 among all group conditions (Figure 3A). The over-represented function of the two closely clustered genes between KD and severe COVID-19 featured by the DAVID annotation tool is shown in Figure 3B. The featured functions included neutrophil chemotaxis, chemokine signal pathway, chemokine-mediated signal pathway and cytokine-cytokine receptor interaction for the cluster 1 genes, while MHC Class II activity, immunoglobulin/major histocompatibility complex, MHC Class II-like antigen recognition protein, interferon-γ-mediated signal pathway, and viral myocarditis represented the cluster 2 genes.

The 12 neutrophil activation markers demonstrated a significant increase in KD when compared with FC, including IL1B, CXCL8, IL6, S100A8, S100A9, S100A12, FCGR1A, CCL3L1, PADI4, CCL4, BCL2A1 and CCL4L2 (all $p < 0.001$, except PADI4, $p < 0.05$) (Figure 4). Meanwhile, CXCL8, S100A8, S100A9, S100A12, FCGR1A, PADI4, and BCL2A1 showed significant increases in severe COVID-19 when compared with mild COVID-19 ($p < 0.05$). All 12 markers of neutrophil activation were significantly higher in KD and severe COVID-19 when compared with adult HC ($p < 0.001$). The eight MHC class II gene expressions were significantly decreased in the KD group compared to FC, including HLA-DMA, HLA-DMB, HLA-DPA1, HLA-DPB1, HLA-DQA1, HLA-DRA, HLA-DRB1, and HLA-DRB5, as well as in severe COVID-19 compared to mild COVID-19 (Figure 5). All nine MHC class II genes showed significant decreases in both KD and severe COVID-19 conditions compared to their respective control groups.

Neutrophil maturation and aging trajectories

According to known gene signatures, we further conducted differentiating neutrophil populations along possible granulopoiesis trajectories in pseudo-time using Monocle 2

10.3389/fimmu.2022.995886

TABLE 1 DAVID enrichment analysis for 219 overlapped DEGs between KD and severe COVID-19.

GOID	Term	Count	%	Genes	Fold Enrichment	FDR
GO:0006955	Immune response	32	15.61	IFITM3, IFITM2, CXCL8, CCL4L2, CXCL3, THBS1, CXCL2, CRIP1, HLA-DMA, HLA-DMB, NFIL3, IGKC, CCL4, CCL3, FCGR1A, HLA-DQA2, HLA-DQA1, HLA-DPA1, CD74, HLA-DRB5, IL1R2, OSM, PPBP, CD4, IL6, IGLV1-51, IL1B, HLA-DPB1, HLA-DRA, HLA-DRB1, PF4, HLA-DQB1	6.718	8.79E-14
GO:0042613	MHC class II protein complex	11	5.366	CD74, HLA-DMA, HLA-DRB5, HLA-DMB, HLA-DPB1, HLA-DRA, HLA-DQA2, HLA-DRB1, HLA-DQA1, HLA-DPA1, HLA-DQB1	46.97	1.54E-12
GO:0060333	Interferon-γ-mediated signaling pathway	14	6.341	HLA-DRB5, IFNGR1, STAT1, IFI30, MT2A, HLA-DPB1, HLA-DRA, FCGR1A, HLA-DMA, HLA-DMB, HLA-DQA1, HLA-DRB1, HLA-DPA1, HLA-DQB1	16.18	9.79E-09
GO:0006954	Inflammatory response	23	11.22	CSF1R, CXCL8, CCL3L1, CCL4L2, CXCR4, TNFAIP3, PPBP, FOS, CXCL3, PTGS2, CXCL2, THBS1, IL6, IL1B, NFKBIZ, CCL4, CCL3, S100A12, NLRP3, NFKBID, S100A9, S100A8, PF4	5.363	8.84E-08
GO:0030593	Neutrophil chemotaxis	11	5.366	CXCL8, CCL3L1, IL1B, CCL4L2, CCL4, CCL3, S100A12, PPBP, CXCL3, S100A9, S100A8	14.73	7.37E-07
GO:0019882	Antigen processing and presentation	10	4.878	CD74, HLA-DRB5, HLA-DMB, HLA-DPB1, HLA-DRA, HLA-DQA2, HLA-DRB1, HLA-DQA1, HLA-DPA1, HLA-DQB1	16.07	1.71E-06
GO:0031295	T cell co-stimulation	12	5.366	HLA-DRB5, CD4, LGALS1, HLA-DPB1, HLA-DRA, MAP3K8, HLA-DMA, HLA-DMB, HLA-DRB1, HLA-DQA1, HLA-DPA1, HLA-DQB1	12.46	2.61E-06
GO:0070098	Chemokine-mediated signaling pathway	10	4.878	CXCL8, CCL3L1, CCL4L2, CCL4, CCL3, CXCR4, PPBP, CXCL3, CXCL2, PF4	12.45	1.06E-05

algorithm. As shown in Figure 6A, neutrophil maturation and aging organized on a tightly associated trajectory, starting from S4 cells and S2 cells, and ending at the left-branched S1 cells and right-branched aging neutrophils (S5-S7 cells). Neutrophil differentiation in S3 concluded with a less mature state that highly expressed CXCL2 but lower CCL4 and CXCL8 than S1, all of which are vital for neutrophil inflammation and mobilization (Figure 6B). S1 cells exhibited the highest expressions of alarmins S100A8, S100A9, S100A12 and toll-like receptors TLR4 and TLR8, all of which are involved in neutrophil activation and were the most mature neutrophils in both KD and Severe COVID-19 patients. S5, S6, and S7 cells exhibited relatively aged states that highly expressed CXCL4 and ARG1 but lower SELL, which accounted for the majority of aged neutrophils, while S7 cells also showed the highest TNF-α expression in both KD and severe COVID-19 patients. Furthermore, S6 and S7 cells highly expressed pyroptotic genes (such as NLRC4/5, NLRP1/12 and CASP1) in both KD and severe COVID-19 patients (data not shown). Notably, the percentages of aged neutrophils were largely increased in KD as well as severe COVID-19 patients (24.3% in KD vs. 8% in FC, 44.3% in severe COVID-19 vs. 26.9% in HC, respectively). However, there was no significant change of aged neutrophils in both influenza and mild COVID-19 patients (25.8% and 23.5%, respectively). The aging tendency of neutrophils was further concluded by reducting the transcription factors LEF1, MYC, CTNNB1, MAX and ATF2, which mediates the proliferation, survival and differentiation of granulocyte progenitor cells (Figure 6C). These observations indicate a comparable dysregulation of neutrophilic granulopoiesis, the occurrence of which may play a critical role in the defective aging program of granulocyte progenitors in patients with KD as well as those with severe COVID-19.

Altogether, these results suggested that the transcriptomic change for elevated neutrophil activation, inflammation and suppressive interferon-γ-mediated signaling pathway through general MHC class II reduction could be a “comparable” immune response between KD and severe COVID-19 patients compared to their controls. Overactivated and dysregulated aging neutrophils represent two pronounced hyperinflammatory states in both KD and severe COVID-19 and could be mediated *via* impaired antigen presentation.

Discussion

On clinical grounds, both KD and severe COVID-19 have been shown to be caused by accompanying hyperinflammatory states (19, 20). In particular, inflammatory cytokines secreted by over-activated classical monocytes and macrophages have been given a central role in not only the acute phase of KD but also the severe progression of COVID-19 (21, 22). Recently, one study

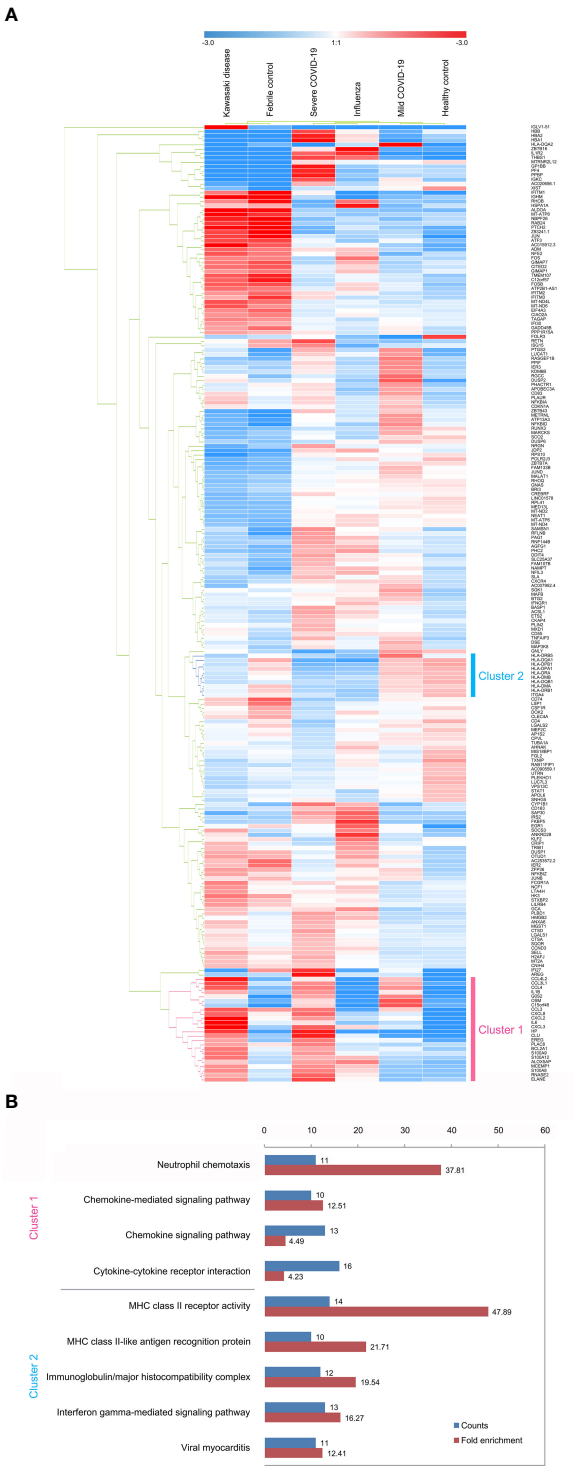

FIGURE 3
Subpopulation analysis of neutrophils. **(A)** Heatmap of 219 differentially expressed genes in neutrophil subsets across disease conditions (KD, FC, severe COVID-19, mild COVID-19, FLU, and HC). The color bars indicate gene expression clustered by hierarchical clustering for normalized gene expression levels. Cluster 1 genes (pink) represent heightened levels, whereas cluster 2 genes (cyan) are drastically reduced in both KD and severe COVID-19 compared to the controls (FC and HC, respectively). **(B)** The lists of over-represented gene ontology function of the two closely clustered genes featured by the DAVID annotation tool. The fold enrichment is defined as the ratio of the two proportions, where one is the proportion of the input 219 DEGs belonging to a certain GO term, and the other is the proportion of genes in the universal background belonging to that specific GO term. Adjusted *p* values are calculated from modified Fisher's exact test with FDR multiple-testing correction.

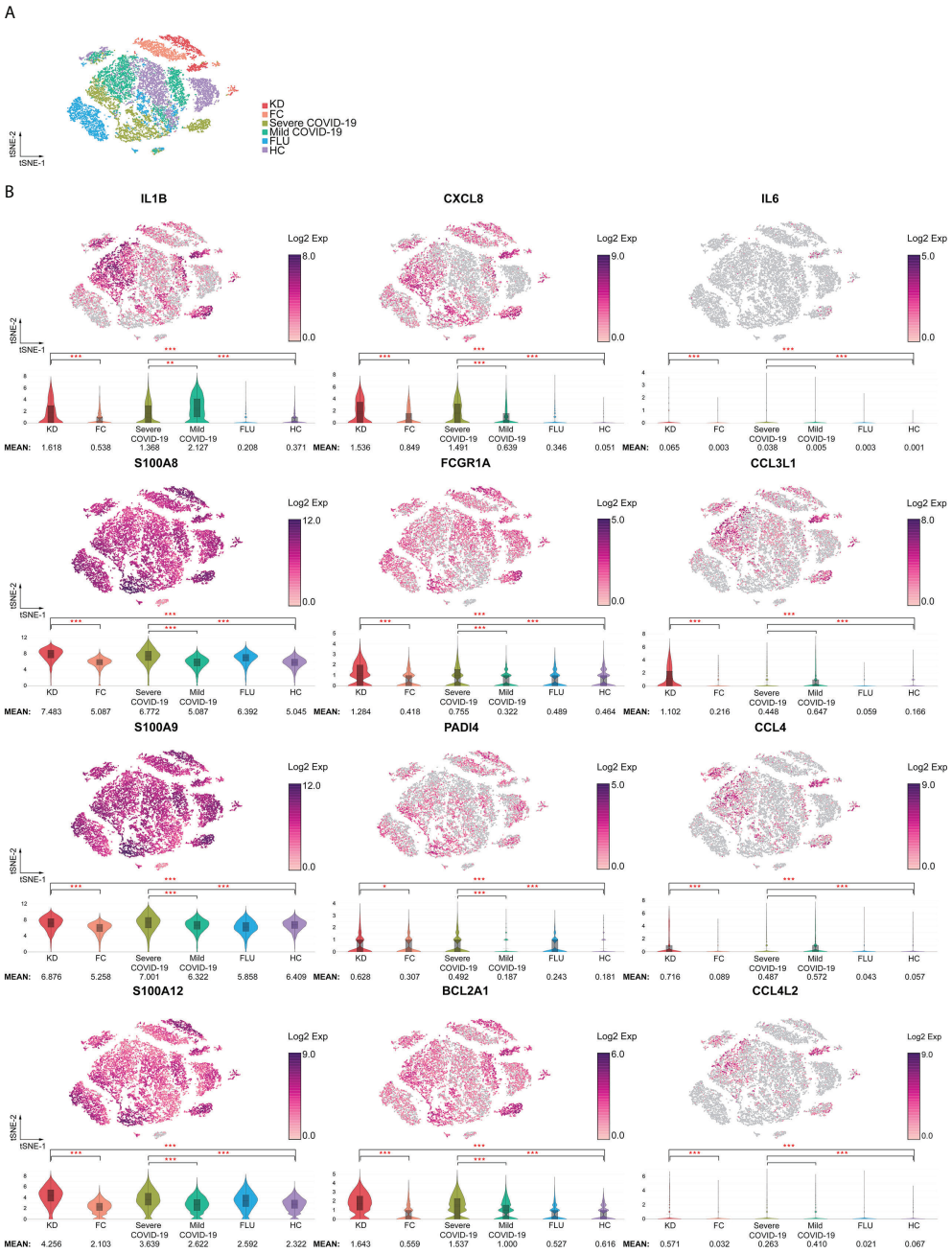

FIGURE 4
Increased activation signatures in neutrophils from both KD and severe COVID-19 patients. **(A)** t-SNE projection of neutrophils across disease conditions. **(B)** t-SNE and violin plots of normalized log2 expression levels of activation genes in cluster 1 identified in Figure 3A. The panel of genes was chosen based on their known role in neutrophil activation (IL1B, IL6, CXCL8, S100A8, S100A9, and S100A12), infiltration (CCL3L1, CCL4, CCL4L2, and FCGR1A), survival (BCL2A1), and neutrophil extracellular trap formation (PADI4). < 0.05 (*), < 0.005 (**) or < 0.0005 (***).

demonstrated that the TNF/IL1B–driven inflammatory response was dominant in COVID-19 across all types of cells among PBMCs using single-cell RNA sequencing (23). Classical monocytes in severe COVID-19 were found to be accompanied by the IFN-I response that was characterized by the up-regulation of various interferon-stimulating genes (ISGs), including ISG15, IFITM1/2/3, ISG20, IFI27, and MX1 when compared to mild COVID-19. Furthermore, an important objective in the study of KD has been identifying the pro-inflammatory cytokines that play a role in the pathogenesis of

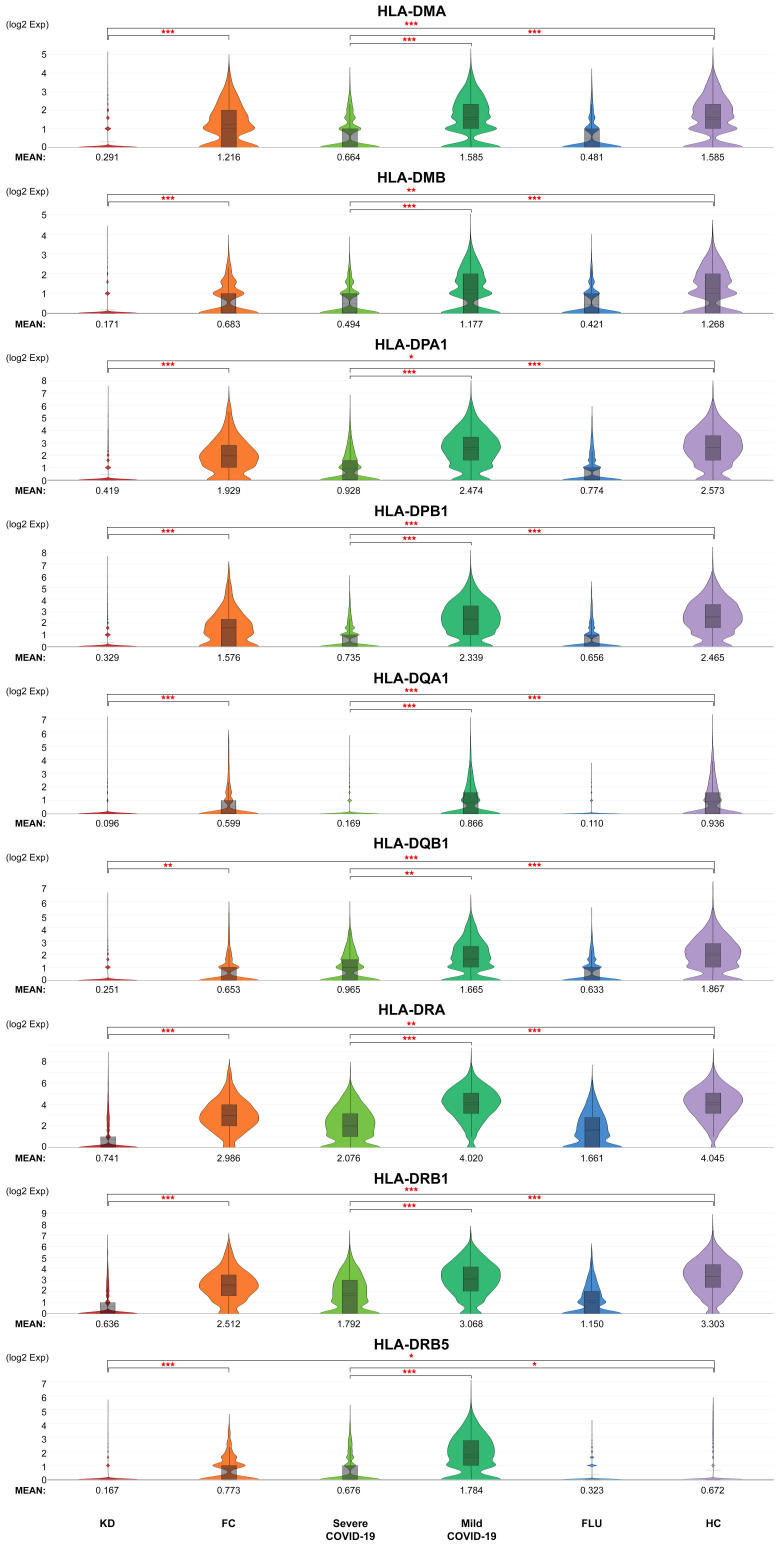

FIGURE 5
Generally reduced MHC class II in neutrophils of both KD and severe COVID-19 patients. Violin plots of normalized log2 expression levels of MHC class genes in cluster 2 identified in Figure 3A. The panel of genes was chosen based on their known role in antigen presentation and interferon-γ-mediated signaling pathway. < 0.05 (*), < 0.005 (**) or < 0.0005 (***).

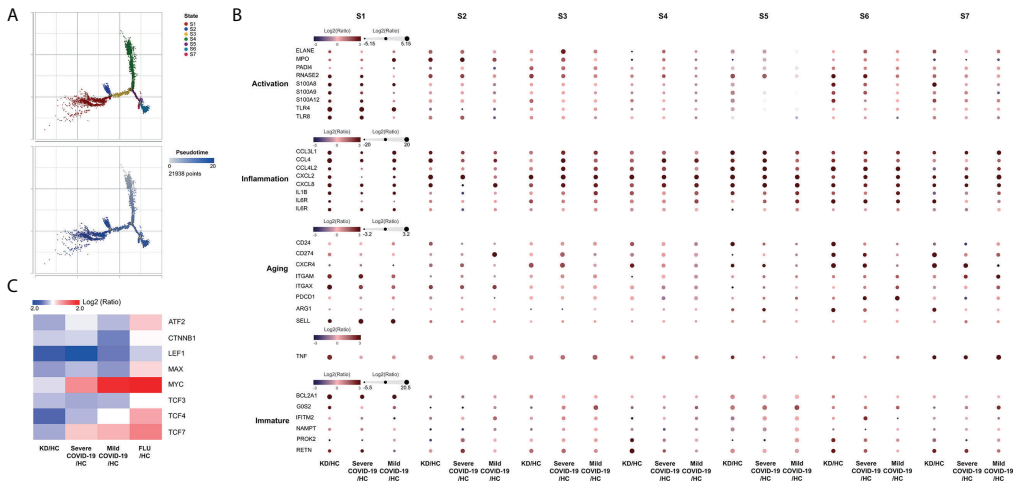

FIGURE 6
Monocle trajectory of neutrophils. **(A)** Trajectory analysis of neutrophils using Monocle 2 was colored by states (upper panel) and pseudotime maps (lower panel) showed changes in neutrophil differentiation. Cell states were inferred from the expression genes in neutrophils. **(B)** Activation-, inflammation-, aging- and immaturation-related genes in neutrophil subpopulations of different states. **(C)** Heatmap showing the significant differential expression of aging-related cell proliferation genes in neutrophils.

cardiac inflammation, and both TNF and IL-1 have been identified as potential *in vitro* and *in vivo* candidates. In the current study, we performed direct comparisons of cytokine expressions in KD and severe COVID and found that the expressions of IL1A, IL1R1, and TNF were about 2.6- to 10-fold higher in severe COVID-19 than in KD. Only levels of IL1B, neutrophil chemotactic CXCL8, and alarmins S100A8/S100A9 were comparably elevated in KD and COVID-19 compared to their respective controls. These four inflammatory markers were mainly expressed by neutrophils, which have a high expression of the CXCL8 receptors CXCR1 and CXCR2, which showed a significant increase in both KD and severe COVID-19 when compared with the respective controls (Figure S4). Furthermore, MIS-C represents a cytokine storm induced by SARS-CoV-2 with elevated inflammatory markers, including C-reactive protein (CRP), procalcitonin, neutrophilia, lymphopenia, and pro-inflammatory cytokine levels (i.e., IL-6, IL-10, ferritin, and D-dimers), that often meets the criteria for macrophage activation syndrome (MAS) of children and shares certain characteristics with KD (3, 24, 25). It has been recently reported that patients with MAS had higher absolute neutrophil counts which may also be associated with neutrophil activation (26, 27). Therefore, the mechanism underlying the neutrophil activation involved in the pathogenesis of KD could be, at least in part, comparable with that of COVID-19 as well as MIS-C. In animal models, IL-1 has been determined to be non-essential for the development of acute myocarditis, which is driven by TNF in the acute phase of KD, but plays an essential role in the subsequent development of coronary vasculitis (28). It has been demonstrated that IL1B triggers the activation of aortic infiltrated neutrophils and further leads to the formation of abdominal aortic aneurysms in an experimental murine model (29). Therefore, the comparable molecular mechanisms underlying neutrophil activation could be critical in both diseases and may contribute to unveiling the pathogenesis of KD.

Neutrophils have been demonstrated to have an important role in a variety of innate immune processes in KD. Mounting evidence has indicated that the regulation of toll-like receptors participates in the pathogenesis of KD (30) by stimulating neutrophil migration (31–33). More importantly, both neutrophil migration and transformation were associated with shock syndrome, a refractory response to IVIG and coronary artery lesions (CAL) in KD (34–36). Neutrophil activation has been reported to be enhanced with a marked increase in ROS, which contributes to the excessive formation of neutrophil extracellular traps (NETs), which has been suggested as being involved in the pathogenesis of KD (31, 37–39), as well as the severity of acute respiratory syndrome caused by SARS-CoV-2 and severe COVID-19 patients who have cardiovascular injuries (40–42). One recent study profiled whole blood transcriptomes of COVID-19 patients and found that neutrophil activation signatures were predominantly enriched in the severe COVID-19 group, which was confirmed *via* granulocyte sample validation of an independent cohort of COVID-19 patients (43). In said study, they found that alarmins S100A/8/9/12 and NETs-involved PADI4 exhibited heightened expressions of granulocytes from severe COVID-19 patients. In our study, neutrophil heterogeneity with distinct subsets of orchestrated maturation associated with KD and disease severity of COVID-19 were revealed using single-

cell RNA-seq analysis in the blood of patients with these diseases. We identified a comparably heightened expression of alarmin genes S100A8/9/12 toll-like receptors TLR4/8, together with markedly increased neutrophil activation-associated signatures PADI4, ELANE, OSM, and anti-apoptotic BCL2A1, PLAC8, and CLU in neutrophil subsets from both KD and severe COVID-19 patients (S1 cells in Figure 6). We also found that aged neutrophils highly expressing CXCR4 and ARG1 were concomitantly increased in PDCD1 in both KD and severe COVID-19 patients (S5-S7 cell populations in Figure 6). CXCR4 phays a critical role in orchestrating the distribution and trafficking of senescent neutrophils. The over-activated/aged phenotype of neutrophils was recently shown to contribute to vascular inflammation and myocardial infarction (44) and to be associated with severity of stroke patients (45). Moreover, neutrophils with increased PDCD1 expression represented immunosuppression of $CD8^+$ T cells in patients living with HIV infection (46). Our data indicated that the aged neutrophils may have an immunosuppressive effect on T cells in both KD and severe COVID-19 patients. Furthermore, MHC class II genes attributed to antigen presentation abilities were highly decreased in KD compared to FC, as well as in severe COVID-19 compared to either HC or mild COVID-19 patients (cluster 2 genes in Figure 3). Reduced HLA class II expression in innate myeloid cells, which is considered an established marker of immunosuppression in sepsis, may imply a dysregulated innate response to inflammation in both KD and severe COVID-19 patients. As for immunosuppressive properties, PD-L1 (CD274) is up-regulated and dysregulated in several types of immune cells of COVID-19 patients' monocytes, neutrophils, gamma delta T cells, and CD4+ T cells. It has been demonstrated that neutrophils from severe COVID-19 patients were persistently increased in PD-L1 (CD274) expression compared to those from healthy controls by single-cell transcriptomes and proteomics (47). We confirmed those findings and further observed that elevated PD-L1 expression on neutrophils was observed in severe COVID-19 but not in KD patients. Nevertheless, the ITGA4 that was attributed to the "mildly activated" neutrophils was also reduced and clustered together with MHC class II genes in both KD and severe COVID-19 patients. FLU patients also exhibited a drastic reduction of MHC class II genes in neutrophils, but their alarmins, neutrophil activation-associated signatures, and anti-apoptotic genes were not significantly altered. Therefore, we identified that neutrophils could mediate both KD and COVID-19 immunopathology, which represents a simultaneous appearance of over activation and immunosuppressant signatures.

Collectively, we provided the first evidence using single-cell transcriptomes that KD represents similar molecular phenotypes of bidirectional over-activated neutrophils with severe COVID-19. The identification of the underlying mechanisms in immune dysfunction associated with maturation and aging of neutrophils behind KD may be essential for developing preventive strategies or focused therapies, but its etiology has remained unknown for decades. Our data implicate defective crosstalk between innate and adaptive immune responses with direct relevance for tissue destruction during the acute phase of KD. When comparing KD to severe COVID-19, the pathological features of neutrophils have important implications for diagnostic and prognostic testing. In particular, the heightened alarmins, reduced MHC class II molecules, and bidirectionally promoted neutrophil survival as well as the aging that we identified, are all crucial for clinical application for improved diagnosis and may be able to predict disease severity early in both KD and COVID-19 patients. Our study has some limitations, including the relatively low number of cases in each group and lack of a comparison with healthy children. We usually compared biochemical and molecular characteristics between Kawasaki disease with common fever to identify true features that differentiated suspected Kawasaki disease patients with febrile children for mechanistic investigation. In this study, the key innate immune response genes and abundantly expressed alarmins that currently known as important features of KD as well as those MHC class II genes were not significantly altered in febrile controls. Thus, the use of febrile children as control of KD patients is suitable at least in investing in the key molecular events occurred in KD and comparing with those in COVID-19 patients. The febrile children may have altered adaptive immune response that will take days and even a week. The altered adaptive immunity in febrile children might affected those genes that also involved in that of KD patients. A further longitudinal analysis of polymorphonuclear leukocytes of KD, febrile children and healthy controls will be required.

Methods

Enrollment of human subjects

We obtained ethical approval for this study from the Institutional Review Board of the Chang Gung Memorial Hospital (No. 202001350A3 and 201800472B0), as well as written informed consent from the parents or guardians of all participants. The KD patients were treated with a single dose of IVIG (2 g/kg) over a 12-hour period and aspirin. Patients whose symptoms did not fit the diagnostic criteria of KD according to the American Heart Association, had an acute fever for less than 5 days, or had an incomplete collection of pre- and post-IVIG blood samples were excluded. The patients in the fever control group had diagnoses of upper respiratory tract infection, as previously described (32).

Preparation of single-cell suspension

Peripheral blood samples were collected from three KD patients within 24 hours before IVIG treatment and two

febrile control subjects in EDTA collection tubes (vender) and centrifuged at 400 × g for 5 min at 4°C. The cell viability of purified white blood cells (WBC) exceeded 90%.

Single-cell RNA-sequencing

Immune cell suspensions were loaded on a GemCode Single-Cell Instrument (10x Genomics, Pleasanton, CA, USA) to generate single-cell GEMs. Single-cell RNA-Seq libraries were prepared using GemCode Single-Cell 3' Gel Bead and Library Kit (now sold as P/N 120262, 1000009, 120267, 10x Genomics). GEM-RT was performed in a Veriti 96-Well Thermal Cycler 2020/7/29 Version1 (Applied Biosystems; Model#: 9902)at 53°C for 45 min, 85°C for 5 min, and held at 4°C. After RT, GEMs were broken, and the single-strand cDNA was cleaned up with DynaBeads MyOneSilane Beads (Thermo Fisher Scientific; P/N 37002D) and the SPRIselect Reagent Kit (0.6 × SPRI; Beckman Coulter; P/N B23318). cDNA was amplified using the Veriti 96-Well Thermal Cycler Module at 98°C for 3 min, cycled 12× at 98°C for 15 s, at 67°C for 20 s, and at 72°C for 1 min and was then held at 4°C. Amplified cDNA product was cleaned up with the SPRIselect Reagent Kit (0.6×SPRI). The cDNA was subsequently sheared to ~200 bp using a Covaris S2 Focused Ultrasonicator system (Covaris; P/N 600028). Indexed sequencing libraries were constructed using the reagents in the GemCode Single-Cell 3' Library Kit, following these steps (1): end repair and A-tailing (2); adapter ligation (3); post-ligation cleanup with SPRIselect (4); sample index PCR and cleanup. The barcode sequencing libraries were quantified using quantitative PCR (KAPA Biosystems Library Quantification Kit for Illumina P/N KK4824 platforms). Sequencing libraries were loaded at 250 pM on an Illumina Hiseq 4000 with 2 × 150 paired-end kits using the following read lengths: 98 bp Read1, 14 bp I7 Index, 8 bp I5 Index, and 10 bp Read2.

ScRNA-seq data analysis

We used the Cell Ranger Single Cell Pipeline v.4.0.0 to process data de-multiplexing, barcode processing, and single cell 3' gene counting, which was generated using the 10X Chromium platform (Kawasaki disease) or downloaded from the SRA/GEO repository (COVID-19, GSE149689/PRJNA629752). All raw and processed ScRNA-seq data of KD patients and febrile controls have been deposited in the GEO database under accession number GSE200743. For all data analyses, we used publicly available software. The Loupe Cell Browser (v.5.0.1) and Seurat (v.4.0) were used for data processing, differential expression analysis, and visualization. For the scRNA-seq dataset, we removed cells with a low number of genes detected (< 200), cells with a high number of UMI detected (> 300,000), and cells with a high proportion of UMI counts attributed to mitochondrial genes (> 20%). The filtered expression matrix was then normalized and scaled to exclude unwanted sources of variation driven by the number of UMIs and mitochondrial content.

Clustering and visualization of scRNA-seq data using t-SNE

Before clustering the cells, we ran principal component analysis (PCA) on the normalized, log-transformed, centered, and scaled gene-barcode matrix to reduce the number of feature (gene) dimensions. The pipeline adopted a python implementation of the IRLBA algorithm, which produced a projection of each cell onto the first N principal components. After running PCA, we then performed the t-distributed Stochastic Neighbor Embedding (t-SNE), a machine learning algorithm for visualization developed by Laurens van der Maaten and Geoffrey Hinton, to visualize cells in a 2-D space. Clustering was then ran in order to group cells that have similar expression profiles together based on their projection into PCA space. Two clustering methods were performed: graph-based and k-means. Cell Ranger also produced a table indicating that genes were differentially expressed in each cluster relative to all other clusters. Classification of immune cells was inferred from the annotation of cluster-specific genes and based on the expression of some well-known markers of immune cell types. Loupe™ Cell Browser (v5.0) was generally used to view the entire dataset and interactively find significant genes, cell types, and substructure within cell clusters.

Gene Ontology enrichment analysis

Functional enrichment was performed on overlapped genesets from Gene Ontology (GO) annotation within the neutrophils by using the DAVID gene functional classification tool. The *p*-value and the Benjamini-Hochberg FDR were used to determine the significance of enrichment or the overrepresentation of terms for each annotation.

Data availability statement

The datasets presented in this study can be found in online repositories. The names of the repository/repositories and accession number(s) can be found below: https://www.ncbi.nlm.nih.gov/geo/query/acc.cgi?acc=GSE200743.

Ethics statement

The studies involving human participants were reviewed and approved by the Institutional Review Board of the Chang Gung Memorial Hospital. Written informed consent to participate in this study was provided by the participants' legal guardian/next of kin.

Author contributions

K-DC, Y-HH and H-CK contributed to the experimental design, data interpretation and writing of the manuscript. K-DC, Y-HH and W-SW contributed to statistical analysis for all genomic data and retrieved clinical data. K-DC and L-SC contributed to genomic data analysis for revision. C-LC contributed all experiments involving sample preparation and single-cell RNA sequencing. All authors contributed to the article and approved the submitted version.

Funding

This study received funding from the following grants: MOST 108-2314-B-182 -037-MY3 from the Ministry of Science and Technology of Taiwan (MOST), and CMRPG8L0021, CMRPG8L0031, CMRPG8L0041, CMRPG8L0401, CMRPG8L0402 and CMRPG8J1641 from Chang Gung Memorial Hospital, Taiwan. Although these institutes provided financial support, they had no influence on the way in which we collected, analyzed, or interpreted the data or wrote this manuscript.

Conflict of interest

The authors declare that the research was conducted in the absence of any commercial or financial relationships that could be construed as a potential conflict of interest.

Publisher's note

All claims expressed in this article are solely those of the authors and do not necessarily represent those of their affiliated organizations, or those of the publisher, the editors and the reviewers. Any product that may be evaluated in this article, or claim that may be made by its manufacturer, is not guaranteed or endorsed by the publisher.

Supplementary material

The Supplementary Material for this article can be found online at: https://www.frontiersin.org/articles/10.3389/fimmu.2022.995886/full#supplementary-material

References

1. Kuo HC, Hsu YW, Wu MS, Chien SC, Liu SF, Chang WC. Intravenous immunoglobulin, pharmacogenomics, and Kawasaki disease. *J microbiology immunology infection = Wei mian yu gan ran za zhi* (2016) 49(1):1–7. doi: 10.1016/j.jmii.2014.11.001

2. Kuo H-C. Preventing coronary artery lesions in Kawasaki disease. *Biomed J* (2017) 40(3):141–6. doi: 10.1016/j.bj.2017.04.002

3. Huang PY, Huang YH, Guo MM, Chang LS, Kuo HC. Kawasaki Disease and allergic diseases. *Front Pediatr* (2020) 8:614386. doi: 10.3389/fped.2020.614386

4. Ouldali N, Pouletty M, Mariani P, Beyler C, Blachier A, Bonacorsi S, et al. Emergence of Kawasaki disease related to sars-Cov-2 infection in an epicentre of the French covid-19 epidemic: A time-series analysis. *Lancet Child Adolesc Health* (2020) 4(9):662–8. doi: 10.1016/S2352-4642(20)30175-9

5. Riphagen S, Gomez X, Gonzalez-Martinez C, Wilkinson N, Theocharis P. Hyperinflammatory shock in children during covid-19 pandemic. *Lancet* (2020) 395(10237):1607–8. doi: 10.1016/S0140-6736(20)31094-1

6. Verdoni L, Mazza A, Gervasoni A, Martelli L, Ruggeri M, Ciuffreda M, et al. An outbreak of severe Kawasaki-like disease at the Italian epicentre of the sars-Cov-2 epidemic: An observational cohort study. *Lancet* (2020) 395(10239):1771–8. doi: 10.1016/S0140-6736(20)31103-X

7. Salah NB, Lahouel I, Mariem CB, Trimech K, Bellallah A, Chouchene S, et al. Multisystem inflammatory syndrome in children associated with erythema multiforme-like eruption following covid-19. *Int J rheumatic Dis* (2022) 25(3):375–7. doi: 10.1111/1756-185X.14294

8. Weng KP, Hsieh KS, Huang SH, Ou SF, Ma CY, Ho TY, et al. Clinical relevance of the risk factors for coronary artery lesions in Kawasaki disease. *Kaohsiung J Med Sci* (2012) 28(1):23–9. doi: 10.1016/j.kjms.2011.09.002

9. Haslak F, Gunalp A, Cebi MN, Yildiz M, Adrovic A, Sahin S, et al. Early experience of covid-19 vaccine-related adverse events among adolescents and young adults with rheumatic diseases: A single-center study. *Int J rheumatic Dis* (2022) 25(3):353–63. doi: 10.1111/1756-185X.14279

10. Curtis N, Sparrow A, Ghebreyesus TA, Netea MG. Considering bcg vaccination to reduce the impact of covid-19. *Lancet* (2020) 395(10236):1545-6. doi: 10.1016/S0140-6736(20)31025-4

11. Escobar LE, Molina-Cruz A, Barillas-Mury C. Bcg vaccine protection from severe coronavirus disease 2019 (Covid-19). *Proc Natl Acad Sci United States America* (2020) 117(30):17720–6. doi: 10.1073/pnas.2008410117

12. Grau-Exposito J, Sanchez-Gaona N, Massana N, Suppi M, Astorga-Gamaza A, Perea D, et al. Peripheral and lung resident memory T cell responses against sars-Cov-2. *Nat Commun* (2021) 12(1):3010. doi: 10.1038/s41467-021-23333-3

13. Renner K, Schwittay T, Chaabane S, Gottschling J, Muller C, Tiefenbock C, et al. Severe T cell hyporeactivity in ventilated covid-19 patients correlates with prolonged virus persistence and poor outcomes. *Nat Commun* (2021) 12(1):3006. doi: 10.1038/s41467-021-23334-2

14. Ulloa-Gutierrez R, Alphonse MP, Dhanranjani A, Yeung RSM. Kawasaki disease-associated cytokine storm syndrome. In: Cytokine Storm Syndrome. Springer Int Publish; (2019) 393–406. doi: 10.1007/978-3-030-22094-5_23

15. Bhaskar S, Sinha A, Banach M, Mittoo S, Weissert R, Kass JS, et al. Cytokine storm in covid-19-Immunopathological mechanisms, clinical considerations, and therapeutic approaches: The reprogram consortium position paper. *Front Immunol* (2020) 11:1648. doi: 10.3389/fimmu.2020.01648

16. Bordallo B, Bellas M, Cortez AF, Vieira M, Pinheiro M. Severe covid-19: What have we learned with the immunopathogenesis? *Adv Rheumatol* (2020) 60(1):50. doi: 10.1186/s42358-020-00151-7

17. Ramaswamy A, Brodsky NN, Sumida TS, Comi M, Asashima H, Hoehn KB, et al. Immune dysregulation and autoreactivity correlate with disease severity in sars-Cov-2-Associated multisystem inflammatory syndrome in children. *Immunity* (2021) 54(5):1083–95.e7. doi: 10.1016/j.immuni.2021.04.003

18. Ghosh P, Katkar GD, Shimizu C, Kim J, Khandelwal S, Tremoulet AH, et al. An artificial intelligence-guided signature reveals the shared host immune response in mis-c and Kawasaki disease. *Nat Commun* (2022) 13(1):2687. doi: 10.1038/s41467-022-30357-w

19. Pedersen SF, Ho YC. Sars-Cov-2: A storm is raging. *J Clin Invest* (2020) 130 (5):2202–5. doi: 10.1172/JCI137647

20. Cherqaoui B, Kone-Paut I, Yager H, Bourgeois FL, Piram M. Delineating phenotypes of Kawasaki disease and sars-Cov-2-Related inflammatory multisystem syndrome: A French study and literature review. *Rheumatology* (2021) 60 (10):4530-7. doi: 10.1093/rheumatology/keab026

21. Merad M, Martin JC. Pathological inflammation in patients with covid-19: A key role for monocytes and macrophages. *Nat Rev Immunol* (2020) 20(6):355–62. doi: 10.1038/s41577-020-0331-4

22. Ichiyama T, Yoshitomi T, Nishikawa M, Fujiwara M, Matsubara T, Hayashi T, et al. Nf-kappab activation in peripheral blood Monocytes/Macrophages and T cells during acute Kawasaki disease. *Clin Immunol* (2001) 99(3):373–7. doi: 10.1006/clim.2001.5026

23. Lee JS, Park S, Jeong HW, Ahn JY, Choi SJ, Lee H, et al. Immunophenotyping of covid-19 and influenza highlights the role of type I interferons in development of severe covid-19. *Sci Immunol* (2020) 5(49): eabd1554. doi: 10.1126/sciimmunol.abd1554

24. Dufort EM, Koumans EH, Chow EJ, Rosenthal EM, Muse A, Rowlands J, et al. Multisystem inflammatory syndrome in children in New York state. *New Engl J Med* (2020) 383(4):347–58. doi: 10.1056/NEJMoa2021756

25. Feldstein LR, Rose EB, Horwitz SM, Collins JP, Newhams MM, Son MBF, et al. Multisystem inflammatory syndrome in U.S. children and adolescents. *New Engl J Med* (2020) 383(4):334–46. doi: 10.1056/NEJMoa2021680

26. Aydin F, Celikel E, Ekici Tekin Z, Coskun S, Sezer M, Karagol C, et al. Comparison of baseline laboratory findings of macrophage activation syndrome complicating systemic juvenile idiopathic arthritis and multisystem inflammatory syndrome in children. *Int J rheumatic Dis* (2021) 24(4):542–7. doi: 10.1111/1756-185X.14078

27. Huang LW, Wei JC, Chen DY, Chen YJ, Tang KT, Ko TM, et al. Bidirectional association between systemic lupus erythematosus and macrophage activation syndrome: A nationwide population-based study. *Rheumatology* (2022) 61(3):1123–32. doi: 10.1093/rheumatology/keab502

28. Stock AT, Jama HA, Hansen JA, Wicks IP. Tnf and il-1 play essential but temporally distinct roles in driving cardiac inflammation in a murine model of Kawasaki disease. *J Immunol* (2019) 202(11):3151–60. doi: 10.4049/jimmunol.1801593

29. Meher AK, Spinosa M, Davis JP, Pope N, Laubach VE, Su G, et al. Novel role of il (Interleukin)-1beta in neutrophil extracellular trap formation and abdominal aortic aneurysms. *Arteriosclerosis thrombosis Vasc Biol* (2018) 38(4):843–53. doi: 10.1161/ATVBAHA.117.309897

30. Kuo HC, Li SC, Huang LH, Huang YH. Epigenetic hypomethylation and upregulation of matrix metalloproteinase 9 in Kawasaki disease. *Oncotarget* (2017) 60(10):4530–7. doi: 10.18632/oncotarget.19650

31. Aomatsu K, Kato T, Fujita H, Hato F, Oshitani N, Kamata N, et al. Toll-like receptor agonists stimulate human neutrophil migration *Via* activation of mitogen-activated protein kinases. *Immunology* (2008) 123(2):171–80. doi: 10.1111/j.1365-2567.2007.02684.x

32. Huang YH, Li SC, Huang LH, Chen PC, Lin YY, Lin CC, et al. Identifying genetic hypomethylation and upregulation of toll-like receptors in Kawasaki disease. *Oncotarget* (2017) 8(7):11249–58. doi: 10.18632/oncotarget.14497

33. Kim J, Shimizu C, Kingsmore SF, Veeraraghavan N, Levy E, Ribeiro Dos Santos AM, et al. Whole genome sequencing of an African American family highlights toll like receptor 6 variants in Kawasaki disease susceptibility. *PLoS One* (2017) 12(2):e0170977. doi: 10.1371/journal.pone.0170977

34. Kang SJ, Kim NS. Association of toll-like receptor 2-positive monocytes with coronary artery lesions and treatment nonresponse in Kawasaki disease. *Korean J Pediatr* (2017) 60(7):208–15. doi: 10.3345/kjp.2017.60.7.208

35. Cho HJ, Bak SY, Kim SY, Yoo R, Baek HS, Yang S, et al. High neutrophil: Lymphocyte ratio is associated with refractory Kawasaki disease. *Pediatr international: Off J Japan Pediatr Soc* (2017) 59(6):669–74. doi: 10.1111/ped.13240

36. Muto T, Masuda Y, Numoto S, Kodama S, Yamakawa K, Takasu M, et al. White blood cell and neutrophil counts and response to intravenous immunoglobulin in Kawasaki disease. *Global Pediatr Health* (2019) 6:2333794X19884826. doi: 10.1177/2333794X19884826

37. Yoshida Y, Takeshita S, Kawamura Y, Kanai T, Tsujita Y, Nonoyama S. Enhanced formation of neutrophil extracellular traps in Kawasaki disease. *Pediatr Res* (2020) 87(6):998–1004. doi: 10.1038/s41390-019-0710-3

38. Ko TM, Chang JS, Chen SP, Liu YM, Chang CJ, Tsai FJ, et al. Genome-wide transcriptome analysis to further understand neutrophil activation and lncrna transcript profiles in Kawasaki disease. *Sci Rep* (2019) 9(1):328. doi: 10.1038/s41598-018-36520-y

39. Li SC, Huang LH, Chien KJ, Pan CY, Lin PH, Lin Y, et al. Mir-182-5p enhances in vitro neutrophil infiltration in Kawasaki disease. *Mol Genet genomic Med* (2019) 7(12):e990. doi: 10.1002/mgg3.990

40. Arcanjo A, Logullo J, Menezes CCB, de Souza Carvalho Giangiarulo TC, Dos Reis MC, de Castro GMM, et al. The emerging role of neutrophil extracellular traps in severe acute respiratory syndrome coronavirus 2 (Covid-19). *Sci Rep* (2020) 10(1):19630. doi: 10.1038/s41598-020-76781-0

41. McCarthy CG, Saha P, Golonka RM, Wenceslau CF, Joe B, Vijay-Kumar M. Innate immune cells and hypertension: Neutrophils and neutrophil extracellular traps (Nets). *Compr Physiol* (2021) 11(1):1575–89. doi: 10.1002/cphy.c200020

42. Borges L, Pithon-Curi TC, Curi R, Hatanaka E. Covid-19 and neutrophils: The relationship between hyperinflammation and neutrophil extracellular traps. *Mediators Inflammation* (2020) 2020:8829674. doi: 10.1155/2020/8829674

43. Aschenbrenner AC, Mouktaroudi M, Kramer B, Oestreich M, Antonakos N, Nuesch-Germano M, et al. Disease severity-specific neutrophil signatures in blood transcriptomes stratify covid-19 patients. *Genome Med* (2021) 13(1):7. doi: 10.1186/s13073-020-00823-5

44. Adrover JM, Del Fresno C, Crainiciuc G, Cuartero MI, Casanova-Acebes M, Weiss LA, et al. A neutrophil timer coordinates immune defense and vascular protection. *Immunity* (2019) 50(2):390–402.e10. doi: 10.1016/j.immuni.2019.01.002

45. Weisenburger-Lile D, Dong Y, Yger M, Weisenburger G, Polara GF, Chaigneau T, et al. Harmful neutrophil subsets in patients with ischemic stroke: Association with disease severity. *Neurology(R) neuroimmunology Neuroinflamm* (2019) 6(4):e571. doi: 10.1212/NXI.0000000000000571

46. Liu K, Huang HH, Yang T, Jiao YM, Zhang C, Song JW, et al. Increased neutrophil aging contributes to T cell immune suppression by pd-L1 and arginase-1 in hiv-1 treatment naive patients. *Front Immunol* (2021) 12:670616. doi: 10.3389/fimmu.2021.670616

47. Schulte-Schrepping J, Reusch N, Paclik D, Bassler K, Schlickeiser S, Zhang B, et al. Severe covid-19 is marked by a dysregulated myeloid cell compartment. *Cell* (2020) 182(6):1419–40.e23. doi: 10.1016/j.cell.2020.08.001

frontiers | Frontiers in Immunology

TYPE Original Research
PUBLISHED 12 September 2022
DOI 10.3389/fimmu.2022.996637

OPEN ACCESS

EDITED BY
Lokesh Sharma,
Yale University, United States

REVIEWED BY
Kishu Ranjan,
Yale University, United States
Takashi Tanikawa,
Josai University, Japan

*CORRESPONDENCE
Jia Tong Loh
loh_jia_tong@immunol.a-star.edu.sg
Kong-Peng Lam
lam_kong_peng@immunol.a-star.edu.sg

SPECIALTY SECTION
This article was submitted to Molecular Innate Immunity, a section of the journal Frontiers in Immunology

RECEIVED 18 July 2022
ACCEPTED 25 August 2022
PUBLISHED 12 September 2022

CITATION
Loh JT, Teo JKH and Lam K-P (2022) Dok3 restrains neutrophil production of calprotectin during TLR4 sensing of SARS-CoV-2 spike protein. *Front. Immunol.* 13:996637. doi: 10.3389/fimmu.2022.996637

Dok3 restrains neutrophil production of calprotectin during TLR4 sensing of SARS-CoV-2 spike protein

Jia Tong Loh[1]*, Joey Kay Hui Teo[1] and Kong-Peng Lam[1,2,3]*

[1]Singapore Immunology Network, Agency for Science, Technology and Research, Singapore, Singapore, [2]Department of Microbiology and Immunology, Yong Loo Lin School of Medicine, National University of Singapore, Singapore, Singapore, [3]School of Biological Sciences, College of Science, Nanyang Technological University, Singapore, Singapore

Increased neutrophils and elevated level of circulating calprotectin are hallmarks of severe COVID-19 and they contribute to the dysregulated immune responses and cytokine storm in susceptible patients. However, the precise mechanism controlling calprotectin production during SARS-CoV-2 infection remains elusive. In this study, we showed that Dok3 adaptor restrains calprotectin production by neutrophils in response to SARS-CoV-2 spike (S) protein engagement of TLR4. Dok3 recruits SHP-2 to mediate the de-phosphorylation of MyD88 at Y257, thereby attenuating downstream JAK2-STAT3 signaling and calprotectin production. Blocking of TLR4, JAK2 and STAT3 signaling could prevent excessive production of calprotectin by Dok3$^{-/-}$ neutrophils, revealing new targets for potential COVID-19 therapy. As S protein from SARS-CoV-2 Delta and Omicron variants can activate TLR4-driven calprotectin production in Dok3$^{-/-}$ neutrophils, our study suggests that targeting calprotectin production may be an effective strategy to combat severe COVID-19 manifestations associated with these emerging variants.

KEYWORDS

neutrophils, calprotectin, SARS-CoV-2, Dok3, TLR4

Introduction

The Coronavirus disease 2019 (COVID-19) pandemic, caused by severe acute respiratory syndrome coronavirus 2 (SARS-CoV-2), has affected more than 490 million individuals and caused more than 6 million deaths to date (who.int). While majority of the patients are presented with asymptomatic or mild disease, more severe and critical illnesses can arise in a subset of patients due to dysregulated innate immune response, leading to the development of cytokine storm, acute respiratory distress syndrome (ARDS), multiple organ failure, and even death (1). While mass COVID-19

vaccination program is currently underway worldwide, a significant proportion of the population remains unvaccinated, and breakthrough infection is increasingly common in fully vaccinated individuals due to the emergence of new SARS-CoV-2 variants (2–4). Moreover, monoclonal antibody therapies which predominantly target the spike (S) protein of SARS-CoV-2 show diminished potency against newly emerging variants such as the Omicron (5, 6). As such, it is necessary for us to expand and diversify our therapeutic toolbox against SARS-CoV-2 to counteract the ongoing COVID-19 pandemic.

One biomarker which distinguishes mild from severe COVID-19 is serum calprotectin level in infected individuals (7–11). Calprotectin is a stable heterodimer of S100a8 and S100a9 which accumulates in the cytoplasm of neutrophils. During infection, they are released in massive amounts to initiate and amplify inflammatory immune responses, including the production of cytokines and recruitment of leukocytes, through binding to Toll-like receptor (TLR) 4 and receptor for advanced glycation end products (RAGE) (12). However, uncontrolled release of calprotectin by neutrophils can lead to life-threatening systemic inflammation in the host. Calprotectin was reported to be the most abundant immune mediator present in the plasma of severe COVID-19 patients (8), and it correlates strongly with disease severity (7–10). Accordingly, therapeutic agents targeting S100a8-TLR4 or S100a9 can alleviate inflammatory responses and improve survival in preclinical models of SARS-CoV-2 infection (13), thereby emphasizing the clinical significance of calprotectin in COVID-19 pathogenesis (7, 10, 14). However, how SARS-CoV-2 can be sensed by and how calprotectin production can be regulated in neutrophils remain elusive.

Dok3 is an adaptor protein which regulates signaling pathways downstream of various immune receptors. As it lacks intrinsic catalytic activity, it functions primarily as a molecular scaffold to facilitate protein-protein interaction through distinct protein-binding domains (15). Dok3 has been shown to be highly expressed in neutrophils where they play a role in suppressing anti-fungal response downstream of C-type lectin receptors (16). Interestingly, RNA-seq analysis of neutrophils from COVID-19 patients revealed that Dok3 expression is elevated in severe disease cases, suggesting a possible role for Dok3 in SARS-CoV-2 infection in humans (17). However, whether Dok3 is involved in the regulation of calprotectin production in response to SARS-CoV-2 infection remains unexplored.

In this study, we report that Dok3 could suppress the production of calprotectin in neutrophils during SARS-CoV-2 infection when the viral S protein engages TLR4. Dok3 recruits protein tyrosine phosphatase SHP-2 to mediate the de-phosphorylation of MyD88 at Y257, thereby suppressing JAK2-STAT3 signaling axis to prevent excessive calprotectin production by neutrophils. Hence, our study provides novel insight into the mechanism underlying calprotectin production by neutrophils in response to SARS-CoV-2 infection and helps to uncover potential therapeutic signaling molecules which can be targeted to alleviate the massive inflammation in severe COVID-19 patients.

Results

Loss of Dok3 enhances calprotectin production by neutrophils in response to SARS-CoV-2 S protein stimulation

Recent RNA-seq analysis of neutrophils from COVID-19 patients revealed that Dok3 expression is elevated in severe disease cases, suggesting an association with SARS-CoV-2 infection in humans (17). To investigate if Dok3 is involved in calprotectin production in neutrophils during SARS-CoV-2 infection, we stimulated wild-type (WT) and *Dok3*$^{-/-}$ neutrophils isolated from mouse bone marrow cells with the ancestral WT SARS-CoV-2 S protein, which has previously been shown to activate both mouse and human immune cells (18), and analyzed for the release of calprotectin (S100a8/9 heterodimer) into the culture medium by ELISA. We observed that treatment with S protein induces a significant increase in calprotectin secretion by *Dok3*$^{-/-}$ but not WT neutrophils (Figure 1A). Similarly, we found that S100a8 and S100a9 expression were significantly higher in *Dok3*$^{-/-}$ as compared to WT neutrophils upon S protein stimulation (Figure 1B), suggesting that Dok3 is required to suppress calprotectin production by neutrophils during SARS-CoV-2 infection. Since the S protein can activate immune responses in mouse neutrophils, we further examine the production of calprotectin *in vivo* upon intranasal instillation of S protein in mice. Our histological and flow cytometry analyses revealed higher levels of S100a8 and S100a9 expressed by *Dok3*$^{-/-}$ as compared to WT neutrophils in the lungs 24h following S protein administration (Figures 1C, D). Moreover, circulating level of calprotectin is significantly increased in *Dok3*$^{-/-}$ mice treated with the S protein (Figure 1E). Calprotectin are potent initiators and amplifiers of inflammation *via* activation and recruitment of circulating leukocytes. Indeed, we detected increased numbers of S100a8- and S100a9-producing cells, which are defined to be neutrophils *via* flow cytometry, accumulating in the lungs of *Dok3*$^{-/-}$ mice (Figure 1D and Supplementary Figure S1). These reflect a positive feedback loop, in which loss of Dok3 leads to elevated calprotectin production by neutrophils, which subsequently triggers further recruitment of calprotectin-producing neutrophils into the lungs, thereby amplifying aberrant immune responses. Taken together, our data indicate that Dok3 plays a key role in the negative regulation of calprotectin production by neutrophils in response to S protein of SARS-CoV-2.

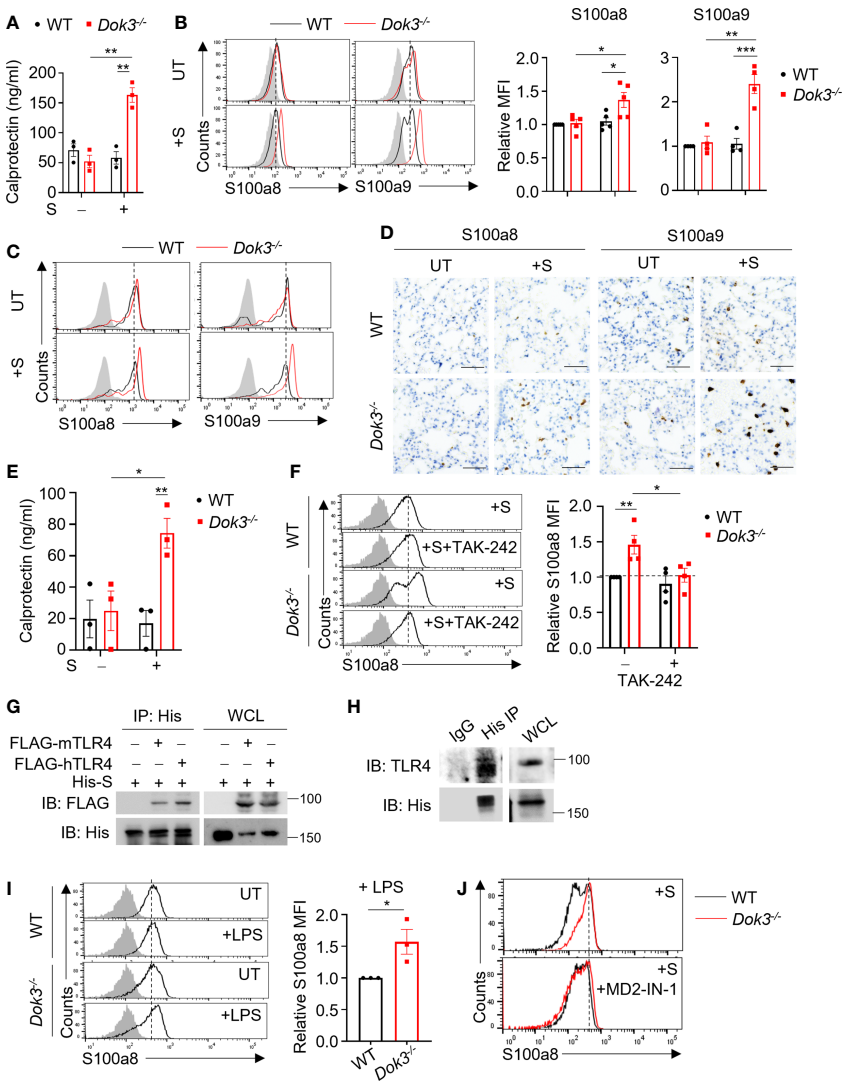

FIGURE 1
Dok3 suppresses calprotectin production by neutrophils in response to SARS-CoV-2 S protein through a TLR4-dependent pathway. **(A)** WT and *Dok3*$^{-/-}$ neutrophils were stimulated with or without S protein for 5h. Calprotectin level in culture medium is measured by ELISA. Data is shown as mean ± S.E.M. (n = 3, 3 independent experiments). **p = 0.002, unpaired two-tailed Student's t-test. **(B)** Flow cytometric analysis of S100a8 and S100a9 expression in WT and *Dok3*$^{-/-}$ neutrophils following 3h stimulation with S protein. Histograms were pre-gated on singlet, Ly6G^{+} cells. Filled histogram represents isotype control. Bar graph depicting MFI of S100a8 or S100a9 fluorescence in *Dok3*$^{-/-}$ neutrophils relative to WT neutrophils. Data is shown as mean ± S.E.M. (n = 5, 5 independent experiments). *p = 0.02, 0.03, **p = 0.002, ***p = 0.001, unpaired two-tailed Student's t-test. (C and D) Lungs were harvested from WT and *Dok3*$^{-/-}$ mice 24h after intranasal instillation of S protein. **(C)** Flow cytometric analysis of S100a8 and S100a9 expression in WT and *Dok3*$^{-/-}$ neutrophils following S protein administration. Histograms were pre-gated on singlet, CD45^{+}, Ly6G^{+} cells. Filled histogram represents isotype control. **(D)** Lung sections were stained with anti-S100a8 and anti-S100a9 antibodies. Scale bar, 50μm. Data shown are representative of 3 biological replicates. **(E)** Circulating calprotectin levels in WT and *Dok3*$^{-/-}$ mice 24h after intranasal instillation of S protein are measured by ELISA. Data is shown as mean ± S.E.M. (n = 3). *p = 0.03, **p = 0.01, unpaired two-tailed Student's t-test. **(F)** Flow cytometric analysis of S100a8 expression in WT and *Dok3*$^{-/-}$ neutrophils following 3h stimulation with S protein in the presence or absence of TAK-242. Histograms were pre-gated on singlet, Ly6G^{+} cells. Filled histogram represents isotype control. Bar graph depicting MFI of S100a8 fluorescence relative to untreated WT neutrophils. Data is shown as mean ± S.E.M. (n = 4, 4 independent experiments). *p = 0.03, **p = 0.01, unpaired two-tailed Student's t-test. **(G)** HEK293T cells were transfected with FLAG-tagged mouse (m) or human (h) TLR4. Cell lysates were incubated with His-tagged S protein and immunoprecipitated (IP) with anti-His antibody overnight. Precipitates and whole cell lysates (WCL) were immunoblotted with anti-FLAG and anti-His antibodies. Data shown are representative of 3 independent experiments. **(H)** WT neutrophils were incubated with His-tagged S protein and cell lysates were IP with anti-His or IgG control. Precipitates and WCL were probed for TLR4 and His. Data shown are representative of 3 independent experiments. **(I)** Flow cytometric analysis of S100a8 expression in WT and *Dok3*$^{-/-}$ neutrophils following 3h stimulation with or without LPS. Histograms were pre-gated on singlet, Ly6G^{+} cells. Filled histogram represents isotype control. Bar graph depicting MFI of S100a8 fluorescence in *Dok3*$^{-/-}$ neutrophils relative to WT neutrophils. Data is shown as mean ± S.E.M. (n = 3, 3 independent experiments). *p = 0.04, unpaired two-tailed Student's t-test. **(J)** Flow cytometric analysis of S100a8 expression in WT and *Dok3*$^{-/-}$ neutrophils following 3h stimulation with S protein in the presence or absence of MD2-IN-1. Histograms were pre-gated on singlet, Ly6G^{+} cells. Filled histogram represents isotype control.

TLR4/MD2 is required for sensing of SARS-CoV-2 S protein in neutrophils

The S protein of SARS-CoV-2 has been reported to interact with host receptors TLR2, TLR4 and ACE2 to activate inflammatory immune responses (18–21). To determine which receptor is responsible for sensing S protein upstream of Dok3, we treated WT and *Dok3*$^{-/-}$ neutrophils with various inhibitors in the presence of S protein and compare their expression of calprotectin. Treatment with selective TLR4 inhibitor Resatorvid (TAK-242) abolished the enhanced production of S100a8 by *Dok3*$^{-/-}$ neutrophils (Figure 1F), whereas inhibition of other receptors involved in viral recognition, such as the cell surface ACE2 and TLR2, and the intracellular TLR7 and TLR9, had no effect on S100a8 expression (Supplementary Figure S2). These suggest that TLR4 signaling drives calprotectin production in *Dok3*$^{-/-}$ neutrophils. To verify if S protein can interact directly with TLR4, we perform co-immunoprecipitation (co-IP) studies with overexpressed TLR4 and SARS-CoV-2 S protein, and observed that both mouse and human TLR4 could interact with the S protein (Figure 1G). Endogenous co-IP using lysates from mouse bone marrow neutrophils also revealed interaction between TLR4 and SARS-CoV-2 S protein (Figure 1H). Moreover, TLR4 agonist lipopolysaccharide (LPS) also induced a significant increase in S100a8 levels in *Dok3*$^{-/-}$ neutrophils (Figures 1G, I). Collectively, these revealed that Dok3 inhibits neutrophil production of calprotectin during TLR4 sensing of SARS-CoV-2 S protein.

MD2 is a co-receptor of TLR4 involved in LPS sensing. To determine if MD2 plays a role during TLR4 sensing of SARS-CoV-2 S protein, we treated WT and *Dok3*$^{-/-}$ neutrophils with a MD2 inhibitor MD2-IN-1. Here, we observed that MD2 inhibition can abolish the enhanced production of S100a8 by *Dok3*$^{-/-}$ neutrophils (Figure 1J), suggesting that TLR4/MD2 complex is required for sensing of SARS-CoV-2 S protein in neutrophils.

Dok3 is not degraded upon TLR4 signaling in neutrophils

Activation of TLR4 signaling by LPS has been reported to induce Dok3 degradation in macrophages (22). To determine if Dok3 is also degraded upon TLR4 activation in neutrophils, we examined Dok3 protein expression in WT neutrophils upon stimulation with S protein or LPS. However, Dok3 expression in TLR4 ligands-stimulated neutrophils remained stable over time, unlike that in LPS-treated macrophages (Supplementary Figure S3). This suggest that Dok3 in neutrophils might function in a distinct signaling pathway from macrophages downstream of TLR4.

Dok3 interacts with MyD88 to mediate its de-phosphorylation on Y257 in response to S protein

MyD88 is a central adaptor protein crucially involved in relaying signals downstream of TLR4 to initiate kinase-dependent signaling during innate immune responses. Recent clinical data suggest that increased expression of MyD88 is associated with the development of severe COVID-19 (23, 24). As such, we postulate that Dok3 may exert an effect on MyD88 during the regulation of TLR4-dependent calprotectin production. To examine possible interactions between Dok3 and MyD88, we overexpressed Dok3 and MyD88 in HEK293T cells, and observed that Dok3 co-IP with MyD88, suggesting an interaction between the two molecules (Figure 2A). Similarly, co-IP experiment using cell lysates from mouse bone marrow neutrophils revealed that Dok3 and MyD88 form a complex endogenously (Figure 2B). Hence, Dok3 is likely to suppress calprotectin production in neutrophils through a MyD88-dependent mechanism.

Dok3 is a non-catalytic adaptor molecule which controls post-translational regulation by directing various enzymes to their target proteins downstream of immuno-receptors (15, 16). A recent study demonstrated that the activity of MyD88 can be regulated post-translationally *via* phosphorylation of tyrosine residues (25). Indeed, we observed that loss of Dok3 led to elevated phosphorylation of MyD88 at Y257 in *Dok3*$^{-/-}$ as compared to WT neutrophils upon stimulation with S protein, indicating that Dok3 mediates the de-phosphorylation of MyD88 in response to SARS-CoV-2 S protein stimulation (Figure 2C).

MyD88 Y257 phosphorylation controls JAK2-STAT3-calprotectin signaling in response to S protein

To delineate the functional role of MyD88 Y257 phosphorylation, we investigated NF-kB and MAPK signaling pathways downstream of MyD88 which are involved in the regulation of inflammatory cytokine production during SARS-CoV-2 infection (24). However, no difference in Erk, NF-kB and p38 activation were observed, and the transcription of inflammatory cytokine genes such as *il1b*, *il6* and *tnfa* were comparable between WT and *Dok3*$^{-/-}$ neutrophils (Supplementary Figures S4A, B). We next examined JAK2-STAT3 signaling which was previously implicated in calprotectin production in *Dok3*$^{-/-}$ colonic neutrophils (26), and detected higher levels of phospho-JAK2 (Y1007/1008) (Figures 2, D, E) and its downstream target, phospho-STAT3 (Y705) (Figures 2F, G), in *Dok3*$^{-/-}$ neutrophils upon stimulation with S protein. On the other hand, phosphorylation of STAT3 at inactivating residue S727 remains unaffected (Supplementary Figure S4C).

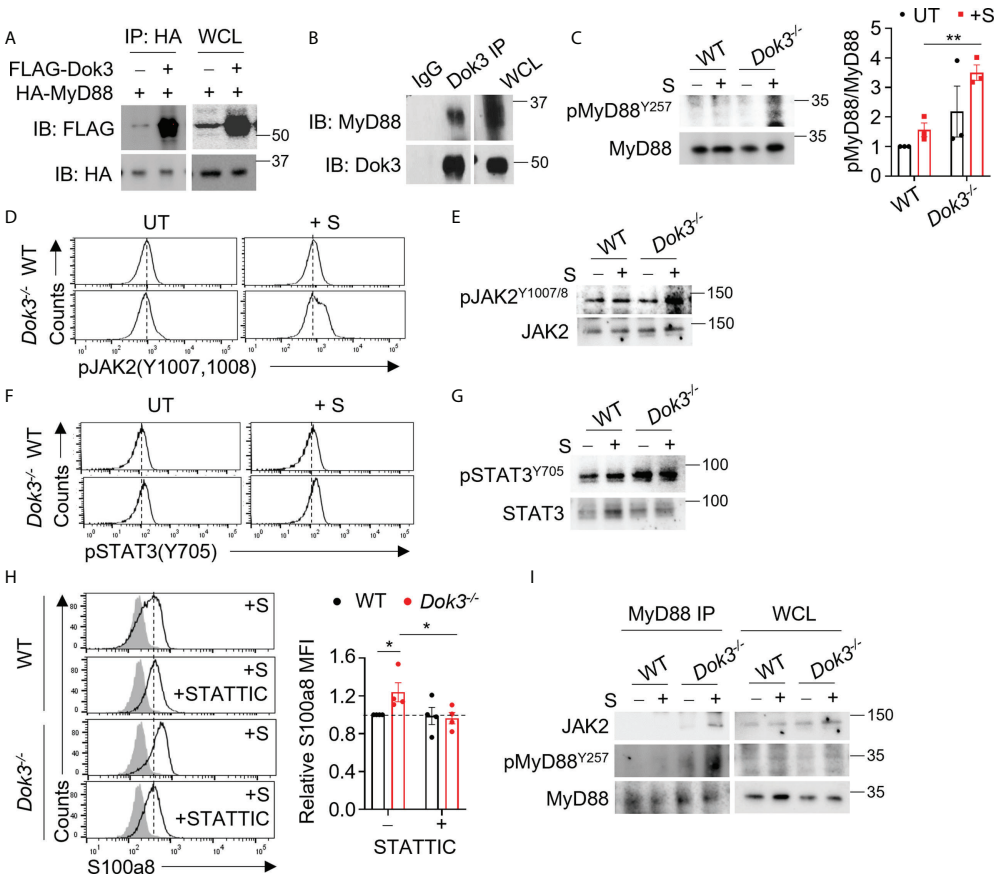

FIGURE 2
Dok3 mediates de-phosphorylation of MyD88 Y257 and suppression of JAK2-STAT3 signaling in response to SARS-CoV-2 S protein stimulation. **(A)** HEK293T cells were transfected with HA-tagged MyD88 and FLAG-tagged Dok3. Cell lysates were IP with anti-HA antibody. Precipitates and WCL were immunoblotted with anti-HA and anti-FLAG antibodies. Data shown are representative of 3 independent experiments. **(B)** Cell lysates from WT neutrophils were IP with anti-Dok3 or IgG control. Precipitates and WCL were probed for Dok3 and MyD88. Data shown are representative of 3 independent experiments. **(C)** Immunoblot analyses of pMyD88(Y257) and total MyD88 in WT and *Dok3*$^{-/-}$ neutrophils treated with or without S protein for 15 mins. Data shown are representative of 3 independent experiments. Bar graph depicts quantification of pMyD88/MyD88 signals from immunoblot. **p = 0.005, unpaired two-tailed Student's t-test. (D, F) Flow cytometric analyses of **(D)** pJAK2 (Y1007,1008) and **(F)** pSTAT3(Y705) in WT and *Dok3*$^{-/-}$ neutrophils treated with or without S protein for 3h. Histograms were pre-gated on singlet, Ly6G^{+} cells. Data shown are representative of 3 independent experiments (n = 3). (E, G), Immunoblot analyses of **(E)** pJAK2(Y1007,1008), total JAK2, **(G)** pSTAT3(Y705) and total STAT3 in WT and *Dok3*$^{-/-}$ neutrophils treated with or without S protein for 15 mins. Data shown are representative of 3 independent experiments. **(H)** Flow cytometric analysis of S100a8 expression in WT and *Dok3*$^{-/-}$ neutrophils following 3h stimulation with S protein in the presence or absence of STATTIC. Histograms were pre-gated on singlet, Ly6G^{+} cells. Filled histogram represents isotype control. Bar graph depicting MFI of S100a8 fluorescence relative to untreated WT neutrophils. Data is shown as mean ± S.E.M. (n = 4, 4 independent experiments). *p = 0.05, unpaired two-tailed Student's t-test. **(I)** Co-IP analysis of WCL from WT and *Dok3*$^{-/-}$ neutrophils treated with or without S protein for 15 mins, and IP with anti-MyD88. Precipitates and WCL were probed for JAK2, pMyD88(Y257) and MyD88. Data shown are representative of 3 independent experiments.

In addition, treatment with a selective STAT3 inhibitor, STATTIC, was able to block S100a8 upregulation in *Dok3*$^{-/-}$ neutrophils efficiently in the presence of S protein (Figure 2H), thus validating the direct involvement of JAK2-STAT3 pathway in calprotectin production. Previous studies revealed that JAK2 can be activated *via* direct association with the TLR4-MyD88 complex during LPS signaling (27), but how this complex formation is being regulated remains unknown. Since the highly phylogenetically conserved Y^{257}KXM motif in MyD88 is a putative SH2 binding site (28), we investigated if phosphorylation of MyD88 at Y257 can regulate JAK2 binding with MyD88. To this end, we performed an endogenous co-IP in neutrophil cell lysates with anti-MyD88 antibody, and found an increased association of JAK2 with MyD88 in *Dok3*$^{-/-}$ neutrophils, and these MyD88 molecules were more highly phosphorylated on Y257 than those in WT neutrophils (Figure 2I). Collectively, these data indicate that Y257 phosphorylation on MyD88 acts as a molecular switch to turn on downstream JAK2-STAT3 signaling for calprotectin production upon TLR4 recognition of SARS-CoV-2 S protein.

Dok3 recruits SHP-2 to de-phosphorylate MyD88 in response to S protein

Since Dok3 is an adaptor protein which lacks intrinsic catalytic activity, we postulate that it could act as a scaffold to recruit a protein tyrosine phosphatase (PTP) to mediate the de-phosphorylation of MyD88 at Y257. SH2 domain-containing protein tyrosine phosphatase-2 (SHP-2) is a PTP highly expressed in hematopoietic cells. To examine possible interactions among Dok3, SHP-2 and MyD88, we overexpress them in HEK293T cells, and observed that Dok3 interacts with MyD88, while SHP-2 co-IP with MyD88 only in the presence of Dok3 (Figure 3A). These data indicate that Dok3 is required to bridge the interaction between SHP-2 and MyD88.

Dok3 is a multidomain adaptor protein containing a N-terminal PH, a central PTB and C-terminal tyrosine-rich SH2 domain (Figure 3B). To further characterize the interaction between Dok3, MyD88 and SHP-2, we overexpressed variants of Dok3 bearing specific domains together with MyD88 or SHP-2 and examined their physical associations *via* co-IP experiments. We observed that MyD88 can co-IP with full-length Dok3 as well as the truncated variant bearing the PH domain of Dok3 (Figure 3C). Similarly, SHP-2 was observed to bind full-length Dok3 and the variant bearing the PH domain of Dok3 (Figure 3D). Hence, Dok3 interacts with both MyD88 and SHP-2 *via* its N-terminal PH domain.

To determine the role of SHP-2 in the de-phosphorylation of MyD88, we treated WT neutrophils with SHP-2 inhibitor PHPS1, and observed a dose-dependent increase in Y257 phosphorylation on MyD88, thus confirming that SHP-2 can act specifically on MyD88 (Figure 3E). Moreover, PHPS1 treatment enhances JAK2 association with MyD88 and results in an increased S100a8 and S100a9 production by WT neutrophils in a dose-dependent manner

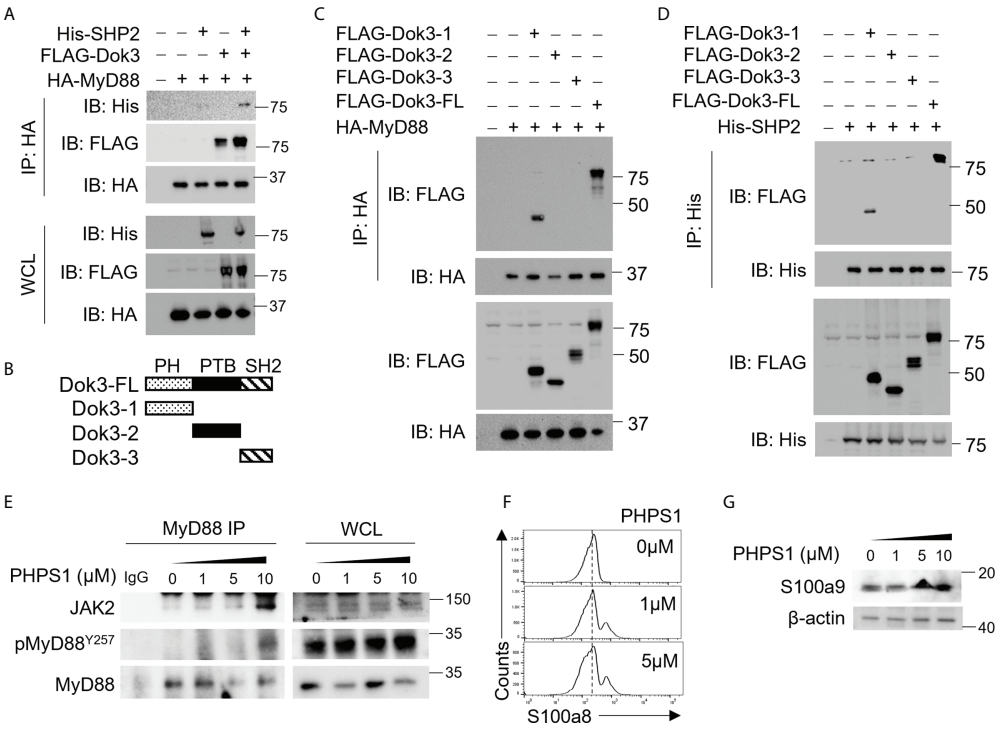

FIGURE 3
Dok3 recruits SHP-2 to de-phosphorylate MyD88 at Y257 in response to SARS-CoV-2 S protein engagement. **(A)** HEK293T cells were transfected with HA-tagged MyD88, FLAG-tagged Dok3 and His-tagged SHP-2. Cell lysates were IP with anti-HA antibody. Precipitates and WCL were immunoblotted with anti-HA, anti-FLAG and anti-His antibodies. Data shown are representative of 3 independent experiments. **(B)** Diagram depicting Dok3 full-length protein and truncation variants bearing individual PH, PTB, and SH2 domains. **(C)** HEK293T cells were transfected with HA-tagged MyD88 and FLAG-tagged Dok3 or its truncation variants. Cell lysates were IP with anti-HA antibody. Precipitates and WCL were immunoblotted with anti-HA and anti-FLAG antibodies. **(D)** HEK293T cells were transfected with His-tagged SHP-2 and FLAG-tagged Dok3 or its truncation variants. Cell lysates were IP with anti-His antibody. Precipitates and WCL were immunoblotted with anti-His and anti-FLAG antibodies. Data shown are representative of 3 independent experiments. **(E, F)** WT neutrophils were treated with increasing dosages of PHPS1 in the presence of S protein. **(E)** WCL were IP with anti-MyD88. Precipitates and WCL were probed for JAK2, pMyD88(Y257) and MyD88. Data shown are representative of 3 independent experiments. **(F)** Flow cytometric analysis of S100a8 expression in WT neutrophils following PHPS1 treatment. Histograms were pre-gated on singlet, Ly6G$^+$ cells. **(G)** Immunoblot analysis of S100a9 expression in WT neutrophils following PHPS1 treatment. Data shown are representative of 3 independent experiments.

upon stimulation with the S protein (Figures 3E-G). We further showed that phosphorylation of SHP-2 on Y580 (Supplementary Figure S5), and hence its activity, is not affected by loss of Dok3, implying that altered SHP-2 activity is unlikely to be responsible for enhanced MyD88 Y257 phosphorylation in the absence of Dok3. Taken together, our results suggest that Dok3 is required to recruit SHP-2 to de-phosphorylate Y257 on MyD88 for the suppression of calprotectin production during SARS-CoV-2 infection.

Fedratinib and Momelotinib suppress S100a8 production by neutrophils in response to SARS-CoV-2 S protein

JAK inhibitors have been proposed as therapy for severe COVID-19 patients on the basis that JAKs are important mediators in the cytokine storm (29–31). However, whether these inhibitors can modulate calprotectin levels to improve COVID-19 outcome remains unknown. To this end, we treated WT and *Dok3*$^{-/-}$ neutrophils with clinically approved JAK2 and STAT3 inhibitors, including Ruxolitinib, Baricitinib, Fedratinib, Momelotinib and Atovaquone, in the presence of S protein. Among them, we observed that Fedratinib and Momelotinib were able to significantly reduce S100a8 expression by *Dok3*$^{-/-}$ neutrophils to WT levels (Figure 4A), suggesting that these 2 inhibitors can efficiently block the JAK2-STAT3 signaling pathway downstream of Dok3 to prevent aberrant release of calprotectin in response to SARS-CoV-2 S protein.

To further examine the relevance of our study in human context, we stimulated human neutrophils isolated from peripheral blood of healthy donors with the S protein of SARS-CoV-2. In line with our mouse data, we do not

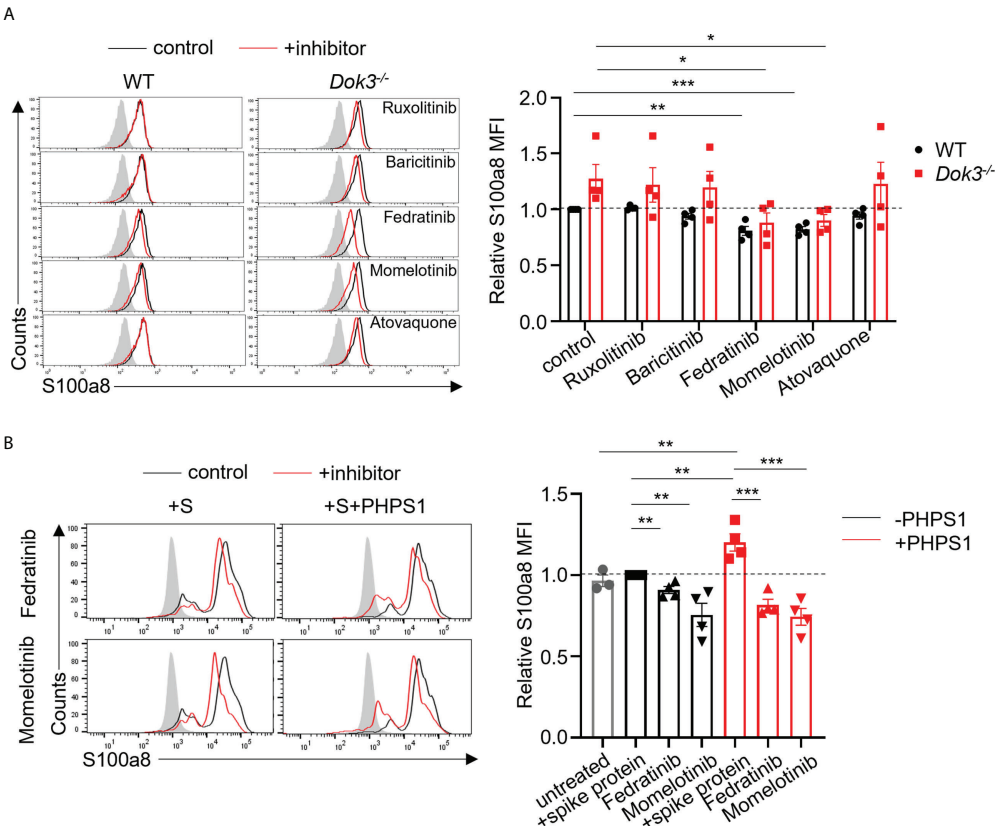

FIGURE 4
Fedratinib and Momelotinib suppress S100a8 expression in mouse and human neutrophils. **(A)** Flow cytometric analysis of S100a8 expression in WT and *Dok3*$^{-/-}$ neutrophils following 3h stimulation with S protein in the presence or absence of indicated inhibitors. Histograms were pre-gated on singlet, Ly6G^{+} cells. Filled histogram represents isotype control. The same control histogram is shown for different inhibitor treatments. Bar graph depicting MFI of S100a8 fluorescence relative to control WT neutrophils. Data is shown as mean ± S.E.M. (n = 4, 4 independent experiments). *p = 0.04, 0.03, **p = 0.003, ***p = 0.0004, unpaired two-tailed Student's t-test. **(B)** Flow cytometric analysis of S100a8 expression in purified human neutrophils following 3h stimulation with S protein in the presence or absence of indicated inhibitors. Filled histogram represents isotype control. The same control histogram is shown for different inhibitor treatments. Bar graph depicting MFI of S100a8 fluorescence relative to S protein-treated WT neutrophils. Data is shown as mean ± S.E.M. (n = 4, 4 independent experiments). **p = 0.01, 0.006, 0.01, 0.008, ***p = 0.0009, 0.0008, unpaired two-tailed Student's t-test.

see an induction of S100a8 by human neutrophils in response to S protein (Figure 4B). This is also consistent with clinical data which shows that plasma calprotectin levels in COVID-19 patients with mild disease are not elevated as compared to healthy controls (8). Consequently, Fedratinib and Momelotinib treatment only resulted in a minor decrease in S100a8 level (Figure 4B). Since our earlier findings indicated that SHP-2 negatively regulates calprotectin production through de-phosphorylating MyD88, we treated human neutrophils with PHPS1 and observed a significant increase in S100a8 production. Moreover, Fedratinib and Momelotinib can block PHPS1-induced S100a8 production (Figure 4B), further confirming that JAK2 functions downstream of SHP-2 during calprotectin production. Together, these findings provide a rationale for the use of JAK2 inhibitors Fedratinib and Momelotinib to treat severe COVID-19 patients since they can attenuate calprotectin production in neutrophils.

SARS-CoV-2 Delta and Omicron variant S proteins bind TLR4 to trigger calprotectin release in the absence of Dok3

The SARS-CoV-2 Delta (B.1.617.2) and Omicron (B.1.1.529) variants harbor distinct amino acid mutations in their S proteins which result in the evasion of host immune responses. As such, we evaluate if these variant S proteins are able to trigger TLR4 signaling in neutrophils by performing co-IP experiments using overexpressed or endogenous TLR4 and Delta or Omicron variant S protein. Interestingly, both Delta and Omicron variant S proteins retained their ability to bind mouse and human TLR4 (Figures 5A–D), and this resulted in an enhanced production of S100a8 and S100a9 by *Dok3*$^{-/-}$ as compared to WT neutrophils (Figures 5E, F). Together, these show that likewise to WT SARS-CoV-2, both Delta and Omicron variant S proteins can activate TLR4-driven calprotectin production in *Dok3*$^{-/-}$ neutrophils.

Discussion

During SARS-CoV-2 infection, aberrant production of calprotectin by neutrophils has been linked to the development of severe COVID-19 (8, 9, 11). Our study revealed that Dok3 plays an essential role in restraining neutrophil production of calprotectin upon binding of SARS-CoV-2 S protein to TLR4. In the absence of Dok3, S protein-mediated TLR4 signaling results in the hyper-phosphorylation of Y257 on MyD88, leading to enhanced JAK2-STAT3 signaling and a resultant calprotectin burst in the neutrophils (Figure 6).

Calprotectin are stable heterodimers of S100a8 and S100a9 involved in neutrophil-mediated inflammatory processes. Given that calprotectin levels are associated with hyperinflammation and poor clinical outcomes in COVID-19 patients, dissecting the molecular mechanism underlying their regulation will be of great significance and contribute towards the identification of potential therapeutic targets for COVID-19 treatments. In our study, we demonstrated for the first time that calprotectin expression in neutrophils is regulated *via* TLR4 pathway in response to SARS-CoV-2 S protein. In WT cells, S100a8 production is generally suppressed upon TLR4 activation, analogous to clinical studies which show that circulating calprotectin levels remain low in majority of the COVID-19 patients who are asymptomatic or have mild symptoms. In this case, Dok3 recruits SHP-2 to maintain MyD88 Y257 in a de-phosphorylated state, thereby dampening downstream JAK2-STAT3 signaling to prevent excessive release of calprotectin. However, in the absence of Dok3, sensing of S protein by TLR4 promotes increased phosphorylation of MyD88 on Y257. This enhances its association with JAK2 and subsequently turns on downstream JAK2/STAT3 signaling, resulting in hyper-production of calprotectin and an uncontrolled inflammation in the host. Collectively, our findings revealed that Dok3 plays a critical role in the negative regulation of TLR4-MyD88-JAK2-STAT3 axis in neutrophils during SARS-CoV-2 infection for the suppression of calprotectin production, and the increased Dok3 levels detected in neutrophils of severe COVID-19 patients (17) could be a compensatory mechanism to blunt elevated calprotectin levels.

Hyperactivation of neutrophils have been implicated in the immunopathogenesis of COVID-19, in which aberrant NETs formation and enhanced calprotectin secretion are prominent features driving inflammation and tissue damage (32–34). Recent studies demonstrated that SARS-CoV-2 can stimulate neutrophils directly through the ACE2-TMPRSS2 axis to induce release of NETs, thus presenting a potential therapeutic approach to inhibit NETs and its associated devastating complications in severe COVID-19 patients (35). On the other hand, the mechanism governing calprotectin production by neutrophils remains poorly understood. A growing body of evidence suggests that the trimeric S protein of SARS-CoV-2 can interact with TLR4 to activate immune responses (18), and TLR4 signaling has recently been associated with calprotectin production during SARS-CoV-2 infection (13). In our study, we provided compelling evidence that calprotectin production is a tightly regulated process which is triggered upon TLR4 activation by S protein. In the absence of Dok3, calprotectin is robustly upregulated in neutrophils, and this increase is abrogated upon blockade of TLR4 signaling by Resatorvid. We further eliminated the contribution of ACE2 in the induction of calprotectin, since treatment with ACE2 inhibitor does not affect calprotectin production by *Dok3*$^{-/-}$ neutrophils, and murine ACE2 harbors differences in amino acids from human ACE2, and hence exhibits poor binding affinity for the S protein (36–38). Thus, our data indicate that SARS-CoV-2 S protein can be

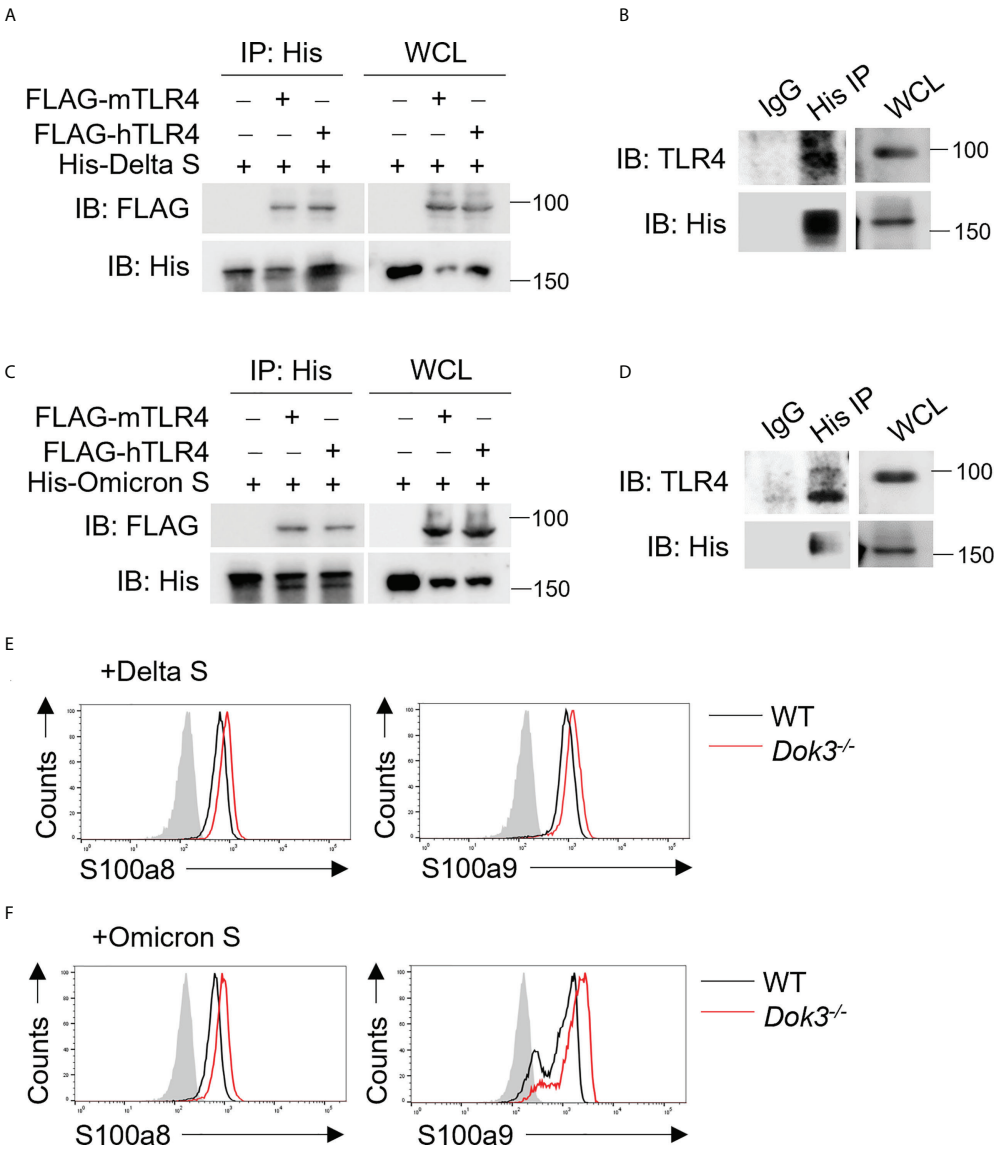

FIGURE 5
SARS-CoV-2 Delta and Omicron variant S proteins can activate TLR4 signaling. **(A, C)** HEK293T cells were transfected with FLAG-tagged mouse (m) or human (h) TLR4. Cell lysates were incubated with His-tagged S protein derived from **(A)** Delta or **(C)** Omicron variant and IP with anti-His antibody overnight. Precipitates and WCL were immunoblotted with anti-FLAG and anti-His antibodies. Data shown are representative of 3 independent experiments. **(B, D)** WT neutrophils were incubated with His-tagged S protein derived from **(B)** Delta or **(D)** Omicron variant and cell lysates were IP with anti-His or IgG control. Precipitates and WCL were probed for TLR4 and His. Data shown are representative of 3 independent experiments. **(E, F)** Flow cytometric analysis of S100a8 and S100a9 expression in WT and *Dok3*$^{-/-}$ neutrophils following 3h stimulation with or without S protein from **(E)** Delta or **(F)** Omicron variant. Histograms were pre-gated on singlet, Ly6G^{+} cells. Filled histogram represents isotype control. Data shown are representative of 3 independent experiments.

sensed directly by TLR4 on neutrophils to regulate calprotectin expression. Consistent with this, it was reported that SARS-CoV-2 infection activates an anti-bacterial like immune response, which was originally proposed to be a result of calprotectin binding to TLR4 (13). Here, our findings suggest that the induction of anti-bacterial pathway genes could be a direct result of interaction between viral S protein and TLR4. We observed that treatment of *Dok3*$^{-/-}$ neutrophils with other TLR4 agonists of bacterial origin such as LPS and cecal bacteria similarly induced elevated levels of calprotectin (26). Hence, it is likely that SARS-CoV-2 is sensed by a TLR4-dependent manner analogous to bacteria, to turn on the production of classical anti-bacterial proteins S100a8 and S100a9 in neutrophils.

Currently, no specific treatment is available for COVID-19 patients, and drug repurposing is the most popular strategy adopted to accelerate drug development against a novel emerging pathogen like SARS-CoV-2. As hyperinflammation stemming from dysregulation of the immune system in response to SARS-CoV-2 may culminate into ARDS, thrombosis and multi-organ damage in severe COVID-19 patients, drugs which act to mitigate the cytokine storm are proposed to be beneficial. However, blockade of cytokines such as IL-6 only yield limited clinical success (39–42). On the other hand, calprotectin levels correlate strongly with COVID-19 severity (8, 9, 11), and inhibiting its function can improve disease outcome in preclinical models of SARS-CoV-2 infection (13). Moreover, the sustained release of calprotectin has been proposed to be a key contributor of hyperinflammation and cytokine storm, hence suggesting that targeting calprotectin production is an attractive strategy to alleviate severe COVID-19 manifestations. Here, we provided the first mechanistic study on the regulation of calprotectin production by neutrophils during SARS-CoV-2 infection, and presented several signaling molecules which can be targeted with currently available drugs to limit calprotectin release (Figure 6). Firstly, TLR4 inhibitors or antibodies can interfere with the recognition of S protein, thereby preventing the release of calprotectin. In addition, inhibitors of JAK2 and STAT3 can dampen calprotectin production, and we have demonstrated the efficacy of JAK2 inhibitors Fedratinib and Momelotinib in blocking S100a8 release in human neutrophils, thus providing a rationale for the repurposing of these clinically approved drugs for severe COVID-19. However, future preclinical animal models are warranted to investigate the *in vivo* potency and specificity of these drugs for treatment of COVID-19.

SARS-CoV-2 is continuously evolving, and several mutations have been detected in the S protein of Delta and Omicron variants which affected their binding affinities to ACE2 and weakened the neutralizing efficacy of therapeutic and vaccine-elicited antibodies (4–6). Surprisingly, we observed that mutations in S proteins of Delta and Omicron variants did not abolish their binding to TLR4, although we were unable to compare their affinities with respect to that of WT SARS-CoV-2. Given that the Delta and

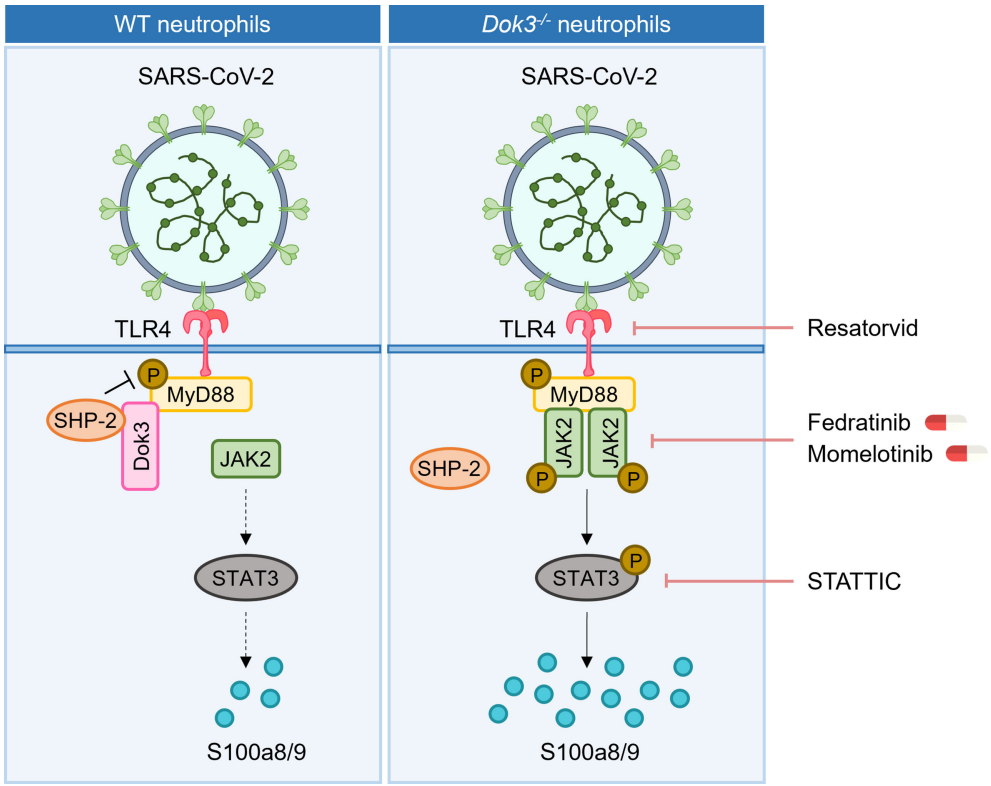

FIGURE 6
Proposed signaling mechanism underlying Dok3 negative regulation of calprotectin production in neutrophils. Binding of the SARS-CoV-2 S protein to TLR4 triggers phosphorylation of MyD88 on Y257. This activates downstream JAK2-STAT3 signaling cascade to turn on the production of calprotectin. Dok3 negatively regulates this pathway by recruiting SHP-2 to mediate the de-phosphorylation of MyD88, as such preventing excessive release of calprotectin which leads to uncontrolled inflammation associated with severe COVID-19. Treatment with TLR4 inhibitor Resatorvid and STAT3 inhibitor STATTIC, as well as clinically approved JAK inhibitors Fedratinib and Momelotinib, can dampen calprotectin production by neutrophils, revealing potential therapeutic targets to improve disease outcome in severe COVID-19 patients.

Omicron variants can elicit enhanced calprotectin production by *Dok3*$^{-/-}$ neutrophils through a TLR4-dependent manner, it is likely that therapeutic strategies which suppress calprotectin production by neutrophils may still be effective in preventing severe COVID-19 manifestations in patients infected with these variants. This is of paramount importance since extensive S protein mutations on the Omicron variant has severely compromised the efficacy of current vaccines and antibody therapies. As such, an immune-based treatment may be more effective in countering emergent variants as opposed to S protein-directed approaches. Moreover, recent study revealed that aberrant production of calprotectin by neutrophils is a common phenotype observed following coronavirus-induced zoonotic infection (13). Hence, the discovery of promising drug targets to suppress calprotectin production may be a milestone for future treatment of divergent coronavirus-infected patients.

In conclusion, our study identified a key immune signaling pathway involved in the regulation of calprotectin production by neutrophils in response to the S protein of SARS-CoV-2, and further revealed potential therapeutic molecules which can be targeted to dampen the over-expression of calprotectin associated with severe cases of COVID-19.

Materials and methods

Mice

C57BL/6 mice were purchased from The Jackson Laboratory. *Dok3*$^{-/-}$ mice were generated as described previously (43). *Dok3*$^{-/-}$ mice were backcrossed to C57BL/6 mice for more than 10 generations. Male and female mice were used at 8 to 10 weeks of age unless otherwise stated. All mice were maintained under specific pathogen-free conditions at A*STAR Biological Resource Centre (BRC).

Isolation of mouse neutrophils

Neutrophils were isolated from tibias and femurs of mice using EasySEP Mouse Neutrophil Enrichment Kit (Stem Cell Technologies). Purity of isolated cells was confirmed by flow cytometry. Cells were stimulated with 1μg/ml recombinant SARS-CoV-2 S protein (10549-CV, R&D Systems), B.1.617.2 S protein (10942-CV), B.1.1.529 S protein (SPN,C52Hz, Acro Biosystems) or LPS for indicated time periods.

Isolation of human neutrophils

Venous blood of healthy human donors was collected and diluted 1:1 in PBS before overlaying on Ficoll-Paque Plus (Cytiva). After density gradient centrifugation, the polymorphonuclear and erythrocyte-rich pellet was collected, and cells were treated with red blood cell lysis buffer for 15 min at room temperature. Cells were subsequently washed with PBS, and neutrophils obtained were resuspended in PBS and rested at 37°C for 1 h.

Inhibitors

Purified neutrophils were treated with the following inhibitors for 2-4 hours at 37°C: TAK-242 (HY-11109, MedChem Express), STATTIC (sc-202818, Santa Cruz Biotechnology Inc.), Ruxolitinib (HY-50856, MedChem Express), Baricitinib (HY-15315, MedChem Express), Fedratinib (HY-10409, MedChem Express), Momelotinib (HY-10961, MedChem Express), Atovaquone (HY-13832, MedChem Express), MLN-4760, C29 (HY-100461, MedChem Express) and AT791 (HY-124603, MedChem Express).

Flow cytometry

Cell suspensions were surface labelled with fluorochrome-conjugated antibodies for 10 minutes at 4°C in staining buffer (PBS containing 1% BSA). For phosphoprotein staining, cells were fixed and permeabilized using the Phosflow kit (BD) according to manufacturer's protocol before staining for 1 hour at room temperature. Data were acquired using LSRII (BD Biosciences) and analyzed using FlowJo software (Tree Star). The following antibodies were used for flow cytometry analysis: anti-CD45 APC/Cy7 (clone 30-F11; BioLegend), anti-Ly6G PE/biotin (clone 1A8; BD, BioLegend), anti-STAT3 (Y705) PE (clone 4/P-STAT3, BD Biosciences), anti-STAT3 (S727) PE (clone 49/P-STAT3, BD Biosciences), anti-pJAK2 (Y1007,1008) Alexa Fluor 647 (clone E132, abcam), anti-Erk1/2 (pT202/Yp204) PE (612593, BD Biosciences), anti-pIKKα/β (S176/180) PE (14938S, Cell Signaling Technology), anti-p-p38 (T180/Y182) FITC (612594, BD Biosciences), anti-S100a8 (clone E4F8V; Cell Signaling Technology), anti-S100a9 (clone D3U8M; Cell Signaling Technology), anti-pSHP2 (Y580) PE (MA5-28045, Invitrogen), goat anti-rabbit IgG (H+L) secondary antibody FITC (Invitrogen).

Intranasal S protein instillation and histology

20μg of S protein was administered intranasally to WT and *Dok3*$^{-/-}$ mice. PBS was used as a negative control. At 24h post-administration, lungs were harvested for flow cytometry analysis or fixed in 4% PFA overnight. For immunohistochemistry, lung sections were stained with anti-S100a8 (clone E4F8V; Cell

Signaling Technology), anti-S100a9 (clone D3U8M; Cell Signaling Technology), according to manufacturer's instructions.

Calprotectin ELISA

Neutrophils were stimulated with or without S protein in RPMI (Gibco), and cell culture medium was collected after 5 hours. The release of calprotectin into the supernatant was measured by ELISA (ab263885), according to the manufacturer's instructions.

Co-IP

For endogenous co-IP, purified neutrophils were stimulated with S protein for 15 minutes before lysis with cell lysis buffer (Cell Signaling Technology) containing protease and phosphatase inhibitors (Cell Signaling Technology). For overexpression studies, HEK293T cells were transfected with the plasmid overnight using lipofectamine (Invitrogen) before lysis with cell lysis buffer. Cell lysates were IP overnight using the indicated antibodies and pulled down using Protein A/G Plus Agarose beads (Santa Cruz Biotechnology Inc.): anti-His (clone H-3; Santa Cruz Biotechnology Inc.), anti-HA (clone F-7; Santa Cruz Biotechnology Inc.), anti-MyD88 (clone E-11; Santa Cruz Biotechnology Inc.), anti-Dok3 (clone H-5; Santa Cruz Biotechnology Inc.), anti-SHP-2 (clone B-1; Santa Cruz Biotechnology Inc.). Precipitates were analyzed by Western blotting according to standard protocol.

Western blotting

Cells were lysed with cell lysis buffer (Cell Signaling Technology) containing protease and phosphatase inhibitors (Cell Signaling Technology). Cell lysates were analyzed by Western blotting according to standard protocol using the indicated antibodies: anti-pSTAT3 (Y705) (clone D3A7; Cell Signaling Technology), anti-STAT3 (clone 79D7; Cell Signaling Technology), anti-pJAK2 (Y1007/1008) (3771S; Cell Signaling Technology), anti-JAK2 (clone C-10; Santa Cruz Biotechnology Inc.), anti-pMyD88 (Y257) (PA5-64835; Invitrogen), anti-MyD88 (clone E-11; Santa Cruz Biotechnology Inc.), anti-S100a8 (clone E4F8V; Cell Signaling Technology), anti-S100a9 (clone D3U8M; Cell Signaling Technology), anti-Dok3 (clone H-5; Santa Cruz Biotechnology Inc.), anti-β actin (clone C-4; Santa Cruz Biotechnology Inc.), anti-GAPDH (clone 1D4; Santa Cruz Biotechnology Inc.), peroxidase affinipure goat anti-rabbit IgG (H+L) (Jackson ImmunoResearch), m-IgGκ BP-HRP (Santa Cruz Biotechnology Inc.).

Quantitative PCR

Purified neutrophils were lysed with TRIzol (Life Technologies), and RNA was purified using phenol/chloroform extraction. Complementary DNA was reversed transcribed using RevertAid First Strand cDNA Synthesis Kit (Thermo Fisher Scientific). The following primers were used for real-time PCR using SYBR Green PCR Master Mix (Applied Biosystems): IL6 (forward): GAGGATACCACTCCCAACAGACC; IL6 (reverse): AAGTGCATCATCGTTGTTCATACA; IL1β (forward): CAACCAACAAGTGATATTCTCCATG; IL1β (reverse): GATCCACACTCTCCAGCTGCA; TNFα (forward): GCCTCTTCTCATTCCTGCTTG; TNFα (reverse): CTGATGAGAGGGAGGCCATT; β-actin (forward): AGATGACCCAGATCATGTTTGAGA; β-actin (reverse): CACAGCCTGGATGGCTACGTA.

Statistics

Figures and statistical analyses were generated using Graphpad Prism software. Mice were allocated to experimental groups based on genotypes and were randomized within their sex- and age-matched groups. No mouse was excluded from the analyses. Unpaired 2-tailed Student's *t* test was performed. A *P* value of less than 0.05 was considered significant.

Study approval

All mouse protocols were conducted in accordance with guidelines from and approved by the A*STAR BRC Institutional Animal Care and Use Committee. Human blood was obtained for research with approval from the Centralised Institutional Research Board of the Singapore Health Services in Singapore.

Data availability statement

The original contributions presented in the study are included in the article/Supplementary Material. Further inquiries can be directed to the corresponding authors.

Ethics statement

The studies involving human participants were reviewed and approved by Centralised Institutional Research Board of the Singapore Health Services in Singapore. Written informed consent for participation was not required for this study in

accordance with the national legislation and the institutional requirements. The animal study was reviewed and approved by A*STAR BRC Institutional Animal Care and Use Committee.

Author contributions

JTL and K-PL conceived and designed the study. JTL and JKHT performed experiments and generated *in vitro* and *in vivo* data which were analyzed and interpreted by JTL. JTL and K-PL wrote the manuscript. All authors reviewed and approved the manuscript.

Funding

This work is supported by the Singapore Ministry of Health's National Medical Research Council under its Open-Fund-Individual Research Grant (NMRC/OFIRG19may-0083) to K-PL and JTL, Open Fund-Young Individual Research Grant (NMRC/OFYIRG21nov-0035) to JTL and A*STAR core grant to K-PL.

Conflict of interest

The authors declare that the research was conducted in the absence of any commercial or financial relationships that could be construed as a potential conflict of interest.

Publisher's note

Supplementary material

The Supplementary Material for this article can be found online at: https://www.frontiersin.org/articles/10.3389/fimmu.2022.996637/full#supplementary-material

References

1. Reusch N, de Domenico E, Bonaguro L, Schulte-Schrepping J, Baßler K, Schultze JL, et al. Neutrophils in COVID-19. *Front Immunol* (2021) 12:652470. doi: 10.3389/fimmu.2021.652470

2. Eyre DW, Taylor D, Purver M, Chapman D, Fowler T, Pouwels KB, et al. Effect of covid-19 vaccination on transmission of alpha and delta variants. *New Engl J Med* (2022) 386:744–56. doi: 10.1056/NEJMoa2116597

3. Lipsitch M, Krammer F, Regev-Yochay G, Lustig Y, Balicer RD. SARS-CoV-2 breakthrough infections in vaccinated individuals: measurement, causes and impact. *Nat Rev Immunol* (2022) 22:57–65. doi: 10.1038/s41577-021-00662-4

4. Chen J, Wang R, Gilby NB, Wei G-W. Omicron variant (B.1.1.529): Infectivity, vaccine breakthrough, and antibody resistance. *J Chem Inf Model* (2022) 62:412–22. doi: 10.1021/acs.jcim.1c01451

5. Iketani S, Liu L, Guo Y, Liu L, Chan JF-W, Huang Y, et al. Antibody evasion properties of SARS-CoV-2 omicron sublineages. *Nature* (2022) 604:553–6. doi: 10.1038/s41586-022-04594-4

6. VanBlargan LA, Errico JM, Halfmann PJ, Zost SJ, Crowe JE, Purcell LA, et al. An infectious SARS-CoV-2 B.1.1.529 omicron virus escapes neutralization by therapeutic monoclonal antibodies. *Nat Med* (2022) 28:490–5. doi: 10.1038/s41591-021-01678-y

7. Mellett L, Khader SA. S100A8/A9 in COVID-19 pathogenesis: Impact on clinical outcomes. *Cytokine Growth Factor Rev* (2022) 63:90–7. doi: 10.1016/j.cytogfr.2021.10.004

8. Silvin A, Chapuis N, Dunsmore G, Goubet A-G, Dubuisson A, Derosa L, et al. Elevated calprotectin and abnormal myeloid cell subsets discriminate severe from mild COVID-19. *Cell* (2020) 182:1401–1418.e18. doi: 10.1016/j.cell.2020.08.002

9. Mahler M, Meroni P-L, Infantino M, Buhler KA, Fritzler MJ. Circulating calprotectin as a biomarker of COVID-19 severity. *Expert Rev Clin Immunol* (2021) 17:431–43. doi: 10.1080/1744666X.2021.1905526

10. Chen L, Long X, Xu Q, Tan J, Wang G, Cao Y, et al. Elevated serum levels of S100A8/A9 and HMGB1 at hospital admission are correlated with inferior clinical outcomes in COVID-19 patients. *Cell Mol Immunol* (2020) 17:992–4. doi: 10.1038/s41423-020-0492-x

11. Shrivastava S, Chelluboina S, Jedge P, Doke P, Palkar S, Mishra AC, et al. Elevated levels of neutrophil activated proteins, alpha-defensins (DEFA1), calprotectin (S100A8/A9) and myeloperoxidase (MPO) are associated with disease severity in COVID-19 patients. *Front Cell Infect Microbiol* (2021) 11:751232. doi: 10.3389/fcimb.2021.751232

12. Wang S, Song R, Wang Z, Jing Z, Wang S, Ma J. S100A8/A9 in inflammation. *Front Immunol* (2018) 9:1298. doi: 10.3389/fimmu.2018.01298

13. Guo Q, Zhao Y, Li J, Liu J, Yang X, Guo X, et al. Induction of alarmin S100A8/A9 mediates activation of aberrant neutrophils in the pathogenesis of COVID-19. *Cell Host Microbe* (2021) 29:222–235.e4. doi: 10.1016/j.chom.2020.12.016

14. Deguchi A, Yamamoto T, Shibata N, Maru Y. S100A8 may govern hyper-inflammation in severe COVID-19. *FASEB J* (2021) 35:e21798. doi: 10.1096/fj.202101013

15. Loh JT, Teo JKH, Lim H-H, Lam K-P. Emerging roles of downstream of kinase 3 in cell signaling. *Front Immunol* (2020) 11:566192. doi: 10.3389/fimmu.2020.566192

16. Loh JT, Xu S, Huo JX, Kim SS-Y, Wang Y, Lam K-P. Dok3-protein phosphatase 1 interaction attenuates Card9 signaling and neutrophil-dependent antifungal immunity. *J Clin Invest* (2019) 129:2717–29. doi: 10.1172/JCI126341

17. Aschenbrenner AC, Mouktaroudi M, Krämer B, Oestreich M, Antonakos N, Nuesch-Germano M, et al. Disease severity-specific neutrophil signatures in blood transcriptomes stratify COVID-19 patients. *Genome Med* (2021) 13:7. doi: 10.1186/s13073-020-00823-5

18. Zhao Y, Kuang M, Li J, Zhu L, Jia Z, Guo X, et al. SARS-CoV-2 spike protein interacts with and activates TLR41. *Cell Res* (2021) 31:818–20. doi: 10.1038/s41422-021-00495-9

19. Khan S, Shafiei MS, Longoria C, Schoggins JW, Savani RC, Zaki H. SARS-CoV-2 spike protein induces inflammation *via* TLR2-dependent activation of the NF-κB pathway. *Elife* (2021) 10:e68563. doi: 10.7554/eLife.68563

20. Shirato K, Kizaki T. SARS-CoV-2 spike protein S1 subunit induces pro-inflammatory responses *via* toll-like receptor 4 signaling in murine and human macrophages. *Heliyon* (2021) 7:e06187. doi: 10.1016/j.heliyon.2021.e06187

21. Lan J, Ge J, Yu J, Shan S, Zhou H, Fan S, et al. Structure of the SARS-CoV-2 spike receptor-binding domain bound to the ACE2 receptor. *Nature* (2020) 581:215–20. doi: 10.1038/s41586-020-2180-5

22. Peng Q, O'Loughlin JL, Humphrey MB. DOK3 negatively regulates LPS responses and endotoxin tolerance. *PloS One* (2012) 7:e39967. doi: 10.1371/journal.pone.0039967

23. Cuevas AM, Clark JM, Potter JJ. Increased TLR/MyD88 signaling in patients with obesity: is there a link to COVID-19 disease severity? *Int J Obes* (2021) 45:1152–4. doi: 10.1038/s41366-021-00768-8

24. Zheng M, Karki R, Williams EP, Yang D, Fitzpatrick E, Vogel P, et al. TLR2 senses the SARS-CoV-2 envelope protein to produce inflammatory cytokines. *Nat Immunol* (2021) 22:829–38. doi: 10.1038/s41590-021-00937-x

25. Gurung P, Fan G, Lukens JR, Vogel P, Tonks NK, Kanneganti T-D. Tyrosine kinase SYK licenses MyD88 adaptor protein to instigate IL-1α-Mediated inflammatory disease. *Immunity* (2017) 46:635–48. doi: 10.1016/j.immuni.2017.03.014

26. Loh JT, Lee K-G, Lee AP, Teo JKH, Lim HL, Kim SS-Y, et al. DOK3 maintains intestinal homeostasis by suppressing JAK2/STAT3 signaling and S100a8/9 production in neutrophils. *Cell Death Dis* (2021) 12:1054. doi: 10.1038/s41419-021-04357-5

27. Akihiro K, Tetsuji N, Tatsushi M, Osamu T, Shizuo A, Ichiro K, et al. Suppressor of cytokine signaling-1 selectively inhibits LPS-induced IL-6 production by regulating JAK–STAT. *Proc Natl Acad Sci* (2005) 102:17089–94. doi: 10.1073/pnas.0508517102

28. Gelman AE, LaRosa DF, Zhang J, Walsh PT, Choi Y, Sunyer JO, et al. The adaptor molecule MyD88 activates PI-3 kinase signaling in CD4+ T cells and enables CpG oligodeoxynucleotide-mediated costimulation. *Immunity* (2006) 25:783–93. doi: 10.1016/j.immuni.2006.08.023

29. Chen C, Wang J, Li H, Yuan L, Gale RP, Liang Y. JAK-inhibitors for coronavirus disease-2019 (COVID-19): a meta-analysis. *Leukemia* (2021) 35:2616–20. doi: 10.1038/s41375-021-01266-6

30. Zhang X, Shang L, Fan G, Gu X, Xu J, Wang Y, et al. The efficacy and safety of janus kinase inhibitors for patients with COVID-19: A living systematic review and meta-analysis. *Front Med* (2022) 8:800492. doi: 10.3389/fmed.2021.800492

31. Melikhov O, Kruglova T, Lytkina K, Melkonyan G, Prokhorovich E, Putsman G, et al. Use of janus kinase inhibitors in COVID-19: a prospective observational series in 522 individuals. *Ann Rheum Dis* (2021) 80:1245. doi: 10.1136/annrheumdis-2021-220049

32. Ackermann M, Anders H-J, Bilyy R, Bowlin GL, Daniel C, de Lorenzo R, et al. Patients with COVID-19: in the dark-NETs of neutrophils. *Cell Death Differ* (2021) 28:3125–39. doi: 10.1038/s41418-021-00805-z

33. Gillot C, Favresse J, Mullier F, Lecompte T, Dogné J-M, Douxfils J. NETosis and the immune system in COVID-19: Mechanisms and potential treatments. *Front Pharmacol* (2021) 12:708302. doi: 10.3389/fphar.2021.708302

34. Zuo Y, Yalavarthi S, Shi H, Gockman K, Zuo M, Madison JA, et al. Neutrophil extracellular traps (NETs) as markers of disease severity in COVID-19. *JCI Insight* (2020) 5(11):e138999. doi: 10.1172/jci.insight.138999

35. Veras FP, Pontelli MC, Silva CM, Toller-Kawahisa JE, de Lima M, Nascimento DC, et al. SARS-CoV-2–triggered neutrophil extracellular traps mediate COVID-19 pathologySARS-CoV-2 directly triggers ACE-dependent NETs. *J Exp Med* (2020) 217:e20201129. doi: 10.1084/jem.20201129

36. Chu H, Chan JF-W. A lethal mouse model using a mouse-adapted SARS-CoV-2 strain with enhanced binding to mouse ACE2 as an important platform for COVID-19 research. *EBioMedicine* (2021) 68. doi: 10.1016/j.ebiom.2021.103406

37. Winkler ES, Bailey AL, Kafai NM, Nair S, McCune BT, Yu J, et al. SARS-CoV-2 infection of human ACE2-transgenic mice causes severe lung inflammation and impaired function. *Nat Immunol* (2020) 21:1327–35. doi: 10.1038/s41590-020-0778-2

38. Dinnon KH, Leist SR, Schäfer A, Edwards CE, Martinez DR, Montgomery SA, et al. A mouse-adapted model of SARS-CoV-2 to test COVID-19 countermeasures. *Nature* (2020) 586:560–6. doi: 10.1038/s41586-020-2708-8

39. Hermine O, Mariette X, Tharaux P-L, Resche-Rigon M, Porcher R, Ravaud P. Group c-19 c. effect of tocilizumab vs usual care in adults hospitalized with COVID-19 and moderate or severe pneumonia: A randomized clinical trial. *JAMA Internal Med* (2021) 181:32–40. doi: 10.1001/jamainternmed.2020.6820

40. Salvarani C, Dolci G, Massari M, Merlo DF, Cavuto S, Savoldi L, et al. Effect of tocilizumab vs standard care on clinical worsening in patients hospitalized with COVID-19 pneumonia: A randomized clinical trial. *JAMA Internal Med* (2021) 181:24–31. doi: 10.1001/jamainternmed.2020.6615

41. Salama C, Han J, Yau L, Reiss WG, Kramer B, Neidhart JD, et al. Tocilizumab in patients hospitalized with covid-19 pneumonia. *New Engl J Med* (2020) 384:20–30. doi: 10.1056/NEJMoa2030340

42. Stone JH, Frigault MJ, Serling-Boyd NJ, Fernandes AD, Harvey L, Foulkes AS, et al. Efficacy of tocilizumab in patients hospitalized with covid-19. *New Engl J Med* (2020) 383:2333–44. doi: 10.1056/NEJMoa2028836

43. Ng C-H, Xu S, Lam K-P. Dok-3 plays a nonredundant role in negative regulation of b-cell activation. *Blood* (2007) 110:259–66. doi: 10.1182/blood-2006-10-055194

frontiers | Frontiers in Immunology

TYPE Original Research
PUBLISHED 19 December 2022
DOI 10.3389/fimmu.2022.1078741

OPEN ACCESS

EDITED BY
Lokesh Sharma,
Yale University, United States

REVIEWED BY
Shamik Majumdar,
National Institute of Allergy and Infectious Diseases (NIH), United States
Nandini Krishnamoorthy,
Brigham and Women's Hospital and Harvard Medical School, United States

*CORRESPONDENCE
Jean-Louis Mege
jean-louis.mege@univ-amu.fr

SPECIALTY SECTION
This article was submitted to Molecular Innate Immunity, a section of the journal Frontiers in Immunology

RECEIVED 24 October 2022
ACCEPTED 05 December 2022
PUBLISHED 19 December 2022

CITATION
Atmeh PA, Gay L, Levasseur A, La Scola B, Olive D, Mezouar S, Gorvel J-P and Mege J-L (2022) Macrophages and γδ T cells interplay during SARS-CoV-2 variants infection. *Front. Immunol.* 13:1078741. doi: 10.3389/fimmu.2022.1078741

Macrophages and γδ T cells interplay during SARS-CoV-2 variants infection

Perla Abou Atmeh[1,2], Laetitia Gay[1,2], Anthony Levasseur[1,2], Bernard La Scola[1,2], Daniel Olive[3], Soraya Mezouar[1,2], Jean-Pierre Gorvel[4] and Jean-Louis Mege[1,2,5]*

[1]Aix-Marseille Univ, Institut de Recherche pour le Développement (IRD), Assistance Publique Hopitaux de Marseille (APHM), Microbe Evolution, Phylogeny and Infection (MEPHI), Marseille, France, [2]Institut Hospitalo-Universitaire (IHU)-Méditerranée Infection, Marseille, France, [3]Institut Paoli-Calmettes; Aix-Marseille Univ, UM105, Centre National de la Recherche Scientifique (CNRS) UMR 7258, Marseille, France, [4]Aix-Marseille Univ, Centre National de la Recherche Scientifique (CNRS), Institut National de la Santé et de la Recherche Médicale (INSERM), Centre d'Immunologie de Marseille Luminy (CIML), Marseille, France, [5]Aix-Marseille Univ, Assitance Publique Hopitaux de Marseille (APHM), Hôpital de la Conception, Laboratoire d'Immunologie, Marseille, France

Introduction: The emergence of several SARS-CoV-2 variants during the COVID pandemic has revealed the impact of variant diversity on viral infectivity and host immune responses. While antibodies and CD8 T cells are essential to clear viral infection, the protective role of innate immunity including macrophages has been recognized. The aims of our study were to compare the infectivity of different SARS-CoV-2 variants in monocyte-derived macrophages (MDM) and to assess their activation profiles and the role of ACE2 (Angiotensin-converting enzyme 2), the main SARS-CoV-2 receptor. We also studied the ability of macrophages infected to affect other immune cells such as γδ2 T cells, another partner of innate immune response to viral infections.

Results: We showed that the SARS-CoV-2 variants α-B.1.1.7 (United Kingdom), β-B.1.351 (South Africa), γ-P.1 (Brazil), δ-B.1.617 (India) and B.1.1.529 (Omicron), infected MDM without replication, the γ-Brazil variant exhibiting increased infectivity for MDM. No clear polarization profile of SARS-CoV-2 variants-infected MDM was observed. The β-B.1.351 (South Africa) variant induced macrophage activation while B.1.1.529 (Omicron) was rather inhibitory. We observed that SARS-CoV-2 variants modulated ACE2 expression in MDM. In particular, the β-B.1.351 (South Africa) variant induced a higher expression of ACE2, related to MDM activation. Finally, all variants were able to activate γδ2 cells among which γ-P.1 (Brazil) and β-B.1.351 (South Africa) variants were the most efficient.

Conclusion: Our data show that SARS-CoV-2 variants can infect MDM and modulate their activation, which was correlated with the ACE2 expression. They also affect γδ2 T cell activation. The macrophage response to SARS-CoV-2 variants was stereotypical.

KEYWORDS

SARS-CoV-2 variants, macrophage, ACE2, γδ T cells, COVID-19

Introduction

Since its emergence in Wuhan (China) in December 2019, severe acute respiratory syndrome coronavirus 2 (SARS-CoV-2) caused COVID-19, a pandemic associated with a global health crisis and more than 6.3 million deaths to date (COVID Live - Coronavirus Statistics - Worldometer). SARS-CoV-2 infection may be asymptomatic or can exhibit mild to moderate respiratory disease associating respiratory and digestive symptoms and neurological abnormalities (1, 2). The patients with comorbidities at risk to develop severe illness expressing as acute respiratory distress syndrome characterized by lung injury, inflammation and pulmonary vascular leakage (3, 4). SARS-CoV-2 infection may be also responsible of long-term invalidating symptoms named post-COVID-19 syndrome (5).

The pathogenesis of SARS-CoV-2 infection has been largely imprinted by host immune response (6). Severe COVID-19 patients exhibit a lymphopenia and an impairment of T-cell mediated anti-viral immunity (7). In contrast, few severe patients experience a macrophage activation syndrome (MAS) (8), followed by respiratory and even multi-organ failure (9, 10); and a cytokine release syndrome (CRS) characterized by large amounts of pro-inflammatory cytokines like interleukin (IL)-1, IL-6, IL-8 and tumor necrosis factor (TNF).

Macrophages play a role in the physiopathology of COVID-19 as shown by histological examination of tissue sample from patients with severe symptoms (11, 12). The accumulation of macrophages in the alveolar lumen has been shown in a humanized mice model of SARS-CoV-2 expressing human angiotensin-converting enzyme 2 (ACE2) (13). In addition, post-mortem COVID-19 lung tissue showed an increased proportion of ACE2-positive cells, including a majority of inflammatory macrophages (14, 15). We previously reported that SARS-CoV-2 infects monocyte-derived macrophages (MDM) with abortive infection, similar to SARS-CoV-1 infection (16). According to their function in pathological conditions, macrophages are considered as activated or alternatively activated also referred to as M1 and M2 polarization phenotype, respectively. We showed that SARS-CoV-2 elicited a transcriptional program associating inflammatory and anti-inflammatory genes in macrophages, which shifted to an anti-inflammatory program of M2 type (16). However, there is not a consensus regarding the activation status of macrophages during SARS-CoV-2 infection. Some studies reported a pro-inflammatory response to viruses (17, 18), while others a lack of macrophage activation (19, 20). We still ignore if the activation status of macrophages *in vivo* results from a cytokine-mediated bystander effect or a direct effect of SARS-CoV-2 including its variants.

During the course of COVID-19, the action of the immune system favors SARS-CoV-2 acquiring mutations notably in the virus Spike (S) protein (21). The World Health organization has classified variants into classes: Variants Being Monitored (VBM), Variants of Interest (VOI) and Variants of Concern (VOC). The least hazardous strains are classified as VBM, while VOI are variants that present a possible risk to public health. Finally, VOC are mutated strains of the Wuhan strain that have increased transmissibility, higher disease progression, severity and mortality. In addition, VOC show a decreased susceptibility to vaccine/infection-induced immune responses but they have the ability to reinfect previously infected and recovered individuals. Five SARS-CoV-2 lineages are designated as the VOC: α-B.1.1.7 (United Kingdom), β-B.1.351 (South Africa), γ-P.1 (Brazil), δ-B.1.617 (India) and B.1.1.529 (Omicron) (22, 23).

Here, we investigated the infection and the inflammatory response of MDM in response to Wuhan strain and 5 variants of concern, compared to Vero E6 cell line as the reference model in the study of SARS-CoV-2 infection (24). We also studied the interaction of macrophages infected with other immune cells such as γδ2 T cells, partners of the innate immune response to viral infections. Indeed, previous studies have highlighted the role of γδ2 T cells during SARS-CoV-2 infection (25, 26). We recently demonstrated that activation of γδ2 T cells leads to inhibition of SARS-CoV-2 replication in co-cultures of MDM infected with γδ2 T cells (27). Our data showed that SARS-CoV-2 variants infected MDM and modulated their activation program, which is correlated with ACE2 expression. γδ2 T cell were also found activated. Our study reveals that the macrophages respond to the infection but this one remains stereotypical without specific response against SARS-CoV-2 variants.

Materials and methods

Cell culture and infection

Vero E6 (African green monkey kidney, American Type Culture Collection (ATCC® CRL-1586™) cell line was cultured using Minimum Essential Media (MEM, Life Technologies, Carlsbad, CA, USA) supplemented with 10% or 4% fetal bovine serum (FBS, Gibco, Life technologies) and 100 U/mL penicillin and 50 µg/mL streptomycin (Life Technologies).

Blood samples (leucopacks) come from the French Blood Establishment (Etablissement français du sang, EFS) that carries out donor inclusions, informed consent and sample collection. Through a convention established between our laboratory and the EFS (N°7828), buffy coats were obtained and peripheral blood mononuclear cells (PBMC) were isolated as previously described (28). Monocytes were purified from PBMC using anti-CD14-conjugated magnetic beads (Miltenyi Biotec, Bergisch Glabach, Germany) and cultured in Roswell Park Memorial Institute-1640 medium (RPMI, Life Technologies) containing 10% FBS, 2 mM L-glutamine, 100 U/mL penicillin and 50 µg/mL

streptomycin. Macrophages derived from monocytes (MDM) were cultured in RPMI-1640 containing 10% inactivated human AB-serum (MP Biomedicals, Solon, OH, USA), 2 mM glutamine, 100 U/mL penicillin and 50 µg/mL streptomycin for 3 days. Then, the medium was replaced by RPMI-1640 containing 10% FBS and 2 mM glutamine, and cells were differentiated into macrophages for 4 additional days.

γδ2 T cells were expanded from fresh PBMCs as previously described (29, 30). Briefly, PBMCs were cultured in RPMI-1640 medium supplemented with 10% FBS, interleukin-2 (IL-2, 200 UI/ml) and Zoledronic acid monohydrate (to a final concentration of 1 µM). IL-2 was added every 2 days beginning on day 5 for 12 days and the purity of the γδ2 T cells was assessed by flow cytometry analysis (>85%) and then frozen at -80°C in 10% dimethyl sulfoxide (Sigma-Aldrich, Saint-Quentin-Fallavier, France) and 90% FBS.

MDM and Vero E6 cells were infected with 20 µl virus suspension at a multiplicity of infection (MOI) of 0.1 for 6, 24, 48 and 72 hours at 37°C in the presence of 5% CO2 and 95% air in a humidified incubator.

SARS-CoV-2 variant production

SARS-CoV-2 strains, including Wuhan-SARS-CoV-2 (from initial outbreak), α-B.1.1.7 (United Kingdom), β-B.1.351 (South Africa), γ-P.1 (Brazil), δ-B.1.617 (India) and B.1.1.529 (Omicron) was obtained after Vero E6 cells (ATCC® CRL-1586™) infection in MEM supplemented with 4% FBS (31) and virus titration using the median tissue culture infectious dose (TCID50) method. All virus strains were stored at -80°C.

Viral RNA extraction and q-RTPCR

Viral RNA was extracted using NucleoSpin® Viral RNA Isolation kit (Macherey-Nagel, Hoerdt, France). Virus detection was performed using One-Step RT-PCR SuperScript™ III Platinum™ (Life Technologies). Thermal cycling was achieved at 55°C for 10 minutes for reverse transcription, pursued by 95°C for 3 minutes and then 45 cycles at 95°C for 15 seconds and 58°C for 30 seconds using a LightCycler 480 Real-Time PCR system (Roche, Rotkreuz, Switzerland). We investigated the N gene for the detection of SARS-CoV-2 as previously described (Table 1) (32).

RNA isolation and q-RTPCR

Total RNA was extracted from MDM (1.10^6 cells/well) using the RNA extraction Kit (ZYMO Research) with DNase I treatment to eliminate DNA contaminants as previously described (33). The extracted RNAs were evaluated using a NanoDrop spectrophotometer (Nanodrop Technologies, Wilmington, DE, USA). Reverse transcription of isolated RNA was performed using a Moloney murine leukemia virus-reverse transcriptase kit (Life Technologies) and oligo(dT) primers. Real time q-PCR was performed using Smart SYBR Green fast Master kit (Roche Diagnostics, Meylan, France) and specific primers (Table 2). Results were normalized using the housekeeping endogenous control *ACTB* gene and were expressed in fold change: $2^{-\Delta\Delta Ct}$ with $\Delta\Delta Ct = \Delta Ct_{Infected} - \Delta Ct_{Uninfected}$.

Cell viability

Cell viability was evaluated using the 3-[4,5-dimethylthiazol-2-yl]-2,5 diphenyl tetrazolium bromide (MTT) assay. After a 24, 48 and 72 hours of SARS-CoV-2 stimulation, 10 µl of MTT (5 mg/ml, Sigma-Aldrich) were added to the cell cultures and incubated at 37°C for 4 hours. The formed formazan crystals were solubilized with 50 µl of dimethylsulphoxide (DMSO) for 30 minutes at 37°C and quantified using a Synergy MxF plate reader at 540 nm (Biotek Instruments, Winooski, VT, USA).

Immunofluorescence

MDM and Vero E6 cells (5.10^5 cells/well) cultured into a 24-well plate containing a glass coverslip were fixed with 4% paraformaldehyde at 4°C for 20 minutes and then permeabilized with 0.1% Triton X-100 in phosphate-buffered saline (PBS) for 3 minutes. Permeabilized cells were incubated with blocking buffer (3% bovine serum albumin diluted in PBS) for 30 minutes and then with primary SARS/SARS-CoV-2 Coronavirus Spike Protein (subunit 1) (1:250, Life Technologies) and ACE2 (1:250, R&D systems, Minneapolis, MN, USA) antibodies for 1 hour. Coverslips were then washed three times with PBS and incubated for 30 minutes at room temperature with secondary antibodies: anti-rabbit Alexa Fluor 633 and anti-mouse Alexa Fluor 488 (1:1000, Invitrogen). Phalloïdin-647 (1:250) and 4',6-diamidino-2-phenylindole (DAPI, 1:250) were also added to reveal F-actin and

TABLE 1 SARS-CoV-2 Nucleocapsid primers and probe.

	Forward primer (5'-3')	Reverse primer (5'-3')
N gene primers	GACCCCAAAATCAGCGAAAT	TCTGGTTACTGCCAGTTGAATCTG
N gene probe	5' FAM-ACCCCGCATTACGTTTGGTGGACC 3'	

TABLE 2 List of primers used for q-RTPCR.

Gene	Forward primer (5′-3′)	Reverse primer (5′-3′)
ACTB	GGAAATCGTGCGTGACATTA	AGGAGGAAGGCTGGAAGAG
TNF	AGGAGAAGAGGCTGAGGAACAAG	GAGGGAGAGAAGCAACTACAGACC
IL1B	CAGCACCTCTCAAGCAGAAAAC	GTTGGGCATTGGTGTAGACAAC
IL6	CCAGGAGAAGATTCCAAAGATG	GGAAGGTTCAGGTTGTTTTCTG
TGFB	GACATCAAAAGATAACCACTC	TCTATGACAAGTTCAAGCAGA
IL10	GGGGGTTGAGGTATCAGAGGTAA	GCTCCAAGAGAAAGGCATCTACA
IFNB	ACAACCTCCCAGGCACAAGGGCTGTATTT	TGATGGCAACCAGTTCCAGAAGGCTCAAG
NOS2	GACTTTCCAAGACACACTTCACC	CTATCTCCTTTGTTACCGCTTCC
IL1R2	CACTCAGGTCAGGGCATACTAA	AGGAGAAGAAGAGACACGGATG
MR	CTTTCATCACCACACAATCCTC	ACCTCACAAGTATCCACACCATC

nuclei, respectively. An LSM800 Airyscan confocal microscope (Zeiss, Germany) with a 63x oil objective was used. Relative ACE2 expression was quantified by fluorescence with ImageJ software (National Institutes of Health, Bethesda, MD, USA). Relative percentage of ACE2 fluorescence was reported to DAPI fluorescence.

Immunoassays

Cytokine release was evaluated from supernatants of infected MDMs at 24 and 48 hours post-infection. Tumor necrosis factor TNF-α, interleukin IL-10, IL-1β (R&D Systems), and IL-6 (CliniSciences, Montrouge, France) were quantified according to the manufacturer's recommendations. The sensitivity was (pg/ml): 5.5 for TNF-α, 3.9 for IL-10, 0.125 for IL-1β, and 15.4 for IL-6.

Flow cytometry

Cells (1.10^6 cells/well) were suspended in PBS containing 5% FBS and 2mM EDTA (Sigma-Aldrich). Suspended cells were incubated with viability dye (Live/Dead Near IR, Invitrogen), CD14-FITC, anti-ACE-2-PE or appropriate isotype control (Miltenyi) for 30 minutes at 4°C. Labelled cells were then permeabilized using BD Cytofix/Cytoperm kit and stained with CD68-PE-Cy7 (Miltenyi). Data were collected on a Navios instrument (Beckman Coulter) and analyzed with FlowJo software (FlowJo v10.6.2, Ashland, OR).

γδ2 T cells activity

MDM were infected for 24 hours with the different SARS-CoV-2 variants studied at an MOI of 0.1. The MDMs were then co-cultured with γδ2 T cells at effector-to-target (E:T) ratio of 1:1 in presence of GolgiStop (BD Biosciences) and CD107(a+b)-FITC (BD Biosciences). Phorbol 12-myristate 13-acetate (PMA, 20 ng/mL) with ionomycine (1 µg/mL) was used as positive control for γδ2 T cell activation. After 4 hours, cells were harvested and stained with a viability marker (Live/Dead Near IR), CD3-PE-Cy7 and TCRγ/δ-PE (Miltenyi Biotec). Fixation/permeabilization kit (BD Biosciences) was used for intracellular staining with TNFα-eFluor 450 and IFNγ-APC (eBioscience). Data were collected on a Navios instrument (Beckman Coulter) and analyzed with FlowJo software (FlowJo v10.6.2).

Statistical analysis

Statistical analysis was performed with GraphPad Prism (7.0, La Jolla, CA), using the two-way ANOVA test. Transcriptional data were analyzed using the ClustVis webtool. Significance was set at $p<0.05$.

Results

Macrophage infection with SARS-CoV-2 variants

We previously showed infection properties of MDM using the Wuhan (china) strain (34). We then wondered if SARS-CoV-2 variants exhibited a similar response in MDM. We infected MDM with viruses at 0.1 MOI for 6, 24, 48 and 72 hours and we measured their infection rate with qRT-PCT. We showed that MDM were infected with all variants (Figure 1). Furthermore, the γ-P.1 (Brazil) variant was more efficient at infecting MDM than the other variants (Figure 1A),

something that was not detected in infected Vero E6 cells (Supplementary Figure 1A), the reference cell model for the study of SARS-CoV-2 (35). In addition, we reported a significant increase in viral load at 24, 48 and 72 hours post-infection compared to the Wuhan (china), δ-B.1.617 (India) and β-B.1.351 South African variants at 6 hours post-infection (Figure 1A). In contrast, all SARS-CoV-2 variants led to a strong increase in viral load in Vero E6 cells (Supplementary Figure 1A). Thus, despite small variations, SARS-CoV-2 variants did not efficiently replicate in MDM.

Then, we studied how can SARS-CoV-2 variants induce a cytopathic effect as assessed by cell viability assay. No cytopathic effect was observed in MDM infected by any of the SARS-CoV-2 variants (Figure 1B). In contrast, all SARS-CoV-2 variants induced a cytopathic effect in Vero E6 cells, with a 70% mortality at 72 hours post-infection (Supplementary Figure 1B).

Finally, we quantified SARS-CoV-2 viral load in MDM supernatants to study viral replication. In contrast to Vero E6 cells (Supplementary Figure 1C), the viral load of all SARS-CoV-2 variants did not change over time (Figure 1C). Taken together, despite the higher infectivity of the γ-Brazil variant, SARS-CoV-2 variants shared the ability to infect MDM without replication.

Macrophage inflammatory response to SARS-CoV-2 variants

Macrophages activation is usually classified in M1 category (pro-inflammatory) and M2 category (anti-inflammatory). We have previously shown that SARS-CoV-2 induces a specific reprogramming of MDM towards an atypical M2 polarization (34). Therefore, we wondered if infection with different SARS-CoV-2 variants could affect the MDM polarization program. We measured the expression of 6 M1-related genes (*IL6, TNF, IL1B, NOS2, IFNB, IL1R2*) and 3 M2-related genes (*IL10, TGFB, MR*) by q-RTPCR in MDM infected with SARS-CoV-2 variants. First, the hierarchical clustering showed two clusters of infected MDM (36): Wuhan, α-B.1.1.7 (United Kingdom) and δ-B.1.617 (India) (1) γ-P.1 (Brazil), β-B.1.351 South Africa, and B.1.1.529 (Omicron) variants (Figure 2A). Interestingly, the principal component analysis of gene expression showed that MDM infected with the β-B.1.351 (South Africa) variant formed a distinct group from the other SARS-CoV-2 variants (Figure 2B). The hierarchical clustering revealed a tendency of increased expression of M1-related genes i.e. *TNF*, *IL1B* and *IL6* in MDM infected with the β-B.1.351 (South Africa) variant compared to the other SARS-CoV-2 variants (Figure 2A). However, only the expression of *IL1B* gene was significantly increased in MDM infected with the β-B.1.351 (South Africa) variant compared to the other variants ($p<0.0001$) (Figure 2C). On the other hand, for M2-related gene expression, a significant increase in *TGFB* expression was found for the Wuhan SARS-CoV-2 compared to the γ-P.1 (Brazil) and B.1.1.529 Omicron variants ($p<0.05$). The expression of *IL10* and *MR* was not modulated upon infection with all variants (Figure 2D).

We then investigated the cytokine secretion induced by SARS-CoV-2 variants at 24 hours (Figure 3A) and 48 hours (Figure 3B) post-infection. The TNF production was significantly increased at 24 hours post-infection in β-B.1.351 (South Africa) infected-MDM compared to uninfected MDM and Wuhan-infected MDM ($p=0.0279$) (Figure 3A). IL-1β over production was also observed in β-B.1.351 (South Africa) infected-MDM at 24h post-infection in comparison to the other SARS-CoV-2 variants and uninfected MDM (all $p<0.0001$) (Figure 3B), respectively. We noticed a significant increase in IL-10 secretion in B.1.1.529 (Omicron) infected MDM compared to infections with the δ-B.1.617 (India) variants ($p=0.0244$). Overall, these results do not illustrate a polarization of MDM. Nevertheless, unlike the other variants, the β-B.1.351 (South Africa) variant induced macrophage activation while the B.1.1.529 (Omicron) was rather inhibitory.

Modulation of ACE2 expression by macrophages infected with SARS-CoV-2 variants

It has been shown that ACE2 expression was higher on the LPS-activated M1 macrophages compared to IL-4-treated M2 macrophages (37). Thus, we tested the activation profile in stimulated MDM infected with SARS-CoV-2 variants in relationship to ACE2 expression. We showed that *ACE2* gene expression was lower in uninfected or stimulated MDM compared to unstimulated Vero E6 cells ($p<0.0001$). *ACE2* gene expression was higher in MDM infected with the β-B.1.351 (South Africa) variant and lower in MDM infected with the α-B.1.1.7 (United Kingdom) and B.1.1.529 (Omicron) variants (Figure 4A). The ACE2 protein expression was quantified by flow cytometry and immunofluorescence in infected MDM. We reported that the ACE2 protein expression was higher in MDM infected with the β-B.1.351 (South Africa) variant compared to the other variants (B.1.1.529 (Omicron), $p=0.0002$) and uninfected cells ($p=0.0002$). In contrast, MDM infected with the B.1.1.529 (Omicron) presented the lowest levels of ACE2 expression (α-B.1.1.7 (United Kingdom), $P=0.0472$ and γ-P.1 (Brazil) variants, $p=0.0355$) (Figure 4B). This high ACE2 expression for the South Africa variant was also found by immunofluorescence analysis. Indeed, an increase of ACE2 expression was observed in MDM infected with the β-B.1.351 (South Africa) variant compared to the other variants (γ-P.1 (Brazil), $p<0.05$) and uninfected cells ($p<0.05$) (Figure 4C).

Taken together, the results showed that SARS-CoV-2 variants modulate ACE2 expression in MDM. In particular, the β-B.1.351 (South Africa) variant induced a higher expression of ACE2, in relationship to MDM activation.

10.3389/fimmu.2022.1078741

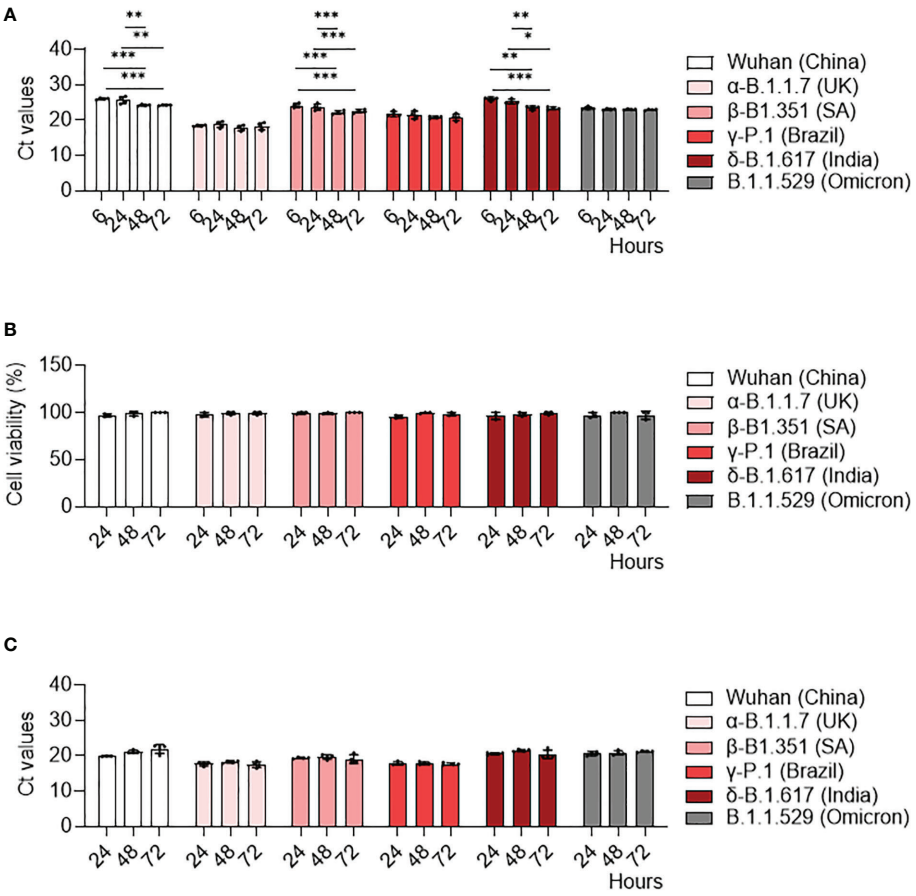

FIGURE 1
MDM infection with SARS-CoV-2 variants. MDM were infected with SARS-CoV-2 variants including Wuhan (China), α-B.1.1.7 (United Kingdom, UK), β-B.1.351 (South Africa, SA), γ-P.1 (Brazil), δ-B.1.617 (India) and B.1.1.529 (Omicron) (0.1 MOI) for 6, 24, 48 and 72 hours. **(A)** SARS-CoV-2 was quantified in cells as Ct values by RT-PCR. **(B)** Cell viability was tested at 24, 48 and 72 hours post-infection. **(C)** SARS-CoV-2 replication was quantified by RT-PCR in cell supernatants and expressed as Ct values. Data values represent the mean ± SD from 4 healthy donors whose experiments were carried out in triplicate. Statistical analysis was performed with two-way ANOVA and Tukey's multiple comparison test. *$p \leq 0.05$, **$p \leq 0.01$ and ***$p \leq 0.001$.

Macrophages infected with SARS-CoV-2 variants induce a different activation of γδ2 T cells

We then tested if MDM infected with SARS-CoV-2 variants affected differently the activation of other immune cells playing an important role in COVID-19. For this purpose, we co-cultured SARS-CoV-2 variants infected-MDM with autologous γδ2 T lymphocytes, which play a role during SARS-CoV-2 infection (25, 27). γδ2 T lymphocytes kill infected cells by direct cytotoxicity through the secretion of cytolytic molecules (perforin and granzymes) and by a cell-mediated non-cytolytic activity based on cytokine production (IFN-γ and TNF-α secretion) (38). Therefore, we assessed γδ2 T cell degranulation (% $CD107ab^+$ cells) by flow cytometry (Figure 5). We showed that MDM infected with the γ-P.1 (Brazil) and β-B.1.351 (South Africa) variants induced a higher degranulation of γδ2 T cells than unstimulated MDM ($p=0.0108$ and $p=0.0071$, respectively) (Figure 5).

Since γδ2 T cells exert their antiviral activity in a cytokine-dependent manner, we analyzed their TNF-α and IFN-γ production by flow cytometry. Infection of MDM with the γ-P.1 (Brazil) and β-B.1.351 (South Africa) variants resulted in highest TNF-α secretion by γδ2 T cells ($p=0.0324$ and $p=0.0101$, respectively).

In summary, all variants were able to activate γδ2 cells. γ-P.1 (Brazil) and β-B.1.351 (South Africa) variants were the most efficient.

Discussion

In this study, we analyzed how SARS-CoV-2 variants differently infect human macrophages and modulate their

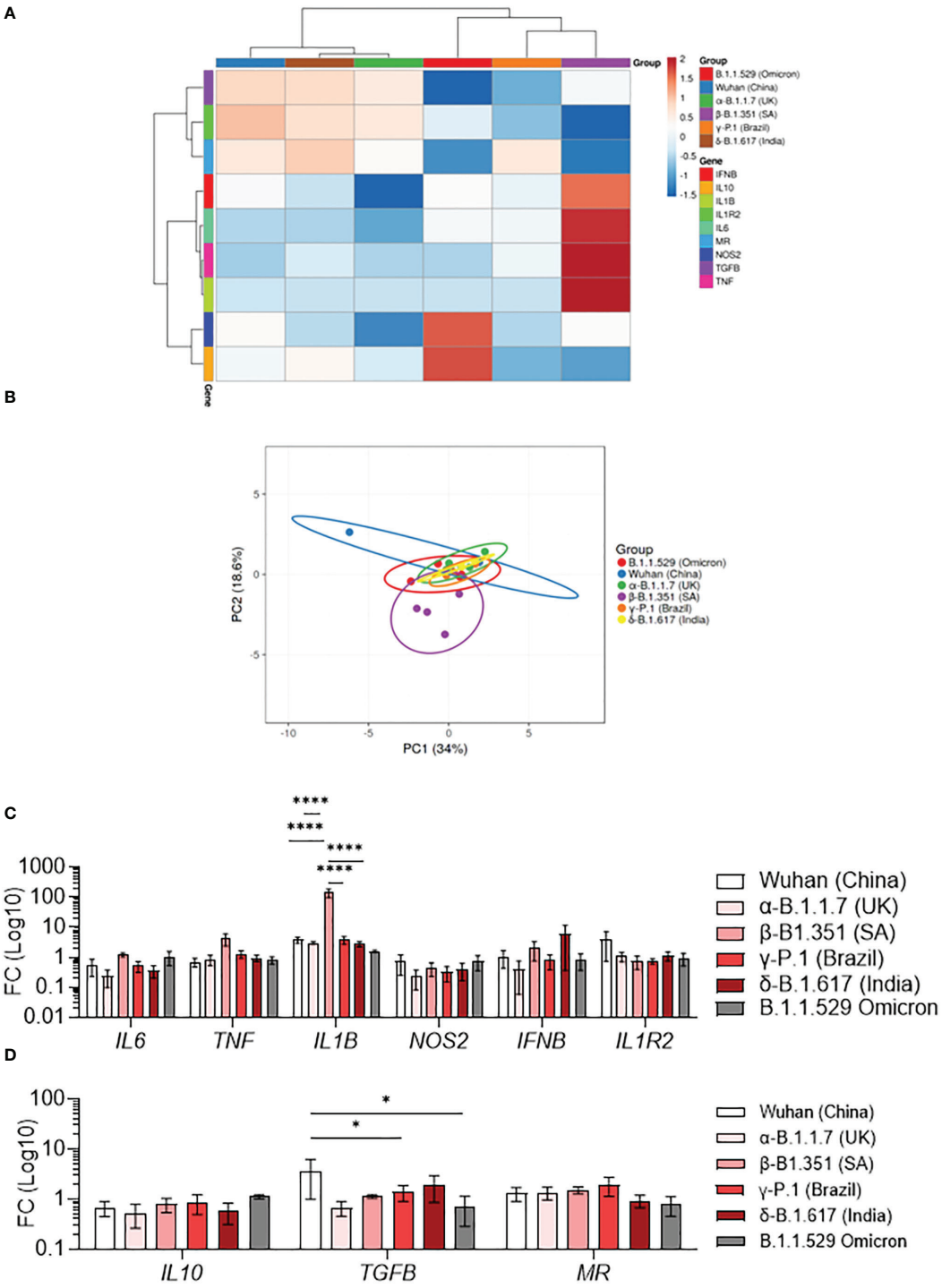

FIGURE 2
Polarization profile of MDM infected with SARS-CoV-2 variants. MDMs were infected with SARS-CoV-2 variants including Wuhan (China), α-B.1.1.7 (United Kingdom, UK), β-B.1.351 (South Africa, SA), γ-P.1 (Brazil), δ-B.1.617 (India) and B.1.1.529 (Omicron) (0.1 MOI). **(A–D)** The polarization status was investigated by measuring the expression of M1 genes (*IL6*, *TNF*, *IL1B*, *NOS2*, *IFNB*, *IL1R2*) and M2 genes (*IL10*, *TGFB*, *MR*) at 6 hours post-infection. Data are illustrated as **(A)** hierarchical clustering and **(B)** principal component analysis obtained using ClustVis webtool. **(C, D)** Fold change (FC) of **(C)** M1 genes and **(D)** M2 genes (Log 10). Data values represent the mean ± SEM from 4 healthy donors whose experiments were carried out in triplicate. Statistical analysis was performed with one-way ANOVA and Tukey's multiple comparison test. *$p \leq 0.05$ and ****$p \leq 0.0001$.

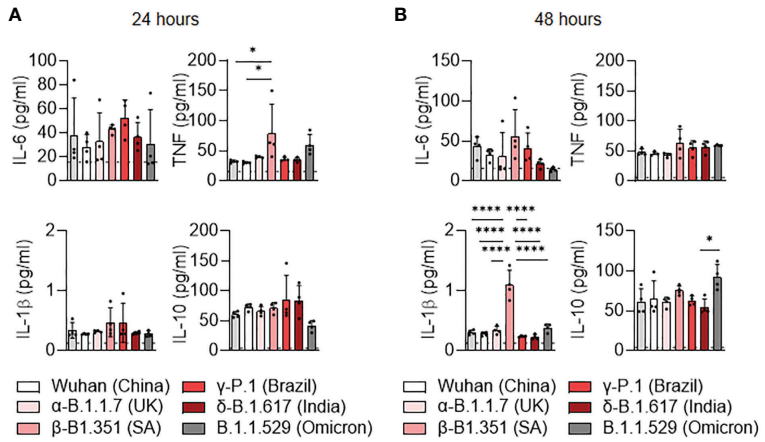

FIGURE 3
Cytokine release of MDM infected with SARS-CoV-2 variants. **(A, B)** Levels of TNF, IL-6, IL-10 and IL1-β were evaluated in the culture supernatants by ELISA at **(A)** 24 and **(B)** 48 hours post-infection. Data values represent the mean ± SEM from 4 healthy donors whose experiments were carried out in triplicate. Statistical analysis was performed with one-way ANOVA and Tukey's multiple comparison test. *$p \leq 0.05$ and ****$p \leq 0.0001$.

function. We compared SARS-CoV-2 variant infection using two cell models, Vero E6, African green monkey kidney cell line, which is widely used for SARS-CoV-2 isolation and virus production, as a positive control (39, 40) and MDM, a model of tissue macrophage of hematopoietic origin (41). Firstly, we showed that Vero E6 were more infectable than macrophages, likely related to abundant expression of ACE2 by Vero E6 cells. This was in accordance with previous study in which Vero E6 are more permissive for SARS-CoV-2 infection than primary cells (42). Secondly, we reported that all SARS-CoV-2 variants were able to infect macrophages, the γ-P.1 (Brazil) variant being most efficient as compared to the other variants. In contrast, we did not find any difference in infectibility among the SARS-CoV-2 variants in Vero E6 cells. This may indicate that internalization of viruses cannot be a means to predict the severity of the disease.

The interaction of viruses like SARS-CoV-2 with macrophages induces their activation, which may lead to tissue damage and severe disease *via* the production of inflammatory and toxic mediators (9). As we previously demonstrated, macrophage activation can be stratified into M1 and M2 states using a combination of markers (11, 43, 44). It was recently reported that polarized M1 and M2 macrophages presented an inhibitory effects on SARS-CoV-2 infection (45). More interestingly the authors showed that, in contrast to M2 macrophages, M1 and un-activated M0 macrophages up-regulated inflammatory factors. Here, we wondered whether infection with the different variants could lead to a distinct immune response in macrophages and contribute to the observed clinical differences. Our results show that infection led to the expression of genes associated with either M1 or M2 profile, suggesting that SARS-CoV-2 does not induce a clear macrophage polarization. This is consistent with a previous study, where we showed that the α-SARS-CoV-2 (Wuhan) variant induced an early M1/M2 followed by a late M2 program in macrophages (16). More specifically, macrophages infected with the β-B.1.351 (South Africa) variant showed a transcriptional program characterized by the up-regulation of M1-type genes validated by an increased secretion of TNF and IL-1β. Although the number of modulated macrophage markers was small, it seems that the β-B.1.351 (South Africa) variant was more efficient than the other variants to reprogram macrophages toward an M1 profile. In contrast, the Omicron variant seems to be less able to polarize macrophages toward an M1 profile *via* its ability to induce IL-10 secretion. These finding highlight the concept of targeting macrophage in COVID-19 as a current and future therapeutic strategy as it was reported that blocking macrophage pro-inflammatory molecules such as the treatment by IL-1α/β inhibitor anakinra provided encouraging perspectives (46).

The viral load in SARS-CoV-2 infected macrophages remained unchanged during the time of the culture. This was emphasized by the lack of cytopathic effects in response to all variants. This shows that infection with all SARS-CoV-2 variants in macrophages presents no replication although a discrete increased viral load was observed with α-SARS-CoV-2 (Wuhan), δ-B.1.617 (India) and β-B.1.351 (South Africa) variants. This is reminiscent of previous studies showing that SARS-CoV-2 efficiently infects human macrophages without replication (17, 47, 48), similar to SARS-CoV-1 (16, 49–51) suggesting a protective role for macrophage during SARS-CoV infection at it was recently reported in humanized mice model

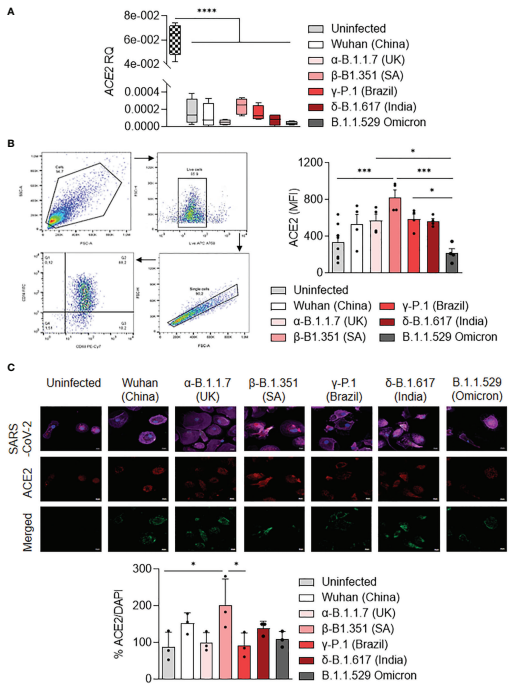

FIGURE 4
ACE2 expression by MDM infected with SARS-CoV-2 variants. MDMs were infected with SARS-CoV-2 variants including Wuhan (China), α-B.1.1.7 (United Kingdom, UK), β-B.1.351 (South Africa, SA), γ-P.1 (Brazil), δ-B.1.617 (India) and B.1.1.529 (Omicron) (0.1 MOI). **(A)** Relative quantity of *ACE2* gene was evaluated by q-RTPCR at 6 hours post-infection after normalization with housekeeping *ACTB* gene as endogenous control. Data values represent the mean ± SD from 4 healthy donors, and the experiments on unstimulated Vero E6 cells were performed in triplicate. **(B)** ACE2 protein expression was quantified by flow cytometry in MDMs at 24 hours post-infection and expressed as mean fluorescence intensity (MFI) values. **(C)** ACE2 was evaluated by immunofluorescence in MDMs at 24 hours post-infection. ACE2 was identified in red, SARS-CoV-2 in green, F-actin in purple and DAPI. Relative ACE2 expression was quantified by fluorescence with ImageJ software. Statistical analysis was performed with two-way ANOVA and Tukey's multiple comparison test. *$p \leq 0.05$, ***$p \leq 0.001$ and ****$p \leq 0.0001$.

(52). It is likely that variations in macrophage response to SARS-CoV-2 variants may be a consequence of changes in ACE2 expression. Several recent studies reported a link between macrophage polarization and ACE2 expression (37, 45, 53). Indeed, ACE2 expression has been shown to be higher in LPS-activated M1 macrophages than in IL-4-treated M2 macrophages (37). The inhibition of viral entry using ACE2 blocking antibody enhances the activity of M2 iPSC-derived macrophages (45). Therefore, we investigated the ACE2 expression in macrophages infected with the different variants. It is noteworthy that the expression of ACE2 by macrophages was markedly lower than that of Vero E6 cells. Interestingly, among the response to different variants of concern, β-B.1.351 (South Africa) infected macrophages expressed higher levels of ACE2 at the cell surface than uninfected macrophages or B.1.1.529 (Omicron) infected macrophages. These results suggest that elevated levels of pro-inflammatory cytokines increase ACE2 expression in an autocrine manner, facilitating cell infectivity. In the case of the β-B.1.351 (South Africa) variant, the M1 profile may induce a higher ACE2 expression, and explains the increased infectivity of macrophages during the infection kinetics. In contrast, IL-10 overproduced in response to B.1.1.529 (Omicron) may decrease ACE2 expression and limit virus-mediated inflammatory response.

Finally, macrophages infected with the variants displayed a different effect on γδ2 T cells whose antiviral properties are promoted by macrophages (54, 55). We recently reported that activated γδ2 T cells elicit *in vitro* strong cytotoxic and non-cytolytic anti-SARS-CoV-2 activities in response to the Wuhan strain (27). Using an *in vitro* co-culture model, we studied SARS-CoV-2 variant-infected macrophage impact on the activation of γδ2 T cells in response to each variant of concern. We revealed that infection of MDM with the γ-P.1 (Brazil) and β-B.1.351 (South Africa) variants resulted in higher γδ2 T cell activation.

Our results suggest that the β-B.1.351 (South Africa) variant possesses molecular characteristics that account for its specific impact on macrophages. β-B.1.351 (South Africa) variant is known to be less sensitive to neutralizing antibodies (56) and to exhibit increased affinity for ACE2 compared with Wuhan receptor binding domain (RBD). This latter is the result of the triple mutation K417N, E484R, and N501Y that is characteristic of the β-B.1.351 (South Africa) RBD. Therefore, antibodies of

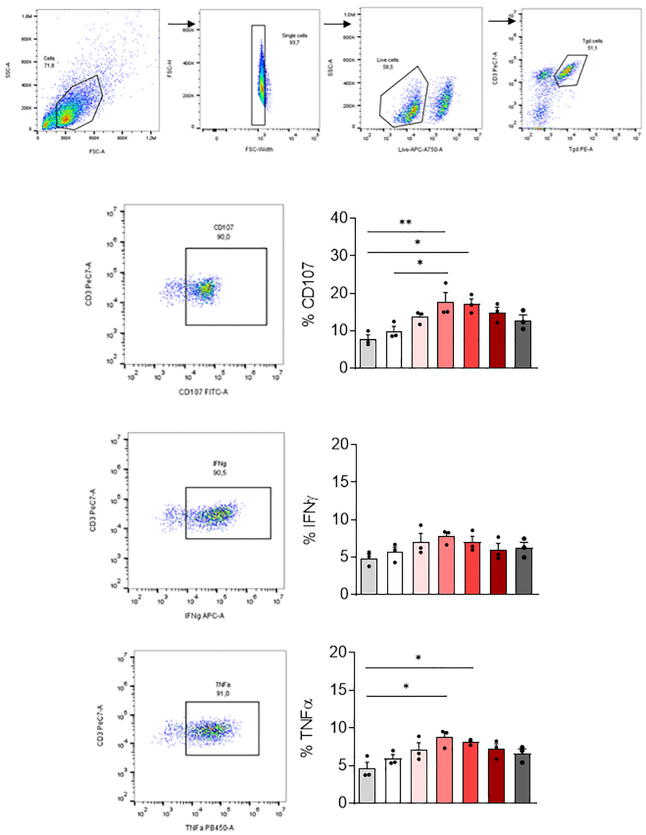

FIGURE 5
γδ2 T cell activation. MDM previously infected 24 hours with SARS-CoV-2 variants including Wuhan (China), α-B.1.1.7 (United Kingdom, UK), β-B.1.351 (South Africa, SA), γ-P.1 (Brazil), δ-B.1.617 (India) and B.1.1.529 (Omicron) (0.1 MOI) were co-cultured with autologous γδ2 T cells (E:T ratio of 1:1). γδ2 T cell degranulation (% CD107ab$^+$ cells) and intracellular TNFα and IFNγ, respectively, were assessed after 4 hours of co-culture in the presence of GolgiStop and analyzed by flow cytometry. Manual gating to identify γδ2 T cell population (CD3$^+$ TCRVδ2$^+$). The percentage of CD107$^+$, IFNγ$^+$ and TNFα$^+$ cells, were then gated in the γδ2 cell population (CD3$^+$ TCRVδ2$^+$). Data values represent the mean ± SD from 3 healthy donors. Statistical analysis was performed with one-way ANOVA and Tukey's multiple comparison test. *$p \leq 0.05$ and **$p \leq 0.01$.

lower affinity will struggle to compete with ACE2 receptor (57). These facts may explain why we observed an upregulation in ACE2 expression in macrophages infected with the β-B.1.351 (South Africa) variant, suggesting that escaping from neutralizing antibodies may enhance the activation of macrophages and innate immunity in an ACE2 receptor-dependent manner.

We have previously reported the importance of several models to investigate SARS-CoV-2 infection *in vitro* and *in vivo* (24). Vero E6 cell line constitutes a reference model in the study of SARS-CoV-2 infection due to an abundant expression of ACE2 receptor on their membrane (58, 59). Nevertheless, Vero E6 presents several disadvantages, such as low expression of *IFN* genes (60, 61) and the absence of TMPRSS2, an essential protein for SARS-CoV-2 viral entry (58). In the absence of TMPRSS2, SARS-CoV-2 may be proteolytically activated following receptor-mediated endocytosis by cathepsin B/L (58, 62). To investigate the role of macrophage in SARS-CoV-2 infection we used the MDM model that it was previously reported to express both ACE2 and TMPRSS2 proteins (37, 63) constituting a more relevant model to the actual disease in humans.

In conclusion, SARS-CoV-2 variants modulate both macrophage activation program including γδ2 T cells and ACE2 expression. Among the variants of concern, the β-B.1.351 (South Africa) variant is highlighted thanks to its efficacy to induce an M1-related program, γδ2 T cell activation and ACE2 overexpression. The characteristics of β-B.1.351 (South Africa) mutations may explain this specific effect on macrophages although the molecular impact of these mutations has still to be clearly deciphered. On the other hand, the Omicron variant is the only one able to stimulate IL-10, known for its immunoregulatory properties, which may account for its decreased pathogenicity. This study demonstrates that the diversity of SARS-CoV-2 has an impact on macrophages and this must be taken into account to

understand the immunopathology of COVID-19 and the treatment of patients with new therapies such as cytokine antagonists or antibody targeting virus receptors.

Data availability statement

The original contributions presented in the study are included in the article/Supplementary Material. Further inquiries can be directed to the corresponding author.

Ethics statement

Peripheral blood mononuclear cells (PBMC) were isolated as previously described (27) from deidentified blood samples (leucopacks) come from the French Blood Establishment (Etablissement français du sang, EFS) that carries out donor inclusions, informed consent and sample collection. Through a convention established between our laboratory and the EFS (N° 7828), buffy coats were obtained and monocytes were isolated for this study. The patients/participants provided their written informed consent to participate in this study.

Author contributions

PA and LG performed the experiments, analyzed the data; PA and SM wrote the first draft of the manuscript; AL performed the bioinformatics experiment and analysis; BL provided SARS-CoV-2 strains; DO, SM, J-PG, and J-LM supervised the work and wrote the final manuscript. All authors contributed to the article and approved the submitted version.

Conflict of interest

The authors declare that the research was conducted in the absence of any commercial or financial relationships that could be construed as a potential conflict of interest.

Publisher's note

All claims expressed in this article are solely those of the authors and do not necessarily represent those of their affiliated organizations, or those of the publisher, the editors and the reviewers. Any product that may be evaluated in this article, or claim that may be made by its manufacturer, is not guaranteed or endorsed by the publisher.

Supplementary material

The Supplementary Material for this article can be found online at: https://www.frontiersin.org/articles/10.3389/fimmu.2022.1078741/full#supplementary-material

SUPPLEMENTARY FIGURE 1
Vero E6 cell line infection with SARS-CoV-2 variants Vero E6 cells were infected with SARS-CoV-2 variants including Wuhan (China), α-B.1.1.7 (United Kingdom, UK), β-B.1.351 (South Africa, SA), γ-P.1 (Brazil), δ-B.1.617 (India) and B.1.1.529 (Omicron) (0.1 MOI) for 6, 24, 48 or 72 hours. **(A)** Cell viability was tested at 24, 48 and 72 hours post-infection. **(B)** The presence of SARS-CoV-2 was evaluated and quantified by immunofluorescence (left panel, virus in green, nucleus in blue and F-actin in purple) and RT-PCR expressed as Ct values (right panel), respectively. **(C)** SARS-CoV-2 replication was quantified by RT-PCR in cell supernatant and expressed as Ct values. Data values represent the mean ± SD from three independent experiments in triplicate. Statistical analysis was performed with two-way ANOVA and Tukey's multiple comparison test. $^{*}p \leq 0.05$, $^{**}p \leq 0.01$, $^{***}p \leq 0.001$ and $^{****}p \leq 0.0001$.

References

1. Guan W, Ni Z, Hu Y, Liang W, Ou C, He J, et al. Clinical characteristics of coronavirus disease 2019 in China. *New Engl J Med* (2020) 382:1708–20. doi: 10.1056/NEJMoa2002032

2. Chen N, Zhou M, Dong X, Qu J, Gong F, Han Y, et al. Epidemiological and clinical characteristics of 99 cases of 2019 novel coronavirus pneumonia in wuhan, China: a descriptive study. *Lancet* (2020) 395:507–13. doi: 10.1016/S0140-6736(20)30211-7

3. Zhou F, Yu T, Du R, Fan G, Liu Y, Liu Z, et al. Clinical course and risk factors for mortality of adult inpatients with COVID-19 in wuhan, China: A retrospective cohort study. *Lancet* (2020) 395:1054–62. doi: 10.1016/S0140-6736(20)30566-3

4. Wang D, Hu B, Hu C, Zhu F, Liu X, Zhang J, et al. Clinical characteristics of 138 hospitalized patients with 2019 novel coronavirus–infected pneumonia in wuhan, China. *JAMA* (2020) 323:1061–9. doi: 10.1001/jama.2020.1585

5. Sudre CH, Murray B, Varsavsky T, Graham MS, Penfold RS, Bowyer RC, et al. Attributes and predictors of long COVID. *Nat Med* (2021) 27:626–31. doi: 10.1038/s41591-021-01292-y

6. Moore JB, June CH. Cytokine release syndrome in severe COVID-19. *Science* (2020) 368:473–4. doi: 10.1126/science.abb8925

7. Moss P. The T cell immune response against SARS-CoV-2. *Nat Immunol* (2022) 23:186–93. doi: 10.1038/s41590-021-01122-w

8. Merad M, Martin JC. Pathological inflammation in patients with COVID-19: a key role for monocytes and macrophages. *Nat Rev Immunol* (2020) 20:355–62. doi: 10.1038/s41577-020-0331-4

9. Xu Z, Shi L, Wang Y, Zhang J, Huang L, Zhang C, et al. Pathological findings of COVID-19 associated with acute respiratory distress syndrome. *Lancet Respir Med* (2020) 8:420–2. doi: 10.1016/S2213-2600(20)30076-X

10. Del Valle DM, Kim-Schulze S, Huang H-H, Beckmann ND, Nirenberg S, Wang B, et al. An inflammatory cytokine signature predicts COVID-19 severity and survival. *Nat Med* (2020) 26:1636–43. doi: 10.1038/s41591-020-1051-9

11. Abou Atmeh P, Mezouar S, Mège J-L. Macrophage polarization in viral infectious diseases: Confrontation with the reality. In: *Macrophages -140 years of their discovery*. (IntechOpen) (2022). doi: 10.5772/intechopen.106083

12. Bain CC, Lucas CD, Rossi AG. Pulmonary macrophages and SARS-Cov2 infection. *Int Rev Cell Mol Biol* (2022) 367:1–28. doi: 10.1016/bs.ircmb.2022.01.001

13. Bao L, Deng W, Huang B, Gao H, Liu J, Ren L, et al. The pathogenicity of SARS-CoV-2 in hACE2 transgenic mice. *Nature* (2020) 583:830–3. doi: 10.1038/s41586-020-2312-y

14. Delorey TM, Ziegler CGK, Heimberg G, Normand R, Yang Y, Segerstolpe Å, et al. COVID-19 tissue atlases reveal SARS-CoV-2 pathology and cellular targets. *Nature* (2021) 595:107–13. doi: 10.1038/s41586-021-03570-8

15. Melms JC, Biermann J, Huang H, Wang Y, Nair A, Tagore S, et al. A molecular single-cell lung atlas of lethal COVID-19. *Nature* (2021) 595:114–9. doi: 10.1038/s41586-021-03569-1

16. Boumaza A, Gay L, Mezouar S, Diallo AB, Michel M, Desnues B, et al. Monocytes and macrophages, targets of SARS-CoV-2: the clue for covid-19 immunoparalysis. *bioRxiv* (2020) 224(3):395–406. doi: 10.1101/2020.09.17.300996

17. Yang D, Chu H, Hou Y, Chai Y, Shuai H, Lee AC-Y, et al. Attenuated interferon and proinflammatory response in SARS-CoV-2–infected human dendritic cells is associated with viral antagonism of STAT1 phosphorylation. *J Infect Dis* (2020) 222:734–45. doi: 10.1093/infdis/jiaa356

18. Lu Q, Liu J, Zhao S, Castro MFG, Laurent-Rolle M, Dong J, et al. SARS-CoV-2 exacerbates proinflammatory responses in myeloid cells through c-type lectin receptors and tweety family member 2. *Immunity* (2021) 54:1304–1319.e9. doi: 10.1016/j.immuni.2021.05.006

19. Niles MA, Gogesch P, Kronhart S, Ortega Iannazzo S, Kochs G, Waibler Z, et al. Macrophages and dendritic cells are not the major source of pro-inflammatory cytokines upon SARS-CoV-2 infection. *Front Immunol* (2021) 12:647824. doi: 10.3389/fimmu.2021.647824

20. Thorne LG, Reuschl A, Zuliani-Alvarez L, Whelan MVX, Turner J, Noursadeghi M, et al. SARS-CoV-2 sensing by RIG-I and MDA5 links epithelial infection to macrophage inflammation. *EMBO J* (2021) 40:e107826. doi: 10.15252/embj.2021107826

21. Li J, Lai S, Gao GF, Shi W. The emergence, genomic diversity and global spread of SARS-CoV-2. *Nature* (2021) 600:408–18. doi: 10.1038/s41586-021-04188-6

22. Choi JY, Smith DM. SARS-CoV-2 variants of concern. *Yonsei Med J* (2021) 62:961–8. doi: 10.3349/ymj.2021.62.11.961

23. Winger A, Caspari T. The spike of concern–the novel variants of SARS-CoV-2. *Viruses* (2021) 13:1002. doi: 10.3390/v13061002

24. Bestion E, Zandi K, Belouzard S, Andreani J, Lepidi H, Novello M, et al. GNS561 exhibits potent antiviral activity against SARS-CoV-2 through autophagy inhibition. *Viruses* (2022) 14:132. doi: 10.3390/v14010132

25. Rijkers G, Vervenne T, van der Pol P. More bricks in the wall against SARS-CoV-2 infection: involvement of γ9δ2 T cells. *Cell Mol Immunol* (2020) 17:771–2. doi: 10.1038/s41423-020-0473-0

26. Odak I, Barros-Martins J, Bošnjak B, Stahl K, David S, Wiesner O, et al. Reappearance of effector T cells is associated with recovery from COVID-19. *EBioMedicine* (2020) 57:102885. doi: 10.1016/j.ebiom.2020.102885

27. Gay L, Rouviere M-S, Mezouar S, Richaud M, Gorvel L, Foucher E, et al. Vγ9Vδ2 T cells are potent inhibitors of SARS-CoV-2 replication and exert effector phenotypes in COVID-19 patients. *Immunology* (2022) 2020:1–10. doi: 10.1101/2022.04.15.487518

28. Gay L, Mezouar S, Cano C, Foucher E, Gabriac M, Fullana M, et al. BTN3A targeting Vγ9Vδ2 T cells antimicrobial activity against coxiella burnetii-infected cells. *Front Immunol* (2022) 13:915244. doi: 10.3389/fimmu.2022.915244

29. Gertner J, Wiedemann A, Poupot M, Fournié J-J. Human γδ T lymphocytes strip and kill tumor cells simultaneously. *Immunol Lett* (2007) 110:42–53. doi: 10.1016/j.imlet.2007.03.002

30. Benyamine A, Loncle C, Foucher E, Blazquez J-L, Castanier C, Chrétien A-S, et al. BTN3A is a prognosis marker and a promising target for Vγ9Vδ2 T cells based-immunotherapy in pancreatic ductal adenocarcinoma (PDAC). *OncoImmunology* (2018) 7:e1372080. doi: 10.1080/2162402X.2017.1372080

31. Andreani J, Le Bideau M, Duflot I, Jardot P, Rolland C, Boxberger M, et al. *In vitro* testing of combined hydroxychloroquine and azithromycin on SARS-CoV-2 shows synergistic effect. *Microbial Pathogenesis* (2020) 145:104228. doi: 10.1016/j.micpath.2020.104228

32. Otmani Idrissi M, Baudoin J-P, Chateau A-L, Aherfi S, Bedotto-Buffet M, Latil A, et al. Presence of SARS-CoV-2 in a cornea transplant. *Pathogens* (2021) 10:934. doi: 10.3390/pathogens10080934

33. Mezouar S, Vitte J, Gorvel L, Ben Amara A, Desnues B, Mege J-L. Mast cell cytonemes as a defense mechanism against. *Coxiella burnetii. mBio* (2019) 10: e02669–18. doi: 10.1128/mBio.02669-18

34. Boumaza A, Gay L, Mezouar S, Bestion E, Diallo AB, Michel M, et al. Monocytes and macrophages, targets of severe acute respiratory syndrome coronavirus 2: The clue for coronavirus disease 2019 immunoparalysis. *J Infect Dis* (2021) 224:395–406. doi: 10.1093/infdis/jiab044

35. Bestion E, Halfon P, Mezouar S, Mège J-L. Cell and animal models for SARS-CoV-2 research. *Viruses* (2022) 14:1507. doi: 10.3390/v14071507

36. *COVID live - coronavirus statistics - worldometer* . Available at: https://www.worldometers.info/coronavirus/ (Accessed June 6, 2022).

37. Song X, Hu W, Yu H, Zhao L, Zhao Y, Zhao X, et al. Little to no expression of angiotensin-converting enzyme-2 on most human peripheral blood immune cells but highly expressed on tissue macrophages. *Cytometry A* (2020) 1–10. doi: 10.1002/cyto.a.24285

38. Gay L, Mezouar S, Cano C, Frohna P, Madakamutil L, Mège J-L, et al. Role of Vγ9vδ2 T lymphocytes in infectious diseases. *Front Immunol* (2022) 13:928441. doi: 10.3389/fimmu.2022.928441

39. Zhou P, Yang X-L, Wang X-G, Hu B, Zhang L, Zhang W, et al. A pneumonia outbreak associated with a new coronavirus of probable bat origin. *Nature* (2020) 579:270–3. doi: 10.1038/s41586-020-2012-7

40. de Souza GAP, Le Bideau M, Boschi C, Ferreira L, Wurtz N, Devaux C, et al. Emerging SARS-CoV-2 genotypes show different replication patterns in human pulmonary and intestinal epithelial cells. *Viruses* (2021) 14:23. doi: 10.3390/v14010023

41. Ginhoux F, Guilliams M. Tissue-resident macrophage ontogeny and homeostasis. *Immunity* (2016) 44:439–49. doi: 10.1016/j.immuni.2016.02.024

42. Essaidi-Laziosi M, Perez Rodriguez FJ, Hulo N, Jacquerioz F, Kaiser L, Eckerle I. Estimating clinical SARS-CoV-2 infectiousness in vero E6 and primary airway epithelial cells. *Lancet Microbe* (2021) 2:e571. doi: 10.1016/S2666-5247(21)00216-0

43. Murray PJ, Allen JE, Biswas SK, Fisher EA, Gilroy DW, Goerdt S, et al. Macrophage activation and polarization: nomenclature and experimental guidelines. *Immunity* (2014) 41:14–20. doi: 10.1016/j.immuni.2014.06.008

44. Mezouar S, Mege J-L. New tools for studying macrophage polarization: Application to bacterial infections. In: Prakash H, editor. *Macrophages*. (IntechOpen) (2021). doi: 10.5772/intechopen.92666

45. Lian Q, Zhang K, Zhang Z, Duan F, Guo L, Luo W, et al. Differential effects of macrophage subtypes on SARS-CoV-2 infection in a human pluripotent stem cell-derived model. *Nat Commun* (2022) 13:2028. doi: 10.1038/s41467-022-29731-5

46. Kyriazopoulou E, Poulakou G, Milionis H, Metallidis S, Adamis G, Tsiakos K, et al. Early treatment of COVID-19 with anakinra guided by soluble urokinase plasminogen receptor plasma levels: a double-blind, randomized controlled phase 3 trial. *Nat Med* (2021) 27:1752–60. doi: 10.1038/s41591-021-01499-z

47. Zheng J, Wang Y, Li K, Meyerholz DK, Allamargot C, Perlman S. Severe acute respiratory syndrome coronavirus 2–induced immune activation and death of monocyte-derived human macrophages and dendritic cells. *J Infect Dis* (2020) 223:785–95. doi: 10.1093/infdis/jiaa753

48. Hui KPY, Cheung M-C, Perera RAPM, Ng K-C, Bui CHT, Ho JCW, et al. Tropism, replication competence, and innate immune responses of the coronavirus SARS-CoV-2 in human respiratory tract and conjunctiva: an analysis in ex-vivo and in-vitro cultures. *Lancet Respir Med* (2020) 8:687–95. doi: 10.1016/S2213-2600(20)30193-4

49. Tseng C-TK, Perrone LA, Zhu H, Makino S, Peters CJ. Severe acute respiratory syndrome and the innate immune responses: Modulation of effector cell function without productive infection. *J Immunol* (2005) 174:7977–85. doi: 10.4049/jimmunol.174.12.7977

50. Junqueira C, Crespo Â, Ranjbar S, de Lacerda LB, Lewandrowski M, Ingber J, et al. FcγR-mediated SARS-CoV-2 infection of monocytes activates inflammation. *Nature* (2022) 606:576–84. doi: 10.1038/s41586-022-04702-4

51. Yilla M, Harcourt BH, Hickman CJ, McGrew M, Tamin A, Goldsmith CS, et al. SARS-coronavirus replication in human peripheral monocytes/macrophages. *Virus Res* (2005) 107:93–101. doi: 10.1016/j.virusres.2004.09.004

52. Kenney DJ, O'Connell AK, Turcinovic J, Montanaro P, Hekman RM, Tamura T, et al. Humanized mice reveal a macrophage-enriched gene signature defining human lung tissue protection during SARS-CoV-2 infection. *Cell Rep* (2022) 39:110714. doi: 10.1016/j.celrep.2022.110714

53. Banu N, Panikar SS, Leal LR, Leal AR. Protective role of ACE2 and its downregulation in SARS-CoV-2 infection leading to macrophage activation syndrome: Therapeutic implications. *Life Sci* (2020) 256:117905. doi: 10.1016/j.lfs.2020.117905

54. Poccia F, Agrati C, Castilletti C, Bordi L, Gioia C, Horejsh D, et al. Anti-severe acute respiratory syndrome coronavirus immune responses: the role played by Vγ9Vδ2 T cells. *J Infect Dis* (2006) 193:1244–9. doi: 10.1086/502975

55. Qin G, Liu Y, Zheng J, Ng IHY, Xiang Z, Lam K-T, et al. Type 1 responses of human Vγ9Vδ2 T cells to influenza a viruses. *J Virol* (2011) 85:10109–16. doi: 10.1128/JVI.05341-11

56. Aleem A, Akbar Samad AB, Slenker AK. Emerging variants of SARS-CoV-2 and novel therapeutics against coronavirus (COVID-19), in: *StatPearls* (2022). Treasure Island (FL: StatPearls Publishing. Available at: http://www.ncbi.nlm.nih.gov/books/NBK570580/ (Accessed April 7, 2022).

57. Zhou D, Dejnirattisai W, Supasa P, Liu C, Mentzer AJ, Ginn HM, et al. Evidence of escape of SARS-CoV-2 variant B.1.351 from natural and vaccine-induced sera. *Cell* (2021) 184:2348–2361.e6. doi: 10.1016/j.cell.2021.02.037

58. Hoffmann M, Kleine-Weber H, Schroeder S, Krüger N, Herrler T, Erichsen S, et al. SARS-CoV-2 cell entry depends on ACE2 and TMPRSS2 and is blocked by a clinically proven protease inhibitor. *Cell* (2020) 181:271–280.e8. doi: 10.1016/j.cell.2020.02.052

59. Ren X, Glende J, Al-Falah M, de Vries V, Schwegmann-Wessels C, Qu X, et al. Analysis of ACE2 in polarized epithelial cells: surface expression and function as receptor for severe acute respiratory syndrome-associated coronavirus. *J Gen Virol* (2006) 87:1691–5. doi: 10.1099/vir.0.81749-0

60. Diaz MO, Ziemin S, Le Beau MM, Pitha P, Smith SD, Chilcote RR, et al. Homozygous deletion of the alpha- and beta 1-interferon genes in human leukemia and derived cell lines. *Proc Natl Acad Sci U.S.A.* (1988) 85:5259–63. doi: 10.1073/pnas.85.14.5259

61. Emeny JM, Morgan MJ. Regulation of the interferon system: evidence that vero cells have a genetic defect in interferon production. *J Gen Virol* (1979) 43:247–52. doi: 10.1099/0022-1317-43-1-247

62. Shang J, Ye G, Shi K, Wan Y, Luo C, Aihara H, et al. Structural basis of receptor recognition by SARS-CoV-2. *Nature* (2020) 581:221–4. doi: 10.1038/s41586-020-2179-y

63. García-Nicolás O, V'kovski P, Zettl F, Zimmer G, Thiel V, Summerfield A. No evidence for human monocyte-derived macrophage infection and antibody-mediated enhancement of SARS-CoV-2 infection. *Front Cell Infect Microbiol* (2021) 11:644574. doi: 10.3389/fcimb.2021.644574

frontiers | Frontiers in Immunology

TYPE Original Research
PUBLISHED 16 March 2023
DOI 10.3389/fimmu.2023.1112870

OPEN ACCESS

EDITED BY
Thierry Roger,
Centre Hospitalier Universitaire Vaudois (CHUV), Switzerland

REVIEWED BY
Sreya Ghosh,
Harvard Medical School, United States
Shamik Majumdar,
National Institute of Allergy and Infectious Diseases (NIH), United States

*CORRESPONDENCE
Amy L. Ryan
amy-l-ryan@uiowa.edu

SPECIALTY SECTION
This article was submitted to Molecular Innate Immunity, a section of the journal Frontiers in Immunology

RECEIVED 30 November 2022
ACCEPTED 03 March 2023
PUBLISHED 16 March 2023

CITATION
Calvert BA, Quiroz EJ, Lorenzana Z, Doan N, Kim S, Senger CN, Anders JJ, Wallace WD, Salomon MP, Henley J and Ryan AL (2023) Neutrophilic inflammation promotes SARS-CoV-2 infectivity and augments the inflammatory responses in airway epithelial cells.
Front. Immunol. 14:1112870.
doi: 10.3389/fimmu.2023.1112870

Neutrophilic inflammation promotes SARS-CoV-2 infectivity and augments the inflammatory responses in airway epithelial cells

Ben A. Calvert[1,2], Erik J. Quiroz[1,2,3], Zareeb Lorenzana[1], Ngan Doan[1], Seongjae Kim[4], Christiana N. Senger[1], Jeffrey J. Anders[2], Wiliam D. Wallace[5], Matthew P. Salomon[6], Jill Henley[6] and Amy L. Ryan[1,2,3*†]

[1]Hastings Center for Pulmonary Research, Division of Pulmonary, Critical Care and Sleep Medicine, Department of Medicine, University of Southern California, Los Angeles, CA, United States, [2]Department of Anatomy and Cell Biology, Carver College of Medicine, University of Iowa, Iowa, IA, United States, [3]Department of Stem Cell Biology and Regenerative Medicine, University of Southern California, Los Angeles, CA, United States, [4]The Salk Institute of Biological Studies, La Jolla, CA, United States, [5]Department of Pathology, University of Southern California, Los Angeles, CA, United States, [6]Department of Medicine, University of Southern California, Los Angeles, CA, United States

Introduction: In response to viral infection, neutrophils release inflammatory mediators as part of the innate immune response, contributing to pathogen clearance through virus internalization and killing. Pre- existing co-morbidities correlating to incidence to severe COVID-19 are associated with chronic airway neutrophilia. Furthermore, examination of COVID-19 explanted lung tissue revealed a series of epithelial pathologies associated with the infiltration and activation of neutrophils, indicating neutrophil activity in response to SARS-CoV-2 infection.

Methods: To determine the impact of neutrophil-epithelial interactions on the infectivity and inflammatory responses to SARS-CoV-2 infection, we developed a co-culture model of airway neutrophilia. This model was infected with live SARS-CoV-2 virus the epithelial response to infection was evaluated.

Results: SARS-CoV-2 infection of airway epithelium alone does not result in a notable pro-inflammatory response from the epithelium. The addition of neutrophils induces the release of proinflammatory cytokines and stimulates a significantly augmented proinflammatory response subsequent SARS-CoV-2 infection. The resulting inflammatory responses are polarized with differential release from the apical and basolateral side of the epithelium. Additionally, the integrity of the \epithelial barrier is impaired with notable epithelial damage and infection of basal stem cells.

Conclusions: This study reveals a key role for neutrophil-epithelial interactions in determining inflammation and infectivity.

KEYWORDS

airway epithelium, cell-cell interactions, cytokines, inflammation, neutrophils, viral infection, COVID-19

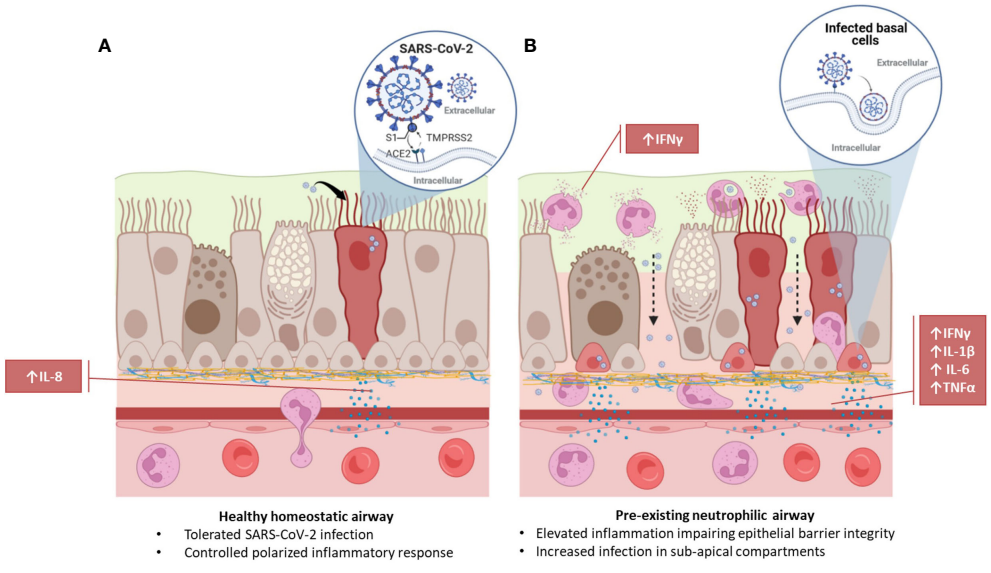

GRAPHICAL ABSTRACT

Introduction

Novel coronavirus infectious disease 2019, COVID-19, is caused by the severe acute respiratory distress syndrome related coronavirus 2, SARS-CoV-2 (1, 2). While COVID-19 is associated with high hospitalization and mortality rates, a substantial proportion of the population is asymptomatic or only experiences mild symptoms. In response to viral infection neutrophils are the first and predominant immune cells recruited to the respiratory tract (3). Neutrophils release inflammatory mediators as part of the innate immune response and contribute to pathogen clearance through virus internalization and killing (4). While the protective versus pathological role of neutrophils in the airways during viral response is poorly understood, it has been shown that the number of neutrophils in the lower respiratory tract correlates to COVID-19 disease severity (5–7). Infiltration of neutrophils is also characteristic of other lung diseases associated with chronic infection and inflammation, such as asthma, chronic obstructive pulmonary disease (COPD) and cystic fibrosis (CF). All these respiratory diseases have been associated with an increased risk of developing severe COVID-19 (8). Evaluating the relationship between SARS-CoV-2 infection and pre-existing airway neutrophilia may provide critical insight into how host and viral factors contribute to disease severity.

Neutrophils have an inherent capacity to recognize infectious agents, in addition to acting as sites of infection and, in both cases, result in an acute inflammatory response (9). Understanding the precise nature of the inflammatory response and the pathophysiological consequences, could identify pathways for therapeutic intervention based on early detection of a prognostic signature for COVID-19 outcomes. An uncontrolled, hyper-inflammatory response, known as a "cytokine storm" can result from a massive influx of innate leukocytes, inclusive of neutrophils and monocytes (10), and has been heavily implicated in patients with severe COVID-19 (11, 12). Cytokine storm and presence of pro-inflammatory mediators can be a predictor of disease severity and often leads to acute respiratory distress syndrome (ARDS), and eventually respiratory failure (13). Retrospective studies have also demonstrated that elevated levels of interleukin-6 (IL-6) are a strong predictor of mortality over resolution (14), and tumor necrosis factor alpha (TNFα) is increased in severe compared to moderate cases (15).

Despite their importance in anti-viral immunity and response to viral pathogens, neutrophils have been somewhat overlooked for their role in the pathogenesis of SARS-CoV-2 infection (16–18). It has been shown that the number of neutrophils in the lower respiratory tract correlates to disease severity in other viral infections, including influenza A infection (19) and, more recently, to also be a feature of COVID-19 pathology (18). Several studies have highlighted the importance of neutrophils in the response to SARS-CoV-2 infection (17, 18, 20, 21) and clinically neutrophil-lymphocyte ratios (NLR) are becoming an important hallmark of severe COVID-19 (22). Furthermore, the expression of angiotensin converting enzyme 2 (ACE2) on neutrophils has also been demonstrated (23–25). These studies, however, have primarily focused on the recruitment of neutrophils post-infection and the production of neutrophil extracellular traps and lack insights into the infection of airways with pre-existing neutrophilia and other neutrophil functional responses such as inflammatory cytokine production and viral internalization.

In this study, the relationship between SARS-CoV-2 infection and pre-existing airway neutrophilia in differentiated airway epithelium was evaluated through the adaption of a co-culture infection model previously used to study viral infections *in vitro*

(26). Primary neutrophils were isolated from peripheral blood and co-cultured with differentiated primary tracheo-bronchial airway epithelium prior to infection with live SARS-CoV-2 virus for 4 hours to characterize the earliest stages of infection. Changes in the inflammatory profile and epithelial response were comprehensively evaluated to determine the impact of pre-existing neutrophilia on SARS-CoV-2 infection of the airway epithelium.

Materials and methods

Isolation of neutrophils from peripheral blood

Neutrophils were isolated from fresh human peripheral blood with patient consent and approval of the Institutional Review Board (IRB) of the University of Southern California (USC), protocol #HS-20-00546. CD15-expressing neutrophils were isolated using the EasySep™ direct neutrophil isolation kit (Stem Cell Technologies, Seattle, WA) within 1 hour of the blood draw as per the manufacturer's instructions. Briefly, 5 ml of peripheral blood was collected into 10 ml EDTA vacutainers (Becton Dickinson, Franklin Lakes, NJ). From this, 3 ml was diluted 1:1 with PBS (Thermo Fisher Scientific, Waltham, MA) and kept on ice for purity analysis by flow cytometry. The remaining 2 ml was transferred to a 5 ml polystyrene round bottomed tube (Genesee Scientific, San Diego, CA) and gently combined with 100 µl of isolation cocktail and 100 µl of RapidSpheres™ (Stem Cell Technologies). After incubation at room temperature for 5 mins, 1.8 ml of 1 mM EDTA was added, gently mixed, and placed into the EasySep™ Magnet (Stem Cell Technologies) for 5 mins. The enriched cell suspension was placed into the EasySep™ Magnet for an additional 5 mins and decanted into a fresh tube. Approximately 4.25 x 10^6 cells were isolated from 5 ml of peripheral blood.

Flow activated cell sorting

To validate the purity of neutrophils isolated from peripheral blood; 1x10^7 $CD15^+$ freshly isolated human neutrophils were resuspended in 100 ul FACS buffer (PBS, 0.5mM EDTA, 1% FBS, 0.1% BSA) and fresh whole human blood diluted 1:5 in FACS buffer and supplemented with 5 ul of human TruStain Fc receptor blocker (Biolegend, San Diego, CA) for 5 mins on ice. Cells were then incubated with anti-human CD15 PE (Biolegend) for 1 hour prior to FACS analysis. Cells were analyzed on the SORP FACS Symphony cell sorter (BD Biosciences) in the Flow Cytometry Facility at USC using FACS Diva software and all analyses was carried out in Flow Jo V10.8.0 (BD Biosciences).

Air-liquid interface differentiation of airway epithelium

Primary human airway basal epithelial cells (HBECs) were isolated from explant human lung tissue as previously described (27) and with approval of IRB at USC (protocol #HS-18-00273). For this study, HBEC donors were randomly paired with blood neutrophil donors (detailed in supplemental table S1&2). HBECs were expanded for 1 to 4 passages in airway epithelial cell growth media (AEGM, Promocell, Heidelberg, DE) and transitioned to Pneumacult Ex+ (Stem Cell Technologies) for 1 passage, prior to growth on Transwells. Cells were routinely passaged at 80% confluence using Accutase™ (Stem Cell Technologies) and seeded at 5 x 10^4 cells per 6.5 mm polyethylene (PET) insert with 0.4 µm pores (Corning, Corning, NY). Media was changed every 24-48 hours and transepithelial electrical resistance (TEER) was monitored every 24-48 hours using an EVOM3 epithelial volt-ohm meter (World Precision Instruments, Sarasota, FL). At resistances ≥ 450Ω ^cm^2, cells were air lifted by removing the apical media and washing the apical surface with phosphate buffered saine (PBS, Sigma-Aldrich, St Louis, MO). The basolateral media was replaced with Pneumacult ALI media (Stem Cell Technologies) and changed every 2 to 3 days for up to 40 days.

SARS-CoV-2 culture

Vero E6 cells overexpressing ACE2 (VeroE6-hACE2) were obtained from Dr. Jae Jung and maintained in DMEM high glucose (Thermo Fisher Scientific), supplemented with 10% FBS (Thermo Fisher Scientific, Waltham, MA), 2.5 µg/ml puromycin (Thermo Fisher Scientific) at 37°C, 5% CO_2 in a humidified atmosphere in the Hastings Foundation and The Wright Foundation Laboratories BSL3 facility at USC. SARS-CoV-2 virus (BEI resources, Manassas, VA) was cultured and passaged 4 times in VeroE6-hACE2 cells and harvested every 48 hours post-inoculation. Plaque forming units (PFU) were determined using a plaque assay by infecting a monolayer of VeroE6-hACE2 cells with serial dilutions of virus stocks and layering semi-solid agar. Plaques were counted at day 3 post infection to determine PFU. Virus stocks were stored at -80°C.

SARS-CoV-2 infection

Differentiated airway epithelium at ALI was cultured with addition of 50 µl of PBS to the apical surface and incubated at 37°C, 5% CO_2 in a humidified atmosphere. After 10 minutes PBS was removed to eliminate the mucus build-up on the apical surface. The basolateral culture media was removed and replaced with 400 µl of assay media (Bronchial Epithelial Growth Media (BEGM), Lonza, Walkersville, MA), without the addition of bovine pituitary extract, hydrocortisone & GA-1000, for 1 hour prior to the addition of neutrophils. Freshly isolated neutrophils were diluted to 5 x10^6 cells/ml in Hank's Balanced Salt Solution (with $Mg2^+$ and $Ca2^+$) (Thermo Fisher Scientific) and 20 µl of this suspension was seeded onto the apical surface of the ALI cultures. Monocultures of airway epithelium and neutrophils were used as controls. The neutrophil-epithelial co-cultures were incubated for 1 hour during which they were transferred to the BSL3 facility for infection. Co-cultures were

infected with $1x10^4$ PFU of SARS-CoV-2 in 100 µl of OptiMEM (Thermo Fisher Scientific) added to the apical surface to a final MOI of 0.1 relative to neutrophils. Infected cell cultures were incubated for 4 hours at 37°C, 5% CO_2 in a humidified atmosphere. After infection, 50µl of apical and 400µl basolateral supernatants were collected, and SARS-CoV-2 was inactivated with a 10x solution of Triton-X (Sigma-Aldrich) in PBS for 1 hour to a final concentration of 1% Triton-X. Culture supernatants were stored at -20°C until required.

For neutrophil monocultures, freshly isolated CD15+ neutrophils were seeded into black walled 96 well plates (Thermo Fisher Scientific) at $2x10^4$ cells per well in 50µl Hank's Balanced Salt Solution (with $Mg2^+$ and $Ca2^+$) with or without 50 ng/ml IFNγ (Peprotech, Cranbury, NJ) for 1 hour. These plates were transferred to the BSL3 facility for infection. Neutrophil monocultures were infected 2 $x10^3$ PFU in 50 µl of OptiMEM of SARS-CoV-2 to a final MOI of 0.1. After 4 hours of infection 90µl of cell culture supernatants were collected, and SARS-CoV-2 inactivated with 10x Triton-X solution in PBS for 1 hour to a final concentration of 1% Triton-X. Culture supernatants were stored at -20°C until required.

Validation of virus inactivation

SARS-CoV-2 virus was inactivated by addition of 10% Triton-X to supernatants to generate a final concentration of Triton-X of 1% and incubating at room temperature for 1 hour. PFU was quantified using a plaque forming assay with ACE2 over-expressing Vero E6 cells (VeroE6-hACE2). Serial dilutions of SARS-CoV-2 virus were performed from a stock concentration of $1x10^5$ PFU/ml and inactivated with 1% Triton-X at room temperature for 1 hour and used to infect Vero E6 cells for a total of 4 days. Cells were monitored routinely for cytopathic effects using the Revolve microscope (Echo Laboratories, San Diego, CA).

RNA isolation and qRT-PCR

RNA was collected in 100 µl of Trizol (Thermo Fisher Scientific) per insert and incubated for 15 mins at room temperature. Cell isolates were gently mixed by pipetting up and down. An additional 900 µl of Trizol was added and cell isolates were collected and stored at -80°C until required. Cellular RNA was isolated by either phenol/chloroform extraction or using the Direct-zol RNA Microprep kit (Zymo Research, Irvine, CA). RT-qPCR was performed in 384 well plates on an Applied Biosystems 7900HT Fast Real-Time PCR system using the QuantiTect Virus Kit (Qiagen, Redwood City, CA) and SARS-CoV-CDC RUO primers and probes (Integrated DNA Technologies (IDT), Coralville, IA). Briefly, each 5 µl reaction contained 1 µl 5x QuantiTect Virus Master Mix, 500 nM forward primer, 500 nM Reverse Primer, 125 nM Probe, 10 ng DNA, 0.05 µl QuantiTect Virus RT Mix, and DNAse/RNAse-free water up to a final volume of 5 µl. Calibration curves for RNAseP primers/probe was performed with 10-fold dilutions of RNA from uninfected Calu3 cells (ATCC, Manassas, VA) from 100 ng to 0.01 ng per reaction. Calibration curves for N1 primers were performed on 5 ng of RNA from uninfected Calu3 cells per reaction spiked with 10-fold dilutions from 50 ng to 0.005 ng of RNA from Calu3 cells collected 48 hours post infection. Relative gene expression was calculated using the Pfaffl method (28).

Immunohisto-/cyto-chemistry

Primary human lung tissue from post-mortem or surgical resection donors (detailed in supplemental table S3) was fixed in 10% neutral buffered Formalin (Thermo Fisher Scientific). The tissue was then dehydrated in 70% ethanol (Thermo Fisher Scientific) prior to embedding in paraffin blocks for sectioning. Tissue sections were mounted on positively charged slides (VWR, Visalia, CA) and tissue was rehydrated through sequentially decreasing concentrations of ethanol (100% - 70%) and finally water. Slides were stained sequentially with Hematoxylin and then Eosin and imaged on the Olympus microscope IX83 (Olympus, Waltham, MA). Alternatively, tissue slides were incubated overnight at 60°C in Tris-based antigen unmasking solution (Vector Laboratories, Burlingame, CA) before permeabilization in 3% BSA, 0.3% Triton-X 100 in PBS for 1 hour and blocking in 5% normal donkey serum (Jackson ImmumoResearch, West Grove, PA) for 1 hour at room temperature. *In vitro* co-cultures were fixed in 4% PFA (Thermo Fisher Scientific) for 1 hour at room temperature and stored in PBS at 4°C to be used for immunohisto/cytochemistry. Co-cultures were then permeabilized and blocked in 3% BSA, 0.3% Triton-X 100 in PBS for 1 hour and blocking in 5% normal donkey serum (Jackson ImmumoResearch, #017-000-121) for 1 hour at room temperature. Tissue sections and *in vitro* cultures were subsequently stained with the antibodies or RNAScope probes listed in supplemental table S4. Slides were mounted in Fluoromount-G (Thermo Fisher Scientific) and imaged on a DMi8 fluorescent microscope (Leica, Buffalo Grove, IL) or a Zeiss LSM 800 confocal microscope (Zeiss, Dublin, CA).

Image analysis

5 random 20x regions were imaged for each ALI section. Sections were prepared from each of the conditions for three random donor pairings. Images were blinded, randomized and analyzed by an independent investigator. Cell frequency was determined by nuclei staining for total cells and KRT5+ staining for basal cells. Infected cells were quantified through positive SARS-CoV-2 staining within an individual cell. Signal thresholds were determined using unstained, uninfected and secondary only control-stained slides. For cell layer thicknesses, 10 random regions from each image were used to measure the thickness in µm. All images were analyzed with Image J 1.53t (Fiji, Bethesda, MD)

Trans epithelial electrical resistance

Pre-warmed assay media (200 µl) was added to the apical surface of the cultures and trans epithelial electrical resistance (TEER) was measured using an EVOM-3 meter (World Precision Instruments).

Meso scale discovery cytokine assay

50 µl of cell culture supernatants were analyzed for cytokines using the Meso Scale Discovery (MSD) Proinflammatory panel 1, Human kit, Lot:K0081459 & K0081080 (Meso Scale Diagnostics, Rockville, MD) as per the manufacturer's instructions. Briefly, 1:5 dilutions of cell supernatant samples were diluted in PBS containing 1% Triton-X. Samples were added to the MSD plate along with a 7-point 4-fold serial dilution (concentrations related to certificate of analysis for each individual standard) of protein standards diluted in PBS with 1% Triton-X. The MSD plate was sealed, and samples incubated at room temperature for 2 hours on a plate shaker (ThermoFisher Scientific) at 700RPM. The plate was washed 3x in wash buffer and 25 µl of secondary antibody was added to each well. Plates were sealed and incubated at room temperature on a plate shaker at 700RPM for a further 2 hours in the dark. Plates were washed 3x with wash buffer and 50 µl of 2x read buffer (MSD R92TC) was added to each well. The plates were read on the MESO Sector S 600 (Meso Scale Diagnostics), and concentrations determined against the standard curves.

Meso scale discovery SARS-CoV-2 spike protein assay

25 µl of cell culture supernatants were analyzed for cytokines using the MSD S-plex SARS-CoV-2 Spike Kit Lot: Z00S0021 as per the manufacturer's instructions. Briefly, plates were washed 3x in wash buffer (PBS 0.05% Tween-20) and coated with 50 µl of coating solution (1:40 dilution of Biotin SARS-CoV-2 spike antibody; 1:200 dilution of S-PLEX Coating reagent C1 in Diluent 100) and incubated at room temperature on a plate shaker at 700RPM for 1 hour. Plates were then washed 3x in wash buffer and blocked in 25 µl blocking solution (1:100 dilution of Blocker s1 in Diluent 61) per well. Samples were added to the MSD plate along with a 7-point 4-fold serial dilution (concentrations related to certificate of analysis for each individual standard) of protein standards diluted in PBS with 1% Triton-X. Plates were incubated at room temperature on a plate shaker at 700RPM for 1.5 hours. Plates were washed 3x in wash buffer and 50 µl per well of TURBO-BOOST antibody (1:200 dilution of TURBO-BOOST SARS-CoV-2 Spike antibody in Diluent 59) was added to each well and plates were incubated at room temperature on a plate shaker at 700RPM for 1 hour. Plates were washed 3x in wash buffer and 50 µl per well of Enhance Solution (1:4 dilution of S-plex Enhance E1 1:4 dilution of S-plex Enhance E2 and 1:200 dilution of S-plex Enhance E3 in molecular biology grade water) was added. Plates were incubated at room temperature on a plate shaker at 700RPM for 30 mins. Plates were washed 3x in wash buffer and 50 µl of Detection solution (1:4 dilution of S-plex Detect D1 and 1:200 dilution of S-plex detect D2 in molecular biology grade water) was added to each well. Plates were incubated at 37°C on a plate shaker at 700RPM for 1 hour. Plates were washed 3x in wash buffer and 150 µl on MSD GOLD Read Buffer B was added to each well. Plates were read immediately on an MSD 1300 MESO QuickPlex SQ 120 plate reader (Meso Scale Diagnostics) and concentrations determined against the standard curve.

Viral internalization assay

CD15+ neutrophils were seeded at 20,000 cells per well in in HBSS with or without 15 µM Cytochalasin D (Sigma Aldrich) black walled 96 well plates (Thermo Fisher Scientific) for 1 hour to allow for attachment. Cells were then infected with SARS-CoV-2 at 2 MOI (80 µl at 5x10^5 PFU/ml) for 4 hours. Cells were then washed 2 x with PBS and fixed in 4% PFA. Cells were stained for SARS-CoV-2 RNA *via* RNAScope and DAPI as per the manufacturer's instructions. Whole wells were supplemented with 50 µl of PBS post staining and well were scanned on the DMi8 fluorescent microscope (Leica, Buffalo Grove, IL). Total cell number was determined by total frequency of DAPI particles and infected cells determined by SARS-CoV-2 particle signal in proximity to DAPI. Images were analyzed with ImageJ software 1.52n (National Institute of Health, Bethesda, MD).

Data analysis and statistics

All data are presented as mean ± S.E.M. Statistical analysis is dependent upon the data set and is specifically indicated in each figure. For comparisons of 2 groups. a two-tailed unpaired Student's T-test was used. For more than 2 groups, an analysis of variance (ANOVA) was used with a *post hoc* Tukey test. Significance is determined to be $p<0.05$. All data represents a minimum of three independent biological replicates (N=3), each with 3 experimental replicates (n=3). Data was presented and analyzed using Graph Pad prism v8.4.3 (GraphPad, San Diego, CA).

All Key reagents for this study are detailed in supplemental table S5.

Results

In vitro models of neutrophilic airways have significant, polarized inflammatory responses to SARS-CoV-2 infection

Given the prevalence of neutrophilia in the airways of patients with chronic airway disease (29) and its association with other SARS-CoV-2 co-morbidities, such as hypertension (30, 31), the impact of chronic neutrophilic airway inflammation in the initial

stages of SARS-CoV-2 infection was evaluated. We adapted a neutrophilic airway *in vitro* model, previously described by Deng and colleagues (26), co-culturing $CD15^+$ peripheral blood polymorphonuclear leukocytes (PMNs) with primary HBECs differentiated at the ALI and infected these cultures with live SARS-CoV-2 virus for 4 hours, shown in the schematic in Figure 1A. This 4-hour time point allows for profiling of the initial stages of infection and acute phase cellular viral response, i.e., neutrophil degranulation. The short time frame for analysis was chosen to eliminate significant viral replication and thus anticipate any detectible intracellular viral load is because of the initial infection (32). It also allows for optimal investigation into neutrophil function without loss of viability interfering with the assays due to the relatively short half-life of neutrophils. Prior to infection we confirmed the expression of ACE2 and Transmembrane Serine Protease 2 (TMPRSS2) in our *in vitro* airway epithelium models (Supplementary Figure S1). While ACE2 RNA was relatively low in expression across basal, secretory and multiciliated cells (Supplementary Figure S1A-C) at the protein level a predominant colocalization was detected with multiciliated cells in the airways (Supplementary Figure S1A, D-F). This data is supported by similar analysis of human lung tissues (Supplementary Information) and Supplementary Figure S2) where we observed a similarly low level of expression in RNA in basal, secretory and multiciliated cells (Supplementary Figure S2A-B) while protein, detected by IF, was associated with multiciliated cells and cells in submucosal glands (Supplementary Figure S2C-F). Confirmation of ACE2 expression at the RNA and protein level in human lung tissues and our *in vitro* model supports currently published data evaluating ACE2 in human lung tissue (33–35).

In our model system the apical side of the epithelium predominantly comprises of multiciliated, and secretory cells directly exposed to neutrophils and the virus, the basolateral side predominantly comprises of basal cells. To understand the immediate inflammatory response of the airway epithelium to SARS-CoV-2 infection we evaluated both the apical and

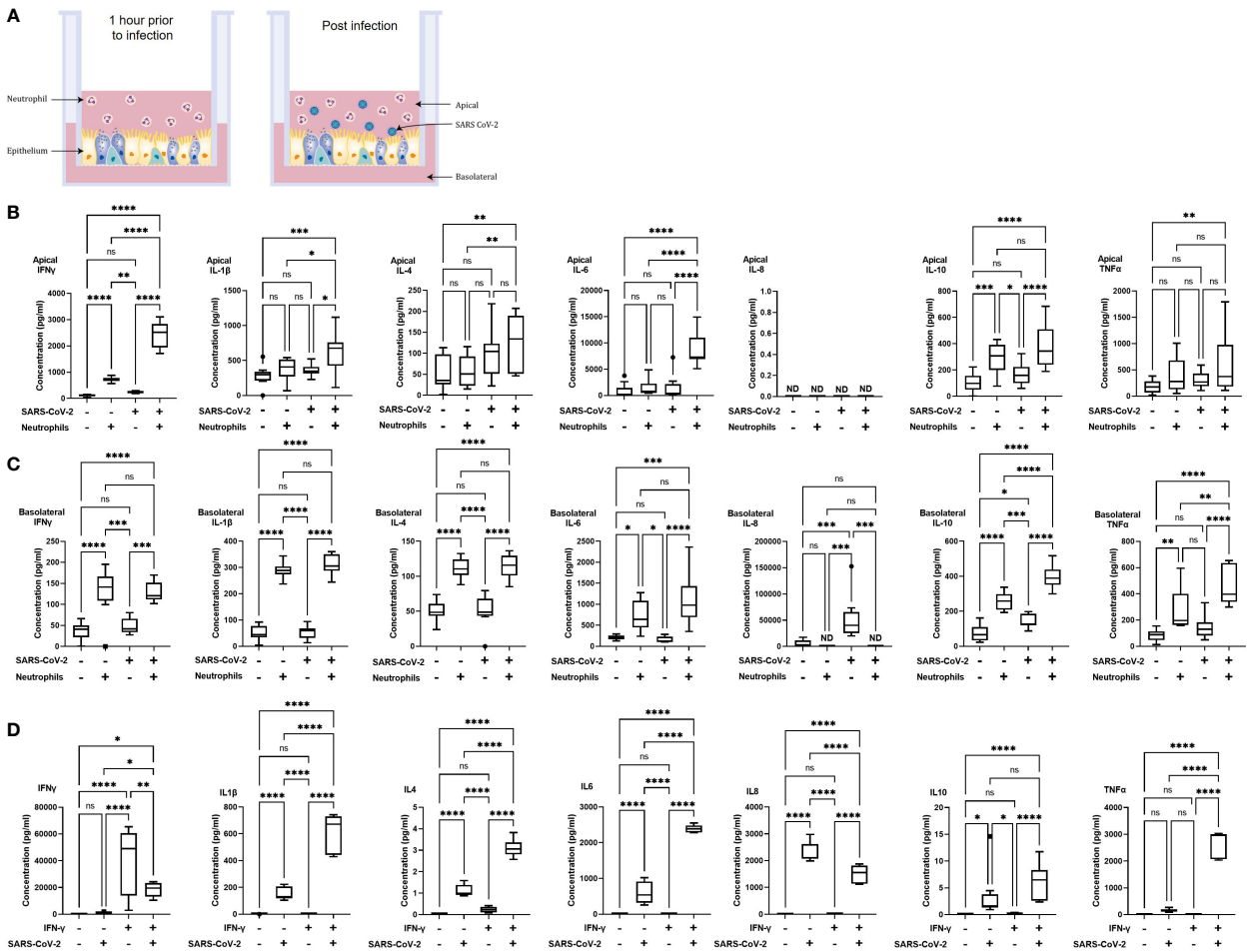

FIGURE 1
Polarized inflammatory response of neutrophils in co-culture with human airway epithelium, infected with SARS-CoV-2. **(A)** Schematic of the *in vitro* model of neutrophilic airways denoting neutrophils in co-culture with differentiated airway epithelial cells and infected with live SARS-CoV-2 virus. Inflammatory profiles of apical **(B)** and basolateral **(C)** supernatants collected 4 hours post infection in the neutrophilic airway model. **(D)** Inflammatory profile of naïve or IFN-γ (50ng/ml 1 hour) neutrophil monocultures infected with SARS-CoV-2 virus for 4 hours. Data is expressed as Tukey method box & whiskers plots. Significance is determined by analysis of variance (ANOVA) followed by Tukey's *post hoc* analysis. *p<0.05,**p<0.01, ***p<0.001, ****, <0.0001 from n=3 experimental repeats from N=3 donors. ns, not significant, ND, not done as an experiment.

basolateral cell culture supernatants using the MSD cytokine assay. All experiments were carried out using three independent HBEC donors and three independent neutrophil donors ensuring significant biological variability in our model system. As shown in Figures 1B, C a differential inflammatory profile exists between the apical and basolateral compartments. Focusing first on the apical cytokine and chemokine release, in the absence of neutrophils there were, surprisingly, no significant changes in cytokine release from the airway epithelial cells upon SARS-CoV-2 infection (Figure 1B). The addition of neutrophils to the model, creating a neutrophil-epithelial co-culture in the absence of any infection, resulted in a significant secretion of interferon gamma (IFNγ) ($p<0.01$) and IL-10 ($p<0.01$) at the apical surface with notable, but not statistically significant, increases in tumor necrosis factor alpha (TNFα) (Figure 1B). In the airway only cultures, only the basolateral release of interleukin-8 (IL-8, $p<0.001$), and IL-10 ($p<0.05$) were significantly changed in response to SARS-CoV-2 infection (Figure 1C). As IL-8 is a major chemoattractant for neutrophils this suggests that the basolateral surface responds to viral infection by releasing IL-8 to recruit neutrophils to infection site (36–38). The addition of neutrophils to the airway stimulated the release of IFNγ ($p< 0.05$) and IL-10 ($p<0.01$) apically (Figure 1B) and additionally, significantly increased the release of IFNγ ($p< 0.0001$) IL-1β ($p<0.0001$), IL-4 ($p<0.0001$), IL-6 ($p<0.05$), IL-10 ($p<0.0001$) and TNFα ($p<0.01$) from the basolateral surface (Figure 1C). Interestingly, the presence of neutrophils did not stimulate significant changes in IL-8 secretion from the basolateral surface supporting the role for IL-8 in the recruitment phase of airway neutrophilia, already established in our neutrophilic airway model (Figure 1C) (39, 40). This data demonstrates that a pro-inflammatory niche is driven primarily by the neutrophils, likely though degranulation. Based on this information we added neutrophils to our airway epithelium to create a pro-inflammatory niche recreating aspects of chronic airway inflammation in the human lung in an *in vitro* model.

Infection of the neutrophilic airway models with live SARS-CoV-2 virus was compared directly to both the infection in the absence of neutrophils and the neutrophilic airway in the absence of infection. Changes in inflammatory cytokine release from both the apical and basolateral surfaces was significantly augmented compared to both the infected epithelial monocultures and the non-infected co-cultures, demonstrating an exacerbation of pro-inflammatory cytokine release in the infected co-cultures (Figures 1B, C). Compared to the infected epithelial monocultures, infection of the co-culture model resulted in a significant increase in the apical secretion of IFNγ ($p<0.0001$), IL1-β ($p<0.05$), IL-6 ($p<0.0001$) and IL-10 ($p<0.001$) (Figure 1B) and in the basolateral secretion of IFNγ ($p<0.05$), IL-4, IL-6 both ($p<0.0001$), IL1-β, IL-10 and TNFα (all $p<0.001$) (Figure 1C). Compared to the uninfected neutrophil-epithelial co-cultures, co-culture infection resulted in a significant increase in the apical secretion of IFNγ, IL-6 (both $p<0.0001$) IL1-β and IL-10 (both $p<0.05$) and in the basolateral secretion of IFNγ, IL-10 (both $p<-.001$), IL-1β, IL-4, IL-6 and TNFα (all $p<0.0001$) (Figure 1B). The only instance where TNFα was significantly changed in the apical supernatants was in the infected co-cultures increased when compared to uninfected epithelial cell monocultures ($p<0.01$). This data supports a significant augmentation of the inflammatory response to SARS-CoV-2 infection occurs in the presence of pre-existing airway neutrophilia. Importantly, this secretion profile closely reflects the cytokine biomarkers that have been clinically identified in patients hospitalized with severe COVID-19 disease (41–43), highlighting the importance of the co-culture models in recapitulating features associated with more severe responses to SARS-CoV-2 and demonstrating a role for neutrophils in the inflammatory profile observed in patients with severe COVID-19.

The innate reactivity of neutrophils in isolation was evaluated independently of the co-culture model. We noted a significant apical increase in IFNγ in the co-cultures in the absence of any stimulation or infection (Figure 1B). As IFNγ is a known activator of neutrophils we evaluated inflammatory cytokine release from neutrophils pre-stimulated with IFNγ in response to SARS-CoV-2 infection using naïve neutrophils as controls to determine whether there was innate recognition of SARS-CoV-2 by neutrophils. Initially we assessed the response of naïve, non-activated neutrophils to SARS-CoV-2 infection. Very small, <1 pg/ml, responses from naïve neutrophils, in the absence of infection or stimulation, was observed for all cytokines assessed except for IL-8. An increase in IL-8 secretion was observed, however this increase equates to an increase of <0.1% of the response to infection. In infected naïve neutrophils, significant increases in cytokine release of IL1-β, IL-4, IL-6, IL-8 (all $p<0.001$) and IL-10 ($p<0.05$) was noted compared to uninfected controls (Figure 1D). Uninfected neutrophils activated with IFNγ produced no significant cytokine release compared to naïve uninfected neutrophils. The observed increase in IFNγ was likely due to the exogenous recombinant IFNγ used to activate the neutrophils and not a response of the neutrophils. Activation of neutrophils with IFNγ produced significant increases in IL-1β, IL-4, IL-6, IL-8, IL-10 and TNFα (all $p<0.0001$). It is worth noting that there was also a significant ($p<0.01$) decrease in IFNγ from the infected neutrophils activated with IFNγ; the presence of exogenous recombinant IFNγ complicates interpretation of this finding (Figure 1D). Finally, we compared IFNγ activated neutrophils with naïve neutrophils after SARS-CoV-2 infection. IFNγ ($p<0.05$), IL-1β, IL-4, IL-6 and TNFα (all $p<0.0001$) were all significantly increased and IL-8 significantly decreased ($p<0.0001$) (Figure 1D). This data demonstrates that naive neutrophils have an innate recognition of SARS-CoV-2 in the absence of any activation and highlight an exacerbation of the response in IFNγ activated neutrophils.

Increased SARS-CoV-2 infection of the airway epithelium is associated with neutrophilia and disruption of epithelial barrier integrity

To determine whether a proinflammatory niche, such as that observed in the presence of pre-existing neutrophilia, impacts epithelial barrier integrity and viral load of the epithelial cells we evaluated barrier resistance and viral content of the airway epithelium. TEER was recorded at 4 and 24 hours after introduction of neutrophils to the airway epithelium. The presence of neutrophils significantly reduced the TEER and,

therefore, epithelial barrier integrity, by 23 ± 9%, ($p<0.05$) after 4 hours. This reduction in TEER was sustained through 24 hours (22 ± 4%, $p<0.05$), all data are compared to epithelial monocultures (Figure 2A). Evaluation of intracellular viral load by qRT-PCR for SARS-CoV-2 nucleocapsid RNA in the epithelial cells under the same conditions indicated a concurrent and significant increase in infection after the addition of neutrophils by 3.1 ± 1.1-fold ($p<0.05$) (Figure 2B). In the absence of infection, no SARS-CoV-2 RNA was detected (data not shown). To determine if the change in epithelial barrier function allowed for increased passage of viral particles from the apical to basolateral surface of the airway epithelium, we also evaluated SARS-CoV-2 spike protein expression in the supernatants (Figures 2C-D). The presence of neutrophils significantly decreased the apical viral load from 69204 ± 9200.1 fg/ml to 6655.6 ± 475.61 fg/ml ($p<0.01$) (Figure 2C) with a concurrent increase in the basolateral viral load from 488.23 ± 129.12 fg/ml to 2307.7 ± 238.94 fg/ml ($p<0.01$) (Figure 2D). This data shows that the presence of neutrophils is allows for increased migration of virus from the apical to the basolateral surface. To determine whether the physical presence of neutrophils is essential or whether the pro-inflammatory cytokines released from neutrophils in epithelial co-cultures (Figure 2) and stimulated by SARS-CoV-2 infection, could induce similar changes in epithelial barrier function, we supplemented the culture media with IFNγ (10 ng/ml), IL-1β (10 ng/ml), IL-6 (10 ng/ml) and TNFα (10 ng/ml) (referred to as cytomix). In the presence of cytomix TEER decreased after 4 hours (18 ± 7%, not significant) with a further and significant decline of 30 ± 5%, $p<0.05$ after 24 hours (Figure 2E). This decrease in TEER corresponded to an increase in viral infection of the airway epithelium (2.6 ± 0.5-fold, $p<0.05$) in the presence of cytomix (Figure 2F). Reflecting the observations in the presence of neutrophils the apical concentrations of SARS-CoV-2 were decreased from 76703 ± 8708.7 fg/ml to 35261 ± 3598.7 fg/ml ($p<0.05$) and basolateral concentrations increased from 479.87 ± 129.21 fg/ml to 12344 ± 906.62 fg/ml ($p<0.001$). This data supports the hypothesis that pro-inflammatory cytokines secreted by neutrophils allow for increased transition of virus from the apical to basolateral surfaces of the airway epithelium.

Neutrophils increase SARS-CoV-2 infection of the epithelium including basal stem cells

To investigate changes in airway pathology associated with SARS-CoV-2 infection we evaluated co-localization of SARS-CoV-2 virus in the presence or absence of neutrophils. Analysis of the airway structure by hematoxylin and eosin (H&E) highlights significant changes in pathology in the presence of neutrophils (Figures 3A-D). We use KRT5 as a marker to identify the sub-apical basal cell layer from the pseudostratified differentiated epithelium.

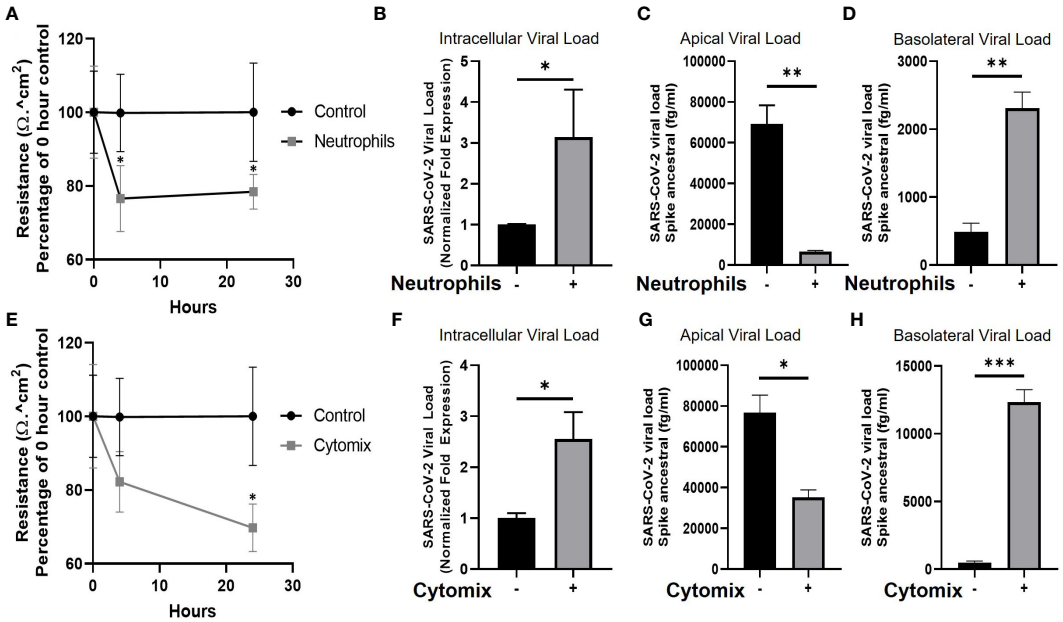

FIGURE 2
Neutrophils and pro-inflammatory cytokines break down the epithelial barrier and increase viral load in human airway epithelial cells. **(A)** TEER of human airway epithelial cells at the air-liquid interface in the presence, or absence (control), of neutrophils. **(B)** Intracellular viral load of SARS-CoV-2 RNA isolated from infected human airway epithelial cells with neutrophils present. **(C)** Apical supernatant SARS-CoV-2 spike protein concentration 4 hours post infection with neutrophils present. **(D)** Basolateral supernatant SARS-CoV-2 spike protein concentration 4 hours post infection with neutrophils present. **(E)** TEER of human airway epithelial cells cultured with a "cytomix" of TNFα, IL-1β, IL-6 and IFN-γ each at 10ng/ml. **(F)** Intracellular viral load of SARS-CoV-2 in airway epithelial cells cultured with cytomix. **(G)** Apical supernatant SARS-CoV-2 spike protein concentration 4 hours post infection from epithelial cells cultured with cytomix. **(H)** Basolateral supernatant SARS-CoV-2 spike protein concentration 4 hours post infection from epithelial cells cultured with cytomix. Data are expressed as mean ± SEM. Statistical significance of TEER data was determined by ANOVA and viral load data was analyzed using an unpaired two-tailed Student's t-test. *p<0.05, **P<0.01, ***p<0.001. Experiments include n=3 experimental repeats of N=3 independent epithelial donors paired with 3 independent neutrophil donors.

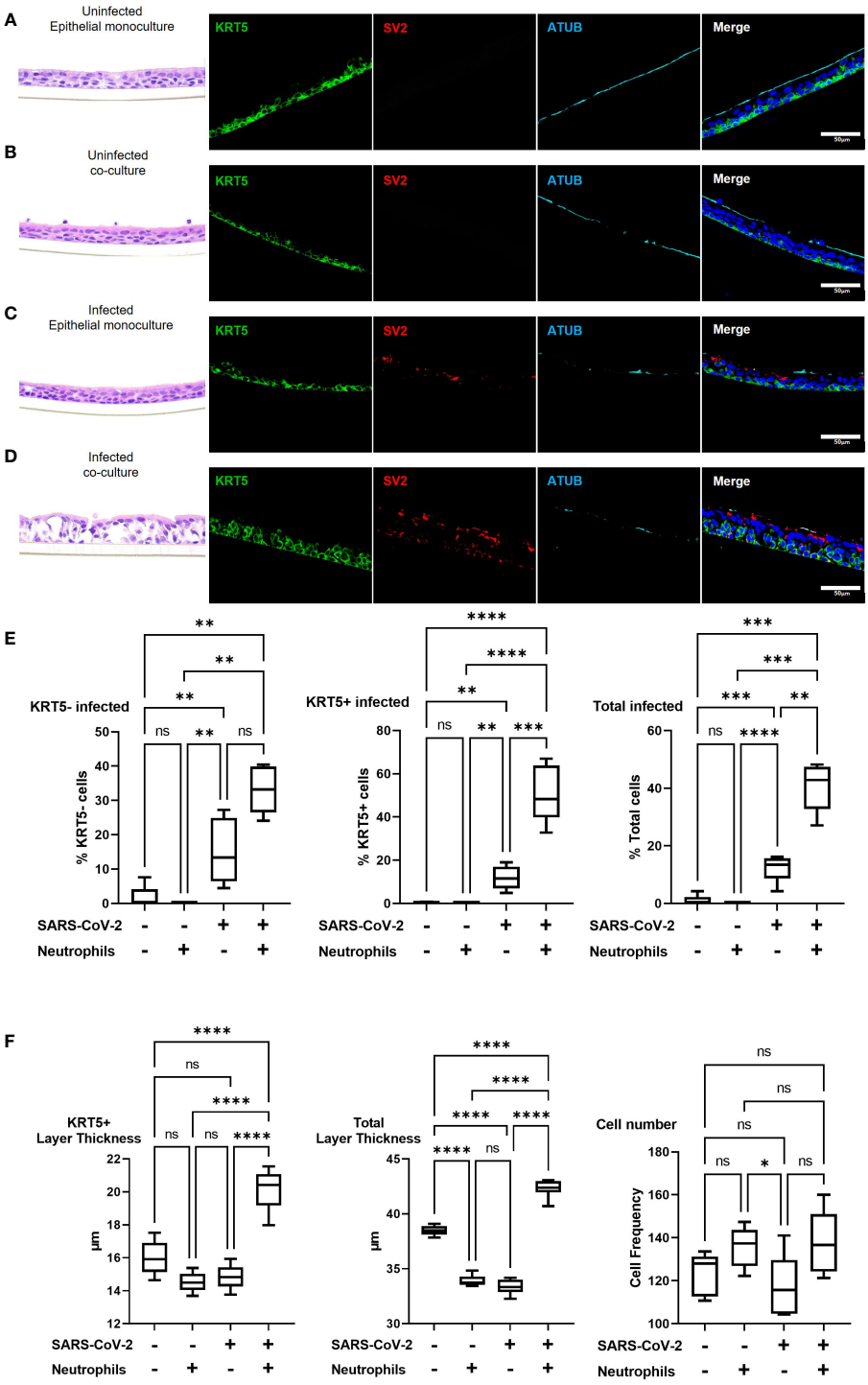

FIGURE 3
Pre-existing neutrophils allow for SARS-CoV-2 infection of KRT5+ Basal cells. a-d representative hematoxylin and eosin (H&E) staining and immunofluorescent images of cross section culture models probed for KRT5 (green) SARS-CoV-2 (red) and alpha-tubulin (cyan). **(A)** uninfected monocultured epithelial cells. **(B)** uninfected epithelial:neutrophil co-cultures. **(C)** SARS-CoV-2 infected epithelial cell monoculture. **(D)** SARS-CoV-2 infected epithelial:neutrophil co-cultures. All IF images have nuclei counterstained with DAPI (blue) and scale bars represent 50 µm. **(E)** Image analysis quantification of infected KRT5-, KRT5+ and total cells. **(F)** Image analysis of cell layer thickness for KRT5+ Cells and Total cells All images are representative of 3 independent experimental repeats of 3 neutrophil and 3 epithelial random donor pairings. Data is expressed as Tukey method box & whiskers plots. Significance is determined by analysis of variance (ANOVA) followed by Tukey's *post hoc* analysis. *p<0.05,**p<0.01, ***p<0.001, **** p<0.0001 from n=3 experimental repeats from N=3 donors. ns, not significant.

In the absence of neutrophils and infection the airways comprise of a typical airway epithelium with KRT5+ basal cells residing on the basolateral surface and ciliated cells lining the airway lumen (Figure 3A). Despite the presence of pro-inflammatory cytokines produced by the neutrophils, epithelial cells appear to tolerate the presence of neutrophils, which can be observed near the apical ciliated cells in the culture model (Figure 3B). In an airway without neutrophils, the epithelial cells are capable of tolerating infection by SARS-CoV-2 after 4 hours of exposure with little evidence of cellular pathology by H&E and only sporadic infection observed in the columnar epithelial cells (Figure 3C and Supplemental Figure S3). Most notably, in the presence of neutrophils, significant cellular pathology is observed by H&E, with evidence for thickening of the basal cell layer, indicative of basal cell proliferation (Figure 3D). Furthermore, SARS-CoV-2 infection in epithelium is more widespread across the entire epithelial layer with KRT5+ basal cells also being infected (Figure 3D and Supplementary Figure S3). To corroborate these findings, we quantified infected KRT5+ basal cells and KRT5- differentiated epithelial cells using blinded image analysis by an independent investigator (Figure 3E). The infection rate in total epithelial cells increased ($p<0.01$) in the presence of neutrophils when compared to monoculture controls. The infection rates increased in KRT5- differentiated epithelium (i.e., ciliated, goblet and club cells) (not significant) and in KRT5+ basal cells in the presence of neutrophils ($p<0.001$). As demonstrated by the H&E staining in Figure 3D, infection in the presence of neutrophils caused significant cellular pathology compared to uninfected controls or infected airways in the absence of neutrophils. To quantify this, we also measured the thickness of the KRT5+ cellular layer and total cell layer and counted the total cells as part of our image analysis. In response to SARS-CoV-2 infection in the presence of neutrophils, the KRT5+ layer thickness increased ($p<0.0001$) and the total cellular layer increased to ($p<0.0001$) compared to uninfected epithelial layer monocultures. Overall, there were no significant changes in total cell numbers, suggesting that the change in thickness is a result of epithelial cellular pathology and remodeling rather than cell proliferation (Figure 3F). Interestingly, we observed a small, but significant decrease in total layer thicknesses in uninfected co-cultures ($p<0.0001$) and infected monocultures ($p<0.0001$) compared to the uninfected monoculture control. In our model system, neutrophils drive significant cellular pathology in response to infection by SARS-CoV-2. Infection of basal cells at such a short timepoint is likely to have significant implications on their function and subsequently airway regeneration.

Airway epithelial pathologies are associated with neutrophil activity in severe COVID-19

The data presented from our *in vitro* models suggests that neutrophils play a role in the pathophysiology of early-stage epithelial infection in COVID-19. To further investigate continued neutrophil related pathologies in severe COVID-19 we evaluated epithelial cell related damage and neutrophil activity in post-mortem human tissues from COVID-19 subjects. Formalin-fixed paraffin embedded (FFPE) tissue sections from two post-mortem COVID-19 subjects, kindly provided by the autopsy service at the University of Vermont Medical Center (UVMMC) were assessed for infection-related pathologies through H&E staining. Pathologies were determined by an independent pathologist to be consistent with severe ARDS with mixed inflammatory cell infiltrates, inclusive of neutrophils, and organizing pneumonia (Figures 4A-D). Tissues from patient Au20-39 (detailed in supplementary table S1) contained a mild infiltrate of chronic inflammatory cells surrounding the bronchiole and arterial tissues with involvement in the adjacent surrounding alveolar tissue (Figure 4A and Supplementary Figure S4A). Scattered giant cells were identified in alveolar spaces and within the interstitium (Figure 4B, indicated by the red arrows and Supplementary Figure S4B). No well-formed granulomas or definite viral inclusions were evident in this patient. Images from the second patient; Au20-48 (Supplementary Table S3) also show severe organizing diffuse alveolar damage with evidence of barotrauma (Figure 4C and Supplementary Figure S4D). Alveolar spaces are lined by hyaline membranes or filled with polyps of organizing pneumonia and chronic inflammation (Supplementary Figure S4D). Alveolar walls are expanded with edema and a mixed inflammatory cell infiltrate including neutrophils (Supplementary Figure S4C-D). Bronchioles demonstrate chronic injury with peribronchiolar metaplasia and early squamous metaplasia (Figure 4D and Supplementary Figure S4C). Organizing pulmonary emboli are present in several arteries (Supplementary Figures S4C, D). There are frequent rounded airspaces lined by inflammatory cells and giant cells, consistent with barotrauma from ventilation injury (Supplementary Figure S4D). There are also scattered giant cells in the interstitium not associated with the barotrauma (Supplementary Figures S4C, D). Given the extensive infiltration of inflammatory cells, inclusive of neutrophils, we further evaluated the neutrophil-related epithelial tissue pathology in both patients. An array of airway tissue pathologies was evident in both tissues including 1) basal cell hyperplasia and small airway occlusion (Figure 4E), 2) epithelial damage and tissue remodeling of smaller ciliated airways (Figure 4F), 3) epithelial shedding of large cartilaginous airways (Figure 4G), 4) neutrophil invasion into the airway lumen (Figure 4H). and finally, 5) neutrophil invasion in the alveolar space with associated alveolar tissue damage and remodeling (Supplementary Figure S4e). In each of these examples, neutrophils were detected and frequently demonstrated strong neutrophil elastase (NE) activity (Figure 4E-I), and myeloperoxidase (MPO) expression (a common neutrophil marker) is frequently observed around centers of SARS-CoV-2 infection in postmortem COVID-19 tissues (Supplementary Figure S4F-G). We also observed sporadic formation of neutrophil extracellular traps (NETs) that stained for SARS-CoV-2 (Supplementary Figure 4G). From this data we conclude that neutrophils are a core part of the COVID-19 lung pathophysiology and significantly impact airway infection and injury in response to SARS-CoV-2 infection.

Phagocytosis of SARS-CoV-2 is the predominant mechanism of viral internalization in neutrophils

As previously mentioned, airway diseases, such as CF, that are co-morbidities for severe SARS-CoV-2 infection and progression to severe COVID-19, are also associated with significant infiltration of the airways with neutrophils (Supplementary Figure S5A-B). Interestingly, the neutrophils also colocalized with strong ACE2 expression (Supplementary Figure S5). Despite having significant ACE2 expression our data suggests that internalization of the virus in neutrophils is likely through phagocytosis. The apical concentration of SARS-CoV-2 in the presence of neutrophils was significantly smaller than the apical concentrations of SARS-CoV-2 in the presence of cytomix (Figure 4C, G) at 6655.65 ± 475.61 fg/ml compared to 35260.93 ± 3598.7 fg/ml, $p<0.01$. This suggests that viral clearance is taking place by the neutrophils in their functional role as professional phagocytes. In our experiments SARS-CoV-2 viral RNA was detected in the co-cultures by RNAscope confirming infection of the airway epithelium (Figure 5A). Interestingly, NE

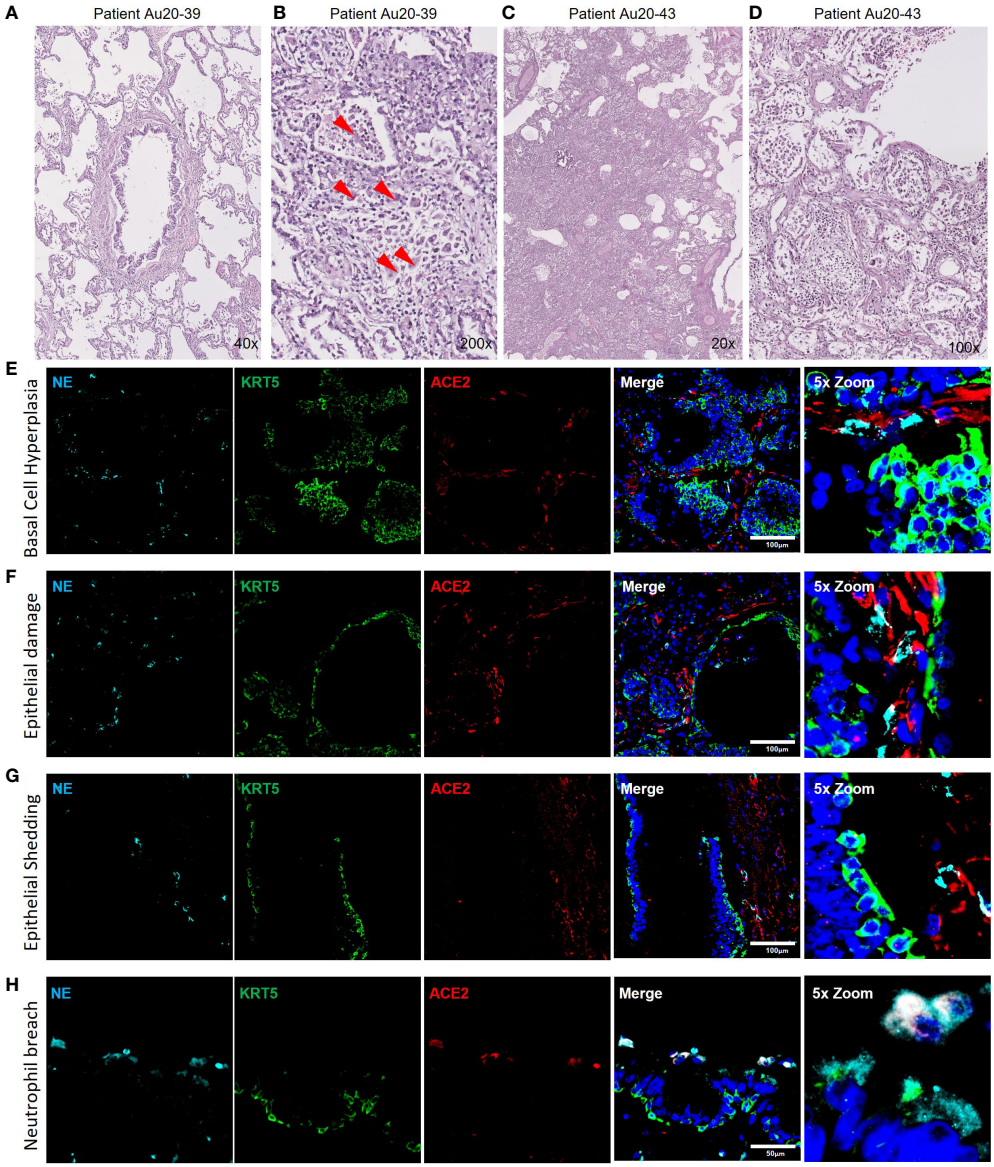

FIGURE 4
Neutrophil associated tissue pathology in post-mortem COVID19 human lung airways. a-d) Representative images of hematoxylin and eosin (H&E) staining of postmortem COVID-19 patient tissues showing patchy organizing pneumonia centered around a major artery and an airway **(A)**; focally expanded interstitium by a mixed cellular infiltrate including scattered giant cells (red arrowheads) **(B)**; diffuse alveolar damage from intense fibroinflammatory process and barotrauma induced rounded airspaces **(C)** and organizing diffuse alveolar damage with fibrin disposition replaced by organizing pneumonia, inflammatory cells and oedema **(D)**. **(E-H)** Representative IF images of postmortem COVID-19 tissue probed for NE (cyan), KRT5 (green) and ACE2 (red). Images highlight; small airway occlusion resulting from basal cell hyperplasia with surrounding neutrophils present **(E)**; epithelial damage with breaching neutrophils into the luminal space **(F)**; epithelial shedding, inclusive of basal cell layer with neutrophil inclusion of mucosal surface **(G)**; neutrophil breach into airway luminal space with high neutrophil elastase activity **(H)**. All IF images have nuclei counterstained with DAPI (blue) and scale bars represent 100 µm. All images are representative of 3 independent regions per donor at least 2 independent donors.

activity was heavily centered around sites of SARS-CoV-2 infection synonymous to that observed in post-mortem patient tissues (Supplementary Figure S4F), and internalization of SARS-CoV-2 by neutrophils was also confirmed by co-localization of staining for NE and SARS-CoV-2 viral RNA (Figure 5A) *in vitro*, indicated by the orange arrows.

Finally, to determine whether the expression of ACE2 protein in neutrophils has a significant impact in the response of neutrophils to SARS-CoV-2, we evaluated whether neutrophils were being actively infected *via* a physical interaction of ACE2 and SARS-CoV-2 or functionally phagocytosing the SARS-CoV-2 virus. The decrease in apical spike protein concentrations when neutrophils are present, compared to epithelial cell monocultures, suggests that the neutrophils are clearing the virus at the apical surface through innate pattern recognition phagocytosis. To better understand this, the frequency of SARS-CoV-2 internalization in monocultures of neutrophils was quantified in the presence or absence of cytochalasin D (15 µM) to inhibit phagocytosis (Figure 5B). The number of neutrophils positive for SARS-CoV-2 RNA, reflecting viral internalization relative to the total number of neutrophils, was calculated after infection of the cells with SARS-CoV-2 (MOI = 2). Infection, detected by RNA scope, occurred at a rate of 7.9 ± 1% of neutrophils in culture. This signal was significantly reduced by from 7.9 ± 1% to 1.3 ± 0.3% in the presence of cytochalasin D (Figure 5C). Disruption of the actin cytoskeleton, a core component of phagocytosis, therefore, significantly reduced viral uptake in neutrophils. This suggests the primary mechanism for SARS-CoV-2 internalization in neutrophils is phagocytosis.

Discussion

It is well established that neutrophils are critical in the development of pathological inflammation which can result in both acute and chronic tissue damage. Evaluation of post-mortem COVID-19 tissues indicated significant neutrophil presence and activation in regions of airway epithelial damage and pathology. In addition, we know that many SARS-CoV-2 co-morbidities, including chronic airway disease (29, 44), aging (45–47) and obesity (48–50), are also associated with chronic airway inflammation. In this study we developed a model of pre-existing airway neutrophilia akin to a model previously developed to investigate other respiratory viruses (26) and applied this to investigate the initial stages of SARS-CoV-2 airway infection. Using this model, we were able to conclude that the pre-existing presence of neutrophils in airway epithelium generates a pro-inflammatory niche, significantly augments initial proinflammatory responses to SARS-CoV-2 infection, increases viral load in basal stem cells and decreases airway epithelial barrier integrity. Our data, therefore, supports a key role for neutrophilic airway inflammation in determining the infectivity and outcome measures of COVID-19.

Establishing a primary cell co-culture model of an inflammatory airway overcomes some of the limitations of using immortalized cell lines and more complex *in vivo* models. While *in vivo* models are perhaps considered gold standard in infection models, they have not been observed to closely mimic human lung pathophysiology, particularly with respect to SARS-COV-2. While infection can be detected, no animal model had closely reflected COVID-19 pathogenesis that leads to severe symptoms and fatal lung disease (5, 51). Furthermore, studying neutrophilia in animal models is challenging, several depleted or knockout models exist (52), however evaluation of elevated lung neutrophilia typically requires pro-inflammatory stimulation with lipopolysaccharide (LPS) (53), this could complicate interpretation of findings in relation to viral infection. Our models use primary HBECs, some of the first cells exposed to inhaled viral particles, that express endogenous levels of ACE2 and TMPRSS2. This allowed for investigation of the initial stages of SARS-CoV-2 infection and characterization of acute phase inflammatory responses.

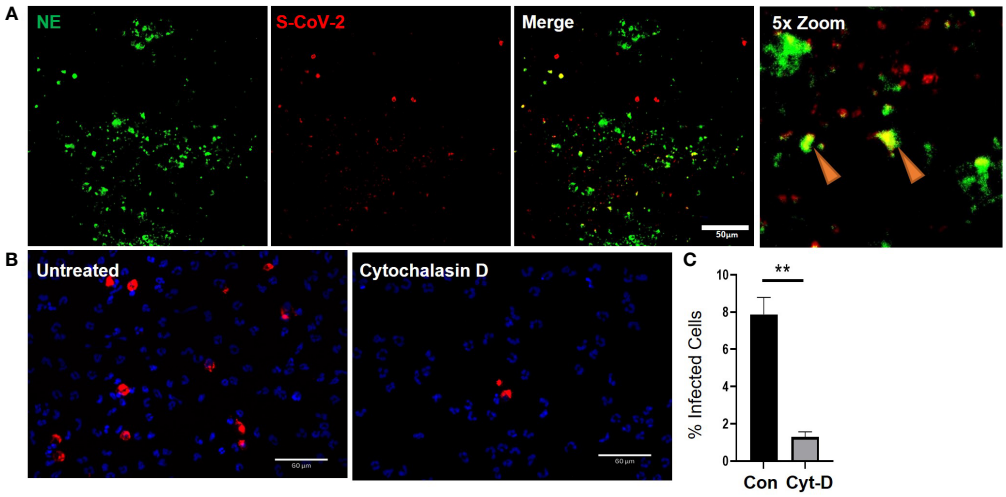

FIGURE 5
Cytochalasin D inhibits internalization of SARS-CoV-2 in neutrophils. a) Representative IF images of ALI cultures probed for neutrophil elastase (NE) (Green) infected with SARS-CoV-2 (red) detected by RNAScope. b) Quantification or SARS-CoV-2 positive neutrophils relative to total number of neutrophils determined by DAPI (blue). Data expressed as mean ± SEM. **p<0.01 unpaired 2-tailed Student's T-test. N=3 independent neutrophil donors, n=3 experimental replicates.

Neutrophil phenotype and function, including those involved in resolving viral infections, is strongly regulated by signals received from their tissue micro-environment (54), in our study we considered neutrophil responses in the presence of an epithelial micro-environment. Our model mimics components of neutrophilic airway inflammation associated with other chronic lung diseases that have been linked with a predisposition to developing more severe COVID-19 disease. Perhaps our most striking finding is the presence of a differential polarized inflammatory response in response to neutrophils and/or SARS-CoV-2. IL-8, the core chemoattractant for neutrophils (36–38, 55), is secreted only on the basolateral surface of the epithelial monocultures, demonstrates that epithelial cells are capable of recognizing neutrophils within their niche and downregulate this chemokine secretion as a result and that the model recapitulates the directionality required to recruit circulating neutrophils into an infected epithelial environment. Furthermore, despite seeding neutrophils on the apical surface of our model, we observed a predominant pro-inflammatory basolateral niche, with increases in IL-1β, IL-4, IL-6 and TNFα. Through paired comparisons to primary airway epithelial cells in monoculture, we were able to demonstrate key differences in the secretion of pro- (IFNγ, IL1β, IL-6, IL-8 and TNFα) and anti-inflammatory (IL-4 and IL-10) mediators, epithelial barrier integrity and infectivity of epithelial cells (Figures 1, 2), which would have been over-looked in monoculture experiments involving airway infection only. Importantly, the secretion of pro-inflammatory cytokines in our model is consistent with clinical studies that have reported an elevated inflammatory profile associated with severe COVID-19 disease. In patient peripheral blood samples, IL-6 (56–59) IL-10 (57, 58) are consistently higher in COVID-19 patients and correlate with disease severity. Additionally, IL-6 and IL-8 are even higher in ICU than the IMU (60). Our data also closely mimics responses observed in primate models of the disease (61). The lack of robust inflammatory response of the epithelium alone may also provide rational for why some people are predisposed to more severe responses than others. In fact, our data evaluating the response of the more proximal, cartilaginous airways may highlight the importance of a robust proximal airway defense mechanism that controls the progression to severe COVID-19 associated with ARDS and distal airway dysfunction.

IFNγ is a known activator of neutrophils (62) and widely studied in virology (63, 64). In addition to IL-10, IFNγ was the only other cytokine increased apically after inclusion of neutrophils in the cultures creating a pro-inflammatory niche. We therefore assessed if IFN activation of neutrophils was required for innate recognition of SARS-CoV-2. We found that IFN activated neutrophils exacerbated their inflammatory response to SARS-CoV-2, however naïve neutrophils still recognized and responded to SARS-CoV-2 (Figure 1D). There are caveats to our neutrophil monoculture analysis. IL-4 and IL-10 concentrations are so low that whilst the assay is sensitive enough to detect such small concentrations it is questionable whether these concentrations would have any significant biological impact. Further, exogenous IFNγ used to activate the neutrophils clearing had a downstream impact in the IFNγ measure in our assay, however, Interestingly we did observe a significant decrease in IFNγ concentration in the IFNγ-treated neutrophil monocultures after SARS-CoV-2 infection (Figure 1D). IFNγ has direct anti-viral mechanisms (63) which may account for a reduction in its expression in the presence of SARS-CoV-2.

Pro-inflammatory cytokines, including IFNγ, IL-1β, IL-6 and TNFα, have extensively been shown to disrupt barrier integrity and permeability of the epithelium (65, 66). This breakdown in barrier integrity exists to allow for leukocyte migration to sites of stress and infection. Theoretically, any tight-junction breakdown that allows for more leukocyte migration, would also allow for increased permeability for viral particles to sub-apical and sub-epithelial structures, thus increasing infectivity and cellular viral loads. Our data supports this phenomenon with both neutrophils and cytomix synonymously decreasing barrier integrity (Figure 2) whilst increasing intracellular viral loads and virus concentrations in sub-apical compartments. This association of epithelial barrier integrity with an increase in intracellular epithelial viral loads, especially in the basal stem cells, suggests that epithelial barrier integrity plays an important functional role in SARS-CoV-2 infection. The changes in airway gross pathology are indicative of responses to neutrophil degranulation and are likely a result of increased reactive oxidative species (ROS) production, we are continuing work to define the mechanisms of action.

Finally, we addressed the key question of whether neutrophils, as professional phagocytes (67, 68), are capable of recognition of SARS-CoV-2 as an invading pathogen through innate recognition pathways, and/or are capable of infection by SARS-CoV-2 through ACE2. Our data supports a high level of expression of ACE2 at the protein level, but not the RNA level in neutrophils; an observation recently reported by Veras and colleagues (23). Furthermore, infection is facilitated by TMPRSS2, and we did not see any evidence for expression on neutrophils by RNA and protein (data not shown). Using cytochalasin D to breakdown actin filament organization we significantly reduced virus internalization, supporting a predominant role for phagocytosis in the internalization of SARS-CoV-2 in neutrophils. Reports are, however, emerging that suggest a significant role for cytoskeletal rearrangement in SARS-CoV-2 entry and, therefore, we cannot entirely rule out infection (69). The use of blocking antibodies has potential to elucidate the mechanisms of internalization, however, neutrophils express copious amounts of Fc receptors (70) and likely to recognize antigens and opsonize through phagocytosis. Our assay attempted to investigate an innate recognition, i.e., a non-humoral opsonization of the SARS-CoV-2 virus. To determine whether the expression of ACE2 on neutrophils is functionally relevant in SARS-CoV-2 infection further investigation will be essential.

In conclusion, we have developed a model to study neutrophil-epithelial interactions which more closely reflects an *in vivo* and more clinically relevant infection of airways than monocultures. Our findings demonstrate that the co-presence of neutrophils generates a polarized pro-inflammatory niche with the conducting airway epithelium that is significantly augmented with SARS-CoV-2 infection. This pro-inflammatory niche breaks down the epithelial barrier integrity allowing for increased epithelial infection including basal stem cells. Overall, this study reveals a

key role for pre-existing chronic airway neutrophilia in determining infectivity and outcomes in response to SARS-CoV-2 infection that highlight neutrophilia as a potential target for prevention of severe COVID-19 disease.

Data availability statement

The original contributions presented in the study are included in the article/Supplementary Material. Further inquiries can be directed to the corresponding author.

Ethics statement

The studies involving human participants were reviewed and approved by Institutional Review Board (IRB) of the University of Southern California (USC), protocol #HS-20-00546. The patients/participants provided their written informed consent to participate in this study.

Author contributions

Conceptualization: BC and AR. Methodology: BC and AR. Formal analysis: JA and MS. Investigation: BC, EQ, ZL, ND, CS, SK, WW, JH, and AR. Writing - original draft: BC and AR. Writing – review and editing: BC and AR. Funding acquisition: AR. All authors contributed to the article and approved the submitted version.

Funding

AR is funded by the Hastings Foundation, Daniel Tyler Health and Education Fund, and the Cystic Fibrosis Foundation (FIRTH17XX0 and FIRTH21XX0).

Acknowledgments

The authors acknowledge the Center for Advanced Research Computing (CARC) at the University of Southern California for providing computing resources that have contributed to the research results reported within this publication. URL: https://carc.usc.edu. All Biosafety Level 3 work was performed within The Hastings Foundation and The Wright Foundation Laboratories at USC. SARS-CoV2 BSL3 resources supported by a grant from the COVID-19 Keck Research Fund. Flow cytometry was performed in the USC Flow Cytometry Facility supported in part by the National Cancer Institute Cancer Center Shared Grant award P30CA014089 and the USC Office of the Provost, Dean's Development Funds, Keck School of Medicine of USC. The content is solely the responsibility of the authors and does not necessarily represent the official views of the National Cancer Institute or the National Institutes of Health. We thank the organ donors and their families for their invaluable donation and the International Institute for the Advancement of Medicine (IIAM), Drs Daniel Weiss and Sharon Mount and the UVMMC autopsy service at the University of Vermont, and Dr. Scott Randell at the University of North Carolina Marsico Lung Institute Tissue Procurement and Cell Culture Core supported in part by NIH DK065988 and grant BOUCHR19R0 from the Cystic Fibrosis Foundation, for their partnership in providing lung tissues for research. Finally, the authors wish to thank the USC COVID-19 Biospecimen Repository for assistance with pathologic analysis

Conflict of interest

The authors declare that the research was conducted in the absence of any commercial or financial relationships that could be construed as a potential conflict of interest.

Publisher's note

Supplementary material

The Supplementary Material for this article can be found online at: https://www.frontiersin.org/articles/10.3389/fimmu.2023.1112870/full#supplementary-material

References

1. Wu Z, McGoogan JM. Characteristics of and important lessons from the coronavirus disease 2019 (COVID-19) outbreak in China: Summary of a report of 72314 cases from the Chinese center for disease control and prevention. *JAMA* (2020) 323(13):1239–42. doi: 10.1001/jama.2020.2648

2. Guan WJ, Ni ZY, Hu Y, Liang WH, Ou CQ, He JX, et al. Clinical characteristics of coronavirus disease 2019 in China. *N Engl J Med* (2020) 382(18):1708–20. doi: 10.1056/NEJMoa2002032

3. Pechous RD. With friends like these: The complex role of neutrophils in the progression of severe pneumonia. *Front Cell Infect Microbiol* (2017) 7:160. doi: 10.3389/fcimb.2017.00160

4. Grommes J, Soehnlein O. Contribution of neutrophils to acute lung injury. *Mol Med* (2011) 17(3-4):293–307. doi: 10.2119/molmed.2010.00138

5. Munoz-Fontela C, Dowling WE, Funnell SGP, Gsell PS, Riveros-Balta AX, Albrecht RA, et al. Animal models for COVID-19. *Nature* (2020) 586(7830):509–15. doi: 10.1038/s41586-020-2787-6

6. Zhang B, Zhou X, Zhu C, Song Y, Feng F, Qiu Y, et al. Immune phenotyping based on the neutrophil-to-Lymphocyte ratio and IgG level predicts disease severity and outcome for patients with COVID-19. *Front Mol Biosci* (2020) 7:157. doi: 10.3389/fmolb.2020.00157

7. Song C-Y, Xu J, He JQ, Lu YQ. COVID-19 early warning score: a multi-parameter screening tool to identify highly suspected patients. *medRxiv* (2020), 2020.03.05.20031906. doi: 10.1101/2020.03.05.20031906

8. Aveyard P, Gao M, Lindson N, Hartmann-Boyce J, Watkinson P, Young D, et al. Association between pre-existing respiratory disease and its treatment, and severe COVID-19: a population cohort study. *Lancet Respir Med* (2021). doi: 10.1016/S2213-2600(21)00095-3

9. Galani IE, Andreakos E. Neutrophils in viral infections: Current concepts and caveats. *J Leukoc Biol* (2015) 98(4):557–64. doi: 10.1189/jlb.4VMR1114-555R

10. Bordon J, Aliberti S, Fernandez-Botran R, Uriarte SM, Rane MJ, Duvvuri P, et al. Understanding the roles of cytokines and neutrophil activity and neutrophil apoptosis in the protective versus deleterious inflammatory response in pneumonia. *Int J Infect Dis* (2013) 17(2):e76–83. doi: 10.1016/j.ijid.2012.06.006

11. Borges L, Pithon-Curi TC, Curi R, Hatanaka E. COVID-19 and neutrophils: The relationship between hyperinflammation and neutrophil extracellular traps. *Mediators Inflamm 2020* (2020) p:8829674. doi: 10.1155/2020/8829674

12. Huang C, Wang Y, Li X, Ren L, Zhao J, Hu Y, et al. Clinical features of patients infected with 2019 novel coronavirus in wuhan, China. *Lancet* (2020) 395(10223):497–506. doi: 10.1016/S0140-6736(20)30183-5

13. Fajgenbaum DC, June CH. Cytokine storm. *N Engl J Med* (2020) 383(23):2255–73. doi: 10.1056/NEJMra2026131

14. Ruan Q, Yang K, Wang W, Jiang L, Song J. Correction to: Clinical predictors of mortality due to COVID-19 based on an analysis of data of 150 patients from wuhan, China. *Intensive Care Med* (2020) 46(6):1294–7. doi: 10.1007/s00134-020-06028-z

15. Chen G, Wu D, Guo W, Cao Y, Huang D, Wang H, et al. Clinical and immunological features of severe and moderate coronavirus disease 2019. *J Clin Invest* (2020) 130(5):2620–9. doi: 10.1172/JCI137244

16. Hemmat N, Derakhshani A, Bannazadeh Baghi H, Silvestris N, Baradaran B, De Summa S, et al. Neutrophils, crucial, or harmful immune cells involved in coronavirus infection: A bioinformatics study. *Front Genet* (2020) 11:641. doi: 10.3389/fgene.2020.00641

17. Shi H, Zuo Y, Yalavarthi S, Gockman K, Zuo M, Madison JA, et al. Neutrophil calprotectin identifies severe pulmonary disease in COVID-19. *J Leukoc Biol* (2021) 109 (1):67–72. doi: 10.1101/2020.05.06.20093070

18. Veras FP, Pontelli M, Silva C, Toller-Kawahisa J, de Lima M, Nascimento D, et al. SARS-CoV-2 triggered neutrophil extracellular traps (NETs) mediate COVID-19 pathology. *medRxiv* (2020), 2020.06.08.20125823. doi: 10.1101/2020.06.08.20125823

19. Radermecker C, Sabatel C, Vanwinge C, Ruscitti C, Marechal P, Perin F, et al. Locally instructed CXCR4(hi) neutrophils trigger environment-driven allergic asthma through the release of neutrophil extracellular traps. *Nat Immunol* (2019) 20(11):1444–55. doi: 10.1038/s41590-019-0496-9

20. Li G, He X, Zhang L, Ran Q, Wang J, Xiong A, et al. Assessing ACE2 expression patterns in lung tissues in the pathogenesis of COVID-19. *J Autoimmun* (2020) 112:102463. doi: 10.1016/j.jaut.2020.102463

21. Tomar B, Anders HJ, Desai J, Mulay SR. Neutrophils and neutrophil extracellular traps drive necroinflammation in COVID-19. *Cells* (2020) 9(6):1383. doi: 10.3390/cells9061383

22. Qin C, Zhou L, Hu Z, Zhang S, Yang S, Tao Y, et al. Dysregulation of immune response in patients with coronavirus 2019 (COVID-19) in wuhan, China. *Clin Infect Dis* (2020) 71(15):762–8. doi: 10.1093/cid/ciaa248

23. Veras FP, Pontelli MC, Silva CM, Toller-Kawahisa JE, de Lima M, Nascimento DC, et al. SARS-CoV-2-triggered neutrophil extracellular traps mediate COVID-19 pathology. *J Exp Med* (2020) 217(12):e20201129. doi: 10.1084/jem.20201129

24. Arcanjo A, Logullo J, Menezes CCB, de Souza Carvalho Giangiarulo TC, Dos Reis MC, de Castro GMM, et al. The emerging role of neutrophil extracellular traps in severe acute respiratory syndrome coronavirus 2 (COVID-19). *Sci Rep* (2020) 10 (1):19630. doi: 10.1038/s41598-020-76781-0

25. Janiuk K, Jablonska E, Garley M. Significance of NETs formation in COVID-19. *Cells* (2021) 10(1):151. doi: 10.3390/cells1001015

26. Deng Y, Herbert JA, Robinson E, Ren L, Smyth RL, Smith CM. Neutrophil-airway epithelial interactions result in increased epithelial damage and viral clearance during respiratory syncytial virus infection. *J Virol* (2020) 94(13):e02161-19. doi: 10.1128/jvi.02161-19

27. Randell SH, Walstad L, Schwab UE, Grubb BR, Yankaskas JR. Isolation and culture of airway epithelial cells from chronically infected human lungs. *In Vitro. Cell Dev Biol Anim* (2001) 37(8):480–9. doi: 10.1290/1071-2690(2001)037<0480:iacoae>2.0.co;2

28. Pfaffl MW. A new mathematical model for relative quantification in real-time RT-PCR. *Nucleic Acids Res* (2001) 29(9):e45. doi: 10.1093/nar/29.9.e45

29. Jasper AE, McIver WJ, Sapey E, Walton GM. Understanding the role of neutrophils in chronic inflammatory airway disease. *F1000Res* (2019) 8(F1000 Faculty Rev):557. doi: 10.12688/f1000research.18411.1

30. Taylor S, Dirir O, Zamanian RT, Rabinovitch M, Thompson AAR. The role of neutrophils and neutrophil elastase in pulmonary arterial hypertension. *Front Med (Lausanne)* (2018) 5:217. doi: 10.3389/fmed.2018.00217

31. Florentin J, Zhao J, Tai YY, Vasamsetti SB, O'Neil SP, Kumar R, et al. Interleukin-6 mediates neutrophil mobilization from bone marrow in pulmonary hypertension. *Cell Mol Immunol* (2021) 18(2):374–84. doi: 10.1038/s41423-020-00608-1

32. Zhu N, Wang W, Liu Z, Liang C, Wang W, Ye F, et al. Morphogenesis and cytopathic effect of SARS-CoV-2 infection in human airway epithelial cells. *Nat Commun* (2020) 11(1):3910. doi: 10.1038/s41467-020-17796-z

33. Jia HP, Look DC, Shi L, Hickey M, Pewe L, Netland J, et al. ACE2 receptor expression and severe acute respiratory syndrome coronavirus infection depend on differentiation of human airway epithelia. *J Virol* (2005) 79(23):14614–21. doi: 10.1128/JVI.79.23.14614-14621.2005

34. Jia HP, Look DC, Tan P, Shi L, Hickey M, Gakhar L, et al. Ectodomain shedding of angiotensin converting enzyme 2 in human airway epithelia. *Am J Physiol Lung Cell Mol Physiol* (2009) 297(1):L84–96. doi: 10.1152/ajplung.00071.2009

35. Zhang H, Rostami MR, Leopold PL, Mezey JG, O'Beirne SL, Strulovici-Barel Y, et al. Expression of the SARS-CoV-2 ACE2 receptor in the human airway epithelium. *Am J Respir Crit Care Med* (2020) 202(2):219–29. doi: 10.1164/rccm.202003-0541OC

36. Baggiolini M, Walz A, Kunkel SL. Neutrophil-activating peptide-1/interleukin 8, a novel cytokine that activates neutrophils. *J Clin Invest* (1989) 84(4):1045–9. doi: 10.1172/JCI114265

37. Yoshimura T, Matsushima K, Tanaka S, Robinson EA, Appella E, Oppenheim JJ, et al. Purification of a human monocyte-derived neutrophil chemotactic factor that has peptide sequence similarity to other host defense cytokines. *Proc Natl Acad Sci U.S.A.* (1987) 84(24):9233–7. doi: 10.1073/pnas.84.24.9233

38. Parsons PE, Fowler AA, Hyers TM, Henson PM. Chemotactic activity in bronchoalveolar lavage fluid from patients with adult respiratory distress syndrome. *Am Rev Respir Dis* (1985) 132(3):490–3. doi: 10.1164/arrd.1985.132.3.490

39. Azevedo MLV, Zanchettin AC, Vaz de Paula CB, Motta Junior JDS, Malaquias MAS, Raboni SM, et al. Lung neutrophilic recruitment and IL-8/IL-17A tissue expression in COVID-19. *Front Immunol* (2021) 12:656350. doi: 10.3389/fimmu.2021.656350

40. Pease JE, Sabroe I. The role of interleukin-8 and its receptors in inflammatory lung disease: implications for therapy. *Am J Respir Med* (2002) 1(1):19–25. doi: 10.1007/BF03257159

41. Del Valle DM, Kim-Schulze S, Huang HH, Beckmann ND, Nirenberg S, Wang B, et al. An inflammatory cytokine signature predicts COVID-19 severity and survival. *Nat Med* (2020) 26(10):1636–43. doi: 10.1038/s41591-020-1051-9

42. Han H, Ma Q, Li C, Liu R, Zhao L, Wang W, et al. Profiling serum cytokines in COVID-19 patients reveals IL-6 and IL-10 are disease severity predictors. *Emerg Microbes Infect* (2020) 9(1):1123–30. doi: 10.1080/22221751.2020.1770129

43. Liu QQ, Cheng A, Wang Y, Li H, Hu L, Zhao X, et al. Cytokines and their relationship with the severity and prognosis of coronavirus disease 2019 (COVID-19): a retrospective cohort study. *BMJ Open* (2020) 10(11):e041471. doi: 10.1136/bmjopen-2020-041471

44. Gernez Y, Tirouvanziam R, Chanez P. Neutrophils in chronic inflammatory airway diseases: can we target them and how? *Eur Respir J* (2010) 35(3):467–9. doi: 10.1183/09031936.00186109

45. Kulkarni U, Zemans RL, Smith CA, Wood SC, Deng JC, Goldstein DR, et al. Excessive neutrophil levels in the lung underlie the age-associated increase in influenza mortality. *Mucosal Immunol* (2019) 12(2):545–54. doi: 10.1038/s41385-018-0115-3

46. Chen MM, Palmer JL, Plackett TP, Deburghgraeve CR, Kovacs EJ. Age-related differences in the neutrophil response to pulmonary pseudomonas infection. *Exp Gerontol* (2014) 54:42–6. doi: 10.1016/j.exger.2013.12.010

47. Sapey E, Patel JM, Greenwood HL, Walton GM, Hazeldine J, Sadhra C, et al. Pulmonary infections in the elderly lead to impaired neutrophil targeting, which is improved by simvastatin. *Am J Respir Crit Care Med* (2017) 196(10):1325–36. doi: 10.1164/rccm.201704-0814OC

48. Kordonowy LL, Burg E, Lenox CC, Gauthier LM, Petty JM, Antkowiak M, et al. Obesity is associated with neutrophil dysfunction and attenuation of murine acute lung injury. *Am J Respir Cell Mol Biol* (2012) 47(1):120–7. doi: 10.1165/rcmb.2011-0334OC

49. Maia LA, Cruz FF, de Oliveira MV, Samary CS, Fernandes MVS, Trivelin SAA, et al. Effects of obesity on pulmonary inflammation and remodeling in experimental moderate acute lung injury. *Front Immunol* (2019) 10:1215. doi: 10.3389/fimmu.2019.01215

50. Manicone AM, Gong K, Johnston LK, Giannandrea M. Diet-induced obesity alters myeloid cell populations in naive and injured lung. *Respir Res* (2016) 17:24. doi: 10.1186/s12931-016-0341-8

51. Kumar S, Yadav PK, Srinivasan R, Perumal N. Selection of animal models for COVID-19 research. *Virusdisease* (2020) p:1–6. doi: 10.1007/s13337-020-00637-4

52. Stackowicz J, Jonsson F, Reber LL. Mouse models and tools for the in vivo study of neutrophils. *Front Immunol* (2019) 10:3130. doi: 10.3389/fimmu.2019.03130

53. Corteling R, Wyss D, Trifilieff A. In vivo models of lung neutrophil activation. comparison of mice and hamsters. *BMC Pharmacol* (2002) 2:1. doi: 10.1186/1471-2210-2-1

54. Parkos CA. Neutrophil-epithelial interactions: A double-edged sword. *Am J Pathol* (2016) 186(6):1404–16. doi: 10.1016/j.ajpath.2016.02.001

55. Kunkel SL, Standiford T, Kasahara K, Strieter RM. Interleukin-8 (IL-8): the major neutrophil chemotactic factor in the lung. *Exp Lung Res* (1991) 17(1):17–23. doi: 10.3109/01902149109063278

56. Yang PH, Ding YB, Xu Z, Pu R, Li P, Yan J, et al. Increased circulating level of interleukin-6 and CD8(+) T cell exhaustion are associated with progression of COVID-19. *Infect Dis Poverty* (2020) 9(1):161. doi: 10.1186/s40249-020-00780-6

57. Liu J, Li S, Liu J, Liang B, Wang X, Wang H, et al. Longitudinal characteristics of lymphocyte responses and cytokine profiles in the peripheral blood of SARS-CoV-2 infected patients. *EBioMedicine* (2020) 55:102763. doi: 10.1016/j.ebiom.2020.102763

58. Godkin A, Humphreys IR. Elevated interleukin-6, interleukin-10 and neutrophil : lymphocyte ratio as identifiers of severe coronavirus disease 2019. *Immunology* (2020) 160(3):221–2. doi: 10.1111/imm.13225

59. Huang H, Zhang M, Chen C, Zhang H, Wei Y, Tian J, et al. Clinical characteristics of COVID-19 in patients with preexisting ILD: A retrospective study in a single center in wuhan, China. *J Med Virol* (2020) 92(11):2742–50. doi: 10.1002/jmv.26174

60. Pandolfi L, Fossali T, Frangipane V, Bozzini S, Morosini M, D'Amato M, et al. Broncho-alveolar inflammation in COVID-19 patients: a correlation with clinical outcome. *BMC Pulm Med* (2020) 20(1):301. doi: 10.1186/s12890-020-01343-z

61. Fahlberg MD, Blair RV, Doyle-Meyers LA, Midkiff CC, Zenere G, Russell-Lodrigue KE, et al. Cellular events of acute, resolving or progressive COVID-19 in SARS-CoV-2 infected non-human primates. *Nat Commun* (2020) 11(1):6078. doi: 10.1038/s41467-020-19967-4

62. Ellis TN, Beaman BL. Interferon-gamma activation of polymorphonuclear neutrophil function. *Immunology* (2004) 112(1):2–12. doi: 10.1111/j.1365-2567.2004.01849.x

63. Kang S, Brown HM, Hwang S. Direct antiviral mechanisms of interferon-gamma. *Immune Netw* (2018) 18(5):e33. doi: 10.4110/in.2018.18.e33

64. Lee AJ, Ashkar AA. The dual nature of type I and type II interferons. *Front Immunol* (2018) 9. doi: 10.3389/fimmu.2018.02061

65. Capaldo CT, Nusrat A. Cytokine regulation of tight junctions. *Biochim Biophys Acta* (2009) 1788(4):864–71. doi: 10.1016/j.bbamem.2008.08.027

66. Al-Sadi R, Boivin M, Ma T. Mechanism of cytokine modulation of epithelial tight junction barrier. *Front Biosci (Landmark Ed)* (2009) 14:2765–78. doi: 10.2741/3413

67. Silva MT, Correia-Neves M. Neutrophils and macrophages: the main partners of phagocyte cell systems. *Front Immunol* (2012) 3:174. doi: 10.3389/fimmu.2012.00174

68. Uribe-Querol E, Rosales C. Phagocytosis: Our current understanding of a universal biological process. *Front Immunol* (2020) 11:1066. doi: 10.3389/fimmu.2020.01066

69. Wen Z, Zhang Y, Lin Z, Shi K, Jiu Y. Cytoskeleton-a crucial key in host cell for coronavirus infection. *J Mol Cell Biol* (2020) 12(12):968–79. doi: 10.1093/jmcb/mjaa042

70. Wang Y, Jonsson F. Expression, role, and regulation of neutrophil fcgamma receptors. *Front Immunol* (2019) 10:1958. doi: 10.3389/fimmu.2019.01958

Frontiers in Immunology

Explores novel approaches and diagnoses to treat immune disorders.

The official journal of the International Union of Immunological Societies (IUIS) and the most cited in its field, leading the way for research across basic, translational and clinical immunology.

Discover the latest Research Topics

See more →

Frontiers

Avenue du Tribunal-Fédéral 34
1005 Lausanne, Switzerland
frontiersin.org

Contact us

+41 (0)21 510 17 00
frontiersin.org/about/contact